Fate of Polymer-Based Coagulants/Flocculants in Oil and Gas Wastewater Treatment

by

JIA LI

A thesis submitted in partial fulfillment of the requirements for the degree of

Doctor of Philosophy

in

Environmental Engineering

Department of Civil and Environmental Engineering
University of Alberta

ABSTRACT

Bitumen is extracted either using surface mining or in situ processes, such as Steam Assisted Gravity Drainage (SAGD), that could produce large quantities of oil sands process water (OSPW) and SAGD produced water. SAGD produced water is generally characterized by a slightly basic pH (7-8), high temperature (80-90 °C), and high levels of colloidal impurities, total dissolved solids (TDS) and total organic carbon (TOC). OSPW is also a highly complex mixture containing sands, silts, heavy metals, and recalcitrant organics such as naphthenic acids (NAs). Currently, OSPW is retained on site in tailings ponds without active return to the regional watershed. In order to treat, recover and recycle these two types of wastewaters, polymer-based coagulants and flocculants are widely applied. However, limited knowledge about the fate of these polymers in wastewater from oil and gas industry is known. Therefore, in this thesis, the interactions and degradations of different polymer-based coagulants/flocculants in oil and gas wastewater were investigated.

Firstly, response surface methodology (RSM) was employed to optimize the thermal softening-coagulation-flocculation-sedimentation process with softeners, poly-DADMAC as the coagulant, and cationic polyacrylamide (PAM) as the flocculant, and assess the interaction effects of operational variables for sludge volume index (SVI) and the removal efficiency of turbidity, total suspended solids (TSS), particulate hardness, silica, total organic carbon (TOC) and total inorganic carbon (TIC) in synthetic SAGD produced water. Poly-DADMAC dose and mixing time with softeners only were demonstrated to be the most influential factors for the treatment process. Temperature was found to facilitate the removal of colloidal impurities by forming larger and denser flocs and changing their surface composition. More importantly, adsorption and subsequent

bridging are the main interaction mechanisms between the polymers and particles in the coagulation-flocculation process.

The long-term fate of dissolved organics in OSPW under various controlled conditions was examined to enhance the understanding of the physiochemical characteristics of OSPW during long-term storage. The highest removal of dissolved organics was observed in ozonated OSPW stored at 20 °C with the highest reduction of COD, DOC, and total NAs. Biodegradation was believed to be the main reason for dissolved organics removal. Additionally, temperature has been demonstrated to be the most important impact factor for the characteristics of OSPW. The limited changes of various parameters in OSPW samples stored at 4 °C supported the common practice of storing OSPW in the cold room as an effective way to preserving the water quality in the laboratory. The microorganism analysis indicated that *Bacillus* and *Fontimonas* might be the key microorganisms for degrading dissolved organics like NAs in OSPW.

Under oxic conditions, the degradation of anionic polyacrylamide (A-PAM) in different temperatures and microorganism conditions in oil sands tailings was studied. The maximum removal efficiency of A-PAM without releasing acrylamide (AMD) monomer was observed in tailings water with augmented microorganisms at 20 °C. No substantial effect on acute toxicity and no genotoxicity were found from aerobic degradation of A-PAM in tailings. It was revealed that in the oil sands tailings oxic zone, macromolecular A-PAM could partially degrade into ammonia and smaller molecules, like organic acids, with help of extracellular amidases.

Finally, anaerobic A-PAM degradation in tailings was studied at various A-PAM dosages. Higher methane yield was observed in the tailings samples with lower concentrations of A-PAM (10 and 100 mg/kg TS) than in higher concentrations of A-PAM (250 to 2000 mg/kg). A-PAM

molecules could be partially degraded into smaller molecules, such as AMD and polyacrylic acid, which could be utilized as both carbon and nitrogen source to microbes. No contribution to the acute toxicity and genotoxicity was found from anaerobic degradation of A-PAM. The A-PAM concentration could affect the degradation via affecting the flocs structure and composition, which subsequently affected the microbial colonization and metabolic activity. The analysis of microbial community suggested that *Smithella*, *Candidatus_Cloacimonas*, *W5*, *XBB1006,* and *DMER64* were critical microorganisms involved in anaerobic degradation of A-PAM. The potential metabolic pathways for producing different volatile fatty acids (VFAs) from the intermediates of A-PAM degradation were proposed.

PREFACE

All the research conducted in this thesis was designed and performed by me, under the supervision of Dr. Mohamed Gamal El-Din. I conducted all the experimental work as well as the data interpretation and the preparation of the manuscripts. Some colleagues also contributed to sample analysis or manuscript edits as described below:

Chapter 2 has been published as "Li J, How ZT, Zeng H, Gamal El-Din M. Treatment Technologies for Organics and Silica Removal in Steam-Assisted Gravity Drainage Produced Water: A Comprehensive Review. Energy & Fuels. 2022; 36(3):1205-31". Dr. Mohamed Gamal El-Din contributed to the supervision, review of the manuscript, and funding acquisition. Dr. Hongbo Zeng contributed to the supervision and review of the manuscript. Dr. Zuo Tong How contributed to the editing of the manuscript.

Chapter 3 has been published as "Li J, How ZT, Benally C, Sun Y, Zeng H, Gamal El-Din M. Removal of colloidal impurities by thermal softening-coagulation-flocculation-sedimentation in steam assisted gravity drainage (SAGD) produced water: performance, interaction effects and mechanism study. Separation and Purification Technology. 2023; 123484". Dr. Mohamed Gamal El-Din contributed to the supervision, review of the manuscript, and funding acquisition. Dr. Hongbo Zeng contributed to the supervision and review of the manuscript. Dr. Zuo Tong How contributed to results, discussion, and manuscript revision. Dr. Chelsea Benally contributed to the editing of the manuscript. Mr. Yongxiang Sun contributed to the analysis of surface force.

Chapter 4 will be submitted to the Journal of Hazardous Materials as "Li J, Arslan M, Yang L, Gamal El-Din M. Fate of dissolved organics in oil sands process water during 4-year storage: mechanistic insights into toxicity removal and microbial processes". Dr. Mohamed Gamal El-Din

contributed to the supervision, review of the manuscript, and funding acquisition. Dr. Muhammad Arslan contributed to the analysis of microbial community and edited the manuscript. Dr. Lingling Yang contributed to the statistical analysis, analyzing samples on ultra-performance liquid chromatograph time-of-flight mass spectrometry (UPLC-TOF-MS), and the editing of the manuscript.

Chapter 5 has been published as "Li J, How ZT, Gamal El-Din M. Aerobic degradation of anionic polyacrylamide in oil sands tailings: Impact factor, degradation effect, and mechanism. Science of the Total Environment. 2023; 856:159079". Dr. Mohamed Gamal El-Din contributed to the supervision, review of the manuscript, and funding acquisition. Dr. Zuo Tong How contributed to the experimental planning, results, discussion and manuscript revision.

Chapter 6 will be submitted to Water Research as "Li J, Usman M, Arslan M, Gamal El-Din M. Molecular and microbial insights towards understanding the anaerobic degradation of anionic polyacrylamide in oil sands tailings". Dr. Mohamed Gamal El-Din contributed to the supervision, review of the manuscript, and funding acquisition. Dr. Muhammad Usman contributed to the experimental planning and the editing of the manuscript. Dr. Muhammad Arslan contributed to the analysis of microbial community and the editing of the manuscript.

DEDICATION

To my beloved parents, Hong Tao & Hongyan Li,

whose love, boundless support, and gift of dream I cherish.

To my incredible boyfriend, my constant companion and source of inspiration,

thank you for your belief in me.

To all my family and friends, who walked this path alongside me, thank you for

your support, encouragement, and love.

And to every dreamer, who never ceases to soar, may you succeed in finding your

own path.

ACKNOWLEDGEMENTS

Lastly, I wish to express my deepest gratitude to my family, my boyfriend Hotaka Kobori, and my friends for their boundless love and unwavering support throughout my academic journey.

TABLE OF CONTENTS

LIST OF TABLES

LIST OF FIGURES

LIST OF ABBREVIATIONS

A-PAM	anionic polyacrylamide
AMD	acrylamide
ANOVA	analysis of variance
ASVs	amplicon sequence variants
ATR FT-IR	attenuated total reflection fourier transform infrared
BBD	Box Behnken design
BBD water	boiler blow-down water
BE-SPME	biomimetic extraction-solid phase microextraction
BFW	boiler feed water
BTEX	benzene, toluene, ethyl benzene, and xylenes
CCD	central composite design
CF	coagulation-flocculation
COD	chemical oxygen demand
CSS	cyclic steam stimulation
DBE	double bond equivalent
DMN	dimethylnaphthalene
DMSO	dimethyl sulfoxide
DO	dissolved oxygen
DOC	dissolved organic carbon
DOM	dissolved organic matter
DOW	de-oiled water
EDS	energy-dispersive x-ray spectroscopy
epi-DMA	epichlorohydrin-dimethylamine
ESI	electrospray ionization
FEEM	fluorescence excitation-emission matrix
FESEM	field emission scanning electron microscopy
FT-ICR-MS	fourier-transform ion cyclotron resonance mass spectrometry
GC-FID	gas chromatography with a flame ion detector
GC-MS	gas chromatography mass spectrometry
GC-TCD	gas chromatography with a thermal conductivity detector
GPC	gel permeation chromatography
HAS	humic acid sodium salt
HLS	hot lime softening
HPiA	hydrophilic acid
HPiB	hydrophilic base
HPiN	hydrophilic neutral
HPLC	high-performance liquid chromatography

HPoA	hydrophobic acid
HPoB	hydrophobic base
HPoN	hydrophobic neutral
ICP-OES	inductively coupled plasma-optical emission spectroscopy
IERW	ion exchange regeneration wastewater
IF	induction factor
MW	molecular weight
MWD	molecular weight distribution
NAs	naphthenic acids
ORP	oxidation-reduction potential
OSPW	oil sands process water
OTSGs	once-through steam generators
PAC	poly(aluminum chloride)
PAFSi	polymeric aluminum ferric silicate
PAHs	polycyclic aromatic hydrocarbons
PALS	phase analysis light scattering
PDI	polydispersity index
PDMS	polydimethylsiloxane
Poly-DADMAC	poly(diallyldimethylammonium chloride)
RDA	redundancy analysis
RSM	response surface methodology
SAGD	steam assisted gravity drainage
SFA	surface forces apparatus
SVI	sludge volume index
TDS	total dissolved solids
TIC	total inorganic carbon
TN	total nitrogen
TOC	total organic carbon
TS	total solids
TSS	total suspended solids
UPLC TOF-MS	ultra-performance liquid chromatography time-of-flight mass spectrometry
UV	ultraviolet
VOCs	volatile organic compounds
WAC	weak-acid cation
WLS	warm lime softening
WSO	water-soluble organics
XPS	x-ray photoelectron spectroscopy
XRD	x-ray powder diffraction
ZP	zeta potential

CHAPTER 1 GENERAL INTRODUCTION AND RESEARCH OBJECTIVES

1.1 Background

1.1.1 Bitumen extraction from oil sands

As the third-largest crude oil reserves in the world, oil sands deposits in northern Alberta, Canada produced 3.6 million barrels of recoverable oil per day in 2019 with an expected production of 4.4 million barrels per day in 2029 (Alberta Energy Regulator, 2020). Depending on how deep the oil sands are deposited, bitumen is extracted either using surface mining or in situ processes (Nimana et al., 2015). For the shallow mines, crude bitumen is extracted via surface mining, which accounts for 46% of the total extraction (Sapkota et al., 2018). Surface mining involves removing the oil sands with shovels and trucks and separating the bitumen by using the Clark caustic hot water process (Bergerson et al., 2012).

However, approximately 80% of Alberta's oil sands deposits are too deep (over 200 m) for surface mining and require in situ methods (Rui et al., 2018). Steam Assisted Gravity Drainage (SAGD) and Cyclic Steam Stimulation (CSS) are two primary in-situ thermal recovery processes used for the bitumen extraction (Qin et al., 2017). CSS is a batch process, and a single well is required for both steam injection and oil production in an alternating batch mode (Radpour et al., 2021). In the SAGD process, the bitumen is extracted through three typical processes with a pair of parallel horizontal wells: (i) hot steam is injected from the upper well to form a steam chamber so that the bitumen can be heated up and its viscosity can be reduced; (ii) the heated bitumen with reduced viscosity flows with the steam condensate and reservoir connate water, and drains almost completely by gravity into the lower well; and (iii) the mixture of bitumen, clay, and water is

pumped to the surface and the water-oil emulsion is separated at a plant (Ku et al., 2012; Manfre Jaimes et al., 2019).

1.1.2 Wastewater from bitumen extraction

1.1.2.1 Oil sands process water

During the Clark caustic hot water extraction process in surface mining, about 0.21-2.5 barrels of water are required for per barrel of bitumen extraction, where a large amount of oil sands process water (OSPW) is generated (NRC, 2022). After the bitumen extraction, OSPW is stored in tailings ponds for water-solid separation. More than 80% of the process water is recovered from tailings ponds and recycled back for the bitumen extraction process (NRC, 2022). OSPW is a complex mixture consisting of suspended solids, salts, inorganic compounds, trace metals, and organic compounds including naphthenic acids (NAs), polycyclic aromatic hydrocarbons (PAHs), phenols, and BTEX (benzene, toluene, ethyl benzene, and xylenes) (Li et al., 2017). As the majority of total organics (~50%) and a major driver of toxicity of OSPW, NAs are oil-derived mixtures of alkyl-substituted saturated cyclic and non-cyclic carboxylic acids with the general formula $C_nH_{2n+Z}O_x$, where n refers to the carbon number, Z (zero or a negative even integer) indicates the hydrogen deficiency caused by rings and/or double bonds introduction, and x is the number of oxygen atoms in the structure (x = 2 is classical NAs and $3 \leq x \leq 6$ is oxidized NAs) (Meshref et al., 2017; Xue et al., 2018).

As OSPW will ultimately need to be incorporated into a reclaimed landscape, such as end-pit lakes, and may introduce NAs to groundwater, understanding and mitigating NAs toxicity is essential for regulatory decision-making (Frank et al., 2014; Marentette et al., 2015). OSPW has been reported to cause acute, sub-chronic and chronic toxicity, to living organisms including fish

(Hughes et al., 2017), mammals (Fu et al., 2017), invertebrates (Bartlett et al., 2017), and microorganisms (Miles et al., 2019). In addition, the acute toxicity of aged OSPW obtained from remediation ponds and wetlands were reduced, which might be due to the changes of NAs composition over time in OSPW (Holowenko et al., 2002; Li et al., 2017). In an aging OSPW, indigenous microbial communities seem to preferentially degrade NAs with lower carbon numbers (< 22), resulting in a larger proportion of NAs with higher carbon fraction (Biryukova et al., 2007; Quagraine et al., 2005). Previous studies have shown that NAs with higher molecular weight are less toxic to *A. fischeri* probably due to the presence of high -COOH content which decreased hydrophobicity (Frank et al., 2009a; Frank et al., 2008; Frank et al., 2009b). However, there are contradicting results on toxicity of fresh and aged OSPW found in studies about other living organisms. For example, Bartlett et al. (2017) have reported that NAs extracted from fresh OSPW were less toxic to invertebrates than those from aged OSPW, while other studies observed reduced toxicity occurring with degradation processes with aging OSPW (Anderson et al., 2012; Holowenko et al., 2002; Wiseman et al., 2013). The different results among various studies could be due to many reasons including different field-OSPW samples (source, aging period, and composition), tested species, exposure time, and extraction methods for NAs. Hence, in order to better understand the aging effect on NAs degradation and toxicity of OSPW, conducting aging experiments in the lab under certain controlling conditions is necessary.

Various technologies have been explored for NAs degradation and OSPW remediation, including active and passive applications (Lillico et al., 2023; Toor et al., 2013; Xue et al., 2018). Successful reclamation of OSPW will require a reduction of NAs concentration and the removal of toxic characteristics. Among different technologies, natural or enhanced bioremediation in lakes or wetlands will likely play a critical role in meeting these requirements (Toor et al., 2013).

Previous studies have shown that a number of microorganisms have the ability to metabolize NAs, including *Acinetobacter anitratum*, *Alcaligenes faecalis*, and *Pseudomonas putida* (Blakley, 1974; Blakley and Papish, 1982; Johnson et al., 2011; Rho and Evans, 1975). It is believed that β-oxidation is the dominant degradation pathway, but α-oxidation and aromatization may also contribute (Han et al., 2008; Quinlan and Tam, 2015). Furthermore, researchers have attempted to utilize indigenous microorganisms to degrade NAs under aerobic and anaerobic conditions. Mahdavi et al. (2015) evaluated an indigenous aerobic algae-bacteria consortium for removal of NAs and toxicity reduction. Their results demonstrated that the indigenous algae-bacteria consortium enhanced detoxification process. Unlike aerobic studies, poor removal of NAs were found in anaerobic studies. For example, Arslan and Gamal El-Din (2021) found toxicity was only slightly reduced and 20% of classical NAs were removed, whereas the oxidized NAs persisted in the OSPW under anaerobic conditions. Therefore, enhanced understanding of the role of indigenous microbes in natural attenuation of NAs is important to improve the efficiency of biotreatment of OSPW.

1.1.2.2 SAGD produced water

During the SAGD process, injected steam is recovered as produced water on the surface. Due to the intensive use of water in the SAGD process, recycling the produced water to regenerate steam is essential for both the protection of environment and minimizing operational costs. With the purpose of recycling SAGD produced water as boiler feed water (BFW) for steam generation, further treatment is required after removing bitumen (Fatema et al., 2015). The de-oiled SAGD produced water is generally characterized by high levels of silica (150-400 mg/L as SiO_2), calcium hardness (5-150 mg/L as $CaCO_3$), magnesium hardness (5-75 mg/L as $CaCO_3$), total dissolved solids (TDS) (1000-2500 mg/L) and total organic carbon (TOC) (150-800 mg/L as C) (Sadrzadeh

et al., 2018; Zhang, K. et al., 2021). The typical conditions of SAGD produced water are slightly basic pH (7-8) and high temperature (80-90 °C) (Sadrzadeh et al., 2015).

In the conventional softening treatment process, the de-oiled water is introduced to the warm lime softening (WLS)/hot lime softening (HLS) treatment unit with addition of hydrated lime ($Ca(OH)_2$), magnesium oxide (MgO), soda ash (Na_2CO_3), coagulant and flocculant under high temperature and high pressure to reduce the pollutant contents (turbidity, silica, hardness) (Heins, 2010). The main challenges for conventional treatment process are the limited reduction of silica and dissolved organics, which have been found to be the predominant causes of fouling in boilers and heat exchangers (Jennings and Shaikh, 2007). Therefore, various technologies, including membrane filtration (Karami et al., 2020), adsorption (Veksha et al., 2016), and coagulation-flocculation (Mohammadtabar et al., 2019), have been developed to enhance the removal of organics and silica in produced water. Among these technologies, coagulation-flocculation, although regarded as a conventional technique, is still considered as a promising and essential technology for separating colloidal impurities from SAGD produced water (Li et al., 2022).

1.1.3 Polymer application

In order to recover water and reduce the amount of tailings stored in ponds, large scale dewatering technologies have been applied (Vedoy and Soares, 2015). Currently, most of dewatering technologies rely heavily on the flocculation capacity of commercial polymer-based flocculants, among which anionic polyacrylamide (A-PAM) with molecular weight averages of several million daltons is one of the most common flocculants (Wang et al., 2016). Given the major particles in tailings ponds are sands, grains, and clay fines, which normally have negative surface charges in a neutral or alkaline solution, it is believed that bridging is the main flocculation

5

mechanism for A-PAM (Lin et al., 2017; Ovenden and Xiao, 2002). As a necessary step of bridging flocculation, adsorption of A-PAM onto the negative particle surface is mainly due to the formation of salt linkage (covalent bonding), in which the presence of a small amount of divalent cations (Ca^{2+} and Mg^{2+}) could promote the adsorption via overcoming the electrical repulsion and linking two negatively charged surfaces (Vedoy and Soares, 2015; Williams, 2008). Besides salt linkage, there are other possible adsorption mechanisms including hydrogen bonding between the hydrogen atoms on the acrylamide groups and oxygen atoms on the surface particles, and electrostatic attraction cause by the spatial inhomogeneity of surface charges on particles, creating attractive regions for an extra opportunity for A-PAM adsorption (Long et al., 2006; Samoshina et al., 2003).

For treating SAGD produced water in WLS process, polymer-based coagulants and flocculants are applied to destabilize the suspended particles to promote their aggregation and settling. Cationic epichlorohydrin-dimethylamine (epi-DMA) and poly-diallyldimethylammonium chloride (Poly-DADMAC) are widely used as coagulants and cationic/anionic polyacrylamide as flocculants (Li et al., 2022; Zeng et al., 2016). As most colloidal impurities in SAGD produced water are negatively charged, electrostatic patch and bridging have been suggested as two main mechanisms of coagulation-flocculation by polymers (Bratby, 2006; Ji et al., 2013). Although previous studies have demonstrated that the performance of polymer-based coagulants and flocculants are impacted by various factors including pH, temperature, dissolved organics, solution salinity, particles concentration and their surface charge (Bratby, 2006; Ji et al., 2013; Zhang, L. et al., 2021), the effect of multiple physiochemical and operational parameters in complex SAGD produced water remains little-known. Therefore, a quantitative understanding of the impact of operations (mixing, dose, temperature) and solution

6

chemistry on the performance of coagulation-flocculation by polymers is of great significance for SAGD produced water treatment processes.

1.1.4 Polymer degradation

With the large application of PAM in tailings treatment, there is a rising concern about the products from PAM degradation and residual acrylamide (AMD), which is the monomer contained in the PAM-based flocculants and has been reported as a neurotoxin to humans (K. Labahn et al., 2010; McCollister et al., 1964). Although commercial PAM typically has a very high molecular weight, it can degrade through various mechanisms such as mechanical, photolytic, chemical, and biodegradation (Guezennec et al., 2015; Xiong et al., 2018a). The following section would present degradation mechanisms investigated for the PAM in oil and gas industry.

1.1.4.1 Mechanical degradation

As one of the most likely degradations in oil and gas industry, mechanical degradation of PAM occurs due to many processes such as stirring, pumping, injecting, and moving via porous media (Brakstad and Rosenkilde, 2016; Guezennec et al., 2015). Mechanical degradation has been reported to be affected by many factors such as the salinity of solution and polymer viscosity (Karami et al., 2018; Mansour et al., 2014). Irreversible changes of PAM have been observed from mechanical degradation, including viscosity reduction, bond scission and formation of free radicals (Avadiar et al., 2013; Mansour et al., 2014; Nguyen and Boger, 1998). However, there are no studies that detected AMD during the mechanical degradation of PAM.

1.1.4.2 Chemical degradation

Although exploring the pathway for chemical degradation is complex due to infinite number of reaction conditions that PAM can be exposed to, the reactivity of the amide group in PAM is the main focus. PAM can undergo hydrolysis under both acidic and basic conditions.

Given that most wastewater produced from oil and gas industry are alkaline solutions, we only focused on the hydrolysis of PAM under basic conditions. As shown in Fig.1.1, the reaction involved in alkaline hydrolysis starting from the nucleophilic addition of hydroxide to the amide carbonyl, followed by the production of acrylic acid residue by eliminating the amide ion ($-NH_2^-$). The amide ion subsequently removes a proton from the acrylic acid residue to produce more stable ammonia and carboxylate anions. In addition, the bottom portion of Fig 1.1 shows the equivalency between the carboxylic anions and the overall ammonia concentration and the concentration of ammonium ion on which the determination of the hydrolysis degree is determined (Caulfield et al., 2002; Ilavsky et al., 1984).
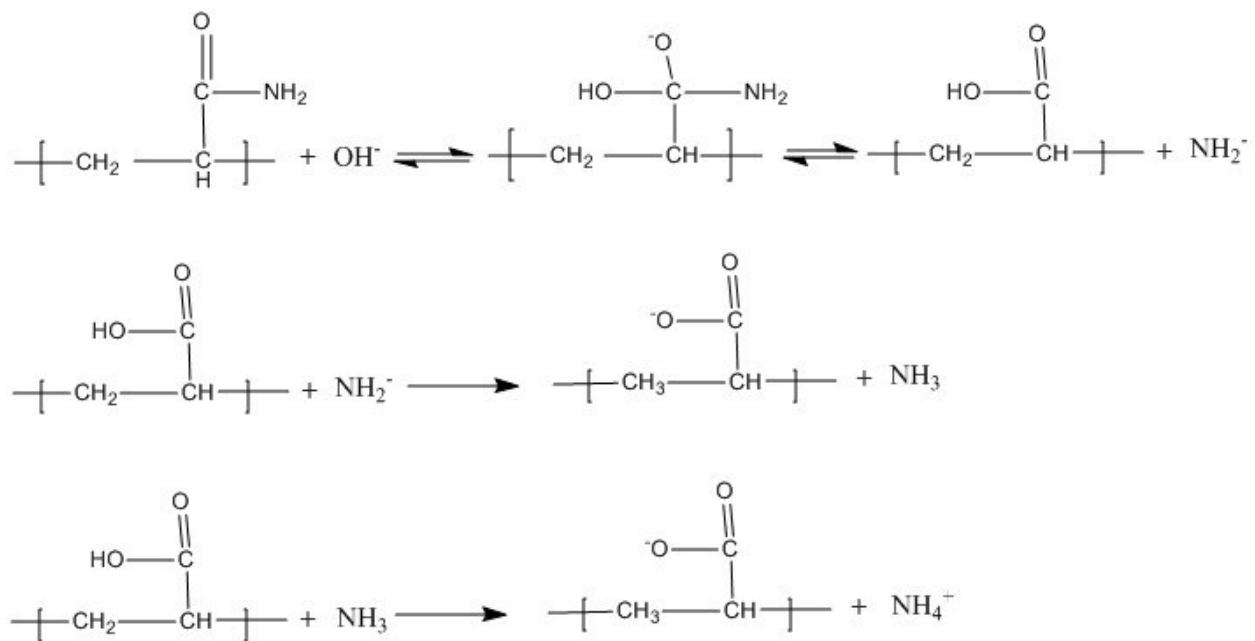
Figure 1.1 Hydrolysis of PAM under alkaline conditions.

In addition to hydrolysis, the chemical degradation through the action of free radicals has also been well studied (Carman and Cawiezel, 2007; Jouenne et al., 2017; Lu et al., 2012; Ramsden and McKay, 1986a; Xiong et al., 2018b). Among different free radicals, hydroxyl radicals are the

most commonly generated from the natural environments. Unlike hydrolysis, free radical induced chain scission has been reported to reduce the molecular weight of PAM without releasing AMD. Generally, as demonstrated in Eq. 1.1-1.4, hydroxyl radicals directly attack the polymer backbone through hydrogen abstraction, generating polymer radicals ($P^{\cdot}$) which can react with dissolved oxygen to form polymer peroxyl radicals ($PO_2^{\cdot}$). After a bimolecular reaction between two polymer peroxyl radicals, chain breakage will occur and polymer fragments ($F_1^{\cdot}$ and F_2) will be formed (Gröllmann and Schnabel, 1982).

$$PH + HO^{\cdot} \rightarrow P^{\cdot} + H_2O \tag{1.1}$$

$$P^{\cdot} + O_2 \rightarrow PO_2^{\cdot} \tag{1.2}$$

$$2PO_2^{\cdot} \rightarrow POOOOP \rightarrow 2PO^{\cdot} + O_2 \tag{1.3}$$

$$PO^{\cdot} \rightarrow F_1^{\cdot} + F_2 \tag{1.4}$$

Numerous studies have highlighted the crucial role of dissolved oxygen and Fe^{2+} in the chemical degradation of PAM under specific environmental conditions like temperature and pH (Jouenne et al., 2017; Ramsden and McKay, 1986b; Seright and Skjevrak, 2015). When the dissolved oxygen is absent, the viscosity of PAM is stable at room temperature, whereas with interactions between oxygen and dissolved Fe^{2+}, hydroxyl radicals can be generated by autoxidation under acidic conditions.

1.1.4.3 Photolytic degradation

Similar to chemical degradation, photolytic degradation is also based on reactions of free radicals generated from light exposure (Caulfield et al., 2002). The irreversible changes of photolytic degradation include bond scission and formation of lower molecular weight of polymer fragments. Different studies have reached different conclusions when it comes to the production

of AMD during photo-degradation of PAM. For example, Woodrow et al. (2008) observed the release of AMD from the acidic/neutral solution of A-PAM and Fe^{3+} exposed to a UV irradiation. However, Holliman et al. (2005) did not detect AMD in the samples of field-conditioned PAM exposed to 365-nm UV radiation in a daily light-black cycle for 5 months. Therefore, further experiments on photolytic degradation of PAM in environmental conditions in the presence of mineral particles are needed.

1.1.4.4 Biological degradation

Since microorganisms can utilize the amide group of PAM as a nitrogen and/or carbon source, biodegradation of PAM can occur in both aerobic and anaerobic conditions (Liu et al., 2012; Wen et al., 2010; Zhao et al., 2016). Given the high molecular weight of PAM, extracellular amidases are necessary for PAM to pass through biological membranes prior to their utilization (Guezennec et al., 2015). Various microorganisms, such as *Enterobacter aerogenes*, *Rhodococcus sp., Helicobacter pylori, Bacillus sp., Acinetobacter sp., Azomonas sp., Pseudomonas sp.,* and *Chlostridium sp.,* have been reported to express PAM-induced amidases (Caulfield et al., 2002; Joshi and Abed, 2017; Ma et al., 2008). It was reported that the aerobic degradation process is relatively faster than the anaerobic degradation process (Zhao et al., 2016). Furthermore, no AMD release has been observed thus far in aerobic culture media, while generated AMD from anaerobic biodegradation of PAM has been documented in studies (Liu et al., 2012; Wang et al., 2018; Zhao et al., 2016). Although a large amount of studies focused on biodegradation of PAM, the reaction pathway under both aerobic and anaerobic conditions for the microbial degradation is still not clearly identified. Hence, it is worthwhile to further investigate the mechanism and impact factors for the biodegradation of PAM in wastewater from oil and gas industry.

1.2 Research scope and Objectives

The overall objective of this research was to investigate the fate of polymer-based coagulants/flocculants in different wastewater from oil and gas industry and to provide fundamental information for their future application on wastewater treatment. To achieve the aim of the project, four sub-objectives were developed and are listed below:

Specific objective 1: Removal of colloidal impurities from synthetic SAGD produced water by using polymeric coagulants/flocculants under high temperature

(1) To assess the effects of operational conditions on the performance of softening-coagulation-flocculation by using poly-DADMAC as coagulant and cationic PAM as flocculant under high temperature (80 °C)

(2) To investigate the interaction effects among operational variables

(3) To optimize the operational conditions

(4) To study the removal mechanisms under different temperatures

Specific objective 2: Long-term fate of dissolved organics in OSPW under various controlled conditions

(1) To evaluate the effect of controlled conditions (temperature, oxygen and ozone pre-treatment) on physicochemical parameters and NAs degradation in OSPW

(2) To investigate the correlation between NAs concentration and other water quality parameters in OSPW

(3) To identify key microorganisms involved in NAs degradation

Specific objective 3: Anionic polyacrylamide (A-PAM) degradation in oil sands tailings under aerobic conditions

(1) To compare the degradation of A-PAM under different temperatures and microbial conditions

(2) To identify the main products of A-PAM degradation

(3) To examine the effects of A-PAM degradation on the chemistry of tailings water

(4) To explore the potential pathway for A-PAM degradation under aerobic conditions

Specific objective 4: Biodegradation of anionic polyacrylamide in oil sands tailings under anaerobic conditions

(1) To investigate the effect of A-PAM dosage on methane production, organic transformation and solid phase during anaerobic degradation

(2) To determine the responsible microbial community for biodegradation of A-PAM

(3) To propose the potential biodegradation mechanisms of A-PAM under anaerobic conditions

1.3 Research significance and hypotheses

Both surface mining and in situ processes for bitumen extraction generate a large amount of wastewater. In order to treat these wastewater, polymer-based coagulants/flocculants are widely applied in different technologies. However, knowledge about the characteristics of wastewater and the stability of polymers during long-term storage, as well as interactions between polymers and impurities in wastewater is still limited. An enhanced understanding of these fundamentals could promote the treatment efficiency of wastewater and eventually be utilized within the framework of meaningful guidance for wastewater management in oil and gas industry. Therefore, in this research, the natural attenuation of OSPW and the fate of polymer-based coagulants/flocculants in

oil sands tailings and SAGD produced water were explored. The following hypotheses were tested in this research:

(1) The effects of temperature on performance of softening-coagulation-flocculation

Hypothesis: Higher temperature will promote the performance of softening-coagulation-flocculation via affecting the removal mechanisms.

(2) The important operational variables for the performance of softening-coagulation-flocculation

Hypothesis: Compared to other operational variables, coagulant dose and softening time with softeners only will be the most important factors.

(3) The effects of temperature on the attenuation of OSPW during long-term storage

Hypothesis: Reduction of NAs concentration, TOC, COD, and toxicity will be faster in aged OSPW stored at 20 °C than in aged OSPW at 4 °C.

(4) Important impact factors for the attenuation of OSPW during long-term storage

Hypothesis: Temperature and oxygen will be crucial factors that affect the characteristics of OSPW during natural attenuation.

(5) The effects of temperature and microbial conditions on degradation of A-PAM in oil sands tailings under aerobic conditions

Hypothesis: Lower molecular weight and concentration of degraded A-PAM will be observed under higher temperatures and augmented microorganisms.

(6) The main products of A-PAM degradation in tailings under aerobic conditions

Hypothesis: AMD will not be released from A-PAM degradation under aerobic conditions, ammonium and polymer fragments with lower molecular weight will be detected.

(7) The effects of A-PAM dosage on the biodegradation of A-PAM under anaerobic conditions

13

Hypothesis: A-PAM with lower dosages would have a faster degradation than A-PAM with higher dosages under anaerobic conditions.

(8) The effects of A-PAM biodegradation on the toxicity of tailings under anaerobic conditions

Hypothesis: No significant impact of A-PAM biodegradation on both acute toxicity and genotoxicity of tailings will be found.

1.4 Thesis organization

This thesis consists of seven chapters that were logically organized according to the research objectives presented above.

Chapter 1 provides a general introduction including the research background, objectives, hypotheses, and research significance. Chapter 1 covers a brief review of bitumen extraction, characteristics of wastewaters, polymer application and degradation.

Chapter 2 is the literature review regarding the use of coagulation-flocculation for removing silica and organics from SAGD produced water. Chapter 2 highlights the literature pertaining to the characteristics of silica and organics, as well as different coagulants and flocculants.

Chapter 3 presents the performance of thermal softening-coagulation-flocculation-sedimentation to remove colloidal impurities from SAGD produced water, focusing on the interaction effects of operational variables and removal mechanisms. First, synthetic SAGD produced water was prepared based on information obtained from industry and jar testers with heaters and temperature controller were applied to conduct the coagulation-flocculation experiments. The interaction effects were studied by applying response surface methodology

(RSM). The removal mechanisms were proposed according to the results of floc characterization and surface measurement.

Chapter 4 describes the fate of dissolved organics in OSPW during 4-year storage under different controlled conditions. Different OSPW samples (raw, ozonated) were stored at different temperatures (4 °C and 20 °C) and oxygen levels (oxic and anoxic). The degradation of NAs was detected by time-of-flight mass spectra (TOFMS). The toxicity of OSPW was evaluated using the *Allivibrio fischeri (A. fischeri)* toxicity screening test. The microbial community in different layers in reactors stored under different conditions were compared to find the microorganisms that are responsible for NAs degradation.

Chapter 5 investigates the degradation of anionic polyacrylamide in oil sands tailings under aerobic environment. The effects of temperature and microorganisms on polymer degradation in both tailings water and pure polymer solution were studied to better understand the degradation performance of polymer. In addition, the impact of polymer degradation on water chemistry of tailings, especially acute toxicity and genotoxicity were also well explored. The mechanism of aerobic biodegradation of polymer were outlined based on the detected products.

Chapter 6 illustrates the results of anaerobic biodegradation of anionic polyacrylamide in oil sands tailings. Different amounts of polymer were added into the oil sands tailings with extra microorganisms collected from the anerobic digester of a municipal wastewater plant to study the effect of initial polymer concentration on biodegradation of the polymer. Methane, intermediates and microbial community were investigated to better understand the degradation performance. The potential metabolic pathways for producing different volatile fatty acids (VFAs) from the intermediates of A-PAM degradation were proposed.

Chapter 7 summarizes the major findings and conclusions of the thesis. Furthermore, recommendations for future work that arise from this thesis are also outlined in this chapter.

1.5 References

Alberta Energy Regulator, 2020. ST98: Alberta Energy Outlook 2020 executive summary. p. 11.

Anderson, J., Wiseman, S.B., Moustafa, A., Gamal El-Din, M., Liber, K., Giesy, J.P., 2012. Effects of exposure to oil sands process-affected water from experimental reclamation ponds on Chironomus dilutus. Water Research 46(6), 1662-1672.

Arslan, M., Gamal El-Din, M., 2021. Bacterial diversity in petroleum coke based biofilters treating oil sands process water. Science of The Total Environment 782, 146742.

Avadiar, L., Leong, Y., Fourie, A., Nugraha, T., 2013. Behaviours of kaolin suspensions with different polyacrylamide (PAM) flocculants under shear, Chemeca 2013: Challenging Tomorrow: Challenging Tomorrow. Engineers Australia Barton, ACT, pp. 249-254.

Bartlett, A.J., Frank, R.A., Gillis, P.L., Parrott, J.L., Marentette, J.R., Brown, L.R., Hooey, T., Vanderveen, R., McInnis, R., Brunswick, P., 2017. Toxicity of naphthenic acids to invertebrates: Extracts from oil sands process-affected water versus commercial mixtures. Environmental pollution 227, 271-279.

Bergerson, J.A., Kofoworola, O., Charpentier, A.D., Sleep, S., MacLean, H.L., 2012. Life cycle greenhouse gas emissions of current oil sands technologies: surface mining and in situ applications. Environmental science & technology 46(14), 7865-7874.

Biryukova, O.V., Fedorak, P.M., Quideau, S.A., 2007. Biodegradation of naphthenic acids by rhizosphere microorganisms. Chemosphere 67(10), 2058-2064.

Blakley, E., 1974. The microbial degradation of cyclohexanecarboxylic acid: a pathway involving aromatization to form p-hydroxybenzoic acid. Canadian Journal of Microbiology 20(10), 1297-1306.

Blakley, E., Papish, B., 1982. The metabolism of cyclohexanecarboxylic acid and 3-cyclohexenecarboxylic acid by Pseudomonas putida. Canadian Journal of Microbiology 28(12), 1324-1329.

Brakstad, K., Rosenkilde, C., 2016. Modelling viscosity and mechanical degradation of polyacrylamide solutions in porous media, SPE Improved Oil Recovery Conference. OnePetro.

Bratby, J., 2006. Coagulation and flocculation in water and wastewater treatment, 430 IWA Publishing. London, UK 431.

Carman, P.S., Cawiezel, K., 2007. Successful breaker optimization for polyacrylamide friction reducers used in slickwater fracturing, SPE hydraulic fracturing technology conference. OnePetro.

Caulfield, M.J., Qiao, G.G., Solomon, D.H., 2002. Some aspects of the properties and degradation of polyacrylamides. Chemical reviews 102(9), 3067-3084.

Fatema, J., Bhattacharjee, S., Pernitsky, D., Maiti, A., 2015. Study of the aggregation behavior of silica and dissolved organic matter in oil sands produced water using Taguchi experimental design. Energy & Fuels 29(11), 7465-7473.

Frank, R.A., Fischer, K., Kavanagh, R., Burnison, B.K., Arsenault, G., Headley, J.V., Peru, K.M., Kraak, G.V.D., Solomon, K.R., 2009a. Effect of carboxylic acid content on the acute toxicity of oil sands naphthenic acids. Environmental science & technology 43(2), 266-271.

Frank, R.A., Kavanagh, R., Burnison, B.K., Arsenault, G., Headley, J.V., Peru, K.M., Van Der Kraak, G., Solomon, K.R., 2008. Toxicity assessment of collected fractions from an extracted naphthenic acid mixture. Chemosphere 72(9), 1309-1314.

Frank, R.A., Roy, J.W., Bickerton, G., Rowland, S.J., Headley, J.V., Scarlett, A.G., West, C.E., Peru, K.M., Parrott, J.L., Conly, F.M., 2014. Profiling oil sands mixtures from industrial developments and natural groundwaters for source identification. Environmental science & technology 48(5), 2660-2670.

Frank, R.A., Sanderson, H., Kavanagh, R., Burnison, B.K., Headley, J.V., Solomon, K.R., 2009b. Use of a (quantitative) structure–activity relationship [(Q) Sar] model to predict the toxicity of naphthenic acids. Journal of Toxicology and Environmental Health, Part A 73(4), 319-329.

Fu, L., Li, C., Lillico, D.M., Phillips, N.A., Gamal El-Din, M., Belosevic, M., Stafford, J.L., 2017. Comparison of the acute immunotoxicity of nonfractionated and fractionated oil sands process-affected water using mammalian macrophages. Environmental science & technology 51(15), 8624-8634.

Gröllmann, U., Schnabel, W., 1982. Free radical-induced oxidative degradation of polyacrylamide in aqueous solution. Polymer degradation and stability 4(3), 203-212.

Guezennec, A.-G., Michel, C., Bru, K., Touze, S., Desroche, N., Mnif, I., Motelica-Heino, M., 2015. Transfer and degradation of polyacrylamide-based flocculants in hydrosystems: a review. Environmental Science and Pollution Research 22(9), 6390-6406.

Han, X., Scott, A.C., Fedorak, P.M., Bataineh, M., Martin, J.W., 2008. Influence of molecular structure on the biodegradability of naphthenic acids. Environmental science & technology 42(4), 1290-1295.

Heins, W., 2010. Is a paradigm shift in produced water treatment technology occurring at SAGD facilities? Journal of Canadian Petroleum Technology 49(01), 10-15.

Holliman, P.J., Clark, J.A., Williamson, J.C., Jones, D.L., 2005. Model and field studies of the degradation of cross-linked polyacrylamide gels used during the revegetation of slate waste. Science of the Total Environment 336(1-3), 13-24.

Holowenko, F.M., MacKinnon, M.D., Fedorak, P.M., 2002. Characterization of naphthenic acids in oil sands wastewaters by gas chromatography-mass spectrometry. Water research 36(11), 2843-2855.

Hughes, S.A., Mahaffey, A., Shore, B., Baker, J., Kilgour, B., Brown, C., Peru, K.M., Headley, J.V., Bailey, H.C., 2017. Using ultrahigh- resolution mass spectrometry and toxicity identification techniques to characterize the toxicity of oil sands process- affected water: The case for classical naphthenic acids. Environmental toxicology and chemistry 36(11), 3148-3157.

Ilavsky, M., Hrouz, J., Stejskal, J., Bouchal, K., 1984. Phase transition in swollen gels. 6. Effect of aging on the extent of hydrolysis of aqueous polyacrylamide solutions and on the collapse of gels. Macromolecules 17(12), 2868-2874.

Jennings, D.W., Shaikh, A., 2007. Heat-exchanger deposition in an inverted steam-assisted gravity drainage operation. Part 1. Inorganic and organic analyses of deposit samples. Energy & fuels 21(1), 176-184.

Ji, Y., Lu, Q., Liu, Q., Zeng, H., 2013. Effect of solution salinity on settling of mineral tailings by polymer flocculants. Colloids and Surfaces A: Physicochemical and Engineering Aspects 430, 29-38.

Johnson, R.J., Smith, B.E., Sutton, P.A., McGenity, T.J., Rowland, S.J., Whitby, C., 2011. Microbial biodegradation of aromatic alkanoic naphthenic acids is affected by the degree of alkyl side chain branching. The ISME journal 5(3), 486-496.

Joshi, S.J., Abed, R.M., 2017. Biodegradation of polyacrylamide and its derivatives. Environmental Processes 4(2), 463-476.

Jouenne, S., Klimenko, A., Levitt, D., 2017. Polymer flooding: Establishing specifications for dissolved oxygen and iron in injection water. SPE Journal 22(02), 438-446.

K. Labahn, S., C. Fisher, J., A. Robleto, E., H. Young, M., P. Moser, D., 2010. Microbially mediated aerobic and anaerobic degradation of acrylamide in a western United States irrigation canal. Journal of environmental quality 39(5), 1563-1569.

Karami, H.R., Rahimi, M., Ovaysi, S., 2018. Degradation of drag reducing polymers in aqueous solutions. Korean Journal of Chemical Engineering 35(1), 34-43.

Karami, P., Khorshidi, B., McGregor, M., Peichel, J.T., Soares, J.B., Sadrzadeh, M., 2020. Thermally stable thin film composite polymeric membranes for water treatment: A review. Journal of Cleaner Production 250, 119447.

Ku, A.Y., Henderson, C.S., Petersen, M.A., Pernitsky, D.J., Sun, A.Q., 2012. Aging of water from steam-assisted gravity drainage (SAGD) operations due to air exposure and effects on ceramic membrane filtration. Industrial & engineering chemistry research 51(21), 7170-7176.

Li, C., Fu, L., Stafford, J., Belosevic, M., Gamal El-Din, M., 2017. The toxicity of oil sands process-affected water (OSPW): A critical review. Science of the Total Environment 601, 1785-1802.

Li, J., How, Z.T., Zeng, H., Gamal El-Din, M., 2022. Treatment Technologies for Organics and Silica Removal in Steam-Assisted Gravity Drainage Produced Water: A Comprehensive Review. Energy & Fuels 36(3), 1205-1231.

Lillico, D.M., Hussain, N.A., Choo-Yin, Y.Y., Qin, R., How, Z.T., Gamal El-Din, M., Stafford, J.L., 2023. Using immune cell-based bioactivity assays to compare the inflammatory activities of oil sands process-affected waters from a pilot scale demonstration pit lake. Journal of Environmental Sciences 128, 55-70.

Lin, Z., Li, P., Hou, D., Kuang, Y., Wang, G., 2017. Aggregation mechanism of particles: Effect of Ca2+ and polyacrylamide on coagulation and flocculation of coal slime water containing illite. Minerals 7(2), 30.

Liu, L., Wang, Z., Lin, K., Cai, W., 2012. Microbial degradation of polyacrylamide by aerobic granules. Environmental technology 33(9), 1049-1054.

Long, J., Li, H., Xu, Z., Masliyah, J., 2006. Role of colloidal interactions in oil sand tailings treatment. AIChE journal 52(1), 371-383.

Lu, M., Wu, X., Wei, X., 2012. Chemical degradation of polyacrylamide by advanced oxidation processes. Environmental technology 33(9), 1021-1028.

Ma, F., Wei, L., Wang, L., Chang, C.-C., 2008. Isolation and identification of the sulphate-reducing bacteria strain H1 and its function for hydrolysed polyacrylamide degradation. International journal of biotechnology 10(1), 55-63.

Mahdavi, H., Prasad, V., Liu, Y., Ulrich, A.C., 2015. In situ biodegradation of naphthenic acids in oil sands tailings pond water using indigenous algae–bacteria consortium. Bioresource technology 187, 97-105.

Manfre Jaimes, D., Gates, I.D., Clarke, M., 2019. Reducing the Energy and Steam Consumption of SAGD Through Cyclic Solvent Co-Injection. Energies 12(20), 3860.

Mansour, A.M., Al-Maamari, R.S., Al-Hashmi, A.S., Zaitoun, A., Al-Sharji, H., 2014. In-situ rheology and mechanical degradation of EOR polyacrylamide solutions under moderate shear rates. Journal of Petroleum Science and Engineering 115, 57-65.

Marentette, J.R., Frank, R.A., Bartlett, A.J., Gillis, P.L., Hewitt, L.M., Peru, K.M., Headley, J.V., Brunswick, P., Shang, D., Parrott, J.L., 2015. Toxicity of naphthenic acid fraction components extracted from fresh and aged oil sands process-affected waters, and commercial naphthenic acid mixtures, to fathead minnow (Pimephales promelas) embryos. Aquatic Toxicology 164, 108-117.

McCollister, D., Oyen, F., Rowe, V., 1964. Toxicology of acrylamide. Toxicology and Applied Pharmacology 6(2), 172-181.

Meshref, M.N., Chelme-Ayala, P., Gamal El-Din, M., 2017. Fate and abundance of classical and heteroatomic naphthenic acid species after advanced oxidation processes: Insights and indicators of transformation and degradation. Water research 125, 62-71.

Miles, S.M., Hofstetter, S., Edwards, T., Dlusskaya, E., Cologgi, D.L., Gänzle, M., Ulrich, A.C., 2019. Tolerance and cytotoxicity of naphthenic acids on microorganisms isolated from oil sands process-affected water. Science of the Total Environment 695, 133749.

Mohammadtabar, F., Pillai, R.G., Khorshidi, B., Hayatbakhsh, A., Sadrzadeh, M., 2019. Efficient treatment of oil sands produced water: Process integration using ion exchange regeneration wastewater as a chemical coagulant. Separation and Purification Technology 221, 166-174.

Nguyen, Q., Boger, D., 1998. Application of rheology to solving tailings disposal problems. International Journal of Mineral Processing 54(3-4), 217-233.

Nimana, B., Canter, C., Kumar, A., 2015. Life cycle assessment of greenhouse gas emissions from Canada's oil sands-derived transportation fuels. Energy 88, 544-554.

NRC, 2022. Water Management in Oil Sands. Natural Resources Canada.

Ovenden, C., Xiao, H., 2002. Flocculation behaviour and mechanisms of cationic inorganic microparticle/polymer systems. Colloids and Surfaces A: Physicochemical and Engineering Aspects 197(1-3), 225-234.

Qin, C., Becerra, M., Shaw, J.M., 2017. Fate of Organic Liquid-Crystal Domains during Steam-Assisted Gravity Drainage/Cyclic Steam Stimulation Production of Heavy Oils and Bitumen. Energy & Fuels 31(5), 4966-4972.

Quagraine, E., Peterson, H., Headley, J., 2005. In situ bioremediation of naphthenic acids contaminated tailing pond waters in the Athabasca oil sands region—demonstrated field studies and plausible options: a review. Journal of Environmental Science and Health 40(3), 685-722.

Quinlan, P.J., Tam, K.C., 2015. Water treatment technologies for the remediation of naphthenic acids in oil sands process-affected water. Chemical Engineering Journal 279, 696-714.

Radpour, S., Gemechu, E., Ahiduzzaman, M., Kumar, A., 2021. Development of a framework for the assessment of the market penetration of novel in situ bitumen extraction technologies. Energy 220, 119666.

Ramsden, D., McKay, K., 1986a. Degradation of polyacrylamide in aqueous solution induced by chemically generated hydroxyl radicals: Part I—Fenton's reagent. Polymer degradation and stability 14(3), 217-229.

Ramsden, D., McKay, K., 1986b. The degradation of polyacrylamide in aqueous solution induced by chemically generated hydroxyl radicals: Part II—Autoxidation of Fe2+. Polymer degradation and stability 15(1), 15-31.

Rho, E., Evans, W., 1975. The aerobic metabolism of cyclohexanecarboxylic acid by Acinetobacter anitratum. Biochemical Journal 148(1), 11-15.

Rui, Z., Wang, X., Zhang, Z., Lu, J., Chen, G., Zhou, X., Patil, S., 2018. A realistic and integrated model for evaluating oil sands development with steam assisted gravity drainage technology in Canada. Applied Energy 213, 76-91.

Sadrzadeh, M., Hajinasiri, J., Bhattacharjee, S., Pernitsky, D., 2015. Nanofiltration of oil sands boiler feed water: Effect of pH on water flux and organic and dissolved solid rejection. Separation and Purification Technology 141, 339-353.

Sadrzadeh, M., Pernitsky, D., McGregor, M., 2018. Nanofiltration for the treatment of oil sands-produced water. InTech Rijeka.

Samoshina, Y., Diaz, A., Becker, Y., Nylander, T., Lindman, B., 2003. Adsorption of cationic, anionic and hydrophobically modified polyacrylamides on silica surfaces. Colloids and Surfaces A: Physicochemical and Engineering Aspects 231(1-3), 195-205.

Sapkota, K., Oni, A.O., Kumar, A., Linwei, M., 2018. The development of a techno-economic model for the extraction, transportation, upgrading, and shipping of Canadian oil sands products to the Asia-Pacific region. Applied Energy 223, 273-292.

Seright, R., Skjevrak, I., 2015. Effect of dissolved iron and oxygen on stability of hydrolyzed polyacrylamide polymers. SPE journal 20(03), 433-441.

Toor, N.S., Franz, E.D., Fedorak, P.M., MacKinnon, M.D., Liber, K., 2013. Degradation and aquatic toxicity of naphthenic acids in oil sands process-affected waters using simulated wetlands. Chemosphere 90(2), 449-458.

Vedoy, D.R., Soares, J.B., 2015. Water- soluble polymers for oil sands tailing treatment: A Review. The Canadian Journal of Chemical Engineering 93(5), 888-904.

Veksha, A., Bhuiyan, T.I., Hill, J.M., 2016. Activation of aspen wood with carbon dioxide and phosphoric acid for removal of total organic carbon from oil sands produced water: Increasing the yield with bio-oil recycling. Materials 9(1), 20.

Wang, C., Han, C., Lin, Z., Masliyah, J., Liu, Q., Xu, Z., 2016. Role of preconditioning cationic zetag flocculant in enhancing mature fine tailings flocculation. Energy & Fuels 30(7), 5223-5231.

Wang, D., Liu, X., Zeng, G., Zhao, J., Liu, Y., Wang, Q., Chen, F., Li, X., Yang, Q., 2018. Understanding the impact of cationic polyacrylamide on anaerobic digestion of waste activated sludge. Water research 130, 281-290.

Wen, Q., Chen, Z., Zhao, Y., Zhang, H., Feng, Y., 2010. Biodegradation of polyacrylamide by bacteria isolated from activated sludge and oil-contaminated soil. Journal of Hazardous Materials 175(1-3), 955-959.

Williams, P.A., 2008. Handbook of industrial water soluble polymers. John Wiley & Sons.

Wiseman, S., Anderson, J., Liber, K., Giesy, J., 2013. Endocrine disruption and oxidative stress in larvae of Chironomus dilutus following short-term exposure to fresh or aged oil sands process-affected water. Aquatic Toxicology 142, 414-421.

Woodrow, J.E., Seiber, J.N., Miller, G.C., 2008. Acrylamide release resulting from sunlight irradiation of aqueous polyacrylamide/iron mixtures. Journal of Agricultural and Food Chemistry 56(8), 2773-2779.

Xiong, B., Loss, R.D., Shields, D., Pawlik, T., Hochreiter, R., Zydney, A.L., Kumar, M., 2018a. Polyacrylamide degradation and its implications in environmental systems. NPJ Clean Water 1(1), 1-9.

Xiong, B., Miller, Z., Roman-White, S., Tasker, T., Farina, B., Piechowicz, B., Burgos, W.D., Joshi, P., Zhu, L., Gorski, C.A., 2018b. Chemical degradation of polyacrylamide during hydraulic fracturing. Environmental science & technology 52(1), 327-336.

Xue, J., Huang, C., Zhang, Y., Liu, Y., Gamal El-Din, M., 2018. Bioreactors for oil sands process-affected water (OSPW) treatment: A critical review. Science of the Total Environment 627, 916-933.

Zeng, T., Li, R.J., Mitch, W.A., 2016. Structural modifications to quaternary ammonium polymer coagulants to inhibit N-nitrosamine formation. Environmental Science & Technology 50(9), 4778-4787.

Zhang, K., Pernitsky, D., Jafari, M., Lu, Q., 2021. Effect of MgO slaking on silica removal during warm lime softening of SAGD produced water. Industrial & Engineering Chemistry Research 60(4), 1839-1849.

Zhang, L., Mishra, D., Zhang, K., Perdicakis, B., Pernitsky, D., Lu, Q., 2021. Impact of influent deviations on polymer coagulant dose in warm lime softening of synthetic SAGD produced water. Water Research 200, 117202.

Zhao, L., Bao, M., Yan, M., Lu, J., 2016. Kinetics and thermodynamics of biodegradation of hydrolyzed polyacrylamide under anaerobic and aerobic conditions. Bioresource Technology 216, 95-104.

CHAPTER 2 LITERATURE REVIEW ON COAGULATION-FLOCCULATION FOR ORGANICS AND SILICA REMOVAL IN STEAM ASSISTED GRAVITY DRAINAGE PRODUCED WATER[1]

2.1 Introduction

In the SAGD process, 0.2 barrels of fresh water were needed for every barrel of bitumen production in 2019 (COSIA). More than 90% of the produced water is recycled after treatment, while the remaining 10% is made up of fresh water (Guha Thakurta et al., 2013; Kawaguchi et al., 2012; Lightbown, 2015; Maiti et al., 2012). SAGD produced water requires treatment prior to being recycled as boiler feed water (BFW) for steam generation (Fatema et al., 2015; Jennings and Shaikh, 2007). In the conventional softening treatment process (Figure 2.1), once-through steam generators (OTSGs) are applied to produce steam. In order to meet the feed water requirement of OTSGs (SiO_2 < 50-75 mg/L, total hardness < 0.5 mg/L as $CaCO_3$, oil and grease < 0.5-1 mg/L) (Fatema et al., 2015), the de-oiled water (DOW) will be mixed with make-up water (fresh and/or brackish) and recycled boiler blow-down (BBD) water, and then treated by warm lime softening (WLS)/hot lime softening (HLS) process or alternatively, evaporators in some facilities. Subsequently, filtration and weak-acid cation (WAC) exchange resin are applied to remove suspended solids and residual divalent ions, such as calcium (Ca^{2+}) and magnesium (Mg^{2+}), to produce boiler feedwater (BFW) suitable for steam generation (Ku et al., 2012; Sadrzadeh et al., 2015). Although OTSGs can tolerate a high amount of TDS (8000-12000 mg/L) and TOC (300-1000 mg/L), the steam quality of OTSGs is low (typically 75-85%) compared to drum boilers

---

[1] This chapter is based on the published paper: Li J, How ZT, Zeng H, Gamal El-Din M. Treatment Technologies for Organics and Silica Removal in Steam-Assisted Gravity Drainage Produced Water: A Comprehensive Review. Energy & Fuels. 2022; 36(3):1205-31.

(100%), resulting in the BBD water flow being ~15-25% of the BFW rate (Sadrzadeh et al., 2018). A portion of BBD water is recycled back to the WLS process, while the rest is discarded (Hayatbakhsh et al., 2016).

Due to the limited removal of silica and organics by conventional processes (Sadrzadeh et al., 2018) and the increasing stricter policy on reduction of freshwater usage (Alberta Energy Regulator, 2019), there are increasing interests in enhancing the removal of organics and silica in produced water. This literature review summarizes the chemistry of SAGD produced water, focusing on the organics matter and silica, and evaluates different coagulants and flocculants for removing the silica and organics from produced water.
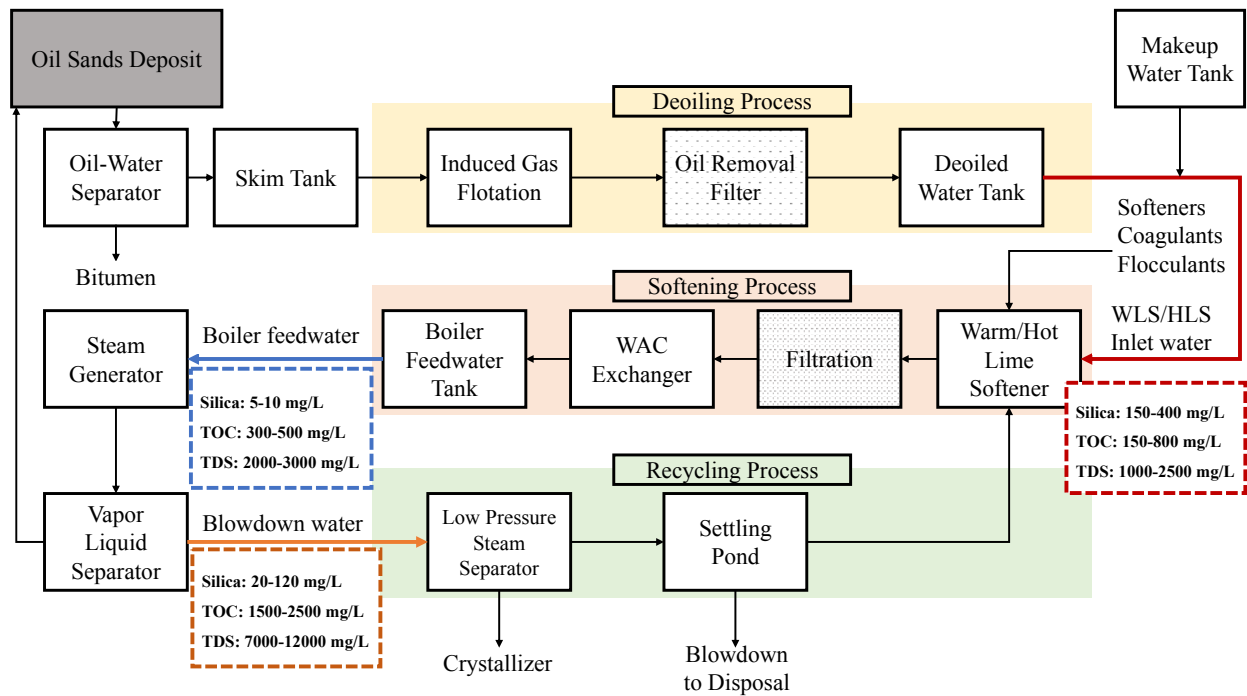
Figure 2.1 Flow diagram of conventional SAGD produced water treatment process (Kawaguchi et al., 2012).

2.2 Silica and organics in SAGD produced water

Due to the complex chemistry of silica and dissolved organics in SAGD produced water, the following section discusses the basic properties of silica in water and the interaction between silica and softener magnesium oxide; while the organic section describes the reason for high dissolved organic content in produced water and also compares different types of organics in different SAGD produced waters.

2.2.1 Silica

Silica and silicates are generic names for the family of silicon dioxide-related compounds which are derived from the dehydration-polymerization of monosilicic acid ($Si(OH)_4$) (Ning, 2005). They are commonly categorized as reactive soluble, non-reactive soluble (colloidal) and non-reactive insoluble (particulate) in waters (Ning, 2003). The initial soluble form of silica, monosilicic acid, is generally deionized at acidic and neutral pH levels, but at pH 10, 50% of the monosilicic acid is ionized (Bouguerra et al., 2007; Sheikholeslami and Tan, 1999). With the increase in concentration of the monosilicic acid ($> 2 \times 10^{-3}$ mol/L) under room temperature (25 °C), polysilicic acids of small molecules as dimers, trimers, or oligomers are formed via polymerization and then colloidal silica, a more highly polymerized species with particles larger than 50 Å down to 10-20 Å, will be formed (Bouguerra et al., 2007; Sheikholeslami and Tan, 1999). The colloidal silica includes the colloidal particles formed by the combination with organic and inorganic species (Sheikholeslami and Tan, 1999). Due to the varied surface properties and the host of ubiquitous organic and inorganic colloidal particles, the interactions among colloidal silica are complicated and difficult to characterize and predict (Ning, 2003). Conversely, particulate silica is larger than colloidal silica (Latour et al., 2014). The rate of silicic acid polymerization is strongly affected by pH and polymerization reaction concentration. For example, the polymerization rate is fast when

the solution is neutral or slightly alkaline (6 < pH < 9) and will continue to increase until the monomeric silica concentration falls to the solubility of amorphous silica. However, when pH drops to 2-3, the polymerization rate decreases (Chan, 1989; Ning, 2003).

Under high pH (9.5-10.5) and high temperature (80-90 °C) conditions, it is reported that silica mostly exists as dissolved silicate and is negatively charged in SAGD produced water (Maiti et al., 2012; Sadrzadeh et al., 2015; Zhang et al., 2021). As mentioned earlier, silica can deposit on the surface of equipment as solid fouling layers (Maiti et al., 2012). It is well known that the silica fouling can be exacerbated via forming silicates with the presence of di- and trivalent cations such as calcium, aluminum, iron, and magnesium (Graham et al., 1989). Therefore, softeners and downstream ion exchange units are used to remove these metal ions so that the formation of silicate scale can be minimized and MgO is added for the removal of silica in the WLS and HLS processes (Alambets, 2014; Sahachaiyunta et al., 2002). Although dissolved organic matter (DOM) can also react with silica, based on studies of interaction of DOM with silica and silicates in SAGD produced water, it could not be concluded definitely that the formed scales are mainly due to the precipitation of DOM-Si complexes (Fatema et al., 2015; Maiti et al., 2012).

In the WLS/HLS process, MgO addition is to interact with silica and precipitate silica compounds from the SAGD produced water. However, the silica removal mechanism has not been fully established (Perdicakis et al., 2019). For silica removal using magnesium compounds during softening in SAGD produced water, two possible competing mechanisms of silica removal were proposed: adsorption onto freshly precipitated $Mg(OH)_2$ or precipitation by forming magnesium silicate precipitates (Parks and Edwards, 2007; Zhang et al., 2021). Different reaction conditions may make one mechanism dominate over the other. As shown in Table 2.1, pH, the type of magnesium compounds and initial molar ratio of Mg:Si were the most significant factors affecting

the silica removal mechanism by magnesium compounds compared to other parameters such as contact time, temperature, and initial silica concentration.

Table 2.1 Dominant mechanism of silica removal by magnesium compounds under different conditions.

| Magnesium compounds | Conditions | | | | | Dominant mechanism | Reference |
	Initial molar ratio Mg:Si	pH	Initial silica concentration (mg/L)	Temperature (°C)	Contact time (min)		
MgCl$_2$	~1	11.2-11.3	250	85	60	Magnesium silicate precipitation	(Zhang et al., 2021)
MgOH$_2$	1.4	11.2-11.3	250	85	60	Adsorption	(Zhang et al., 2021)
Non-slaked MgO	2	11.2-11.3	250	85	60	Magnesium silicate precipitation	(Zhang et al., 2021)
Slaked MgO	2	11.2-11.3	250	85	60	Adsorption	(Zhang et al., 2021)
MgO	1-1.5	8.2-9.5	260	25-50	1440	Magnesium silicate precipitation	(Latour et al., 2015)

MgOH$_2$	> 22	>9	21	25	20	Adsorption	(Chen et al., 2006)
MgCl$_2$	< 6	10.8	12	-	50	Magnesium silicate precipitation	(Parks and Edwards, 2007)

2.2.1 Organics

Similar to other produced waters in the oil and gas industry, such as oil sands process waters (OSPW) from surface mining, SAGD produced water collected in the oil sands region already contains high levels of DOM due to the unique composition of the geological formation (Hurwitz et al., 2015; Maiti et al., 2012; Pillai et al., 2017). During the separation of oil and water, chemicals like diluents and subsequent pH increase during softening in conventional treatment may lead to the solubilization of a broader range of organic matter into the SAGD produced water (Guha Thakurta et al., 2013). Moreover, the limited ability of conventional treatment to remove DOM can result in higher concentrations of dissolved organic carbon (DOC) in the BBD water (typically >2000 mg/L as carbon) (Guha Thakurta et al., 2013; Pillai et al., 2017). Increased water-soluble organics (WSO) and TDS concentrations in BBD water occur using conventional treatment processes, without any treatment of the BBD water, and as more BBD water is recycled. Although extensive literature is available on the chemical characteristics of OSPW (Gamal El-Din et al., 2011; Huang et al., 2015; Li et al., 2017; McQueen et al., 2017; Pourrezaei et al., 2014), knowledge of the nature and effects of DOM in SAGD applications is not well-understood (Guha Thakurta et al., 2013; Kawaguchi et al., 2012). Additionally, the nature of DOM in SAGD produced water may be different from the OSPW DOM due to different oil-sands characteristics and extraction process

(Guha Thakurta et al., 2013). For instance, SAGD process employs higher temperatures (200-250 °C) and pressures (ca. 3.5 MPa) than the surface mining process, which requires moderate temperature (70-90 °C) and atmospheric pressure (Guha Thakurta et al., 2013). The addition of diluent in SAGD emulsion (oil-water mixture) may also contribute to the difference (Guha Thakurta et al., 2013).

By using resin fractionation, the DOM in SAGD produced water can be separated into six hydrophobic and hydrophilic fractions: hydrophobic acid (HPoA), hydrophobic base (HPoB), hydrophobic neutral (HPoN), hydrophilic acid (HPiA), hydrophilic base (HPiB), and hydrophilic neutral (HPiN) (Edzwald and Association, 2011). Guha Thakurta et al. (2013) tested three different resins, including DAX-8, strongly acidic cation exchanger resin, and highly porous weak base anion resin, for the fractionation of DOM in BBD water. Based on the percentage contribution of TOC in Figure 2.2, HPoA and HPiN are the dominant dissolved organic fractions in the BBD water, constituting 39% and 28%, respectively, while the other four fractions constitute the remaining 33%. The percent aromaticity of DOM has been shown to have strong correlation to specific UV absorbance (SUV$_{254}$) values. As shown in Figure 2.3, BBD water and its HPoA and HPoN fractions had higher SUV$_{254}$ values (4.3, 5.0 and 4.0 L mg^{-1} m^{-1}, respectively), which indicated that BBD water and its hydrophobic acid and neutral fractions were rich in aromatic content.
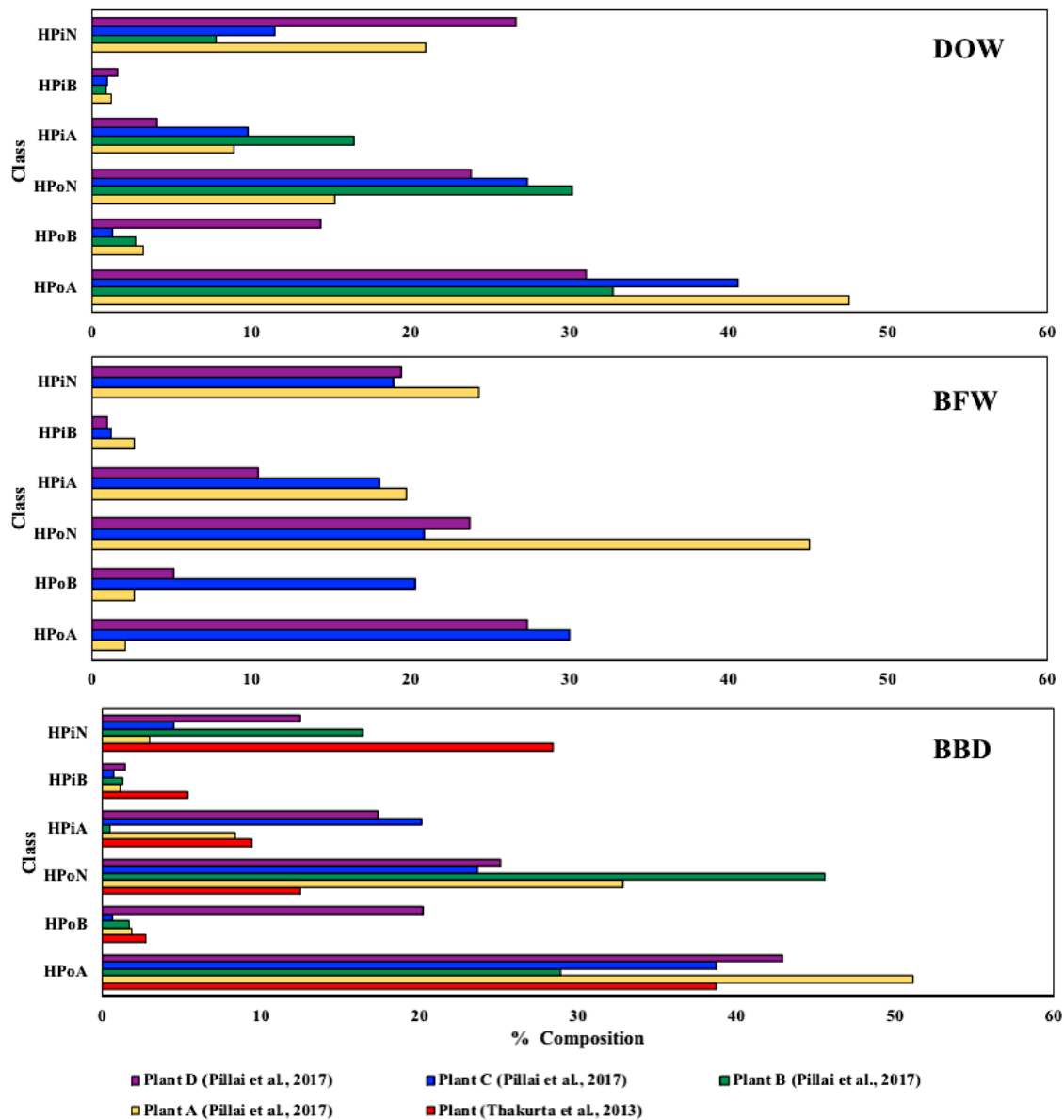
Figure 2.2 Distribution of DOM fractions in DOW, BFW, and BBD water samples from different SAGD plants.
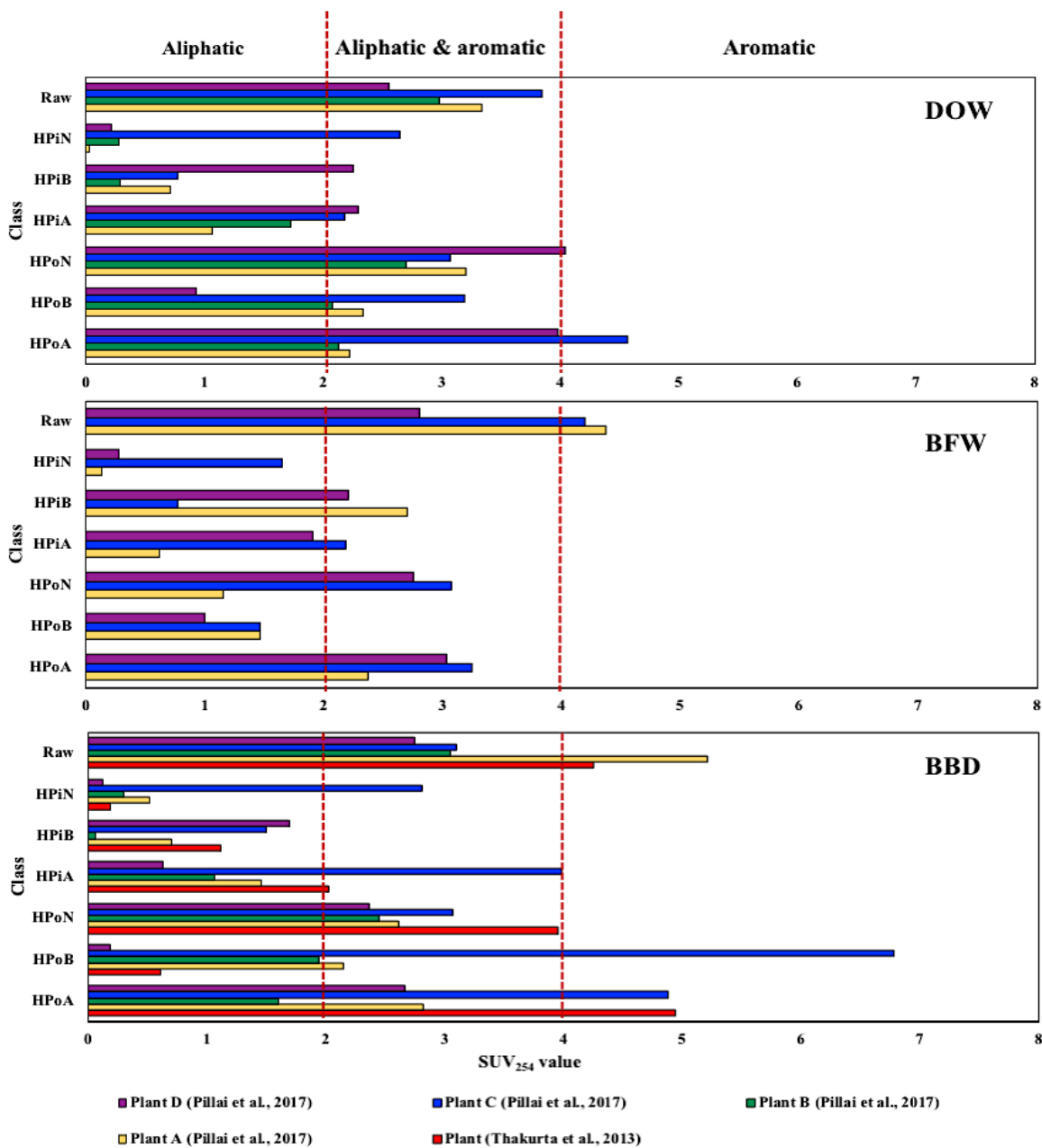
Figure 2.3 SUVA$_{254}$ values of raw DOW, BFW, and BBD water samples and their fractions from different SAGD plants (SUV$_{254}$ >4: predominantly aromatic compounds; SUV$_{254}$ 2-4: mixture of aromatic and aliphatic organic matter; SUV$_{254}$ <2: predominantly aliphatic compounds).

In addition, fluorescence excitation-emission matrix (FEEM) spectroscopy was also used to characterize the fractions (hydrophobic and hydrophilic) of SAGD produced water. The fluorescence peak intensities of fluorophores of DOM in different SAGD produced water and of different fractions isolated from BBD water are compared in Table 2.2. Although the range of peaks varied between WLS and BBD in different studies, dominant peaks of tryptophan-like, fulvic-like and humic-like signatures can be found in both WLS and BBD water, suggesting that majority of organic components contain humic-like, fulvic-like and tryptophan-like structural features (Fatema et al., 2015; Guha Thakurta et al., 2013; Hayatbakhsh et al., 2016; Pillai et al., 2017). In terms of DOM fractions isolated from BBD water via the resin-based method, both Guha Thakurta et al. (2013) and Pillai et al. (2017) revealed the presence of humic- and fulvic-like structural elements in HPoA and HPiA, and of tryptophan-like structures in HPoB. However, the observation of HPoN and HPiN fractions in these two studies were inconsistent. Signatures of tyrosine-like and tryptophan-like molecules were found in HPoN by Guha Thakurta et al. (2013) while fulvic- and humic-like structures were mainly distributed in HPoN in the study of Pillai et al. (2017). The reasons for these differences are still unknown but the assumption could be related to the variability of produced water from different plant operations and the source bitumen.

Table 2.2 Summary of FEEM peaks of WLS, BBD water and its fractions from the research literature.

Water Type	Fraction	Peaks location (Ex/Em wavelength nm)	Chem nature	Reference
WLS	-	220-350/350-450	Tryptophan-like; fulvic-like; humic-like	(Hayatbakhsh et al., 2016)
BBD	-	205-250/375-450 and 300-340/375-480	Tryptophan-like, fulvic-like, humic-like	(Fatema et al., 2015)

BBD	-	250/375-425 and 300-340/375-480	Tryptophan-like, fulvic-like, humic-like	(Guha Thakurta et al., 2013)
BBD	HPoA	310-340/400-500	Humic-like	(Guha Thakurta et al., 2013)
BBD	HPoA	300-350/380-460	Humic-like	(Pillai et al., 2017)
BBD	HPoN	225-250/325-380	Tyrosine-like, tryptophan-like	(Guha Thakurta et al., 2013)
BBD	HPoN	225-275/325-460	Fulvic-like, humic-like	(Guha Thakurta et al., 2013)
BBD	HPoB	260-290/280-320	Tryptophan-like	(Guha Thakurta et al., 2013)
BBD	HPoB	225-250/375-425	Tryptophan-like	(Guha Thakurta et al., 2013)
BBD	HPiA	320-375/375-500	Humic-like	(Guha Thakurta et al., 2013)
BBD	HPiA	300-350/380-460	Humic-like	(Guha Thakurta et al., 2013)
BBD	HPiN	210-225 and 250-275/280-320	Tyrosine-like	(Guha Thakurta et al., 2013)
BBD	HPiB	210-225/275-310 and 210-225/325-400	Tyrosine-like, tryptophan-like	(Guha Thakurta et al., 2013)

Advanced analytical techniques such as GC-MS, FT-ICR-MS and TOF-MS were applied to better define the families of dissolved organic species in SAGD produced water. Kawaguchi et al. (2012) analyzed the DOM in different SAGD produced water by GC-MS and their results demonstrated that organic acids and volatile organic compounds (VOCs) were the predominate organics in the produced water, WLS feed water, and BFW, whereas only organic acids were most abundant in the BBD water because most of the VOCs were significantly removed through steam generation. Pereira et al. (2013) found over 3000 elemental compositions corresponding to a range of heteroatom-containing homologue classes in BBD water by applying HPLC-Orbitrap-MS. As shown in Figure 2.4, classes of O_x and SO_x were more abundant than NO_x and S_2O_x species in

BBD water. Similar results of heteroatom class analysis were also found by Pillai et al. (2017). Besides, by comparing different SAGD produced waters, naphthenic acids (NAs) and larger carboxylic acids were found in all water samples and the relative amounts of acidic compounds increased from BFW to BBD. Among organic acids in SAGD produced water, organic acids with 2−3 oxygen atoms represented the majority of the species.
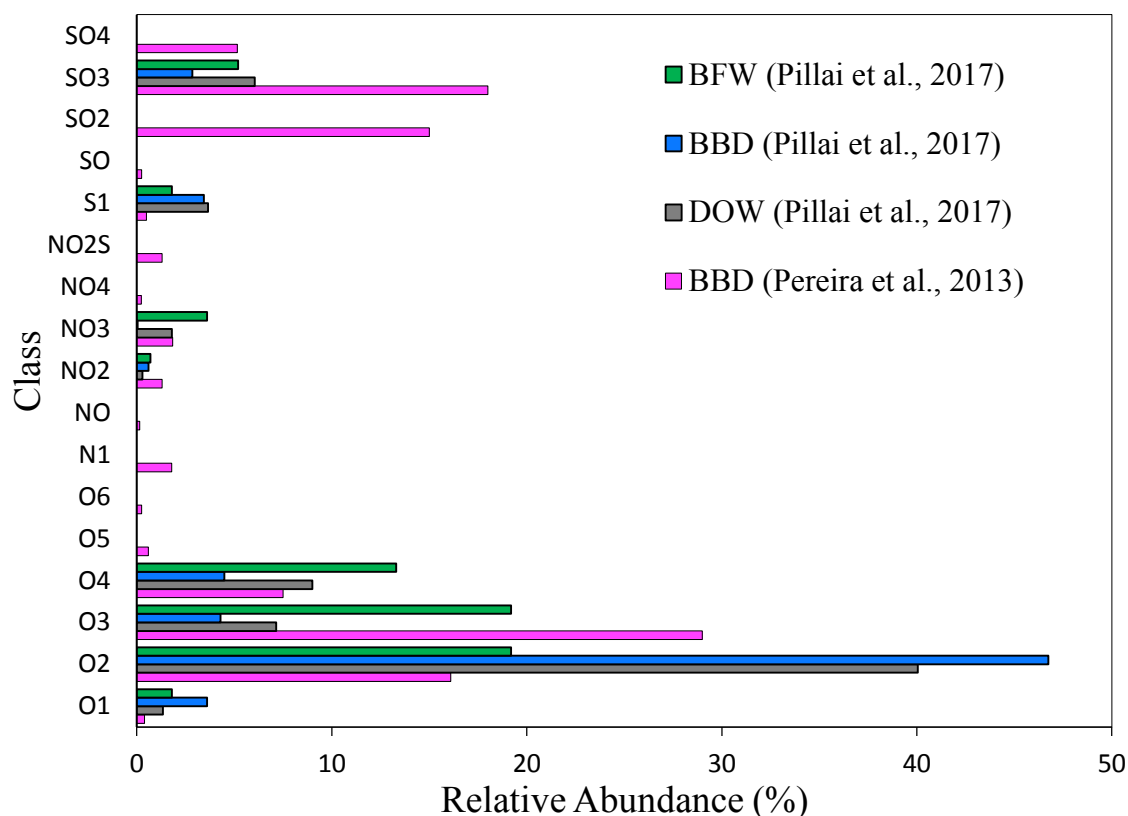
Figure 2.4 Heteroatom class analysis for de-oiled water DOW, Boiler feed water BFW and blowdown water BBD acquired by ESI (-) HPLC-Orbitrap-MS or FT-ICR-MS.

2.3 Coagulation-flocculation for removal organics and silica

Various technologies, such as membrane technologies and adsorption, have been developed to treat SAGD produced water (Atallah et al., 2019; Kimetu et al., 2016). Coagulation-flocculation, although regarded as a conventional technique, is still one of the most widely applied

technologies to remove suspended and dissolved particles, colloids and organic matter in various wastewater owing to its low energy consumption, easy operation, and relatively simple design (Renault et al., 2009; Wu et al., 2019). Coagulation is the process to destabilize colloidal particles by adding coagulants and mixing rapidly to promote agglomeration, while flocculation is the process to enhance agglomeration by slow stirring to form larger flocs that can settle down quickly and are subsequently removed (Prakash et al., 2014). Coagulation and flocculation aim to destabilize the colloidal particles by diminishing the repulsive force and zeta potential between the colloidal particles (Hogg, 2005; Metcalf, 2003; Reynolds and Richards, 1995). Charge neutralization, interparticle bridging, electrostatic patch and sweep/enmeshment coagulation are the main mechanisms for destabilization. The characteristics of each destabilizing mechanism are illustrated in Figure 2.5. These mechanisms are determined by water characteristics, type and doses of coagulant/flocculant, and also treatment conditions such as design of mixing devices (Parsons and Jefferson, 2006).
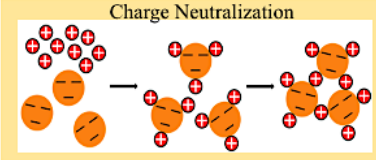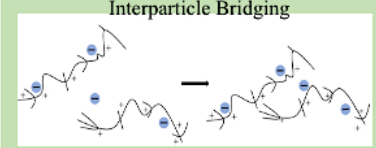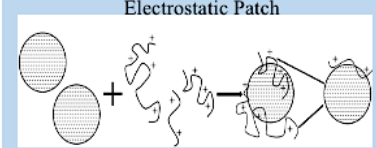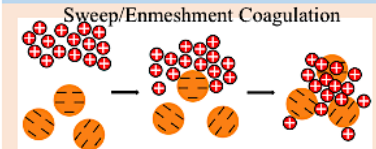
	Condition	Type of coagulant/flocculant
Charge Neutralization	Low pH Low to intermediate concentration of coagulants/flocculants	Metal salts
Interparticle Bridging	Optimum dosage of polymer	Polyelectrolytes
Electrostatic Patch	Highly charged polyelectrolytes Low density of opposite charged sites surface	Polyelectrolytes
Sweep/Enmeshment Coagulation	High coagulant dose High pH	Metal salts

Figure 2.5 Characteristics of destabilizing mechanism for coagulation/flocculation (Sharma et al., 2006; Wills and Finch, 2015).

Since coagulation/flocculation is a well-established method to destabilize and aggregate colloids, the emerging interests are in regard to exploring promising coagulants and flocculants for various wastewater treatment (Mohd-Salleh et al., 2019; Sillanpaa et al., 2018; Zeng, et al., 2007b). Generally, coagulants can be classified into inorganics (metal salts) and organics (mainly polymers), while flocculants are polymers that can be classified as synthetic, natural and grafted. In order to make the discussion below easier, coagulants and flocculants together are classified into two categories: chemical and natural. In SAGD produced water treatment, the performance of different coagulants and flocculants are summarized in Table 2.3.

Table 2.3 Summary of coagulants and flocculants applied in SAGD produced water treatment.

Coagulant	Flocculant	Water type	Temperature (°C)	Feed pH	Optimal removal	Mechanism	Reference
$Al(NO_3)_3$	-	Produced water	80	12	33% of TOC (pH: 3.7)	Surface neutralization; localized enmeshment coagulation	(Al-As'ad and Husein, 2014)
$FeCl_3$	-	Produced water	80	12	73% of TOC (pH:1.6) >80%of silica (pH:7.9)	Surface neutralization; localized enmeshment coagulation	(Al-As'ad and Husein, 2014)
$Ca(NO_3)_2$	-	Produced water	80	12	18% of TOC (pH:9.1)	Surface neutralization	(Al-As'ad and Husein, 2014)

IERW	-	BBD	40, 80	11	81.8% of TOC 98.6% of silica	Surface neutralization	(Mohammadtabar et al., 2019)
PAC	-	BBD	85	12	40% of DOC	Surface neutralization; precipitation of organics in acidification	(Hurwitz et al., 2015)
Alum	-	BBD	85	12	15% of DOC	Surface neutralization; precipitation of organics in acidification	(Hurwitz et al., 2015)
Epi/DMA or poly-DADMAC	Anionic PAM	Produced water	95	4	73% of silica 50% of COD 40% of TOC 99% of O & G	-	(Polizzotti and Khwaja, 2011)
Tannins or chitosan	Cationic and anionic PAM	Produced water	20-100	4	75% of silica 54% of COD 42% of TOC 98% of O & G	-	(Polizzotti and Khwaja, 2011)

2.3.1 Chemical coagulants and flocculants

Multivalent metal salts such as aluminum (aluminum sulfate, aluminum chloride and sodium aluminate), ferric salts (ferric sulfate, ferrous sulfate and ferric chloride), and magnesium chloride are the most commonly used coagulants (Joo et al., 2007). Among them, Al- and Fe-based coagulants are the most popular mainly due to low cost, high availability, as well as high efficiency to remove turbidity and color (Bratby, 2016). As shown in Table 2.3, Al-As'ad and Husein (2014) compared aluminum, calcium and ferric salts as coagulants for treating SAGD produced water under high temperature (80 °C). At higher doses (5-30 g/g organic), the removal of TOC by ferric (73%) and aluminum salts (33%) were higher than calcium salts (18%) due to much higher solubility of $Ca(OH)_2$ than that of $Fe(OH)_3$ and $Al(OH)_3$. Compared to aluminum salts, ferric salt was much more effective because the complexes formed by Fe^{3+} and/or its hydrolysis products with organics are more stable and less soluble. Ferric salt also performed effectively to remove silica (>80%) from SAGD produced water when the pH was around 8. This can be explained by the fact that the bulk precipitation of $Fe(OH)_3$ occurs at pH values of 6-9; $Fe(OH)_3$ precipitate would adsorb hydrolysis soluble silica species with negative charge and be forced to precipitate (Leong, 2005; Mesmer and Baes, 1990). Magnesium has been also proven to be an effective coagulant for removing silica and other contaminants from wastewater at high pH (Latour et al., 2015; Shamaei et al., 2018; Vandamme et al., 2012; Zeng, et al., 2007a). Mohammadtabar et al. (2019) analyzed the use of ion exchange regeneration wastewater (IERW), which contains high concentrations of calcium and magnesium, as a coagulant to treat SAGD produced water. The authors found out that the efficiency of removing of silica and TOC by IERW can achieve 98.7% and 81.3%, respectively. In addition, the study also demonstrated that larger precipitated flocs and

enhanced coagulation process can be achieved by using mixing and increasing the temperature and dosage of the IERW.

Inorganic polymers such as poly(aluminum chloride) (PAC) are commonly used as synthetic inorganic coagulants in conventional wastewater treatments (Cao et al., 2011; Gao et al., 2003). The main mechanisms for these inorganic polymers to remove organics are adsorption, entrapment, complexation, and charge neutralization to a lesser extent (Cheng and Chi, 2002). Compared to the aluminum and ferric salts, the inorganic polymeric coagulants showed better removal efficiency of organics at high pH (Cheng et al., 2008). For example, Hurwitz et al. (2015) evaluated PAC and alum as coagulants to remove DOC from BBD at an elevated temperature of 85 °C. Based on the results from jar tests, there was an observable improvement in organic removal by PAC (40%) over generic alum (15%), especially at higher pH (12) (Table 2.3). The superior performance of PAC as compared to alum may have been due to the fact that when the pH was high, PAC had higher positively charged Al-species and higher positive charge density on Al-precipitate surfaces than alum (Pernitsky and Edzwald, 2006).

Organic polymers are the sole class of coagulants or flocculants used in the SAGD industries because they have effective function at wider pH and water temperature ranges. The nature of charges followed by molecular weight and charge density are important factors for their coagulation or flocculation performance (Lee et al., 2014). When used as coagulants, the advantages of organic polymers over inorganic metal salts are significant, including the need for less coagulant dosage, less sensitive to pH, less sludge volume, and less metallic compound residuals (Gao et al., 2008). The removal efficiency from organic polymeric coagulants is generally higher than that of inorganic polymers. Epichlorohydrin-dimethylamine (epi-DMA) and poly-diallyldimethylammonium chloride (poly-DADMAC) are common cationic polymers used

44

as coagulants. When used as flocculants, organic polymers are preferred because they are convenient to use, easily to dissolve in an aqueous system, independent of pH, efficient at lower doses, and capable of producing larger and stronger flocs (Lee et al., 2014). Common organic flocculants are polyacrylamide (PAM) and polyamine. In SAGD produced water treatment, cationic polymeric coagulant coupled with PAM flocculant have been applied. Polizzotti et al. (2011) have patented a treatment process that employs cationic epi-DMA and poly-DADMAC as coagulants and polyacrylamide (cationic and anionic) as flocculants to reduce chemical oxygen demand (COD), TOC, oil and grease, and silica from SAGD produced water at 95 °C. Promising results of high removal efficiency of COD (50%), TOC (40%), silica (73%) and oil & grease (99%) were observed by using cationic epi-DMA as coagulant with anionic PAM as flocculant (Table 2.3). However, it is worth noting that the pH was adjusted from 7.5 to 4 before adding coagulants in this patent. These promising results need to be further investigated to compare the impact of coagulation-flocculation and pH reduction.

Composite coagulants are designed to gain advantages from both inorganic and organic coagulants while overcoming the shortcomings posed by each. They have presented superior coagulation performance in various wastewater treatments (Gao et al., 2008; Sun et al., 2017; Zhu et al., 2012). For example, Sun et al. (2017) prepared polymeric aluminum ferric silicate (PAFSi) for high-oil-containing wastewater treatment. The coagulation tests showed that 98.2 % COD removal and 98.4% oil removal were achieved under the optimal conditions. However, to our best knowledge, there is no published work in SAGD produced water treatment investigating the composite coagulants so far. The performance of different composite coagulants for treating SAGD produced water under high temperature is worth investigating in the future due to their high removal efficiencies of COD and oil.

2.3.2 Natural coagulants and flocculants

Natural polymers are explored and investigated to use as coagulants and flocculants (Oladoja, 2016; Renault et al., 2009). The significant advantages for natural bio-coagulants/flocculants are that these materials are biodegradable, non-toxic, relatively low cost and no secondary pollution (Bolto and Gregory, 2007). Bio-coagulants/flocculants can destabilize the colloidal particles via two mechanisms: one is increasing the ionic strength and reducing the zeta potential, leading to the reduction of thickness of the diffuse layer in the electrical double layer. The second is adsorbing counterions to neutralize the particle charge by a variety of functional groups such as carboxyl and hydroxyl groups (Özacar and Şengil, 2003). Currently, the commercially available natural coagulants/flocculants are mainly chitosan and tannins (Oladoja, 2016; Renault et al., 2009). Both of them have been applied in SAGD produced water treatment. Polizzotti et al. (2014) have patented a de-oiling method that uses tannins and chitosan as natural coagulants and a cationic and/or anionic flocculant to clarify SAGD produced water under higher temperature (95 °C). This process can achieve 75% of silica, 54% of COD, 42% of TOC and 98% of oil & grease removal by reducing the pH from 7.5 to 4, then adding the tannin based polymeric coagulant, followed by the addition of cationic PAM and anionic PAM flocculant. However, as discussed earlier, the impact of pH reduction and coagulation-flocculation on the removal efficiencies need to be compared to confirm the main contributing factor. Besides, when considering the potential application of natural coagulants/flocculants in SAGD produced water treatment, the disadvantages of natural polymers cannot be ignored. The biodegradability of natural polymers would shorten their shelf life due to the degradation of active components and would lose stability and strength with time (Lee et al., 2014).

2.4 Conclusion

Given the complex chemistry of SAGD produced water, improving removal of both organics and silica faces technical and operational challenges. Although silica has been reported to exist mostly as dissolved silicate and it is negatively charged in SAGD produced water at high temperature (80-90 °C) and high pH (9.5-10.5), the interaction between silica and MgO, which is most commonly used to remove silica, is not fully understood. Two possible mechanisms, which are silica adsorption on the formed $Mg(OH)_2$ or silica precipitation as magnesium silicate precipitates, have been proposed based on studies using synthetic water. However, the real SAGD produced water is a multicomponent mixture that is much more complicated than the simplified synthetic water. Therefore, more studies would be recommended to understand the interaction of silica and MgO as well as the effect of other organics. In terms of dissolved organics, the dominant fraction of dissolved organics is different among different SAGD produced waters. Generally, HPoA, HPoN and HPiN were primary DOM constituents in most SAGD produced water including DOW, BFW and BBD. FEEM results indicated that components of SAGD DOM have humic- and fulvic-like structure features. Based on MS based analytical techniques, organic acids and VOCs were found to be predominant in DOW, WLS feed water and BFW, whereas organic acids were most abundant in the BBD. In addition, phenols, aromatic acids, and aliphatic acids were identified as major classes of organics. However, based on these organics data, no clear linkages between organic species and the degree of fouling observed in the field can be found. Hence, more analyses of dissolved organics are required in the future.

Compared to metal salts and natural coagulants/flocculants, organic polymers are the preferred coagulants and flocculants in SAGD produced water treatment. The advantages of organic polymers over inorganic metal salts are significant, including less dosage of coagulants,

less sensitive to pH, less sludge volume, and less residual of metallic compound. Epi-DMA and poly-DADMAC are common organic coagulants while PAM and polyamine are usually used as organic flocculants. In order to promote the performance of organic polymers, it is worth exploring the impact factor and study the interactions among particles and polymers under high temperatures.

2.5 References

Al-As'ad, A., Husein, M.M., 2014. Treatment of steam-assisted gravity drainage water using low coagulant dose and Fenton oxidation. Environ Technol 35(13-16), 1630-1638. https://doi.org/10.1080/09593330.2013.877086.

Alambets, A., 2014. Magnesium Oxide (MgO) Dosing Systems for Thermal Enhanced Oil Recovery, Alberta WaterSmart Water Management Solution. Calgary.

Alberta Energy Regulator, 2019. Directive 081: Water Disposal Limits and Reporting Requirements for Thermal In Situ Oil Sands Schemes, in: Regulator, A.E. (Ed.).

Atallah, C., Mortazavi, S., Tremblay, A.Y., Doiron, A., 2019. Surface-Modified Multi-lumen Tubular Membranes for SAGD-Produced Water Treatment. Energy & Fuels 33(6), 5766-5776. https://doi.org/10.1021/acs.energyfuels.9b00585.

Bolto, B., Gregory, J., 2007. Organic polyelectrolytes in water treatment. Water research 41(11), 2301-2324.

Bouguerra, W., Ali, M.B.S., Hamrouni, B., Dhahbi, M., 2007. Equilibrium and kinetic studies of adsorption of silica onto activated alumina. Desalination 206(1-3), 141-146.

Bratby, J., 2016. Coagulation and flocculation in water and wastewater treatment, IWA publishing.

Cao, B., Gao, B., Liu, X., Wang, M., Yang, Z., Yue, Q., 2011. The impact of pH on floc structure characteristic of polyferric chloride in a low DOC and high alkalinity surface water treatment. Water Res 45(18), 6181-6188. https://doi.org/10.1016/j.watres.2011.09.019.

Chan, S., 1989. A review on solubility and polymerization of silica. Geothermics 18(1-2), 49-56.

Chen, S., Chang, T., Lin, C., 2006. Silica pretreatment for a RO brackish water source with high magnesium. Water Science and Technology: Water Supply 6(4), 179-187.

Cheng, W.P., Chi, F.H., 2002. A study of coagulation mechanisms of polyferric sulfate reacting with humic acid using a fluorescence-quenching method. Water research 36(18), 4583-4591.

Cheng, W.P., Chi, F.H., Li, C.C., Yu, R.F., 2008. A study on the removal of organic substances from low-turbidity and low-alkalinity water with metal-polysilicate coagulants. Colloids and Surfaces A: Physicochemical and Engineering Aspects 312(2-3), 238-244. https://doi.org/10.1016/j.colsurfa.2007.06.060.

COSIA, Water Performance Goals, https://cosia.ca/performance-goals/water.

Edzwald, J., Association, A.W.W., 2011. Water quality & treatment: a handbook on drinking water. McGraw-Hill Education.

Gamal El-Din, M., Fu, H., Wang, N., Chelme-Ayala, P., Pérez-Estrada, L., Drzewicz, P., Martin, J.W., Zubot, W., Smith, D.W., 2011. Naphthenic acids speciation and removal during petroleum-coke adsorption and ozonation of oil sands process-affected water. Science of the Total Environment 409(23), 5119-5125.

Fatema, J., Bhattacharjee, S., Pernitsky, D., Maiti, A., 2015. Study of the Aggregation Behavior of Silica and Dissolved Organic Matter in Oil Sands Produced Water Using Taguchi Experimental Design. Energy & Fuels 29(11), 7465-7473.

Gao, B., Yue, Q., Miao, J., 2003. Evaluation of polyaluminium ferric chloride (PAFC) as a composite coagulant for water and wastewater treatment. Water science and technology 47(1), 127-132.

Gao, B.Y., Wang, Y., Yue, Q.Y., Wei, J.C., Li, Q., 2008. The size and coagulation behavior of a novel composite inorganic–organic coagulant. Separation and Purification Technology 62(3), 544-550. https://doi.org/10.1016/j.seppur.2008.02.023.

Graham, S., Reitz, R., Hickman, C., 1989. Improving reverse osmosis performance through periodic cleaning. Desalination 74, 113-124.

Guha Thakurta, S., Maiti, A., Pernitsky, D.J., Bhattacharjee, S., 2013. Dissolved organic matter in steam assisted gravity drainage boiler blow-down water. Energy & fuels 27(7), 3883-3890.

Hayatbakhsh, M., Sadrzadeh, M., Pernitsky, D., Bhattacharjee, S., Hajinasiri, J., 2016. Treatment of an in situ oil sands produced water by polymeric membranes. Desalination and water treatment 57(32), 14869-14887.

Hogg, R., 2005. Flocculation and dewatering of fine-particle suspension. Coagulation and flocculation: Second Edition (FL). Boca Raton, CRC Press.

Huang, C., Shi, Y., Gamal El-Din, M., Liu, Y., 2015. Treatment of oil sands process-affected water (OSPW) using ozonation combined with integrated fixed-film activated sludge (IFAS). Water research 85, 167-176.

Hurwitz, G., Pernitsky, D.J., Bhattacharjee, S., Hoek, E.M., 2015. Targeted removal of dissolved organic matter in boiler-blowdown wastewater: integrated membrane filtration for produced water reuse. Industrial & Engineering Chemistry Research 54(38), 9431-9439.

Jennings, D.W., Shaikh, A., 2007. Heat-exchanger deposition in an inverted steam-assisted gravity drainage operation. Part 1. Inorganic and organic analyses of deposit samples. Energy & fuels 21(1), 176-184.

Joo, D.J., Shin, W.S., Choi, J.H., Choi, S.J., Kim, M.C., Han, M.H., Ha, T.W., Kim, Y.H., 2007. Decolorization of reactive dyes using inorganic coagulants and synthetic polymer. Dyes and Pigments 73(1), 59-64.

Kawaguchi, H., Li, Z., Masuda, Y., Sato, K., Nakagawa, H., 2012. Dissolved organic compounds in reused process water for steam-assisted gravity drainage oil sands extraction. Water Res 46(17), 5566-5574. https://doi.org/10.1016/j.watres.2012.07.036.

Kimetu, J.M., Hill, J.M., Husein, M., Bergerson, J., Layzell, D.B., 2016. Using activated biochar for greenhouse gas mitigation and industrial water treatment. Mitigation and Adaptation Strategies for Global Change 21(5), 761-777.

Ku, A.Y., Henderson, C.S., Petersen, M.A., Pernitsky, D.J., Sun, A.Q., 2012. Aging of water from steam-assisted gravity drainage (SAGD) operations due to air exposure and effects on ceramic membrane filtration. Industrial & engineering chemistry research 51(21), 7170-7176.

Latour, I., Miranda, R., Blanco, A., 2014. Silica removal in industrial effluents with high silica content and low hardness. Environmental Science and Pollution Research 21(16), 9832-9842.

Latour, I., Miranda, R., Blanco, A., 2015. Silica removal with sparingly soluble magnesium compounds. Part II. Separation and Purification Technology 149, 331-338.

Lee, C.S., Robinson, J., Chong, M.F., 2014. A review on application of flocculants in wastewater treatment. Process Safety and Environmental Protection 92(6), 489-508.

Leong, Y.-K., 2005. Yield stress and zeta potential of nanoparticulate silica dispersions under the influence of adsorbed hydrolysis products of metal ions—Cu (II), Al (III) and Th (IV). Journal of colloid and interface science 292(2), 557-566.

Li, C., Fu, L., Stafford, J., Belosevic, M., Gamal El-Din, M., 2017. The toxicity of oil sands process-affected water (OSPW): A critical review. Science of the Total Environment 601, 1785-1802.

Lightbown, V., 2015. New SAGD technologies show promise in reducing environmental impact of oil sand production. Journal of Environmental Solutions for Oil, Gas, and Mining 1(1), 47-58.

Maiti, A., Sadrezadeh, M., Guha Thakurta, S., Pernitsky, D.J., Bhattacharjee, S., 2012. Characterization of boiler blowdown water from steam-assisted gravity drainage and silica–organic coprecipitation during acidification and ultrafiltration. Energy & fuels 26(9), 5604-5612.

McQueen, A.D., Kinley, C.M., Hendrikse, M., Gaspari, D.P., Calomeni, A.J., Iwinski, K.J., Castle, J.W., Haakensen, M.C., Peru, K.M., Headley, J.V., 2017. A risk-based approach for identifying constituents of concern in oil sands process-affected water from the Athabasca Oil Sands region. Chemosphere 173, 340-350.

Mesmer, R., Baes, C., 1990. Review of Hydrolysis Behavior of Ions in Aqueous Solutions. MRS Online Proceedings Library (OPL) 180.

Metcalf, W., 2003. Metcalf and Eddy wastewater engineering: treatment and reuse. In Wastewater engineering: treatment and reuse. New York, NY, McGraw Hill.

Mohammadtabar, F., Pillai, R.G., Khorshidi, B., Hayatbakhsh, A., Sadrzadeh, M., 2019. Efficient treatment of oil sands produced water: Process integration using ion exchange regeneration wastewater as a chemical coagulant. Separation and Purification Technology 221, 166-174.

Mohd-Salleh, S.N.A., Mohd-Zin, N.S., Othman, N., 2019. A review of wastewater treatment using natural material and its potential as aid and composite coagulant. Sains Malaysiana 48(1), 155-164.

Ning, R.Y., 2003. Discussion of silica speciation, fouling, control and maximum reduction. Desalination 151(1), 67-73.

Oladoja, N.A., 2016. Advances in the quest for substitute for synthetic organic polyelectrolytes as coagulant aid in water and wastewater treatment operations. Sustainable Chemistry and Pharmacy 3, 47-58. https://doi.org/10.1016/j.scp.2016.04.001.

Özacar, M., Şengil, İ.A., 2003. Evaluation of tannin biopolymer as a coagulant aid for coagulation of colloidal particles. Colloids and Surfaces A: Physicochemical and Engineering Aspects 229(1-3), 85-96. https://doi.org/10.1016/j.colsurfa.2003.07.006.

Parks, J.L., Edwards, M., 2007. Boron removal via formation of magnesium silicate solids during precipitative softening. Journal of Environmental Engineering 133(2), 149-156.

Parsons, S.A., Jefferson, B., 2006. Introduction to potable water treatment processes. Blackwell publishing.

Perdicakis, B., Petersen, M., Gerbino, A., McGregor, M., 2019. In High Temperature Reverse Osmosis Membrane SAGD Process Design Assessment, International Water Conference. Orlando, pp. 19-61.

Pereira, A.S., Bhattacharjee, S., Martin, J.W., 2013. Characterization of oil sands process-affected waters by liquid chromatography orbitrap mass spectrometry. Environmental science & technology 47(10), 5504-5513.

Pernitsky, D.J., Edzwald, J.K., 2006. Selection of alum and polyaluminum coagulants: principles and applications. Journal of Water Supply: Research and Technology—AQUA 55(2), 121-141.

Pillai, R.G., Yang, N., Thi, S., Fatema, J., Sadrzadeh, M., Pernitsky, D., 2017. Characterization and Comparison of Dissolved Organic Matter Signatures in Steam-Assisted Gravity Drainage Process Water Samples from Athabasca Oil Sands. Energy & Fuels 31(8), 8363-8373. https://doi.org/10.1021/acs.energyfuels.7b00483.

Polizzotti, D.M., Khwaja, A.R., 2011. Use of cationic coagulant and acrylamide polymer flocculants for separating oil from oily water. Google Patents.

Polizzotti, D.M., Khwaja, A.R., 2014. Deoiling of SAGD produce water. Google Patents.

Pourrezaei, P., Alpatova, A., Chelme-Ayala, P., Perez-Estrada, L., Jensen-Fontaine, M., Le, X., Gamal El-Din, M., 2014. Impact of petroleum coke characteristics on the adsorption of the organic fractions from oil sands process-affected water. International Journal of Environmental Science and Technology 11(7), 2037-2050.

Prakash, N., Sockan, V., Jayakaran, P., 2014. Waste water treatment by coagulation and flocculation. International Journal of Engineering Science and Innovative Technology (IJESIT) 3(2), 479-484.

Renault, F., Sancey, B., Charles, J., Morin-Crini, N., Badot, P.-M., Winterton, P., Crini, G., 2009. Chitosan flocculation of cardboard-mill secondary biological wastewater. Chemical Engineering Journal 155(3), 775-783.

Reynolds, T.D., Richards, P.A.C., 1995. Unit operations and processes in environmental engineering. PWS Publishing Company.

Sadrzadeh, M., Hajinasiri, J., Bhattacharjee, S., Pernitsky, D., 2015. Nanofiltration of oil sands boiler feed water: Effect of pH on water flux and organic and dissolved solid rejection. Separation and Purification Technology 141, 339-353. https://doi.org/10.1016/j.seppur.2014.12.011.

Sadrzadeh, M., Pernitsky, D., McGregor, M., 2018. Nanofiltration for the treatment of oil sands-produced water, Nanofiltration. InTech, pp. 25-45.

Sahachaiyunta, P., Koo, T., Sheikholeslami, R., 2002. Effect of several inorganic species on silica fouling in RO membranes. Desalination 144(1-3), 373-378.

Shamaei, L., Khorshidi, B., Perdicakis, B., Sadrzadeh, M., 2018. Treatment of oil sands produced water using combined electrocoagulation and chemical coagulation techniques. Science of the Total Environment 645, 560-572.

Sharma, B., Dhuldhoya, N., Merchant, U., 2006. Flocculants—an ecofriendly approach. Journal of Polymers and the Environment 14(2), 195-202.

Sheikholeslami, R., Tan, S., 1999. Effects of water quality on silica fouling of desalination plants. Desalination 126(1-3), 267-280.

Sillanpaa, M., Ncibi, M.C., Matilainen, A., Vepsalainen, M., 2018. Removal of natural organic matter in drinking water treatment by coagulation: A comprehensive review. Chemosphere 190, 54-71. https://doi.org/10.1016/j.chemosphere.2017.09.113.

Sun, Y., Zhu, C., Zheng, H., Sun, W., Xu, Y., Xiao, X., You, Z., Liu, C., 2017. Characterization and coagulation behavior of polymeric aluminum ferric silicate for high-concentration oily wastewater treatment. Chemical Engineering Research and Design 119, 23-32.

Suopajärvi, T., 2015. Functionalized nanocelluloses in wastewater treatment applications. Acta Universitatis Ouluensis C, 526.

Vandamme, D., Foubert, I., Fraeye, I., Meesschaert, B., Muylaert, K., 2012. Flocculation of Chlorella vulgaris induced by high pH: role of magnesium and calcium and practical implications. Bioresource technology 105, 114-119.

Wills, B.A., Finch, J., 2015. Wills' mineral processing technology: an introduction to the practical aspects of ore treatment and mineral recovery. Butterworth-Heinemann.

Wu, C., De Visscher, A., Gates, I.D., 2019. On naphthenic acids removal from crude oil and oil sands process-affected water. Fuel 253, 1229-1246. https://doi.org/10.1016/j.fuel.2019.05.091.

Zeng, Y., Yang, C., Pu, W., Zhang, X., 2007a. Removal of silica from heavy oil wastewater to be reused in a boiler by combining magnesium and zinc compounds with coagulation. Desalination 216(1-3), 147-159.

Zeng, Y., Yang, C., Zhang, J., Pu, W., 2007b. Feasibility investigation of oily wastewater treatment by combination of zinc and PAM in coagulation/flocculation. J Hazard Mater 147(3), 991-996. https://doi.org/10.1016/j.jhazmat.2007.01.129.

Zhang, K., Pernitsky, D., Jafari, M., Lu, Q., 2021. Effect of MgO Slaking on Silica Removal during Warm Lime Softening of SAGD Produced Water. Industrial & Engineering Chemistry Research.

Zhu, G., Zheng, H., Chen, W., Fan, W., Zhang, P., Tshukudu, T., 2012. Preparation of a composite coagulant: Polymeric aluminum ferric sulfate (PAFS) for wastewater treatment. Desalination 285, 315-323.

CHAPTER 3 REMOVAL OF COLLOIDAL IMPURITIES BY THERMAL SOFTENING-COAGULATION-FLOCCULATION-SEDIMENTATION IN STEAM ASSISTED GRAVITY DRAINAGE PRODUCED WATER: PERFORMANCE, INTERACTION EFFECTS AND MECHANISM STUDY[2]

3.1 Introduction

As one of the primary *in situ* thermal recovery processes for bitumen production, steam-assisted gravity drainage (SAGD) extracts bitumen by injecting high temperature and high pressure steam (Butler, 1994). Subsequently, injected steam is recovered as produced water on the surface. Due to the intensive use of water in the SAGD process, recycling the produced water to regenerate steam is essential for both the protection of environment and minimizing operational costs. SAGD produced water is comprised of a complex mixture of bitumen residue, dissolved organic compounds, inorganic salts, and suspended solids. Among these constituents, high levels of dissolved silica (150-400 mg/L) and dissolved organics (150-800 mg/L) are particularly problematic because their precipitation can result in fouling in steam generators and clogging of pipelines (Sadrzadeh et al., 2018). In addition, water hardness components (Ca^{2+}, Mg^{2+}) can cause scaling and corrosion of pipelines and steam generators (Chow and Pham, 2019). Currently after the de-oiling process, produced water is introduced to the warm lime softening (WLS) treatment unit with addition of hydrated lime ($Ca(OH)_2$), magnesium oxide (MgO), soda ash (Na_2CO_3), coagulant and flocculant under high temperature (65-85 °C) and high pressure (Heins, 2010).

---

[2] This Chapter is based on the published paper: Li J, How ZT, Benally C, Sun Y, Zeng H, Gamal El-Din M. Removal of colloidal impurities by thermal softening-coagulation-flocculation-sedimentation in steam assisted gravity drainage (SAGD) produced water: performance, interaction effects and mechanism study. Separation and Purification Technology. 2023; 123484.

In recent decades, various technologies, such as membrane filtration, have been developed to treat produced water (Forshomi et al., 2017; Karami et al., 2020). Coagulation-flocculation, although regarded as a conventional technique, is still considered as a promising and essential technology for separating colloidal impurities from different sources of wastewater (Li et al., 2022b). Previous studies tested inorganic coagulants (Hurwitz et al., 2015; Rasouli et al., 2017) and organic coagulants (epichlorohydrin-dimethylamine (EPI-DMA), poly(diallyldimethylammonium chloride) (poly-DADMAC)) (Polizzotti and Khwaja, 2011; Zhang et al., 2021b) with/without flocculants in real and synthetic produced water. Overall, given that organic coagulants/flocculants are less sensitive to pH and temperature, they showed higher removal efficiency of colloidal impurities with less dosage, less sludge volume, and less residual of metallic compounds than inorganic coagulants/flocculants in SAGD produced water treatment (Gao et al., 2008; Li et al., 2022b). Among different organic coagulants, poly-DADMAC and polyacrylamide (PAM) are the most commonly used polymers in oil and gas industry (Bhandari and Ranade, 2014; Li et al., 2022b; Wang, 2016). However, none of these attempts have been combined with the softening step under high temperature and include total inorganic carbon (TIC) and sludge volume index (SVI) as performance indicators when assessing the efficiency of the technologies. In fact, TIC can significantly affect the surface charges of $CaCO_3$ and $Mg(OH)_2$, which would in turn affect the performance of both softening and subsequent coagulation-flocculation (Zhang et al., 2021b). Besides, SVI is a primary indicator of the readiness levels of the formed flocs to be settled down and thickened (Van Aken et al., 2017). It is known that coagulation-flocculation (CF) is impacted by both water chemistry, such as salinity, total organic carbon (TOC) and pH, and operational conditions including temperature, chemical dose, and mixing (Ji et al., 2013). However, the effect of these multiple physicochemical parameters in a

complex environment like SAGD produced water remains relatively uncovered. In recent published research, Zhang et al. (2020) investigated the interactions among humic acid, silicate, clay and formed $CaCO_3$ and $Mg(OH)_2$, focusing on electrokinetic properties. Their results demonstrated that the existence of silica, clay or humic acid could easily change the surface charge of $Mg(OH)_2$ particles and increase the magnitude of negative charge on $CaCO_3$ particles. Later, Zhang et al. (2021b) also explored the individual impact of water chemistry, including TOC, total suspended solids (TSS) and silica, on the EPI-DMA coagulant demand for treating synthetic produced water at 65 °C. They found that humic acid and silica were two significant factors affecting the coagulant dose. While these studies provide the understanding of the binary interactions and the individual impact of water chemistry at lower temperature of WLS, there is still no clear and unified conclusion on interaction of various particles and the impact of operational conditions in a multi-component system at high temperature.

To explore the effects among operational factors and to further study removal mechanisms under optimal treatment, response surface methodology (RSM) can be incorporated into the research methodology. RSM is a collection of mathematical and statistical techniques and is an effective tool in optimization and modelling of the composite non-linear systems while using less experimental runs compared to the one factor at a time approach (Kusuma et al., 2021). RSM has been utilized to successfully optimize the CF process in various types of wastewater, including turbid wastewater (Kusuma et al., 2022), palm oil mill effluent (Huzir et al., 2019), and crude oil-polluted water (Rehman et al., 2022). However, to the best of our knowledge, there are no published studies about optimization and modelling of the softening with CF process under high temperature in SAGD produced water by using RSM.

Furthermore, due to the high pH of SAGD produced water (7-8), most of the colloidal impurities are negatively charged and remain suspended due to the strong repulsive forces which prevent them from collision (Maiti et al., 2012). The removal mechanisms were mainly studied by focusing on inorganic coagulants without flocculant, and charge neutralization and enmeshment were found as the two main mechanisms (Hurwitz et al., 2015). A limited number of research has investigated removal mechanism by organic coagulants under high temperature and the effect of temperature on removal mechanism in produced water. Mohammadtabar et al. (2019) examined the mechanism of removing turbidity from blowdown water with the temperature range of 40-80 °C using ion exchange regeneration wastewater as the coagulant. Based on their observation, increasing temperature could produce larger flocs and hence promote turbidity removal. Zhang et al. (2021a) studied the removal mechanism of silica by using MgO and two competing mechanisms including adsorption on formed $Mg(OH)_2$ and precipitation as magnesium silicate were proposed. However, the synthetic water used in their study only contained Na_2SiO_3, indicating interactions with other impurities that might change the removal mechanism were neglected. Hence, the removal mechanism of different colloidal impurities and temperature effect in softening-coagulation-flocculation process need to be further investigated. Advanced understanding of the impact of operation conditions and removal mechanism are of great significance for SAGD produced water treatment processes.

Therefore, this study aims to evaluate effects of operating conditions on the performance of softening-coagulation-flocculation in synthetic water, following the industrial practice of utilizing poly-DADMAC as the coagulant and cationic PAM as the flocculant at high temperature (80 °C, a typical temperature operated in WLS treatment process in SAGD plant). Systematic numerical investigations based on RSM were performed to study the interaction among operational

variables and optimize the operating conditions. Furthermore, the characterization of formed flocs at optimal conditions under room temperature and high temperature were compared, and surface force measurements between polymers and particles were conducted to examine the mechanisms for removing colloidal impurities in the treatment process and the temperature effect on removal mechanisms. The findings of this study provide new insights into the influence of operating conditions on colloidal impurities removal, and have a greater significance in the guidance for improving efficiency in on-site produced water treatment.

3.2 Materials and methods

3.2.1 SAGD WLS water and chemicals

A typical SAGD WLS feed composition was used for preparing the synthetic water sample, as shown in Table 3.1. $Ca(OH)_2$, Na_2CO_3, sodium chloride (NaCl), calcium chloride dehydrate ($CaCl_2 \cdot 2H_2O$), magnesium chloride hexahydrate ($MgCl_2 \cdot 2H_2O$), sodium bicarbonate ($NaHCO_3$) were purchased from Fisher Chemicals. Kaolinite clay ($Al_2O_3 \cdot 2SiO_2 \cdot 2H_2O$) was obtained from Fluka. Sodium metasilicate (Na_2SiO_3), humic acid sodium salts ($C_9H_8Na_2O_4$) and MgO were purchased from Sigma Aldrich. Poly-DADMAC (Sigma Aldrich) and cationic polyacrylamide (855 BS, Praestol, Gernany) were applied as cationic coagulant and flocculant, respectively. Milli-Q water (Millipore Corp) was used for the synthetic water and all working solutions.

Table 3.1 Synthetic SAGD WLS feed water component.

Parameters	Value	Representative properties
Na^+ (NaCl and Na_2SO_4)	2000 mg/L	Total dissolved solids (TDS)

CaCl₂ · 2H₂O and MgCl₂ · 2H₂O	250 mg/L as CaCO₃	Total hardness
Kaolinite	500 mg/L	Total suspended solids (TSS)
NaHCO₃	650 mg/L as HCO₃⁻	Bicarbonate alkalinity
Humic acid sodium salt (HAS)	150 mg/L as C	Total organic carbon (TOC)
Na₂SiO₃	250 mg/L as SiO₂	Silica

3.2.2 Softening-coagulation-flocculation test

A Phipps & Bird PB-700^{TM} JarTester was used to perform the jar tests using 2L of synthetic water. A Magni-Whirl constant temperature water bath (Blue M) was applied to heat up the water samples and maintain the temperature at 80 °C before and after the jar test (Fig. A.1 in appendix A). During the jar test, a temperature controller (Inkbird) was applied to control a portable heater (Diximus) to maintain the temperature of water samples on the jar tester. Softeners including $Ca(OH)_2$ (125 mg/L), MgO (258 mg/L) and Na_2CO_3 (150 mg/L) were added into jars immediately after the start of rapid mixing. After softening, poly-DADMAC was added as coagulant while the speed was kept the same for 2 min. This was followed by slow mixing at 20 rpm with addition of 1 mg/L of cationic PAM as flocculant and sedimentation for 15 min in the water bath. 200 mL of supernatant was collected using a syringe from approximately 2 cm below the water surface. After settling, the flocs at the bottom of the jars were collected and dried at 105 °C in the oven overnight for further analysis.

3.2.3 Experimental design and data analysis

StatEase Design-Expert software (version 11.0) was used for statistical design and data analysis. The central composite design (CCD), the most common fractional factorial design used in RSM model, was applied in this study. CCD is favored over other designs such as the Box Behnken design (BBD) because it offers more axial design points compared to the BBD while

being suitable for testing four variables (Nair et al., 2014). In addition, CCD is better at extreme conditions and gives better results for quadratic models (Ahmadi et al., 2005). The coded independent variables are poly-DADMAC dose (x_1), mixing time with softeners only (x_2), coagulation speed (x_3) and flocculation time (x_4); turbidity removal (Y_1), TSS removal (Y_2), particulate hardness removal (Y_3), silica removal (Y_4), TOC removal (Y_5), TIC removal (Y_6), and SVI (Y_7) are the responses of interest. Table 3.2 shows the CCD in the form of a 2^4 full factorial design, along with ranges and levels for each independent variable. For each response, regression coefficients and analysis of variance (ANOVA) were estimated based on the quadratic polynomial model Eq. 3.1.

$$Y = \beta_0 + \sum_{i=1}^{4} \beta_i x_i + \sum_{i=1}^{4} \beta_{ii} x_i^2 + \sum_{i=1}^{} \sum_{i \neq j=1}^{} \beta_{ij} x_i x_j + \varepsilon \tag{3.1}$$

where Y is the response, x_i and x_j are the coded values of the operational variables i and j, β_0 is the intercept, β_i, β_{ii}, β_{ij} denote linear coefficient, the quadratic coefficient for i and the interaction coefficient between i and j, respectively. ε is the random error. The reduced quadratic model was then used to develop the corresponding response surfaces where two operational variables were varied within the experimental ranges with the other two variables kept at central level (level 0). Moreover, in order to quantitatively evaluate the influences of terms on all the responses, Pareto analysis was also conducted, and Pareto charts were generated by using the MINITAB 19.

Table 3.2 Experimental range and levels of the independent variables according to RSM.

Variables	Unit	Range and levels				
		-2	-1	0	1	2
Poly-DADMAC dose	mg/L	50	60	70	80	90

Mixing time with softeners only	min	2	6	10	14	18
Coagulation speed	rpm	50	100	150	200	250
Flocculation time	min	4	8	12	16	20

3.2.4 Water quality analysis

Treated water samples were stored at 4 °C prior to analysis. Turbidity was measured by a turbidity meter (Oakton T100) and pH was determined using an Accumet Research AR20 pH/conductivity meter (Fisher Scientific). Hardness, TSS and SVI were determined by Standard Methods 2340B, 2540D and 2710D, respectively (AWWA, 2017). Zeta potential analysis was performed in a Malvern Zetasizer Nano (Malvern Instruments). TOC and TIC were analyzed by Shimadzu TOC-L. Chemical oxygen demand (COD) of filtered water samples (0.45 μm nylon filter) was measured by using a Spectrophotometer (DR 3900, HACH, Germany) with Hach TNTplus Vial Test kit 822. The concentration of calcium (Ca^{2+}) and magnesium (Mg^{2+}) ions and silica were quantified by inductively coupled plasma-optical emission spectroscopy (ICP-OES) (Thermo Fisher ICAP6300).

3.2.5 Flocs and surface analysis

Field emission scanning electron microscopy (FESEM, Zeiss Sigma 300 VP) was used to observe the structure of particles in raw (untreated) water and formed flocs after optimal treatment under room and high temperature (80 °C). Further particle size analysis was conducted by using the open-source software ImageJ distributed by Fiji (Srivastava et al., 2022). The elemental compositions of the particles and flocs were analyzed using energy-dispersive X-ray spectroscopy (EDS, Bruker), X-ray powder diffraction (XRD, Rigaku Ultima IV), and X-ray photoelectron spectroscopy (XPS, Kratos AXIS ULTRA). The chemical functional groups of the particles and

flocs were assessed by an attenuated total reflection Fourier transform infrared (ATR-FTIR) spectrometer (Nicolet 8700, Thermo Fisher Scientific). The detailed procedure for sample preparation and measurement method of FTIR was previously reported (Li et al., 2022a).

In order to further understand the interactions between polymers and solid surfaces, a surface forces apparatus (SFA) was employed to directly measure their interaction forces by following the procedure used by Lu et al. (2016). In brief, a thin mica sheet (model clay) was glued onto a cylindrical silica disk with a silver coated back surface. The two curved mica surfaces were mounted into the SFA chamber with cross-cylinder configuration, followed by polymer solutions injection between mica surfaces. Then the two surfaces were brought close or separated apart. The distance D between the two mica surfaces was quantified via the multiple-beam interferometry optical technique and the force F between two surfaces was obtained as a function of separation distance based on the Hooke's law. In this work, 1000 mg/L poly-DADMAC stock solution and 100 mg/L cationic PAM stock solution were prepared separately in 2500 mg/L NaCl solution, which was the common salt concentration of SAGD WLS feed water.

3.3 Results and discussion

3.3.1 Development of regression models and statistical analysis

Table A.1 (found in appendix A) summarizes 36 experiments designed by CCD, including operational conditions, the observed and the predicted values for responses. The coded reduced quadratic models for each response are shown in Eq 3.2-3.8. Insignificant terms (*p*-value >0.05) were removed from the models (except those required to support hierarchy) (Table A.2). ANOVA results (Table 3.3) showed that all responses models were statistically significant (*p*-value <0.01), indicating a good fit of reduced quadratic models to the experimental results. High values of R^2 for all responses also demonstrate high model fitness. Besides, values higher than 4 for the

adequate precision (A.P.) and lower than 10% for the coefficient of variance (C.V.) further proved the models' adequacy and reproducibility (Ooi et al., 2018). Fig. 3.1 plots the predicted response values of the model against the observed values. As shown, data points were distributed relatively close and had linear behavior, suggesting highly accurate prediction power of the models.

$$\text{Turbidity removal } (Y_1)\% = 98.37 - 0.7422 * A + 0.7903 * B + 0.7328 * C - 0.0953 * D \\ + 0.5119 * AB - 0.3569 * BC - 0.2076 * A^2 - 0.2982 * B^2 \tag{3.2}$$

$$\text{TSS removal } (Y_2)\% = 95.91 - 0.8444 * A + 1.10 * B + 0.7687 * C + 0.3506 * D \\ + 0.5825 * AB + 0.4795 * C^2 + 0.3582 * D^2 \tag{3.3}$$

$$\text{Particulate hardness removal } (Y_3)\% = 99.58 - 0.0544 * A + 0.5631 * B + 0.7469 * C$$

$$+ 0.2294 * D - 0.3825 * BC + 0.2138 * BD - 0.4837 * CD \\ - 0.4085 * B^2 - 0.3756 * C^2 - 0.2625 * D^2 \tag{3.4}$$

$$\textit{S}\text{ilica removal } (Y_4)\% = 16.89 + 1.50 * A + 1.90 * B + 0.2775 * C - 0.005 * D + 1.72 * AB$$

$$- 1.29 * AC + 1.33 * BC + 1.79 * BD + 1.58 * CD + 1.31 * B^2 + 1.32 * C^2 + 1.09 * D^2 \tag{3.5}$$

$$\text{TOC removal } (Y_5)\% = 72.79 + 3.90 * A - 0.6053 * B + 0.1434 * C + \\ 0.2041 * D - 1.71 * BC - 1.18 * A^2 - 0.7143 * D^2 \tag{3.6}$$

$$\text{TIC removal } (Y_6)\% = 30.38 + 0.7734 * A - 0.1647 * B - 0.6528 * C - 0.6628 * D \\ - 2.12 * AC + 1.50 * AD + 1.79 * CD + 0.4008 * A^2 - 0.3955 * B^2 \tag{3.7}$$

$$\text{SVI } (Y_7)(\text{mL/g}) = 38.83 - 1.89 * A + 2.35 * B - 0.3828 * C + 2.24 * D \\ - 1.08 * AB + 1.56 * AD - 1.77 * CD - 1.22 * B^2 - 0.8624 * C^2 - 1.47 * D^2 \tag{3.8}$$

where Y is the predicted value, A, B, C, and D represent poly-DADMAC dose, mixing time with softeners only, coagulation speed, and flocculation speed, respectively. AB, AC, AD, BC, BD, and CD are the interaction effect terms, and A^2, B^2, C^2 and D^2 each represent the quadratic effect terms.

Table 3.3 Fit statistics and ANOVA results showing the adequacy of the model.

	Turbidity removal	TSS removal	Particulate hardness removal	Silica removal	TOC removal	TIC removal	SVI
ANOVA for quadratic model							
Sum of Squares	66.58	106.42	49.28	509.06	622.87	226.95	688.45
Degree of freedom(df)	8	7	10	12	7	9	10
Mean Square	8.32	15.20	4.93	42.42	88.98	25.22	68.85
F-value	34.16	41.41	33.10	23.20	53.44	30.28	27.17
p-value	<0.0001	<0.0001	<0.0001	<0.0001	<0.0001	<0.0001	<0.0001
Fit statistics							
Standard deviation	0.49	0.61	0.39	1.35	1.29	0.91	1.59
Mean	97.92	96.71	98.59	20.20	71.10	30.39	35.67
R^2	0.91	0.91	0.93	0.92	0.93	0.91	0.92
Adjusted R^2	0.88	0.89	0.90	0.88	0.91	0.88	0.88
Predicted R^2	0.84	0.86	0.85	0.79	0.89	0.82	0.81
Coefficient of variance (C.V.)%	0.50	0.63	0.39	6.69	1.81	3.00	4.46
Adequate precision (A.P.)	21.07	22.17	16.29	19.13	28.22	22.91	18.75
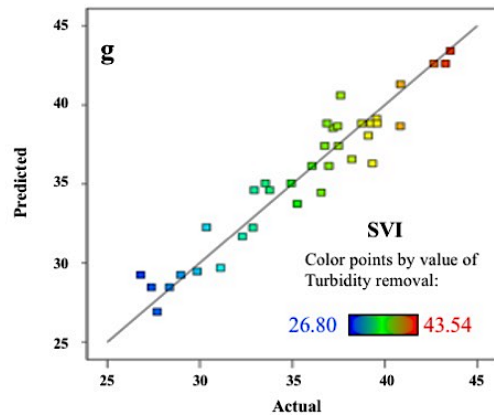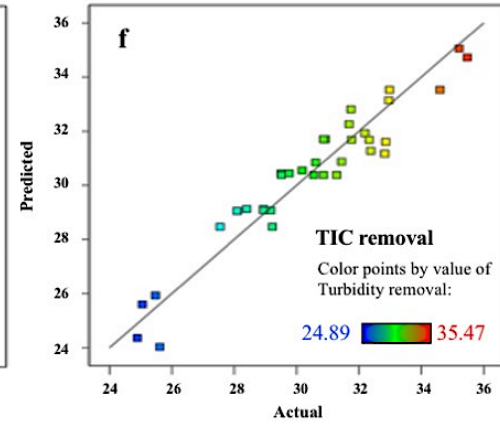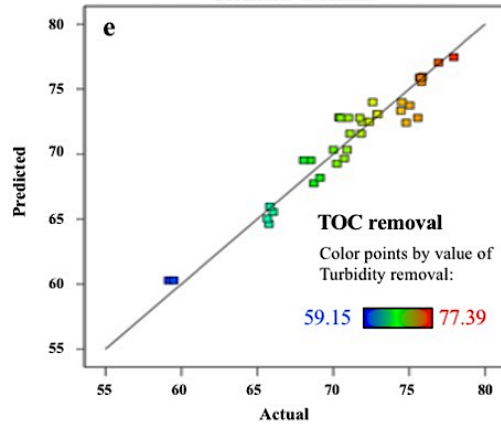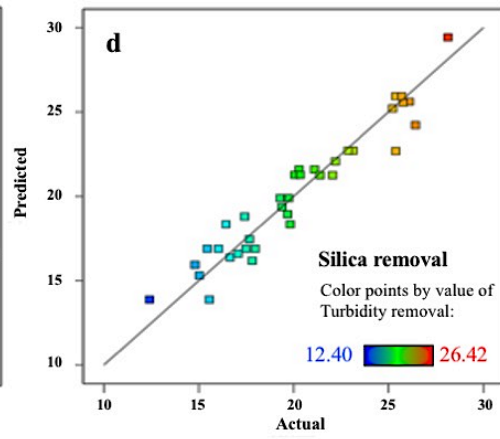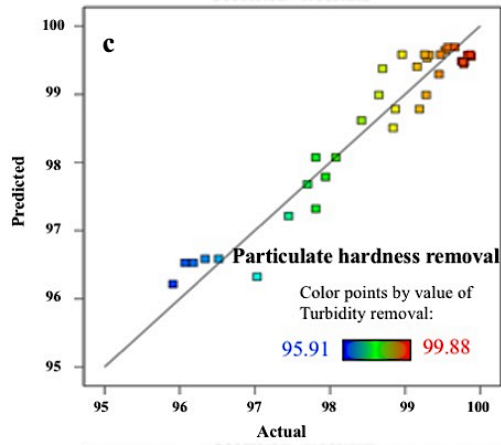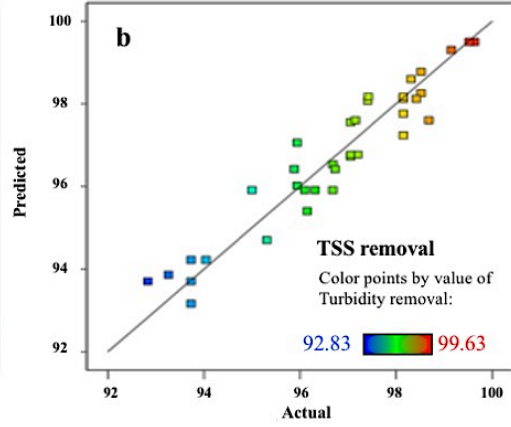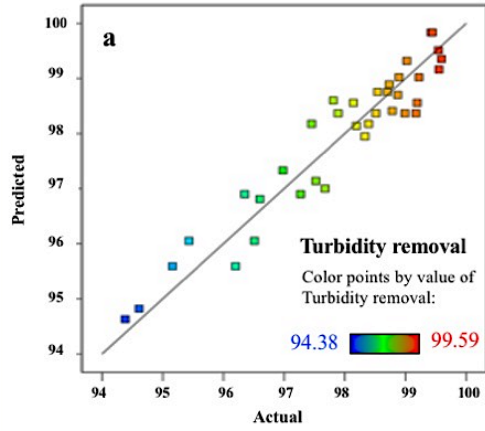
Figure 3.1 Correlation between the actual and predicted (a) turbidity removal, (b) TSS removal, (c) particulate hardness removal, (d) silica removal, (e) TOC removal, (f) TIC removal, and (g) SVI.

Fig.3.2 presents the Pareto charts, which are a set of bars whose lengths represent the frequency or impact of independent variables. The red vertical lines in the Pareto charts are located at a critical *p-value* of 0.05 to indicate the minimum statistically significant effect. Therefore, the independent variables with bars that extend to the right of red reference line are relatively more significant. As observed, poly-DADMAC dose (A), mixing time with softeners only (B), and coagulation speed (C) had the salient impacts on the turbidity and TSS removal (Fig. 3.2a, 2b). For particulate hardness removal, the corresponding Pareto chart (Fig. 3.2c) indicates significant linear and quadratic effects of mixing time with softeners only and coagulation speed. On the other hand, linear, quadratic and interaction effects of most variables, except coagulation speed and flocculation time, were significant for silica removal (Fig. 3.2d). As shown in Fig. 3.2e, 2f, poly-DADMAC dose imposed the greatest effect on TOC removal whereas the interactions among poly-DADMAC dose, coagulation speed and flocculation time had marked effects on TIC removal. From Fig. 3.2g, SVI is largely affected by mixing time with softeners only, flocculation time, and poly-DADMAC dose. The analysis also suggested that the interaction effects of coagulation speed and flocculation time, poly-DADMAC dose and flocculation time, as well as poly-DADMAC dose and mixing time with softeners only were significant for SVI. Given the significant linear, quadratic and interaction effects of poly-DADMAC dose and mixing time with softeners only were observed in most of responses, poly-DADMAC dose and mixing time with softeners only were the most important operational variables in the treatment process.
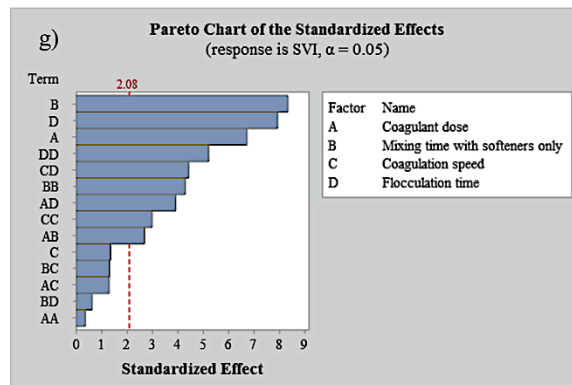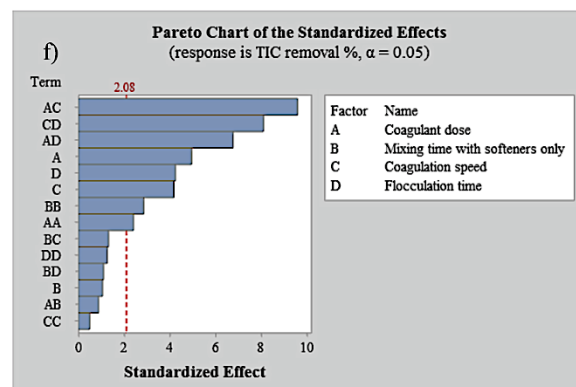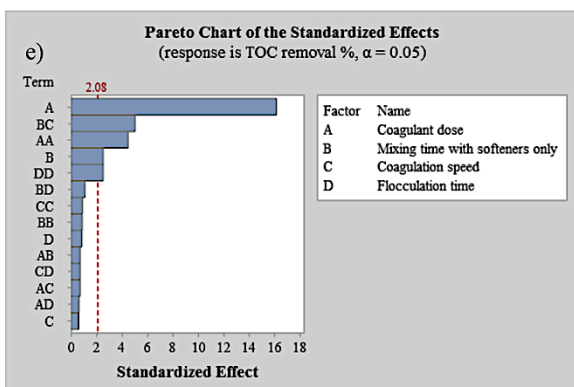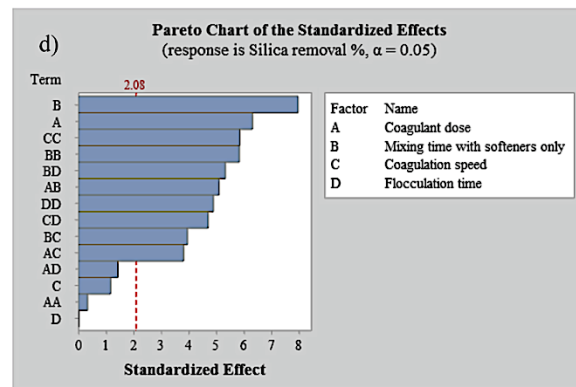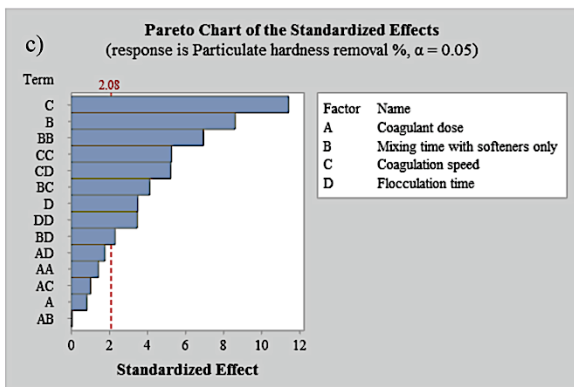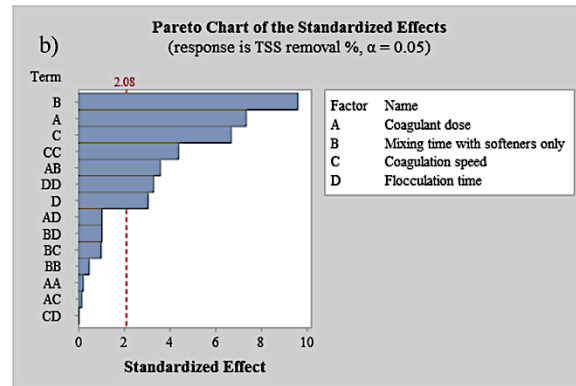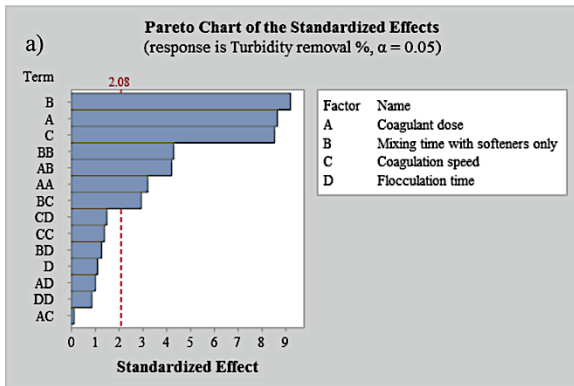
Figure 3.2 Standardized Pareto charts for responses: (a) turbidity removal, (b) TSS removal, (c) particulate hardness removal, (d) silica removal, (e) TOC removal, (f) TIC removal, and (g) SVI. (A, B, C, and D represent poly-DADMAC dose, mixing time with softeners only, coagulation speed, and flocculation speed, respectively. AB, AC, AD, BC, BD, and CD are the interaction effect terms, and A^2, B^2, C^2 and D^2 each represent the quadratic effect terms).

3.3.2 Performance of thermal treatment and interaction effects

3.3.2.1 Turbidity and TSS removal

Figure 3.3 shows the response surface of turbidity and TSS removal for variable interaction effects. Fig. 3.3a and 3b illustrate the interaction effect for the turbidity removal between poly-DADMAC dose and mixing time with softeners only, and between coagulation speed and mixing time with softeners only, respectively. The highest turbidity removal was observed at 99.2% with a coagulation speed of 250 rpm and mixing time with softeners only of 18 min (with poly-DADMAC dose at 70 mg/L and flocculation time at 12 min). When the mixing time of softeners only was below 14 min, decreasing the poly-DADMAC dose led to the increase of turbidity removal whereas no significant difference could be found at different levels of poly-DADMAC dose when mixing time of softeners only was above 14 min. A similar interaction was also observed in TSS removal (Fig. 3.3c). The results may be related to more precipitate produced in softening with longer mixing time with softeners, which can compromise the overdosing effect of coagulant, and the maximum available sites on produced precipitant for coagulant adsorption found at 14 min of mixing with softeners only. As shown in Fig. 3.3b, increasing coagulation speed, accompanied by the increase in mixing time with softeners only, could result in higher turbidity removal. The improvement was probably due to the fraction of successive collision and the precipitation (Dayarathne et al., 2022).
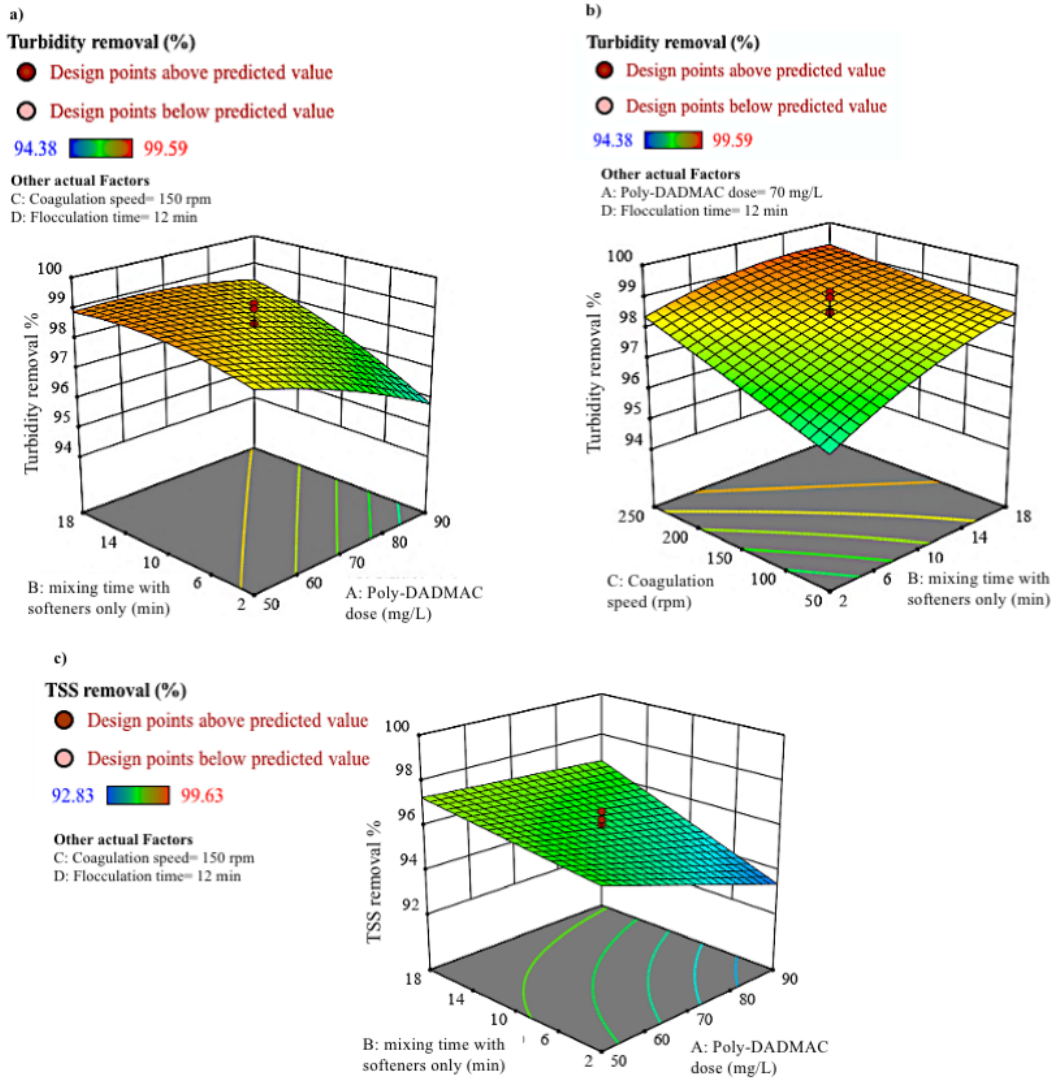
Figure 3.3 Response surface of turbidity removal with the interaction effect of variables: (a) poly-DADMAC dose and mixing time with softeners only, (b) coagulation speed and mixing time with softeners only; and (c) TSS removal with the interaction effects of poly-DADMAC dose and mixing time with softeners only.

3.3.2.2 Particulate hardness removal

The response surface of particulate hardness removal is presented in Fig. 3.4. Fig. 3.4a shows that increasing the mixing time with softeners only and coagulation speed resulted in an increase in the particulate hardness removal to an optimum point, after which further increase in

72

both two variables caused a negative effect on the response. Similarly, Nason and Lawler (2009) found that the mixing intensity strongly influenced $CaCO_3$ production in softening-coagulation. As shown in Fig. 3.4b, increasing flocculation time promoted the hardness removal with longer mixing time with softeners only (> 10 min). Fig. 3.4c shows that for coagulation speed up to 150 rpm, longer flocculation time would increase the removal of particulate hardness. Increasing coagulation speed beyond 150 rpm led to the maximum particulate hardness removal near 100% at coagulation speed of 240 rpm and flocculation time of 12 min (poly-DADMAC dose of 70 mg/L and mixing time with softeners only of 10 min). The results of particulate hardness demonstrated that the removal of hardness is mainly affected by mixing conditions during softening and coagulation.
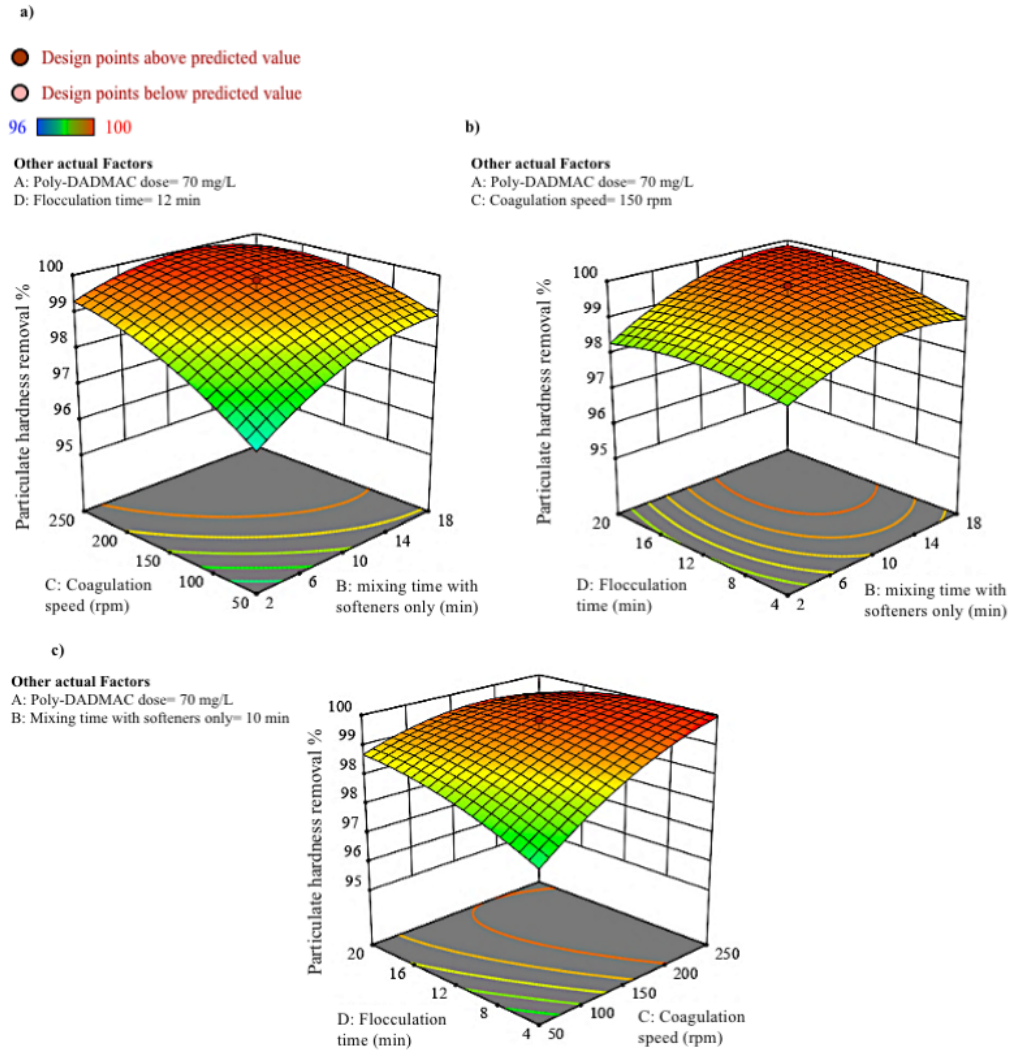
Figure 3.4 Response surface of particulate hardness removal with the interaction effects of variables: (a) coagulation speed and mixing time with softeners only; (b) flocculation time and mixing time with softeners only; and (c) flocculation time and coagulation speed.

3.3.2.3 Silica removal

As shown in Fig. 3.5, significant interactions occurred among poly-DADMAC dose, coagulation speed, flocculation time and mixing time with softeners only on silica removal. In Fig. 3.5a, an increase in poly-DADMAC dose promoted silica removal with longer mixing time with softeners only (>10 min). On the contrary, increasing poly-DADMAC dose enhanced silica removal at lower levels of coagulation speed (<150 rpm) (Fig. 3.5b). To explain these results, it is

hypothesized that more magnesium silicate was produced, or silica adsorption was facilitated by increasing mixing time with softeners only and their settlement was increased with higher poly-DADMAC dose. However, the positive effect of coagulant dose could be hindered by floc breakage due to excessive coagulation speed, which is commonly found in coagulation studies (Yu et al., 2011; Zeng et al., 2007). In Fig. 3.5c, increasing both coagulation speed and mixing time with softeners only would first reduce and later increase the removal efficiency of silica. Similar effects were observed for flocculation time versus mixing time with softeners only and coagulation speed (Fig. 3.5d, 5e), respectively, which indicated the mixing conditions were essential for optimizing silica removal. The highest removal efficiency of silica was found to be 23.3%, with the poly-DADMAC dose of 90 mg/L and mixing time with softeners only of 18 min (coagulation speed was 150 rpm and flocculation time was 12 min).
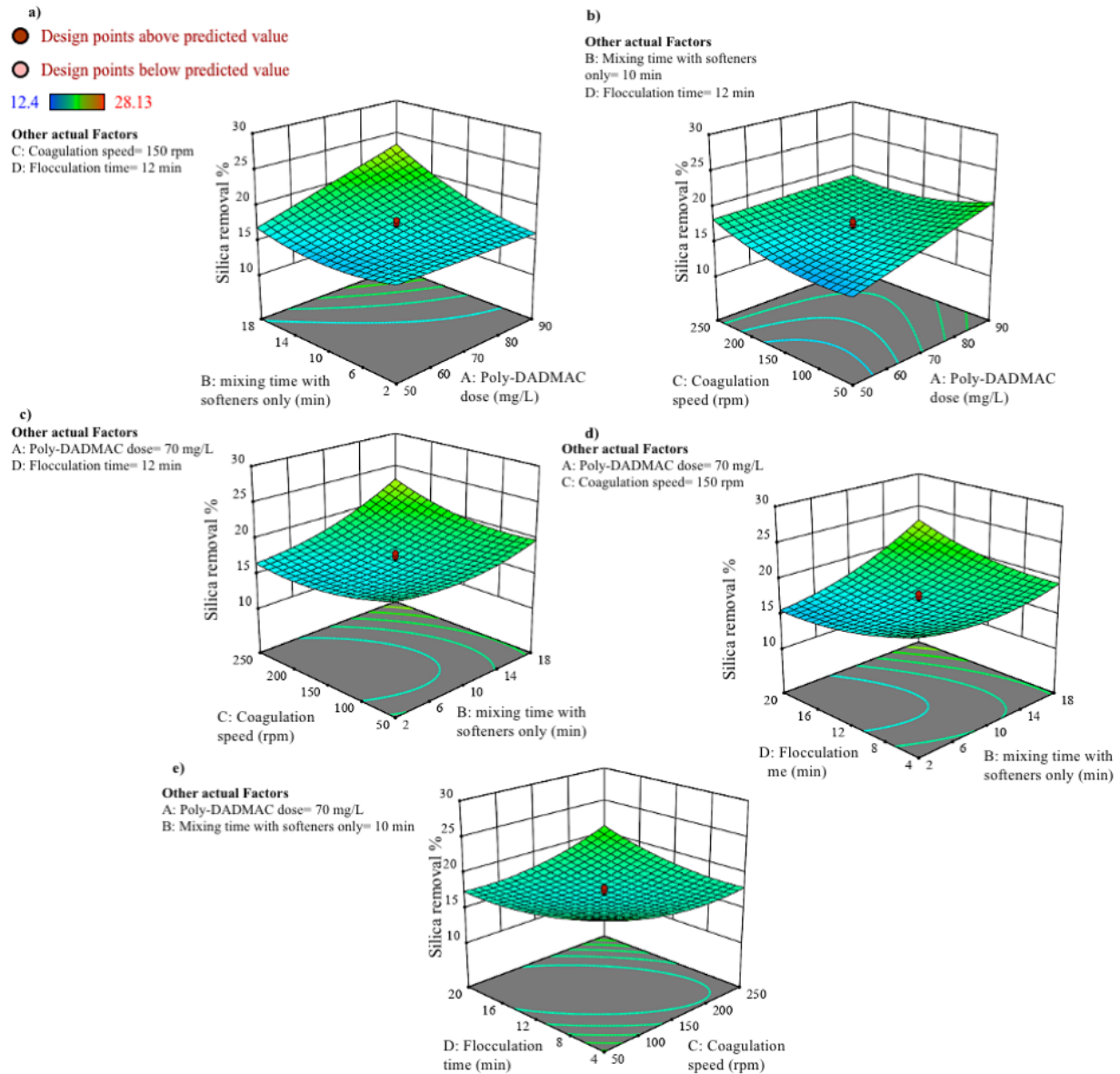
Figure 3.5 Response surface of silica removal with the interaction effects of variables: (a) mixing time with softeners only and poly-DADMAC dose; (b) coagulation speed and poly-DADMAC dose; (c) coagulation speed and mixing time with softeners only; (d) flocculation time and mixing time with softeners only, and (e) flocculation time and coagulation speed.

3.3.2.4 TOC and TIC removal

Fig. 3.6 presents the interaction effects on TOC and TIC removal. From Fig. 3.6a, TOC removal improved with increasing coagulation speed with shorter mixing time with softeners only

(<6 min) while the opposite, lower TOC removal, was observed with faster coagulation speed at longer mixing time with softeners only (>6 min). These results suggest that the organic compounds were mainly removed through adsorption onto the precipitate with prolonged rapid mixing leading to the occurrence of floc breakage. The highest TOC removal achieved was 75.2%, with mixing time with softeners only of 2 min and coagulation speed of 250 rpm (poly-DADMAC dose was 70 mg/L and flocculation time was 12 min). In terms of TIC removal, the positive effects of poly-DADMAC dose mainly occurred at slower coagulation speed (<150 rpm) or longer flocculation time (>12 min) (Fig. 3.6b, 6c). When coagulation speed was slow, TIC removal reduced with longer flocculation time, but this was reversed at faster coagulation speeds (Fig. 3.6d). The highest TIC removal was 34.3%, with poly-DADMAC dose of 90 mg/L and coagulation speed of 50 rpm (mixing time with softeners only was 10 min and flocculation time was 12 min).
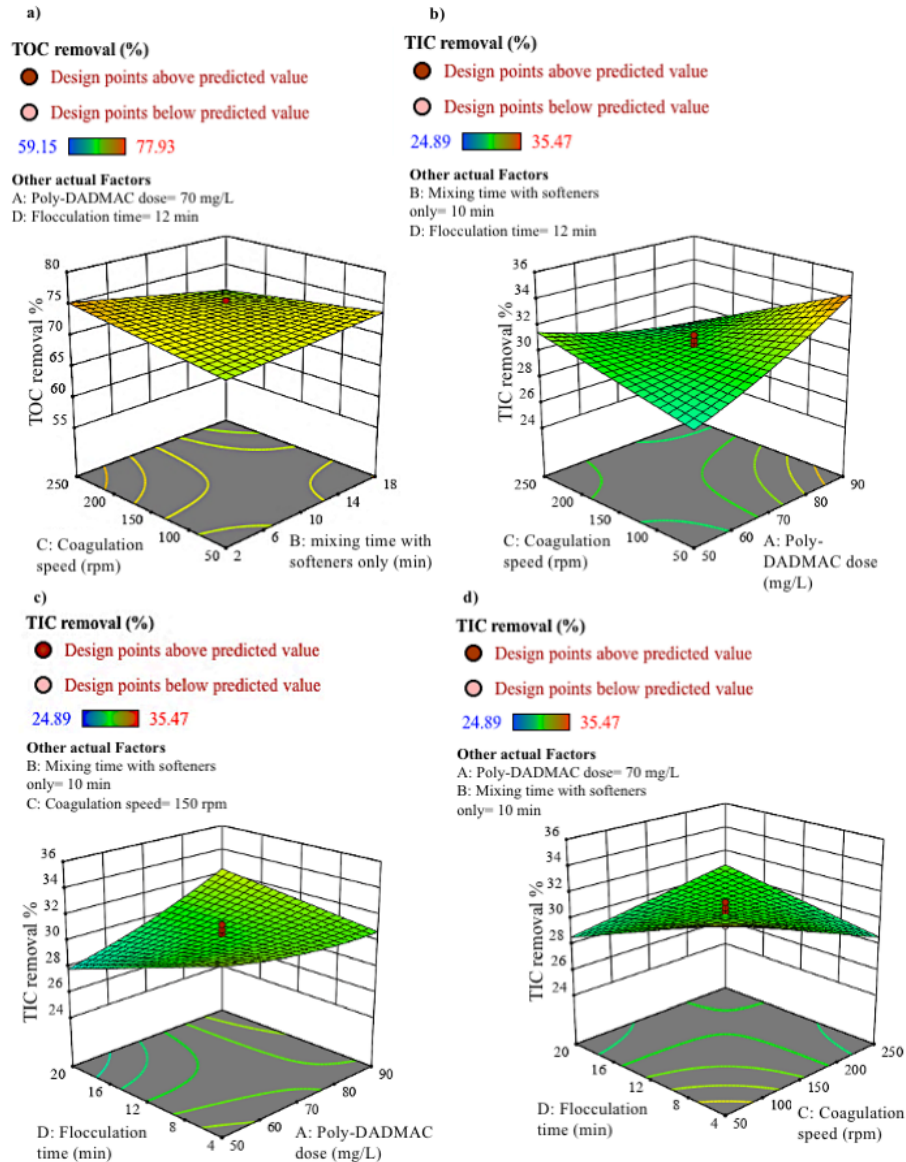
Figure 3.6 Response surface of (a) TOC removal with the interaction effect of coagulation speed and mixing time with softeners only, and TIC removal with the interaction effects on variables: (b) coagulation speed and poly-DADMAC dose; (c) flocculation time and poly-DADMAC dose; and (d) flocculation time and coagulation speed.

3.3.2.5 SVI

Fig. 3.7 shows the interaction effects on SVI. Based on Fig. 3.7a, 7b, poly-DADMAC had limited effect at shorter mixing time with softeners only (<10 min) and at longer flocculation time (>12 min). On the other hand, increasing poly-DADMAC dose could reduce SVI when mixing time with softeners only was long (>10 min) and flocculation time was short (<12 min), respectively. The SVI results implied that longer mixing time with softeners only with higher coagulant dose allowed particles were bridged and rapidly settled; however longer flocculation time would hinder this positive interaction due to floc breakage. Wu et al. (2019) also found floc breakage as flocculation time increased. Fig. 3.7c shows that reduction of SVI with increasing coagulation speed was observed at longer flocculation time (>12 min). Previous studies (Wu et al., 2019; Zhou et al., 2012) suggested that the size of flocs decreased with increase of mixing speed, resulting in an increase of the total surface areas of flocs and hence more polymers could adsorb. Under this situation, longer flocculation time would allow more bridging to occur and denser flocs could be settled. In CF processes, low SVI values (< 200 mL/g) are indicative of good quality of flocs that can be readily settled or densified (Crittenden et al., 2005). The lowest SVI was observed at 31.8 mL/g, with poly-DADMAC dose of 90 mg/L, and flocculation time of 4 min (mixing time with softeners only was 10 min and coagulation speed was 150 rpm, respectively).
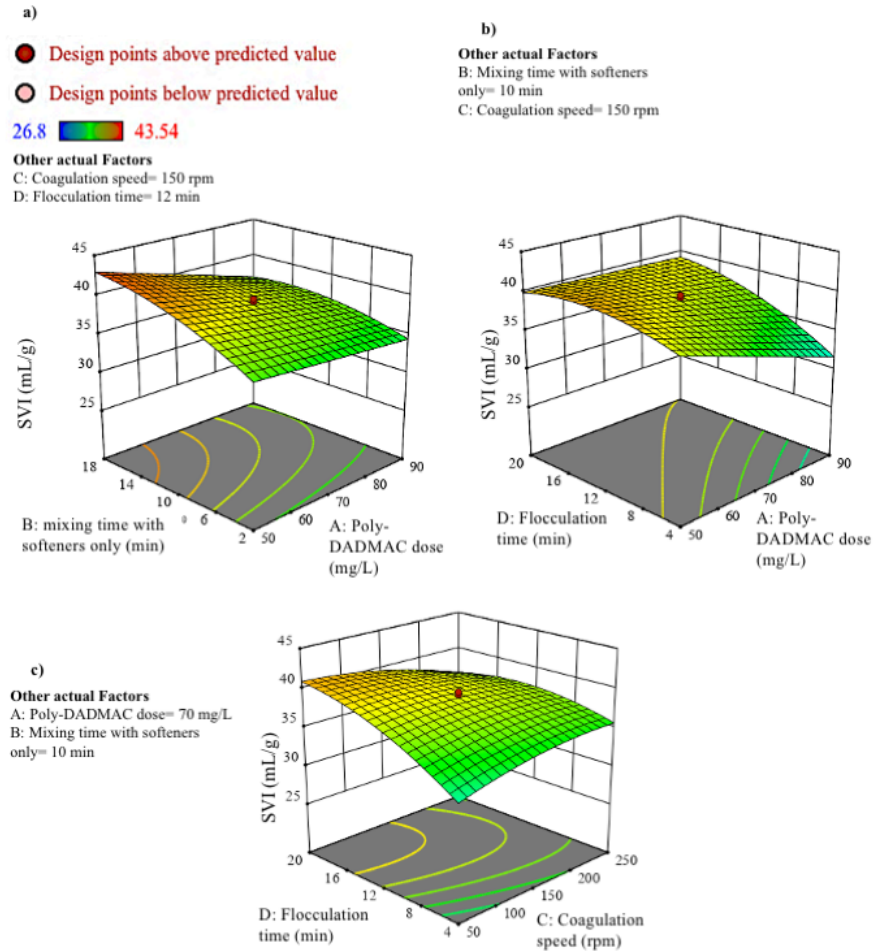
Figure 3.7 Response surface of SVI with the interaction effects of variables: (a) mixing time with softeners only and poly-DADMAC dose; (b) flocculation time and poly-DADMAC dose; and (c) flocculation time and coagulation speed.

3.3.3 Optimization and validation experiments

To determine the optimal conditions, a numerical optimization was carried out. The desired goals for each variable and response are presented in Table 3.4. The goal was set to "maximize" for the most of removal efficiency and was set "within the range" for SVI. For the operational variables, the poly-DADMAC dose was minimized as less chemical dose is more desirable in industry whereas other variables were set as "within the range". Subsequently,

among 100 potential solutions, the optimal condition with 0.93 desirability was identified at 67

mg/L, 14 min mixing time with softeners only, 200 rpm coagulation speed, and 16 min

flocculation time (Fig. 3.8). This solution corresponds to 38.1 mL/g, 99.2%, 99.1%, 99.4%,

27.0%, 69.0%, and 30.3% for SVI and the removal efficiencies of turbidity, TSS, particulate

hardness, silica, TOC, and TIC, respectively. The validity of estimated optimum conditions was

confirmed with triplicated experimental runs. Table 3.5 shows that the average experimental

results were in agreement with the predicted values with deviation < 2%.

Table 3.4 The constraints adopted for the determination of desirability.

	Variables	Goal	Lower limit	Upper limit	Lower weight	Upper weight	Importance coefficients
Inputs	Poly-DADMAC dose	minimize	60	80	1	0.1	5
	Mixing time with softeners only	within range	6	14	1	0.1	3
	Coagulation speed	within range	100	200	0.1	1	3
	Flocculation time	within range	8	16	1	0.1	3
Outputs	Turbidity removal	maximize	94.38	99.59	1	1	2
	TSS removal	maximize	92.83	99.63	1	1	2
	Particulate hardness removal	maximize	95.91	99.88	0.1	1	4
	Silica removal	maximize	12.4	26.42	0.1	1	4
	TOC removal	maximize	59.15	77.93	1	1	1
	TIC removal	maximize	24.89	35.47	0.1	1	3
	SVI	within range	26.8	43.54	1	1	2

Table 3.5 Validation results of multiple-response process optimization.

Variable	Response-predicted (observed)

Poly-DADMAC dose (x_1)	Mixing time with softeners only (x_2)	Coagulation speed (x_3)	Flocculation time (x_4)	Turbidity removal (%)	TSS removal (%)	Particulate hardness removal (%)	Silica removal (%)	TOC removal (%)	TIC removal (%)	SVI (mL/g)
67 mg/L	14 min	200 rpm	16 min	99.18 (98.99)	99.11 (98.83)	99.36 (99.53)	27.00 (25.16)	69.01 (68.56)	30.28 (30.55)	38.07 (39.52)
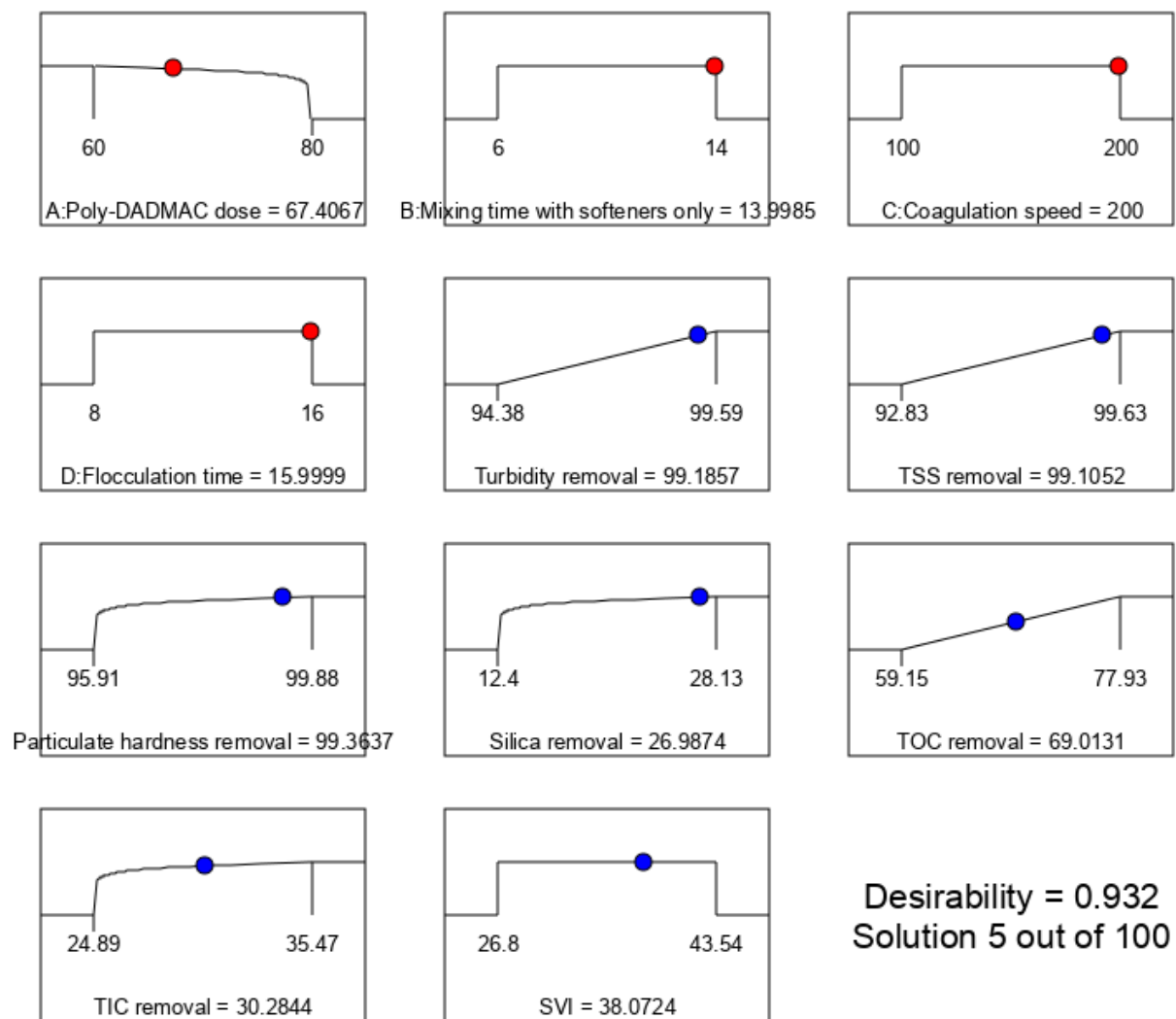
Figure 3.8 Ramp plots of numerical optimized conditions and responses.

3.3.4 Floc characterization and surface interaction

3.3.4.1 Floc analysis

According to SEM images in Fig. 3.9, the formed flocs (Fig. 3.9b, 9c) had an irregular and polyhedral shape with relative rough and non-uniformly distributed porous structures compared to the raw particles (Fig. 3.9a). This observation revealed that the aggregation of fine particles occurred during the treatment process. It is also evident from the SEM images that the treatment process led to the formation of larger and aggregated flocs (Fig. 3.9d, 9e, 9f). In addition, the flocs formed after optimal process at high temperature (80 °C) had a wider range from 0-120 μm with the peak of particle size distribution at 30 μm while the flocs formed under room temperature had narrower range of 0-80 μm with the peak of particle size distribution at 20 μm, indicating that increasing temperature could facilitate settling by forming larger and denser flocs. Several reports have shown that floc settling is temperature dependent (Dayarathne et al., 2022; Mohammadtabar et al., 2019; Zhou et al., 2012). An increase in temperature would increase the proportion of particles activated to overcome repulsive forces to aggregate, thus enhancing the overall aggregation rate.

Table 3.6 presents the detailed elemental composition of raw particles and flocs determined by EDS analysis. In both raw particles and flocs, O and C were the most abundant elements, while Na, Al, Si, Ca, Mg, S, and K were found at relatively low concentrations. The percentage of C, O, Al, Si, Ca, and Mg on the formed flocs increased, indicating that the hardness component (Ca^{2+}, Mg^{2+}), kaolinite, silica, and organics could be removed after the treatment process. In addition, it is worthy to notice that the percentage of O (41.00 %), Al (10.57%), Si (8.53%), Ca (6.45%), and Mg (4.50%) in the flocs formed at high temperature (80 °C) are higher than the flocs formed at room temperature (O:39.65%, Al:8.46%, Si:7.10%, Ca:5.30%, Mg:3.20%). Percent C is higher in

room temperature flocs (28.04%) as compared with the high temperature (80 °C) flocs. This finding suggests that increasing the temperature can be beneficial for the treatment by affecting not only the floc size but also the floc composition by influencing the surface charge, metal-ion species, and adsorption of polymers (Dayarathne et al., 2022; Mpofu et al., 2004).
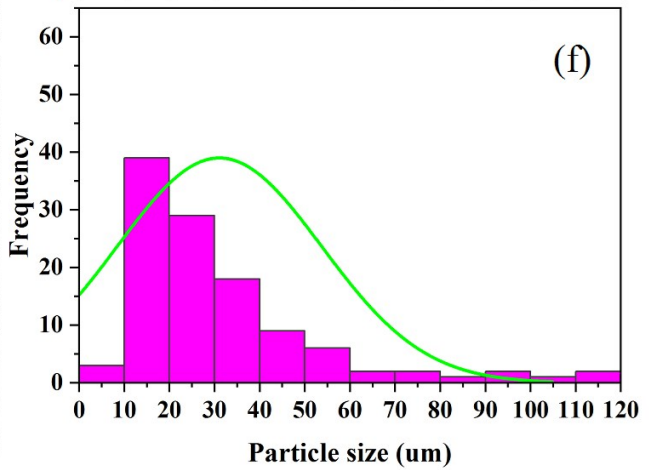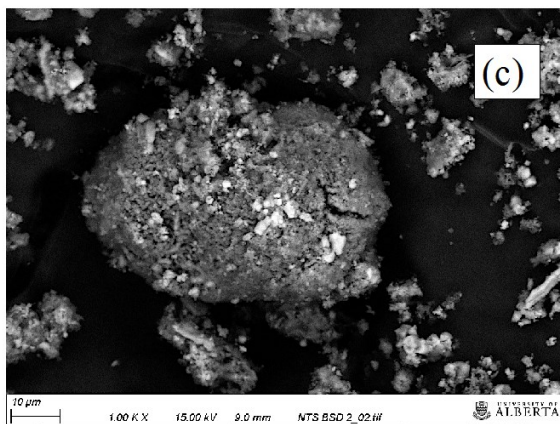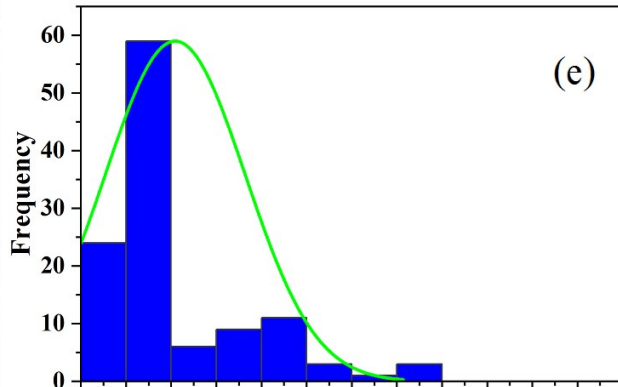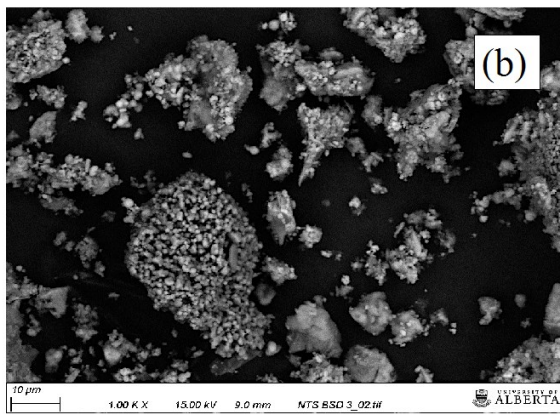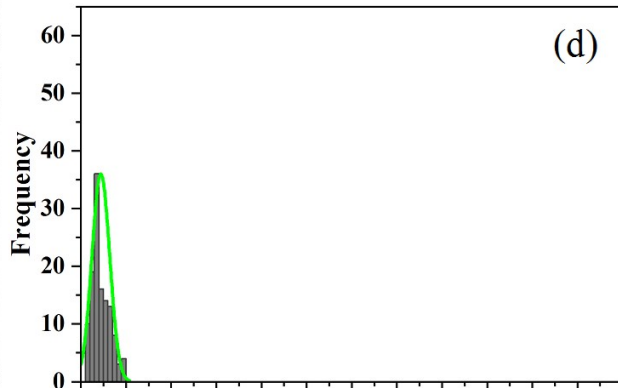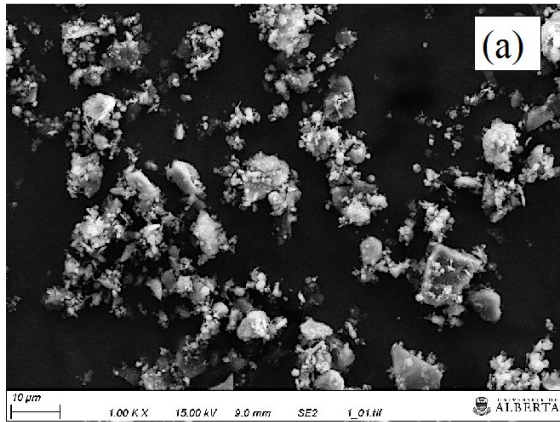
Figure 3.9 SEM images of (a) raw particles, (b) flocs after treatment at 20 °C, (c) flocs after treatment at 80 °C and particle size distribution of (d) raw particles, (e) flocs after treatment at 20 °C, and (f) flocs after treatment at 80 °C.

Table 3.6 Chemical composition of raw particles and flocs after treatment at optimal condition under different temperatures by EDS analysis.

Sample	Element (wt%)										Sum
	O	C	Na	Al	Si	Cl	Ca	Mg	S	K	
Raw	15.50	22.90	17.20	5.10	3.60	29.70	1.50	0.10	2.63	1.80	100.03
After treatment at 20 °C	39.65	27.60	4.68	8.46	7.10	3.90	5.30	3.20	0.10	0.00	99.99
After treatment at 80 °C	41.00	28.04	0.50	10.57	8.53	0.40	6.45	4.50	0.00	0.00	99.99

The XRD patterns of the raw particles and flocs are shown in Fig. 3.10a. The appearance of kaolinite and $CaCO_3$ in the formed flocs demonstrated that they were successfully removed from water. The observed peaks in the formed flocs at $2\theta = 42.5°$, $50.3°$, and $73.8°$ were associated with MgO (Zhang et al., 2021a), which was probably a residual of added MgO. It is interesting to note that the peaks of amorphous magnesium silicate was only observed in the formed flocs at room temperature, while the $Mg(OH)_2$ peaks ($2\theta = 44.8°$, $60.5°$ and $68.9°$) were only found at high temperature. This indicates that silica and Mg^{2+} removals at room temperature were achieved mainly by the coprecipitation as magnesium silicates while at high temperature this occurred through adsorption of silica on $Mg(OH)_2$. Additionally, very weak peaks of $Ca(OH)_2$ appeared in the flocs formed under high temperature, which can be explained by the decreased solubility of $Ca(OH)_2$ at elevated temperature (Deschner et al., 2013).

Fig. 3.10b shows the FTIR spectra of raw particles and flocs. The peaks at 3691 cm^{-1}, 1030 cm^{-1}, 1006 cm^{-1}, 913 cm^{-1} are the characteristic peaks of kaolinites (Osacky et al., 2013; Sam-Tunsa Alarba et al., 2022). For the formed flocs, the intensity of the kaolinite peaks increased dramatically, especially for peaks at 1030 cm^{-1} and 1006 cm^{-1} in the flocs formed under high temperature (80 °C). The band at 3618 cm^{-1} is associated with the structural hydroxyl group (Geçer, 2022), which can belong to magnesium silicates or Ca(OH)$_2$ and Mg(OH)$_2$. The peak at 1407 cm^{-1} can be attributed to the carboxylic group, which could come from humic acid salts and also polymers (Hay and Myneni, 2007; Parvathy and Jyothi, 2012). Similar to kaolinite, the peaks of carboxylic group were found to be more intense in the flocs formed under high temperature. The 1112 cm^{-1} peak and the 873 cm^{-1} peak observed in the low-frequency region can represent NaCl and carbonates, respectively (Kumar et al., 2012; Osacky et al., 2013). The intensity of carbonate peaks in the flocs increased probably due to produced CaCO$_3$ during the softening process. The peaks centered at 795 cm^{-1} and 740 cm^{-1} can be assigned to Si-O (Sam-Tunsa Alarba et al., 2022), which may originate from magnesium silicates or from silica. The higher intensity of these two peaks in the formed flocs demonstrates that silica can be removed by the treatment process. The peak at 650 cm^{-1} could be due to the presence of residual MgO (Chen et al., 2008). Therefore, the FTIR data are in agreement with the EDS and XRD results, confirming that Mg, Ca, Si, kaolinite, and humic acid are in the precipitated sludge and increasing the temperature can promote the removal process.

The zeta potentials of the suspended particles in raw water and the supernatant of treated water are presented in Fig. 3.10c. In the raw water sample, the zeta potential was -40.45 mV ($\pm$ 2.75) which suggested that the kaolinite and silica particles had a negative surface charge. After adding softeners and cationic polymers, the zeta potential became less negative, confirming that

charge neutralization was occurring during the treatment process. Besides, an increase of zeta potential of supernatant, from -31.24 mV ($\pm$ 0.85) to -26. 93 mV ($\pm$ 2.28), with increasing temperature was observed, which indicated that higher temperature could promote charge neutralization via increasing the adsorbed polymers density (Mpofu et al., 2004) and having a more stretched conformation of polymer chains (Wiśniewska, 2012).
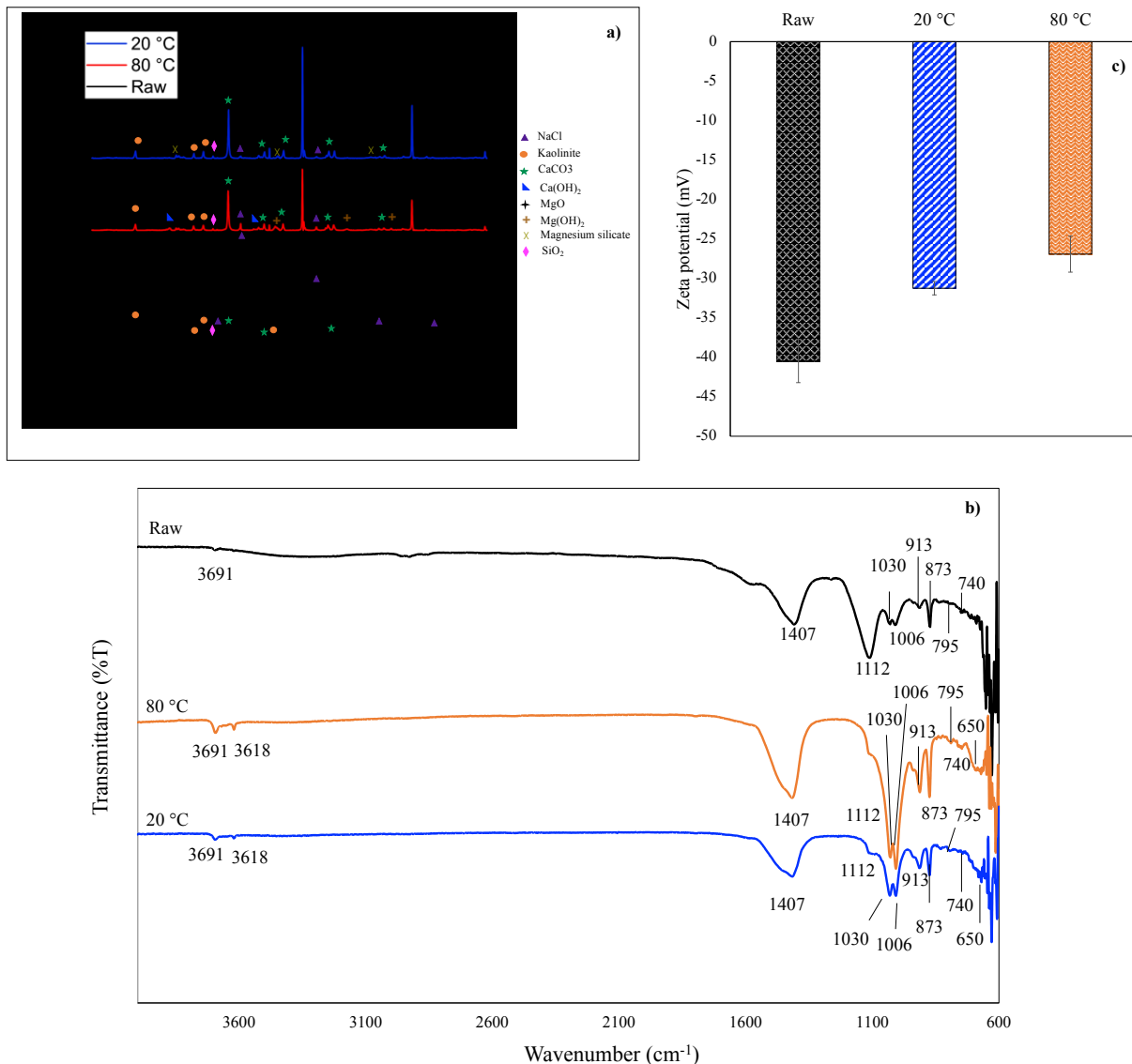
Figure 3.10 XRD, FTIR and zeta potential analysis of raw particles and flocs after optimal treatment under 20 °C and 80 °C: (a) XRD patterns, (b) FTIR spectra, and (c) zeta potential.

The XPS survey spectrum is shown in Fig. A.2 and the high-resolution Ca 2p, Mg 2p, Si 2p, O 1s, C 1s spectra of each solid are shown in Fig. 3.11. Due to shifting that was observed in most XPS peaks of the formed flocs at room temperature (~ 3.5 mV), the reported values are the results after correction. The shifting can be explained by internal errors from instruments and difference of materials, which may result in poor agreement between the results obtained by different groups (Ni and Ratner, 2008; Ulgut and Suzer, 2003). As shown in Fig. 3.11a, the Ca 2p high-resolution spectra in the formed flocs at room temperature clearly shows well-defined peaks at 350.6 eV and 347.1 eV with a peak area ratio of 1:2, which can be assigned to $CaCO_3$ (Xiao et al., 2021). For the flocs formed at high temperature (Fig. 3.11b), the Ca 2p was deconvoluted into four peaks at 350.8 eV, 346.9 eV, 349.8 eV, and 346.2 eV, suggesting that the solids were a mixture of $CaCO_3$ and $Ca(OH)_2$ (Feng et al., 2018; Ni and Ratner, 2008). For the Mg 2p, two peaks at 50.4 eV and 49.8 eV ascribable to Mg-O-Si and Mg-O, respectively, were observed in the formed flocs at room temperature, whereas two peaks at 48.71 eV and 49.29 eV, corresponding to Mg-OH and Mg-O, respectively (Keikhaei and Ichimura, 2019; Zhang et al., 2021a), were found at high temperature. These peaks indicate that the formed solids at room temperature were a mixture of magnesium silicates and residual MgO, while they were a mixture of MgO and $Mg(OH)_2$ at high temperature. The Si 2p peak for the solids formed at room temperature was deconvoluted into two peaks, at 102.1 eV and 102.8 eV, corresponding to the Si-O and Mg-O-Si bonds of the formed magnesium silicate, respectively (Zhang et al., 2021a). However, only one peak of Si-O (102.2 eV) was present at high temperature, suggesting that the silica was removed mainly through precipitation at room temperature, while it was removed by adsorption at high temperature. The peaks of O 1s at 533.0 eV and 532.7 eV in the formed flocs can be assigned to the O-C=O (Zhao et al., 2021). At the same time, the C 1s contains peaks at 284.8 eV (C-C and C-H) (Zhang et al.,

2018), 287.8 eV and 288.0 eV (O-C=O) (Chen et al., 2020), were also observed in formed flocs. The peaks of O 1s and C 1s indicate that humic acids were removed and settled with polymers after the treatment. Overall, XPS data is in agreement with the FTIR and XRD results.
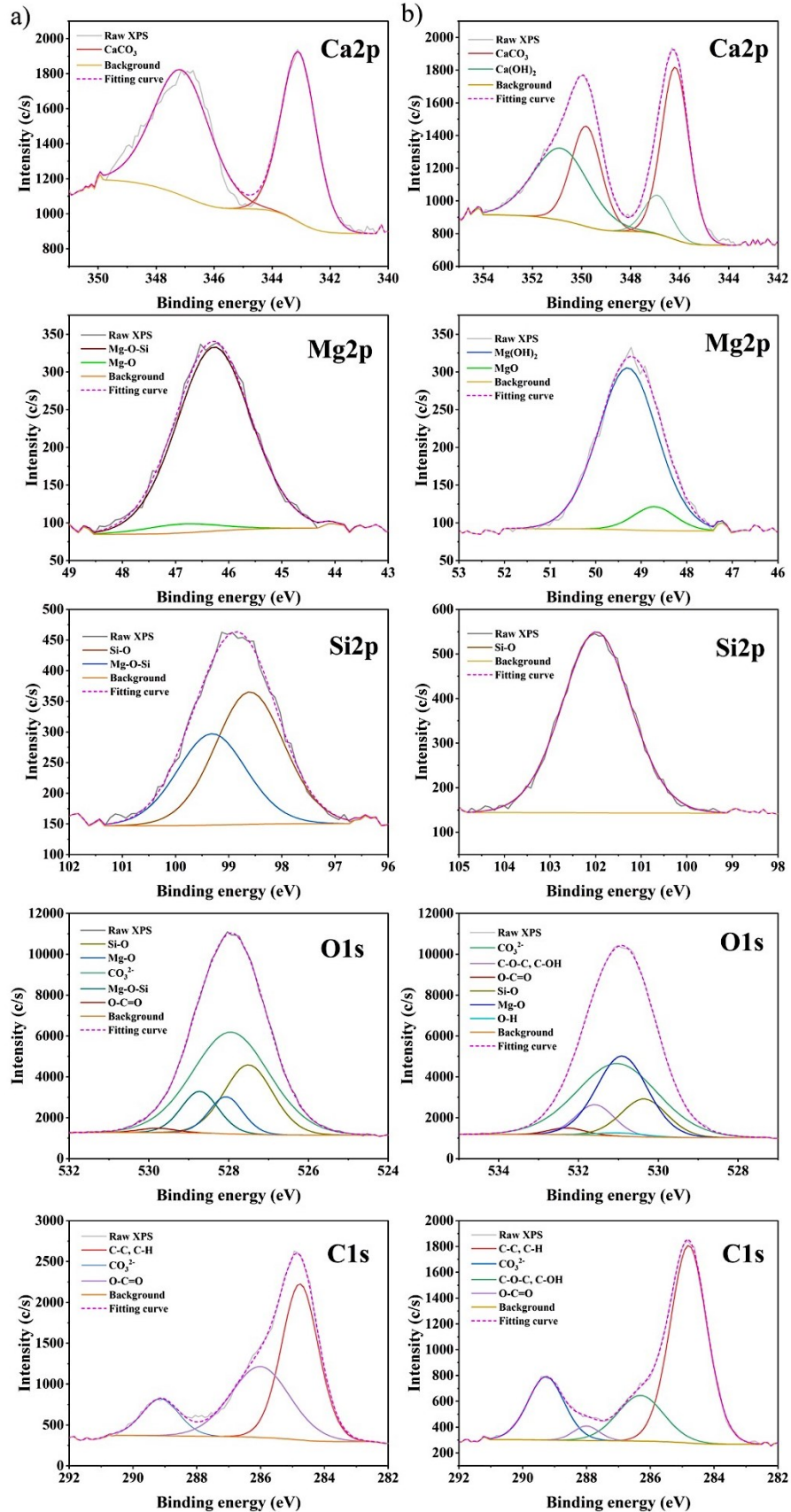
Figure 3.11 High-resolution XPS of Ca 2p, Mg 2p, Si 2p, O 1s, C 1s spectra of (a) flocs after optimal treatment at 20 °C and (b) flocs after treatment at 80 °C.

3.3.4.2 Surface force measurement

To further unravel the adsorption behavior and interaction mechanisms of polymers on the particle surfaces underlying the coagulation-flocculation process, surface force measurements using an SFA were performed. The force-distance profiles between two mica surfaces in 1000 mg/L poly-DADMAC solution and in a mixture of 1000 mg/L of poly-DADMAC and 100 mg/L cationic PAM are presented in Fig. 3.12. As in Fig. 3.12a, about 6.5 nm of polymer film was confined between mica surfaces whereas no adhesion (F_{ad}/R) was detected, which indicates that the main function of poly-DADMAC was to neutralize negative charge by adsorbing on the surface of particles. When mica surfaces were in the mixture of poly-DADMAC and cationic PAM (Fig. 3.12b), an adhesion F_{ad}/R value of ~ -1.8 mN/m with adsorbed polymer thickness of ~11.1 nm between two mica surfaces was measured during the separation. Such increased thickness and adhesion force observed in the polymer mixture suggested that the adhesion was mainly due to cationic PAM that bridged two mica surfaces via electrostatic attraction. The surface force results demonstrated that adding poly-DADMAC as coagulant and cationic PAM as flocculant could enhance the attractive interactions between the suspended particles via adsorption and subsequent bridging.
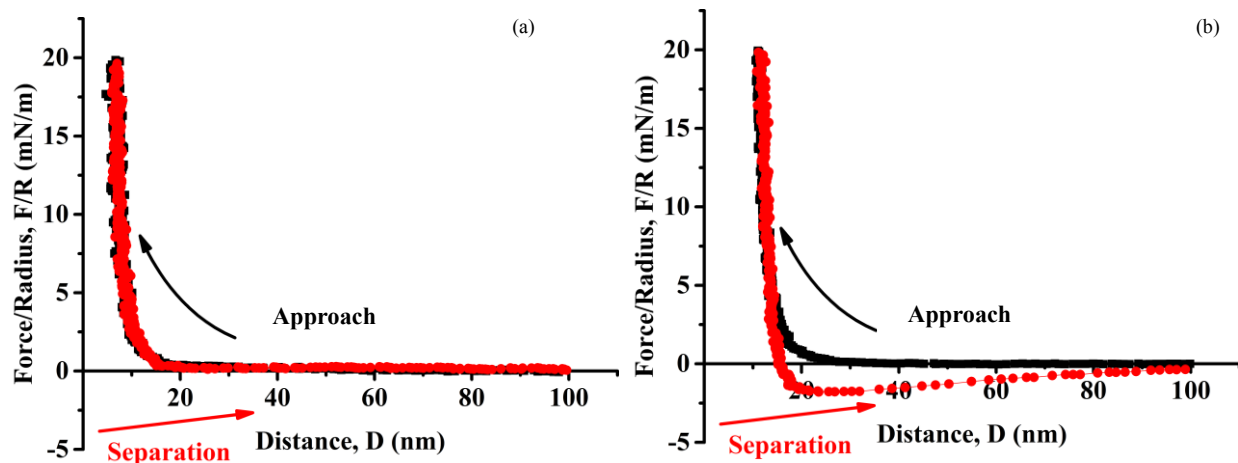
Figure 3.12 Normalized forces-distance profiles between mica surfaces in (a) 1000 mg/L poly-DADMAC solution and (b) mixture of 1000 mg/L poly-DADMAC and 100 mg/L cationic PAM.

3.3.5 Removal mechanisms of softening-coagulation-flocculation

The removal mechanisms for impurities in softening-CF at 20 °C and 80 °C are outlined in Fig. 3.13. According to floc characterization results, the hardness components (Ca^{2+} and Mg^{2+}) were removed by forming $CaCO_3$ and $Mg(OH)_2$ particles simultaneously during lime softening at high temperature (80 °C), whereas Mg^{2+} would be removed by coprecipitation with silica at room temperature. For silica removal with MgO, the above results at room temperature confirmed the formation of magnesium silicates and demonstrated that the precipitation would be the dominant mechanism, which is in agreement with reported studies (Latour et al., 2015; Zhang et al., 2021a). However, only the $Mg(OH)_2$ peak appeared in the flocs formed under high temperature, indicating that the adsorption on freshly precipitated $Mg(OH)_2$ from MgO became the main mechanism for silica removal. Similar results were also observed by Zhang et al. (2021a). With increasing temperature, the solubility of $Mg(OH)_2$ decreases, resulting in the limited amount of Mg^{2+} ions in the water and hence the formation of magnesium silicate would be hindered. Besides, the pH of treated water was about 10.4 at high temperature. Due to the fact that the freshly precipitated

Mg(OH)$_2$ is positively charged and silica is negatively charged with a pH ranging from 10.2 to 11.2 (Black and Christman, 1961; Zhang et al., 2020), silica adsorption on Mg(OH)$_2$ at high temperature is likely to occur. Previous studies demonstrated that natural organic matter can be removed via coprecipitation with other precipitated particles (Russell et al., 2009a; Russell et al., 2009b). Additionally, the humic acid could be removed through coprecipitation with formed inorganics solids such as CaCO$_3$ and Mg(OH)$_2$ during the lime softening. The adsorption of humic acids on these inorganic surfaces could occur through ligand exchange of functional groups on the humic substances with hydroxyl groups on the surface of metal oxides, or via the binding of metal ions to the carboxyl and hydroxyl groups on humic acids in a bidentate form (Stumm and Morgan, 1992). After the softening process, as confirmed by SFA results, poly-DADMAC coagulant was added first to neutralize the surface charge and create a collision condition between particles, thus forming small flocs. Then cationic PAM was added to increase larger flocs by forming bridges between small flocs. The increase in zeta potential and in adhesion force after treatment validated that the charge neutralization and bridging process occurred during the coagulation-flocculation process. It is worth noting that other impurities like residual bitumen may affect the findings of interactions and removal mechanism during coagulation/flocculation obtained in this study. Both positive and negative effect of residual bitumen on coagulation/flocculation have been observed in previous studies (Carreras et al., 2013; Klein et al., 2013). Future experiments may be planned to explore the effect of residual bitumen and other impurities on the performance of the treatment.
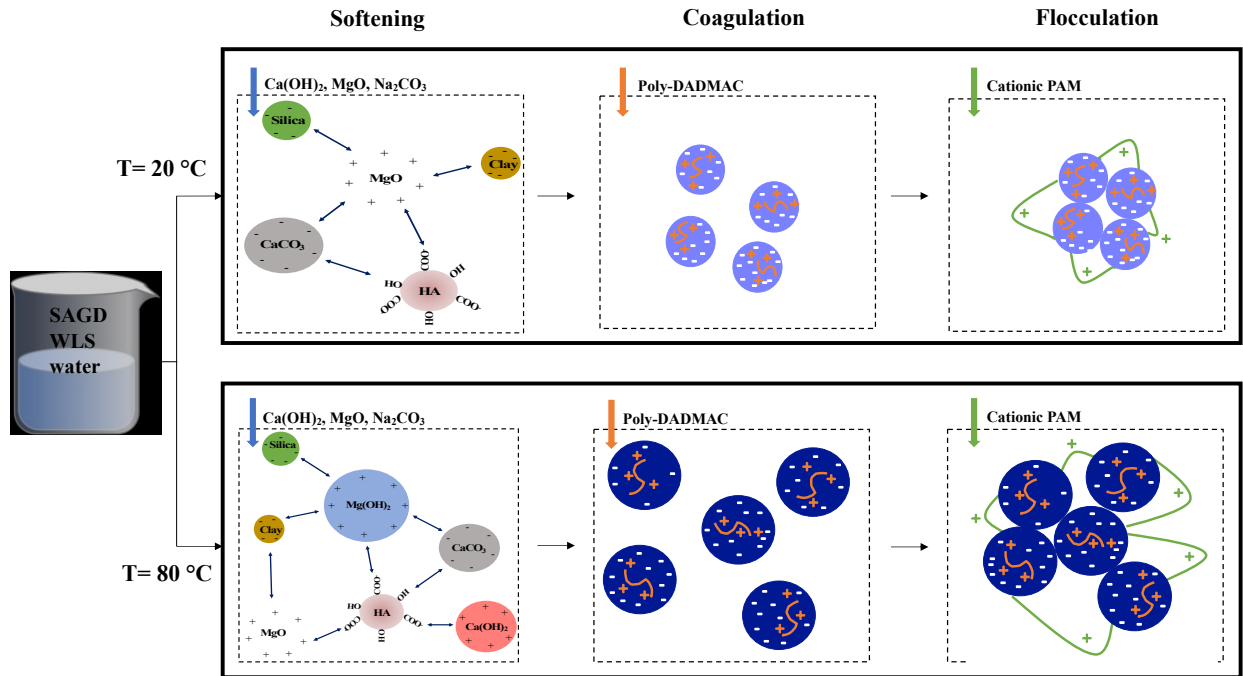
Figure 3.13 A schematic for proposed removal mechanisms in softening-coagulation-flocculation at 20 °C and 80 °C.

3.4. Conclusion

In this study, CCD-RSM was adopted to determine the optimal conditions for softening-CF-sedimentation and to investigate the interaction effects of operational variables in synthetic SAGD WLS water under high temperature (80 °C) by testing the responses of the SVI and the removal of turbidity, TSS, particulate hardness, silica, TOC and TIC. Overall, the statistical analysis suggested that poly-DADMAC dose and mixing time with softeners only were the most important factors for the treatment process due to their significant linear, quadratic and interaction effects on most responses. Increasing mixing time with softeners only could negate negative effect of poly-DADMAC dose on both turbidity and TSS removal, indicating that more precipitate produced in softening can compromise the overdosing effect of coagulant. Increasing coagulation speed could magnify the positive effect of mixing time with softeners only on silica removal, which

is contrary to their interaction effect on particulate hardness removal, suggesting that their removal mechanisms were different even though they can be removed simultaneously in softening. The results of interaction effects on the removal of TOC and TIC demonstrated that TOC were affected mainly by softening and coagulation whereas coagulation and flocculation were important for TIC removal. The interaction results for SVI confirmed that particles with more segments allowed for the addition of polymeric chains which could then be bridged and rapidly settled with increasing polymer dose whereas longer flocculation time would cause floc breakage. The optimal conditions for softening-CF-settling at 0.93 desirability were 67 mg/L poly-DADMAC dose, 14 min mixing time with softeners only, 200 rpm coagulation speed, and 16 min flocculation time. At these conditions, the predicted maximum removal of turbidity, TSS, particulate hardness, silica, TOC and TIC were 99.2%, 99.1%, 99.4%, 27.0%, 69.0%, and 30.3%, respectively, and the value of SVI was 38.1 mL/g. The temperature effect on the removal mechanisms was explored by comparing the characteristics of flocs formed under optimal conditions at room temperature and high temperature (80 °C). The results indicated that increasing temperature could facilitate the removal of colloidal impurities by forming larger and denser flocs and changing their surface composition. In addition, SFA results confirmed that the adsorption and subsequent bridging are the main mechanisms for poly-DADMAC and cationic PAM in the CF process. Our research covers a wide range of operational variables, their interactions and provide in-depth insight into the mechanisms of removing impurities. Given other impurities like residual bitumen may affect current findings of interactions and removal mechanism during CF process, future experiments may be planned to explore the effect of residual bitumen and other impurities on the performance of the treatment. Nevertheless, the insights gained from this study can be applied to enhance the removal efficiency in on-site produced water treatment processes.

95

3.5 References

Ahmadi, M., Vahabzadeh, F., Bonakdarpour, B., Mofarrah, E., Mehranian, M., 2005. Application of the central composite design and response surface methodology to the advanced treatment of olive oil processing wastewater using Fenton's peroxidation. Journal of Hazardous Materials 123(1-3), 187-195.

AWWA, 2017. Standard methods for the examination of water and wastewater. 23rd Edition. American Public Health Association, American Water Works Association, Water Envrionmental Federation, New York.

Bhandari, V.M. and Ranade, V.V., 2014. Advanced physico-chemical methods of treatment for industrial wastewaters. Industrial wastewater treatment, recycling and reuse, 81-140.

Black, A., Christman, R.F., 1961. Electrophoretic Studies of Sludge Particles Produced in Lime-Soda Softening. Journal- American Water Works Association 53(6), 737-747.

Butler, R.M., 1994. Steam-assisted gravity drainage: concept, development, performance and future. Journal of Canadian Petroleum Technology 33(02), 44-50.

Carreras, E.S., Passade-Boupat, N., Bourrel, M., Sedgwick, A., Yang, X., Junaid, A., 2013. Residual bitumen and flocculation: do we understand its effects?, Proceedings of the Seventeenth International Conference on Tailings and Mine Waste, November. pp. 3-6.

Chen, H., Li, Q., Wang, M., Ji, D., Tan, W., 2020. XPS and two-dimensional FTIR correlation analysis on the binding characteristics of humic acid onto kaolinite surface. Science of the Total Environment 724, 138154.

Chen, L., Xu, C., Zhang, X.-F., 2008. DFT calculations of vibrational spectra and nonlinear optical properties for MgO nanotube clusters. Journal of Molecular Structure: THEOCHEM 863(1-3), 55-59.

Chow, H., Pham, A.L.-T., 2019. Effective removal of silica and sulfide from oil sands thermal in-situ produced water by electrocoagulation. Journal of hazardous materials 380, 120880.

Dayarathne, H., Angove, M.J., Jeong, S., Aryal, R., Paudel, S.R., Mainali, B., 2022. Effect of temperature on turbidity removal by coagulation: Sludge recirculation for rapid settling. Journal of Water Process Engineering 46, 102559.

Deschner, F., Lothenbach, B., Winnefeld, F., Neubauer, J., 2013. Effect of temperature on the hydration of Portland cement blended with siliceous fly ash. Cement and concrete research 52, 169-181.

Feng, B., Guo, W., Peng, J., Zhang, W., 2018. Separation of scheelite and calcite using calcium lignosulphonate as depressant. Separation and Purification Technology 199, 346-350.

Forshomi, Z.D., Alva-Argaez, A., Bergerson, J.A., 2017. Optimal design of distributed effluent treatment systems in steam assisted gravity drainage oil sands operations. Journal of cleaner production 149, 1233-1248.

Gao, B.Y., Wang, Y., Yue, Q.Y., Wei, J.C., Li, Q., 2008. The size and coagulation behavior of a novel composite inorganic–organic coagulant. Separation and Purification Technology 62(3), 544-550.

Geçer, A., 2022. Relation of the grain size, petrophysical parameters, and Fourier transform infrared analysis of Kusuri sandstones in the Zonguldak subbasin of the West Black Sea, Turkey. BULGARIAN CHEMICAL COMMUNICATIONS 4(3), 235-241.

Hay, M.B., Myneni, S.C., 2007. Structural environments of carboxyl groups in natural organic molecules from terrestrial systems. Part 1: Infrared spectroscopy. Geochimica et cosmochimica acta 71(14), 3518-3532.

Heins, W., 2010. Is a paradigm shift in produced water treatment technology occurring at SAGD facilities? Journal of Canadian Petroleum Technology 49(01), 10-15.

Hurwitz, G., Pernitsky, D.J., Bhattacharjee, S., Hoek, E.M., 2015. Targeted removal of dissolved organic matter in boiler-blowdown wastewater: integrated membrane filtration for produced water reuse. Industrial & Engineering Chemistry Research 54(38), 9431-9439.

Huzir, N.M., Aziz, M.M.A., Ismail, S., Mahmood, N.A.N., Umor, N., Muhammad, S.A.F.a.S., 2019. Optimization of coagulation-flocculation process for the palm oil mill effluent treatment by using rice husk ash. Industrial Crops and Products 139, 111482.

Ji, Y., Lu, Q., Liu, Q., Zeng, H., 2013. Effect of solution salinity on settling of mineral tailings by polymer flocculants. Colloids and Surfaces A: Physicochemical and Engineering Aspects 430, 29-38.

Karami, P., Khorshidi, B., McGregor, M., Peichel, J.T., Soares, J.B., Sadrzadeh, M., 2020. Thermally stable thin film composite polymeric membranes for water treatment: A review. Journal of Cleaner Production 250, 119447.

Keikhaei, M., Ichimura, M., 2019. Fabrication of Mg (OH) 2 thin films by electrochemical deposition with Cu catalyst. Thin Solid Films 681, 41-46.

Klein, C., Harbottle, D., Alagha, L., Xu, Z., 2013. Impact of fugitive bitumen on polymer- based flocculation of mature fine tailings. The Canadian Journal of Chemical Engineering 91(8), 1427-1432.

Kumar, K., Ravi, M., Pavani, Y., Bhavani, S., Sharma, A., VVR, N.R., 2012. Electrical conduction mechanism in NaCl complexed PEO/PVP polymer blend electrolytes. Journal of non-crystalline solids 358(23), 3205-3211.

Kusuma, H.S., Amenaghawon, A.N., Darmokoesoemo, H., Neolaka, Y.A., Widyaningrum, B.A., Anyalewechi, C.L., Orukpe, P.I., 2021. Evaluation of extract of Ipomoea batatas leaves as a green coagulant–flocculant for turbid water treatment: Parametric modelling and optimization using response surface methodology and artificial neural networks. Environmental Technology & Innovation 24, 102005.

Kusuma, H.S., Amenaghawon, A.N., Darmokoesoemo, H., Neolaka, Y.A., Widyaningrum, B.A., Onowise, S.U., Anyalewechi, C.L., 2022. A comparative evaluation of statistical empirical and neural intelligence modeling of Manihot esculenta-derived leaves extract for optimized bio-coagulation-flocculation of turbid water. Industrial Crops and Products 186, 115194.

Latour, I., Miranda, R., Blanco, A., 2015. Silica removal with sparingly soluble magnesium compounds. Part II. Separation and Purification Technology 149, 331-338.

Li, J., How, Z.T., Gamal El-Din, M., 2022a. Aerobic degradation of anionic polyacrylamide in oil sands tailings: Impact factor, degradation effect, and mechanism. Science of The Total Environment, 159079.

Li, J., How, Z.T., Zeng, H., Gamal El-Din, M., 2022b. Treatment Technologies for Organics and Silica Removal in Steam-Assisted Gravity Drainage Produced Water: A Comprehensive Review. Energy & Fuels 36(3), 1205-1231.

Lu, Q., Yan, B., Xie, L., Huang, J., Liu, Y., Zeng, H., 2016. A two-step flocculation process on oil sands tailings treatment using oppositely charged polymer flocculants. Science of the Total Environment 565, 369-375.

Maiti, A., Sadrezadeh, M., Guha Thakurta, S., Pernitsky, D.J., Bhattacharjee, S., 2012. Characterization of boiler blowdown water from steam-assisted gravity drainage and

silica–organic coprecipitation during acidification and ultrafiltration. Energy & Fuels 26(9), 5604-5612.

Mohammadtabar, F., Pillai, R.G., Khorshidi, B., Hayatbakhsh, A., Sadrzadeh, M., 2019. Efficient treatment of oil sands produced water: Process integration using ion exchange regeneration wastewater as a chemical coagulant. Separation and Purification Technology 221, 166-174.

Mpofu, P., Addai-Mensah, J., Ralston, J., 2004. Temperature influence of nonionic polyethylene oxide and anionic polyacrylamide on flocculation and dewatering behavior of kaolinite dispersions. Journal of Colloid and Interface Science 271(1), 145-156.

Nair, A.T., Makwana, A.R., Ahammed, M.M., 2014. The use of response surface methodology for modelling and analysis of water and wastewater treatment processes: a review. Water science and technology 69(3), 464-478.

Nason, J.A., Lawler, D.F., 2009. Particle size distribution dynamics during precipitative softening: Declining solution composition. water research 43(2), 303-312.

Ni, M., Ratner, B.D., 2008. Differentiating calcium carbonate polymorphs by surface analysis techniques—an XPS and TOF- SIMS study. Surface and Interface Analysis: An International Journal devoted to the development and application of techniques for the analysis of surfaces, interfaces and thin films 40(10), 1356-1361.

Ooi, T.Y., Yong, E.L., Din, M.F.M., Rezania, S., Aminudin, E., Chelliapan, S., Rahman, A.A., Park, J., 2018. Optimization of aluminium recovery from water treatment sludge using Response Surface Methodology. Journal of environmental management 228, 13-19.

Osacky, M., Geramian, M., Ivey, D.G., Liu, Q., Etsell, T.H., 2013. Mineralogical and chemical composition of petrologic end members of Alberta oil sands. Fuel 113, 148-157.

Parvathy, P.C., Jyothi, A.N., 2012. Synthesis, characterization and swelling behaviour of superabsorbent polymers from cassava starch- graft- poly (acrylamide). Starch- Stärke 64(3), 207-218.

Polizzotti, D.M., Khwaja, A.R., 2011. Use of cationic coagulant and acrylamide polymer flocculants for separating oil from oily water. Google Patents.

Rasouli, Y., Abbasi, M., Hashemifard, S.A., 2017. Investigation of in-line coagulation-MF hybrid process for oily wastewater treatment by using novel ceramic membranes. Journal of Cleaner Production 161, 545-559.

Rehman, K., Arslan, M., Müller, J.A., Saeed, M., Anwar, S., Islam, E., Imran, A., Amin, I., Mustafa, T., Iqbal, S., 2022. Operational parameters optimization for remediation of crude oil-polluted water in floating treatment wetlands using response surface methodology. Scientific Reports 12(1), 1-11.

Russell, C.G., Lawler, D.F., Speitel Jr, G.E., 2009a. NOM coprecipitation with solids formed during softening. Journal- American Water Works Association 101(4), 112-124.

Russell, C.G., Lawler, D.F., Speitel Jr, G.E., Katz, L.E., 2009b. Effect of softening precipitate composition and surface characteristics on natural organic matter adsorption. Environmental science & technology 43(20), 7837-7842.

Sadrzadeh, M., Pernitsky, D., McGregor, M., 2018. Nanofiltration for the treatment of oil sands-produced water. InTech Rijeka.

Sam-Tunsa Alarba, A., Epey, N., Nana, A., Tome, S., Mache, J.R., Nchare, M., 2022. Mineralogical and physicochemical characterization of clayey materials from Meiganga (Adamawa-Cameroon): potential application in traditional ceramic. Journal of Building Pathology and Rehabilitation 7(1), 1-12.

Srivastava, S., Saxena, K., Brighu, U., Gupta, A.B., 2022. Comparative evaluation of pilot-scale reactors based on pulsating floc blanket clarification and conventional clariflocculation technologies in simultaneous treatment of natural organic matter and turbidity. Water Supply 22(8), 6945-6958.

Stumm, W., Morgan, J., 1992. Surface charge and the electric double layer. Chemistry of the Solid±Water Interface.

Ulgut, B., Suzer, S., 2003. XPS studies of SiO2/Si system under external bias. The Journal of Physical Chemistry B 107(13), 2939-2943.

Van Aken, P., Van den Broeck, R., Degrève, J., Dewil, R., 2017. A pilot-scale coupling of ozonation and biodegradation of 2, 4-dichlorophenol-containing wastewater: The effect of biomass acclimation towards chlorophenol and intermediate ozonation products. Journal of Cleaner Production 161, 1432-1441.

Wang, X., 2016. Review of characterization methods for water-soluble polymers used in oil sand and heavy oil industrial applications. Environmental Reviews 24(4), 460-470.

Wiśniewska, M., 2012. The temperature effect on the adsorption mechanism of polyacrylamide on the silica surface and its stability. Applied Surface Science 258(7), 3094-3101.

Wu, M., Yu, W., Qu, J., Gregory, J., 2019. The variation of flocs activity during floc breakage and aging, adsorbing phosphate, humic acid and clay particles. Water research 155, 131-141.

Xiao, D., Cheng, J., Liang, W., Sun, L., Zhao, J., 2021. Metal-phenolic coated and prochloraz-loaded calcium carbonate carriers with pH responsiveness for environmentally-safe fungicide delivery. Chemical Engineering Journal 418, 129274.

Yu, W.-z., Gregory, J., Campos, L., Li, G., 2011. The role of mixing conditions on floc growth, breakage and re-growth. Chemical Engineering Journal 171(2), 425-430.

Zeng, Y., Yang, C., Zhang, J., Pu, W., 2007. Feasibility investigation of oily wastewater treatment by combination of zinc and PAM in coagulation/flocculation. Journal of hazardous materials 147(3), 991-996.

Zhang, K., Pernitsky, D., Jafari, M., Lu, Q., 2021a. Effect of MgO slaking on silica removal during warm lime softening of SAGD produced water. Industrial & Engineering Chemistry Research 60(4), 1839-1849.

Zhang, L., Mishra, D., Zhang, K., Perdicakis, B., Pernitsky, D., Lu, Q., 2020. Electrokinetic study of calcium carbonate and magnesium hydroxide particles in lime softening. Water Research 186, 116415.

Zhang, L., Mishra, D., Zhang, K., Perdicakis, B., Pernitsky, D., Lu, Q., 2021b. Impact of influent deviations on polymer coagulant dose in warm lime softening of synthetic SAGD produced water. Water Research 200, 117202.

Zhang, Q., Yan, Z., Ouyang, J., Zhang, Y., Yang, H., Chen, D., 2018. Chemically modified kaolinite nanolayers for the removal of organic pollutants. Applied clay science 157, 283-290.

Zhao, P., Geng, T., Zhao, Y., Tian, Y., Li, J., Zhang, H., Zhao, W., 2021. Removal of Cu (Ⅱ) ions from aqueous solution by a magnetic multi-wall carbon nanotube adsorbent. Chemical Engineering Journal Advances 8, 100184.

Zhou, Z., Yang, Y., Li, X., Gao, W., Liang, H., Li, G., 2012. Coagulation efficiency and flocs characteristics of recycling sludge during treatment of low temperature and micro-polluted water. Journal of Environmental Sciences 24(6), 1014-1020.

CHAPTER 4 FATE OF DISSOLVED ORGANICS IN OIL SANDS PROCESS WATER DURING FOUR-YEAR STORAGE: MECHANIC INSIGHTS INTO TOXICITY AND MICROBIAL PROFILING

4.1 Introduction

During bitumen extraction from surface mining of oil sands in Canada, a large volume of water known as oil sands process water (OSPW) is generated from the Clark Hot Water Extraction process (Clarke, 1980; Masliyah et al., 2004; Xue et al., 2018). OSPW is a complex mixture consisting of suspended solids, salts, inorganic compounds, heavy metals, and organic compounds including naphthenic acids (NAs), polycyclic aromatic hydrocarbons (PAHs), phenols, and BTEX (benzene, toluene, ethyl benzene, and xylenes) (Li et al., 2017). As the major contributor to the OSPW toxicity to aquatic and terrestrial lives, NAs are oil-derived mixtures of alkyl-substituted saturated cyclic and non-cyclic carboxylic acids with the general formula $C_nH_{2n+Z}O_x$, where n refers to the carbon number, Z (zero or a negative even integer) indicates the hydrogen deficiency caused by rings and/or double bonds introduction, and x is the oxygen atoms in the structure (x = 2 is classical NAs and $3 \leq x \leq 6$ is oxidized NAs) (Meshref et al., 2017; Xue et al., 2018). Previous studies have reported the mechanisms of toxicity associated with NAs in OSPW, including endocrine disruption, oxidative damages to lipids and nucleic acids, as well as narcosis (Garcia-Garcia et al., 2011; Goff et al., 2013; Li et al., 2017). Currently, huge amounts of OSPW are stored in tailings ponds and oil sands companies do not actively discharge OSPW mainly due to NAs (Lo et al., 2006; Martin et al., 2010). With increasing water demands for oil sands extraction and reports calling for further regulation of water imports from the Athabasca River, the reclamation

of OSPW is an important challenge facing the oil sands industry today (Han et al., 2009; Schindler et al., 2007).

Various technologies have been explored to degrade NAs and reclaim OSPW, including engineering (i.e. active) and biological (i.e. semi-passive/passive) applications (Lillico et al., 2022; Toor et al., 2013; Xue et al., 2018). While active treatment technologies, such as advanced oxidation processes (AOPs), have shown promising results in bench-scale studies (Abdalrhman et al., 2019; Abdelrahman et al., 2023; Meng et al., 2021; Zhang et al., 2017), these technologies have been tested using OSPW samples collected on-site that may have been stored for long time periods (e.g. several months) while tests were being conducted, potentially limiting their applicability due to the unrepresentative sample water quality (Petersen et al., 2015). In addition to active treatment technologies, semi-passive/passive strategies, such as constructed wetlands and end-pit lakes, have gained increased attention. These strategies aim to retain OSPW over a prolonged period of time to facilitate the natural degradation of organic acid components and mitigate the toxicity of OSPW (McQueen et al., 2017; Morandi et al., 2020). However, there is limited knowledge of how the characteristics of OSPW change over time and how these changes may impact the effectiveness in reducing toxicity. Although previous research has investigated the fate of NAs in OSPW during storage on-site and their results indicated that indigenous microbial communities in tailings water can degrade NAs given appropriate nutrient conditions (Brown et al., 2013; Han et al., 2009; Mahdavi et al., 2015; Quagraine et al., 2005b), many unknowns and uncontrolled variables can influence the fate of dissolved organics in OSPW-containing aquatic systems (Han et al., 2009). Therefore, further controlled studies under laboratory conditions are needed to understand the long-term fate of NAs in OSPW.

The objective of this study was to investigate the long-term fate of dissolved organics in OSPW under various controlled conditions. The impacts of temperature, oxygen, and ozone pre-treatment on water quality parameters such as turbidity, NAs degradation and toxicity reduction, were thoroughly investigated. Moreover, at the end of the experiments, the microbial community structure on the top and bottom layer of reactors was examined to identify key bacterial taxa involved in degradation of dissolved organics in OSPW during storage for approximately 4 years. To the best of the authors' knowledge, this is the first study to comprehensively demonstrate the long-term fate of dissolved organics in OSPW under different conditions, providing valuable insights into the management and treatment of OSPW.

4.2 Materials and methods

4.2.1 OSPW and chemicals

OSPW was collected from a tailings pond in Alberta, Canada, and stored in 200 L barrels located in a cold room (4 °C) before conducting the experiments. The characteristics of OSPW are shown in Table. 4.1. All solutions used in the experiments were prepared with Milli-Q water (Millipore Corp., USA). Solutions used in NAs analysis were prepared with Optima-grade water (Fisher Scientific, USA). 100-μm (d_f) SPME fibers (Sigma-Aldrich, Canada) coated with polydimethylsiloxane (PDMS), 0.612 μL PDMS per fiber, were used for the extraction of OSPW samples. HPLC grade sulfuric acid (H_2SO_4) (Sigma-Aldrich, Canada) was used for pH adjustment. Analytical grade 2,3-dimethylnaphthalene (DMN) was purchased from Sigma-Aldrich.

Table 4.1. Characteristics of oil sands process-affected water.

Parameter	Raw oil sands process-affected water
pH	8.5 ± 0.1

Chemical oxygen demand (COD), mg/L	204 ± 2.8
Dissolved organic carbon (DOC), mg/L	60.5 ± 0.5
Total naphthenic acids (NAs), mg/L	43.0 ± 1.1
Turbidity, NTU	85.3 ± 8.3
Dissolved oxygen (DO), mg/L	6.9 ± 0.2

4.2.2 Experimental Set-up

In order to investigate the effect of pre-treatment on the characteristics of OSPW during long-term storage under ambient temperature, pure nitrogen (N_2), oxygen (O_2), and a mild-dose (10 mg/L) of ozone were purged separately into different barrels to produce anoxic, oxic, and ozonated environments for OSPW. In addition, the temperature effect was also examined by storing raw (no pre-treatment) and ozonated OSPW under 4 °C. Duplicated reactors were set up for each condition. Samples (250 mL) were collected on each sampling date. All samples were filtered through a nylon filter (0.45 μm) before further analysis.

4.2.3 NAs degradation analysis

The degradation of NAs concentration during the storage of OSPW samples was measured by ultra-performance liquid chromatography time-of-flight mass spectrometry (UPLC TOF-MS) (Synapt G2, Waters, ON). In brief, the chromatographic separation was achieved by a Waters Phenyl BEH column with 2 mM ammonia acetate buffer in both water and 50/50 methanol/ acetonitrile. TOF-MS was operated in negative electrospray ionization (ESI) mode using MS scan over the mass range of 50-1200 Da in high-resolution mode (mass resolution = 40,000 FWHM at 1431 m/z). Myristic acid-1-^{13}C was used as an internal standard. All samples were filtered by using a 0.45 μm nylon filter prior to the analysis. Details of chromatographic separation and sample

analysis using UPLC TOF-MS have been reported elsewhere (Huang et al., 2018). The data was acquired by MassLynx (Waters) and processed by TargetLynx®V 4.2 software (Waters).

The biodegradation process of NAs in OSPW follows pseudo first order reaction kinetics (Arslan et al., 2022). The rate constant (k) and the corresponding half-life period ($t_{1/2}$) for the degradation of NAs were determined by Eq. 4.1-4.3:

$$C_t = C_0 e^{-kt} \tag{4.1}$$

$$k = \frac{(\ln(C_0) - \ln(C_t))}{t} \tag{4.2}$$

$$t_{1/2} = \frac{\ln(2)}{k} \tag{4.3}$$

where C_0 is the initial concentration of NAs in OSPW, C_t is the concentration of NAs in OSPW at time t.

4.2.4 Toxicity test

The acute toxicity of OSPW samples was evaluated via Microtox® acute toxicity test (81.9% screening test) with the bacterial reagent *A. fischeri*, a luminescent marine bacterium. Microtox® has been reported previously in many research studies regarding the toxicity of OSPW and it was commonly used as a reliable bioassay in toxicity studies due to its high correlation with other animal-based toxicity assays (Arslan and Gamal El-Din, 2021; Ganiyu et al., 2022; Islam et al., 2015). The pH of OSPW samples was adjusted to the required range (6.5-7.5) using 0.1 mM H_2SO_4. Then the suspension of *A. fischeri* was exposed to OSPW samples at 15 °C and bioluminescence inhibition tests were undertaken in duplicates in 96-well plates with a Synergy Microplate reader. The percentage inhibition was calculated after 15 min as recommended by the manual based on the Microtox® 81.9% screening test protocol. The luminescence intensity of *A. fischeri* in dilution

(2% NaCl in deionized water) and in phenol solution were measured as a negative control and positive control, respectively. The decrease in luminescence intensity of OSPW samples was calculated based on the equations shown below:

$$R_t = \frac{I_{t-B}}{I_{0-B}} \tag{4.4}$$

$$G_{t-s} = \frac{I_{0-s} \times R_t}{I_{t-s}} - 1 \tag{4.5}$$

$$\text{Inhibition effect \%} = \frac{G_{t-s}}{(G_{t-s} + 1)} \times 100 \tag{4.6}$$

where R_t is the correction factor, I_{0-B} is the luminescence intensity of the negative control without *A. fischeri*, I_{t-B} is the luminescence intensity of the negative control with *A. fischeri* under t exposure time (t = 5 min or 15 min), G_{t-s} is Gamma for OSPW samples and the positive control under t exposure time.

4.2.5 Analytical methods

The OSPW pH was measured using an Accumet Research AR20 pH/conductivity Meter. The turbidity was tested with a turbidimeter (OAKTON). Dissolved oxygen (DO) was monitored by YSI model 50B DO meter (YSI Incorporated, Oh, USA). The oxidation-reduction potential (ORP) was analyzed in-situ with a YSI probe (1003 pH/ORP Sensor). The dissolved organic carbon (DOC) in filtered (0.45 μm) OSPW was measured using a Shimadzu VCSH total organic carbon (TOC) analyzer (Shimadzu, TOC-V CHS/CSN) based on thermal catalytic principle and non-purgeable organic carbon method. The chemical oxygen demand (COD) of OSPW was analyzed by using a thermal reactor (HACH) for digesting samples at 150 °C for 120 min and a

spectrophotometer (HACH) for reading samples after cooling down to room temperature. Each physicochemical parameter was analyzed in duplicate.

The biomimetic extraction-solid phase microextraction (BE-SPME) has been developed as a tool to estimate total body residues in biota after exposure to organic mixtures, and is based on the principle that the SPME-water partition coefficients correlate well with octanol-water and membrane-water partition coefficients and provide a good surrogate for lipid partitioning (Van Loon et al., 1997; Verbruggen et al., 2000). BE-SPME has been reported as an industry benchmark for the measurements of bioavailable organics and acid-extractable organics (AEOs) in OSPW (Huang et al., 2021; Redman et al., 2018). Briefly, 20 mL OSPW samples were collected into glass vials and were acidified with 50 µL of phosphoric acid (85%, ACS grade) bringing the sample pH to the range of 2.0-2.4. Then samples were transferred to the SPME autosampler, where they were equilibrated with the 30 µm PDMS fiber for 100 min with orbital agitation (250 rpm) at 30 °C. After completion of the extraction period, the fiber was automatically retracted and injected into the GC-FID (Agilent 7890B) at 280 °C via the autosampler. The average molar response factor of 2,3-dimethylnaphthalene (2,3-DMN) was used to convert the GC-FID response to nanomoles of organic constituents on the PDMS fiber. Based on the calibration curve of 2,3-DMN, the BE-SPME/GC-FID results were expressed as µmol 2,3-DMN/mL PDMS according to the equation displayed below:

$$\text{Conc.}\left(\mu\text{mol}\,\frac{\text{DMN}}{\text{mL}}\,\text{PDMS}\right) = \frac{(A_S - A_B) \times V_{DMN}}{a \times MW_{DMN} \times V_{PDMS}} \tag{4.7}$$

where A_S is the sample peak area, A_B is the blank run peak area, MW_{DMN} is the molecular weight of 2,3-DMN (156.22 g/mol), V_{DMN} is the 2,3-DMN injection volume (0.5 µL), V_{PDMS} is PDMS

fiber volume (0.612 μL) and a is the constant (the slope) of the calibration curve. The detection limit for BE-SPME/GC-FID was about 0.5 μmol as DMN/ mL PDMS.

4.2.6 DNA extraction, 16S amplicon sequencing and bioinformatics

Total bacterial communities were examined to study the overall composition as well as to identify key players under different storage conditions. Bacterial communities were analyzed at the end of the sampling period by taking samples from the top and bottom of the reactor. For the analysis of bacterial communities, 100 mL OSPW samples were filtered using a 0.45 μm nylon filter. Then, DNA on the filter was extracted by using DNeasy Blood and Tissue Kit (Qian Inc, USA).

The analysis of microbial communities in OSPW has been reported in our previous reports (Arslan and Gamal El-Din, 2021; Arslan et al., 2022). In brief, sequencing was performed with an Illumina MiSeq platform (Micro300 PE) and the V3-V4 hypervariable region was targeted at the Applied Genomics Core facility (University of Alberta, Canada). 341F and 785R primers were used for library preparation. DADA2 computational pipeline (v1.8.0) was used for processing raw reads in R language, where true sequences were identified as amplicon sequence variants (ASVs). To assess the community diversity, richness, and pattern similarity, the alpha and beta diversity were calculated. The taxonomic assignment of each sequence was performed by using the "assignTaxonomy" function in R and using the non-redundant SILVA taxonomic training set ("silva_nr_v128_train_set.fa", https://www.arb-silva.de/). Then, the microbial profiles were collapsed to phylum to species. The taxonomy-assigned ASV table was generated and imported into R language, where "Phyloseq" package was used to perform diversity analyses and make bar plots, and a heatmap of the top 20 abundant ASVs was plotted in "Ampvis2" package.

4.2.7 Statistical analysis

Statistical analysis including multiple regression, one-way analysis of variance (ANOVA), redundancy analysis (RDA), and correlation analysis were applied to analyze the quantitative correlation among characteristics of OSPW, and the impact of storage conditions on water quality. Multiple regressions were developed in OriginPro (v. 2021) to examine the relationship among characteristics of OSPW. The RDA plot and a correlation matrix were further performed to evaluate the relationship between storage conditions (temperature, oxygen, pH) and dependent variables including removal efficiency of turbidity, COD, DOC, NAs, and toxicity by using R language.

4.3 Results and discussions

4.3.1 Attenuation of OSPW

4.3.1.1 Water quality

The DO and pH of OSPW samples stored at 20 and 4 °C were monitored throughout the study period (Fig. 4.1). As shown in Fig. 4.1a, the DO was kept at less than 0.3 mg/L in the OSPW stored at anoxic conditions, whereas DO remained at ~7.2 mg/L in raw OSPW, ~7.7 mg/L in ozonated OSPW, and ~8.0 mg/L in the oxic OSPW under 20 °C. Accordingly, the oxidation-reduction potential (ORP) values in anoxic OSPW at 20 °C were negative (Top: -207 mV, Bottom: -206 mV) whereas those in raw (Top: 129 mV, Bottom: 126 mV), ozonated (Top: 154 mV, Bottom: 153 mV), and oxic OSPW (Top:142 mV, Bottom: 139 mV) at 20 °C were positive. It is well-established that positive ORP supports the oxidation of organics; whereas its negative value below -200 mV facilitates methanogenesis at high rates that allow the transformation of organics in a syntrophic manner (Arslan et al., 2022). The initial pH values of all OSPW samples at 20 °C were approximately 8.7 due to the presence of sodium hydroxide used in the extraction of bitumen (Fig.

4.1b). A minimal decrease in pH was observed after ozonation, resulting in the initial pH of 8.5 for the ozonated OSPW, which could be attributed to the buffering effect of bicarbonate ions present in OSPW. Similarly, the limited impact of ozonation on pH of OSPW was also reported by Zhang et al. (2016) and Martin et al. (2010). The pH values of all OSPW samples were relatively stable during the storage at 20 °C. For OSPW samples stored at 4 °C, both raw and ozonated OSPW had higher DO than the OSPW stored at 20 °C (Fig. 4.1c). It is well-known that DO is temperature-dependent and water in lower temperature water would hold more DO (Butcher and Covington, 1995). In addition, similar ORP values were observed at the top layer and bottom layer in raw (Top: 136 mV, Bottom: 134 mV) and ozonated OSPW (Top: 92 mV, Bottom: 87 mV) at 4 °C. Unlike DO, temperature had minimal impact on the pH of OSPW, which led to similar pH values between OSPW samples stored at 4 °C and OSPW samples stored at 20 °C (Fig. 4.1d).
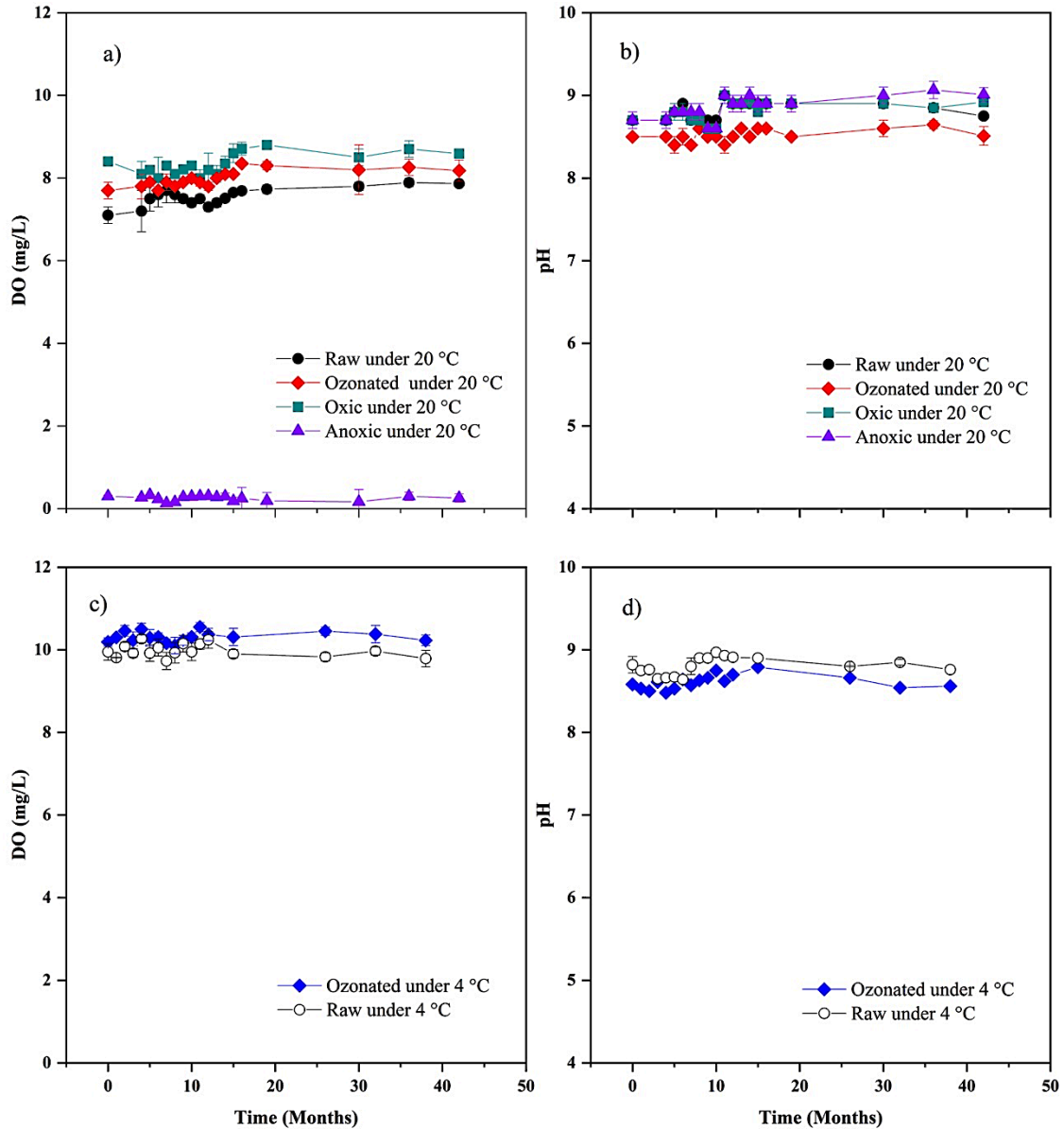
Figure 4.1 DO and pH of OSPW under different conditions: (a) DO of OSPW samples stored at 20 °C; (b) pH of OSPW samples stored at 20 °C; (c) DO of OSPW samples stored at 4 °C; (d) pH of OSPW samples stored at 4 °C.

The removal of COD, DOC, and turbidity were studied to determine the basic water quality of OSPW during the 4-year storage under different conditions (Fig. 4.2). The initial COD in raw OSPW, OSPW stored at oxic condition and OSPW stored at anoxic condition under 20 °C were at

around 210.0 mg/L, whereas the initial COD reduced to 197.3 mg/L in OSPW after ozonation pre-treatment (Fig. 4.2a). Similarly, lower initial DOC was also found in ozonated OSPW (60.7 mg/L) compared to initial DOC in other OSPW (62.0 mg/L) under room temperature (Fig. 4.2b). The COD decreased gradually in all reactors stored at 20 °C, reducing to 157.1 mg/L (24.5%) in raw OSPW, 147.3 mg/L (25.3%) in ozonated OSPW, 155.0 mg/L (25.1%) in OSPW at oxic condition, and 165.1 mg/L (21.5%) in OSPW at anoxic condition. Similar reduction trends were observed in DOC, with the final concentration of 50.8 mg/L (17.8%) in raw OSPW, 48.7 mg/L (19.8%) in ozonated OSPW, 49.7 mg/L (19.3%) in OSPW stored at oxic condition, 51.7 mg/L (15.9%) in OSPW stored at anoxic condition. Among different conditions, ozonated OSPW had the lowest initial COD and DOC values and the highest decrease in both of them, indicating the positive effect of mild ozonation as a pre-treatment on removing COD and DOC from OSPW, which has been reported in previous studies (Islam et al., 2014a; Shi et al., 2015; Zhang et al., 2016). In addition, the COD reached a plateau in all reactors stored at 20 °C after 2.5 years and the DOC reached the plateau in all reactors stored at 20 °C within two years. Our results of COD and DOC demonstrated that the limited change (< 30%) of COD and DOC would occur in lab stored OSPW samples at 20 °C, especially under anoxic condition, and the organic content remain stable in aged OSPW (>3 years), which is consistent with the observation in naturally aged OSPW in isolated oil tailings ponds (> 10 years) (Brown et al., 2013). Unlike COD and DOC, turbidity in OSPW samples (Fig. 4.2c) stored at 20 °C reduced dramatically in the first few weeks, among which ozonated OSPW was the first to reach the plateau with the lowest turbidity of 0.5 NTU, followed by 0.6 NTU in OSPW under oxic condition, 0.9 NTU in raw OSPW, and 4.3 NTU in OSPW under anoxic condition. It has previously been demonstrated that a suitable dose of ozone can promote particle settling via particle destabilization and aggregation (Li et al., 2009; Liang et al., 2014; Liu et al.,

2007). Several mechanisms of ozone-assisted particle destabilization and aggregation have been proposed, such as in situ production of coagulants by released oxidized metal ions from ozone, inducing polymerization of natural organic matter to form aggregates, and increasing carboxylic acids on solid surfaces to produce greater aluminum, magnesium, and calcium association that enables precipitation of metal humate complexes (Chheda and Grasso, 1994; Reckhow et al., 1986). Compared to the initial turbidity in raw OSPW (85.3 NTU), higher initial turbidity values were observed in OSPW samples under oxic (128.3 NTU) and anoxic (115.5 NTU) conditions due to the nitrogen and oxygen gas purging, respectively.

For raw and ozonated OSPW stored at 4 °C, no remarkable decreases (< 10%) were observed in COD and DOC during the 4-year storage (Fig. 4.2d. 4.2e), suggesting that the aging effect of 4-year lab-aged OSPW stored at 4 °C would be minimum for any treatment that the water might undergo. Additionally, a slight reduction of turbidity removal was found in raw and ozonated OSPW stored at 4 °C (~ 90%) (Fig. 4.2f) when compared with turbidity removal in OSPW stored at 20 °C (> 95%). The significant change of turbidity in OSPW samples at both temperatures suggested that it is essential to mix OSPW before taking samples for testing. It is worth noting that ozonated OSPW had higher reductions of COD (7.3%), DOC (6.9%) and turbidity (90.1%) than the reductions observed in raw OSPW stored at 4 °C (COD: 4.6%, DOC: 4.2%, turbidity: 82.2%), indicating the ozonation can enhance the removal of COD, DOC and turbidity in OSPW even at low temperature. The findings of this study are in agreement with previous research which observed a positive effect of ozonation on particle removal in a pilot plant, even at low temperatures in the range of 3.0-7.0 °C (Jasim et al., 2008).
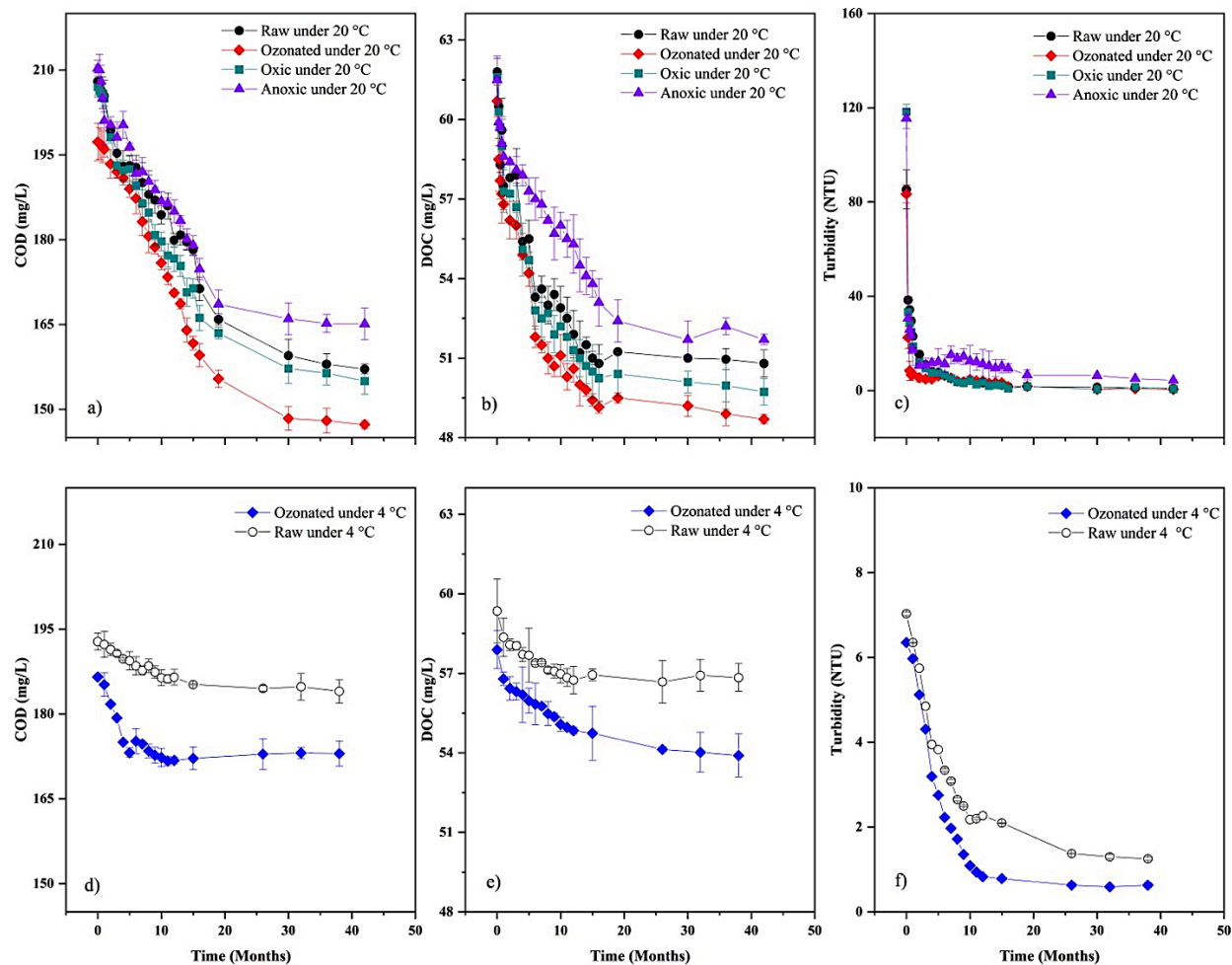
Figure 4.2 Chemistry of OSPW stored at 20 °C: (a) COD, (b) DOC, (c) turbidity and stored at 4 °C: (d) COD, (e) DOC, and (f) turbidity.

4.3.1.2 Dissolved organics

The removal of total, classical and oxidized NAs in OSPW under different storage conditions is shown in Fig. 4.3. OSPW with ozonation pre-treatment had the highest removal of total and classical NAs at 20 °C, decreasing from 40.4 mg/L to 11.1 mg/L (72.6%) (Fig. 4.3a), and from 22.5 mg/L to 1.8 mg/L (91.9%) (Fig. 4.3b), respectively. For other OSPW samples stored at 20 °C, the removal of total and classical NAs shared the same order: oxic OSPW > raw OSPW > anoxic OSPW. It is suggested that biodegradation is responsible for the natural attenuation of NAs

117

in aged OSPW (Han et al., 2009; Quagraine et al., 2005b). Kinetics analysis was performed for biodegradation of total NAs and classical NAs in each OSPW sample stored at 20 °C, the corresponding rate constants were calculated (Fig. A.3), and the degradation half-lives for NAs are summarized in Table. 4.2. The shortest half-life for both total (474.8 days) and classical NAs (266.6 days) were observed in ozonated OSPW, indicating that integrating mild ozone with the biological process can effectively enhance the removal of NAs from OSPW (Zhang et al., 2019). It has been previously reported that the half-life of classical NAs in an OSPW sample with combined treatment of mild-ozonation and aerobic biodegradation was within the range of 48-55 days (Martin et al., 2010). The longer half-life of classical NAs observed in the ozonated OSPW in this study could be due to lower concentrations of indigenous microorganisms in the OSPW samples. In oxic OSPW, the half-life for classical NAs was 346.6 days, which is in accordance with the earlier study where a half-life of 203-315 days was observed during aerobic biodegradation of classical NAs (Mahdavi et al., 2015). However, poor degradation of total and classical NAs were found in anoxic OSPW, with the longest half-lives of 877.4 days and 577.6 days, respectively, indicating that oxygen plays a role in the fate of dissolved organics in OSPW at 20 °C.

In this study, the removal of oxidized NAs was also evaluated, as they are considered as oxidation products of classical NAs. As shown in Fig. 4.3c-4.3f, the concentrations of oxidized NAs in all OSPW samples stored at 20 °C were found to be lower than those of classical NAs, in the following order: O_3-NAs > O_4-NAs > O_5-NAs > O_6-NAs. This result is consistent with the earlier findings that classical NAs are the dominant NAs species in OSPW (Huang et al., 2018; Xue et al., 2017). Compared to classical NAs, oxidized NAs exhibited less reduction in all OSPW samples stored at 20 °C, with O_3-NAs 71.5%, O_4-NAs 40.7%, O_5-NAs 35.8%, and O_6-NAs 27.7%

118

in raw OSPW, followed by oxic OSPW (O_3-NAs 68.2%, O_4-NAs 32.9%, O_5-NAs 32.5%, O_6-NAs 27.6%), ozonated OSPW (O_3-NAs 64.0%, O_4-NAs 30.0% , O_5-NAs 27.0%, O_6-NAs 25.9%), and anoxic OSPW (O_3-NAs 64.2%, O_4-NAs 32.5%, O_5-NAs 22.5%, O_6-NAs 17.4%). The comparatively high removal of O_3-NAs, limited removal of O_4-NAs and O_5-NAs, and lowest removal of O_6-NAs could be due to the preferential biodegradation of compounds with low carbon number and cyclicity (Scott et al., 2005; Zhang et al., 2016), and a higher degree of alkyl branching and oxygenation in persistent oxidized NAs (Han et al., 2009; Smith et al., 2008). In addition, it should be noted that anoxic condition resulted in a removal of oxidized NAs that is comparable to oxidized NAs removal in both the oxic and ozonated conditions, implying that certain microorganisms active under anoxic conditions are capable of metabolizing oxidized NAs (Xue et al., 2018). In fact, some β-Proteobacteria have been reported to possesss the capability to concurrently denitrify and metabolize recalcitrant hydrocarbons (Xue et al., 2016). More detailed discussion on microbial community structures is found in section 4.3.2.

Compared to OSPW samples stored at 20 °C, a much smaller amount of NAs was removed in both raw and ozonated OSPW at 4 °C, with a removal efficiency of total NAs recorded at 29.6% and 32.8%, respectively (Fig. 4.3g-4.3l). The results demonstrated that temperature, in addition to oxygen, holds a significant influence on the determination of the concentration of dissolved organics in OSPW. Moreover, the findings confirmed the effectiveness of storing OSPW samples in a cold room (4 °C) before experiments, which is a common practice in most OSPW studies (Abdelrahman et al., 2023; Arslan et al., 2022; Huang et al., 2021). In line with the results obtained from OSPW samples stored at 20 °C, ozonation could also enhance the degradation for both total and classical NAs at 4 °C. However, there was no dramatic difference in the removal of oxidized NAs between raw and ozonated OSPW stored at 4 °C.

To better understand of the different characteristics of aged OSPW in field conditions and in controlled laboratory settings, the removal of total NAs in OSPW aged in the reclamation pond and in the laboratory were compared in Table 4.3. It is interesting to note that the removal of total NAs in 4 years-aged OSPW at 20 °C in the laboratory (highest 72.6%) is higher than that in OSPW aged over 10 years in the reclamation ponds (highest 48.3%), indicating that controlled laboratory settings can be more efficient in removing NAs from OSPW than *in situ* field conditions. Furthermore, the estimated *in situ* degradation half-lives for total NAs in the field were between 12.8 and 13.6 years (Han et al., 2009), which is considerably longer than the longest half-life for total NAs in lab-aged OSPW of 877.4 days (~3 years) at 20 °C. This could be due to the differences in environmental factors and degradation mechanisms between field and laboratory conditions. For example, the field conditions may not provide optimal conditions for the growth and activity of microorganisms involved in NAs degradation. The decrease of NAs may result from various processes in the ponds such as dilution from natural water (e.g. rainfall and runoff), biodegradation, partitioning onto suspended solids and residual bitumen, and water-air partitioning in summertime. In contrast, biodegradation is likely the main mechanism for the reduction of NAs under laboratory conditions and the controlled conditions can be enhanced for NAs removal, providing a more suitable environment for the microorganism.
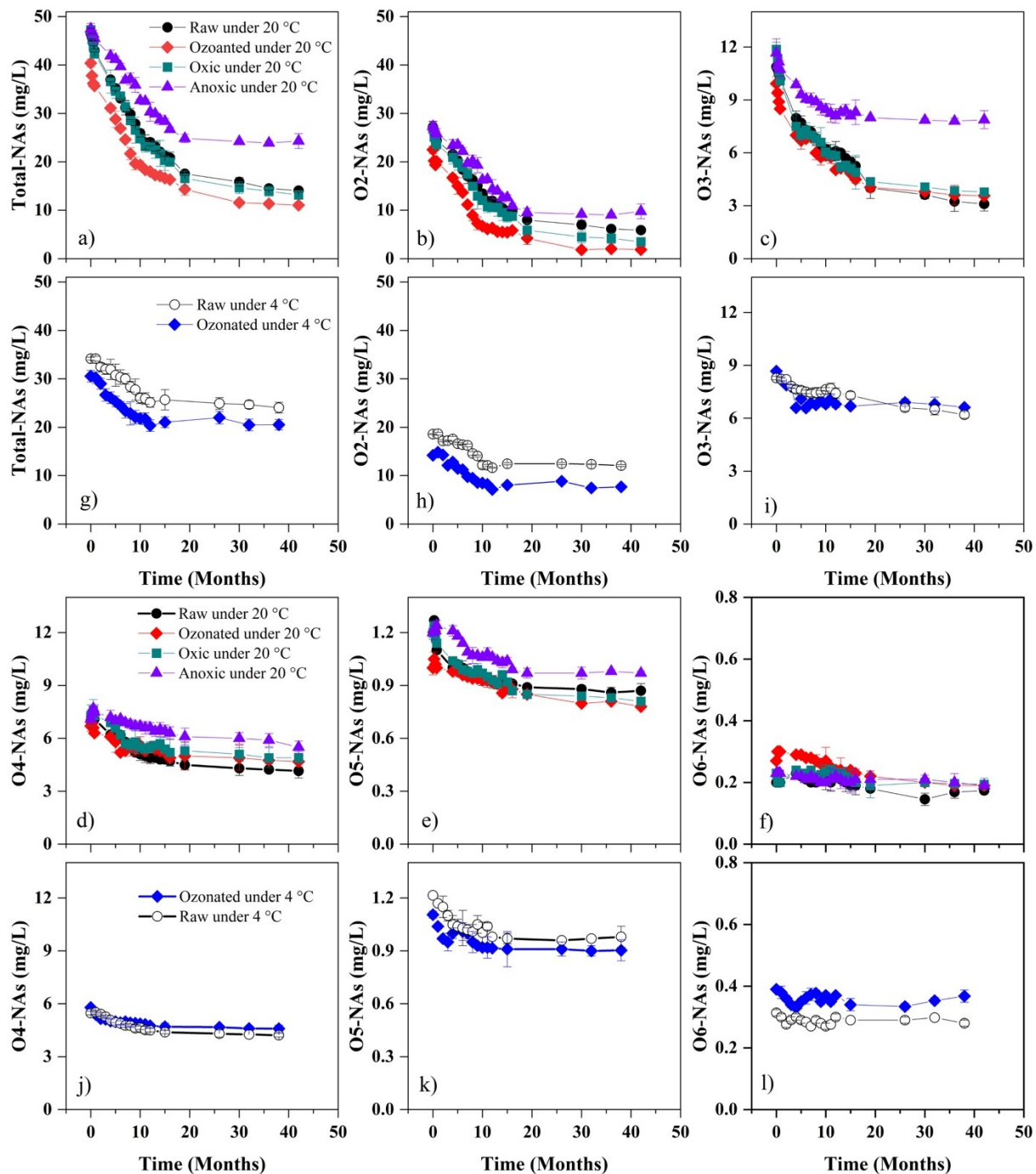
Figure 4.3 Removal of NAs in OSPW: (a) total NAs in OSPW stored at 20 °C; (b) classical NAs in OSPW stored at 20 °C, (c) O3-NAs in OSPW stored at 20 °C; (d) O4-NAs in OSPW stored at 20 °C; (e) O5-NAs in OSPW stored at 20 °C; (f) O6-NAs in OSPW stored at 20 °C; (g) total NAs in OSPW stored at 4 °C; (h) classical NAs in OSPW stored at 4 °C, (i) O$_3$-NAs in OSPW

stored at 4 °C; (j) O_4-NAs in OSPW stored at 4 °C; (k) O_5-NAs in OSPW stored at 4 °C; (l) O_6-NAs in OSPW stored at 4 °C.

Table 4.2 Summary of estimated half-life times for total and classical NAs measured at 20 °C for each condition.

Reactors	Total NAs	Classical NAs
	$t_{1/2}$ (days)	$t_{1/2}$ (days)
Raw	537.3	433.2
Ozonated	474.8	266.6
Oxic	502.3	346.6
Anoxic	877.4	577.6

Table 4.3 Comparison of concentration of total NAs in field-aged and lab-aged OSPW.

Sample designation	Description	Aging time (years)	Total NAs removal (%)	Analytical instrument	Reference
TPW	A pond containing OSPW only	13	48.3	FT-IR	(Han et al., 2009)
TPW	A pond containing OSPW only	16	41.6	FT-IR	(Anderson et al., 2012)
CT POND	A pond containing OSPW only	9	38.6	FT-IR	(Han et al., 2009)
Raw 20	Raw OSPW stored at 20 °C in the lab	~4	69.8	UPLC-TOF-MS	Present study
Ozonated 20	Ozonated OSPW stored at 20 °C in the lab	~4	72.6	UPLC-TOF-MS	Present study
Oxic 20	OSPW stored at oxic condition at 20 °C in the lab	~4	72.2	UPLC-TOF-MS	Present study

Anoxic 20	OSPW stored at anoxic condition at 20 °C in the lab	~4	48.8	UPLC-TOF-MS	Present study
Raw 4	Raw OSPW stored at 4 °C in the lab	~4	29.6	UPLC-TOF-MS	Present study
Ozonated 4	Ozonated OSPW stored at 4 °C in the lab	~4	32.8	UPLC-TOF-MS	Present study

BE-SPME was employed in this study to investigate the bioavailable organics and acid-extracable organics in OSPW on the basis of system exposure (i.e., lipid uptake) as opposed to external water concentrations (Fig. 4.4). Similar to NAs results, SPME fiber concentration decreased over time in OSPW samples at 20 °C, following the order of ozonated OSPW (35.2%) > oxic OSPW (32.3%) > raw OSPW (30.9%) > anoxic OSPW (30.6%) (Fig. 4.4a), while only minimal decline was found in raw (8.0%) and ozonated OSPW (9.7%) at 4 °C (Fig. 4.4b). In addition, ozonated OSPW had higher SPME fiber concentrations than raw OSPW at both temperatures, which may be attributed to the higher partitioning of dissolved organics in ozonated OSPW with the PDMS fiber. Further analysis of organics components and their partitioning behavior with PDMS fiber is required to gain a deeper understanding of the varying BE-SPME results across the OSPW samples.
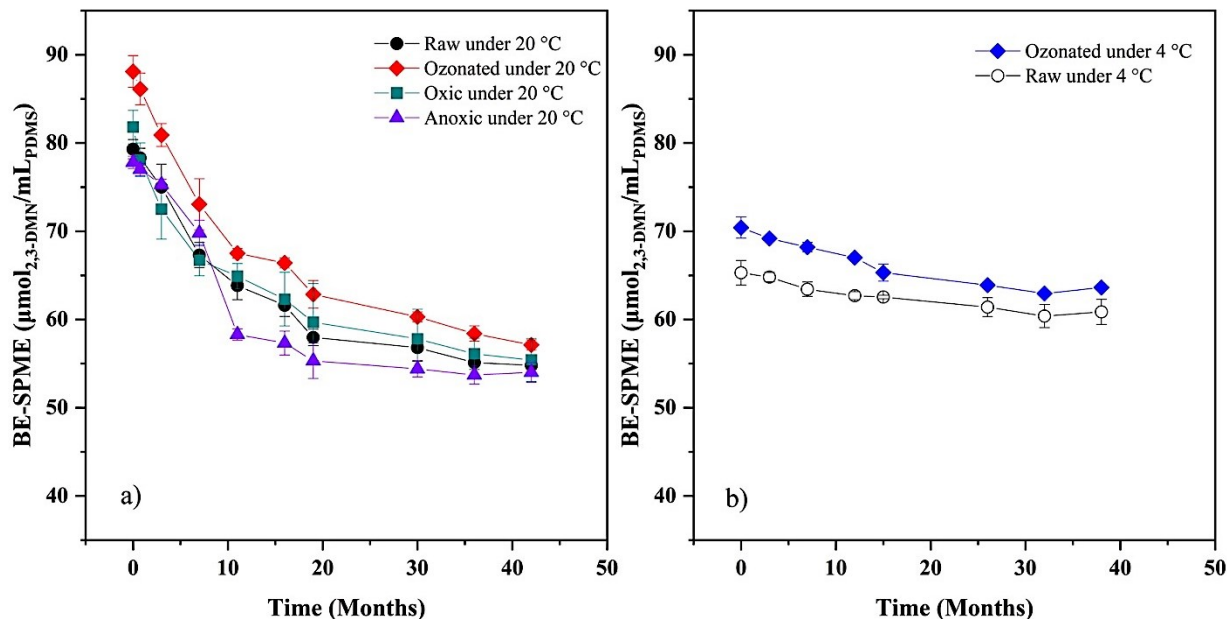
Figure 4.4 Reduction in SPME fiber concentration in OSPW stored at 20 °C (a) and 4 °C (b).

4.3.1.3 Toxicity

The toxicity of OSPW stored under different conditions was evaluated using Microtox® bioassay (Fig. 4.5). As shown in Fig. 4.5a, the inhibition effect of all OSPW samples at 20 °C diminished over time, with the maximum reduction observed in ozonated OSPW (40.5% to 15.9%), followed by oxic OSPW (42.1% to 17.9%) and raw OSPW (43.1% to 19.7%). The smallest reduction was observed in anoxic OSPW (40.1% to 22.7%). Such reductions are expected because the concentration of NAs, which are the main dissolved organic compounds responsible for acute toxicity in OSPW, are depleted to some extent by biodegradation and partitioning onto suspended solids, resulting in the reduction of the acute toxicity of aged OSPW (Del Rio et al., 2006; Han et al., 2009). In contrast to OSPW samples stored at 20 °C, a limited decline in inhibition effect was observed in both raw OSPW (41.3% to 32.6%) and ozonated OSPW (33.3% to 22.6%) at 4 °C (Fig. 4.5b). This result indicated that acute toxicity was not significantly affected by a four-year storage period under 4 °C, which is consistent with findings from a previous study (Whale et al.,

124

2022). Furthermore, the inhibition effects of ozonated OSPW and raw OSPW stored at 4 °C showed comparable reductions, implying that the hindered biological process at 4 °C would diminish the ozonation impact on reducing acute toxicity. In fact, earlier research has reported a positive effect of ozonation on acute toxicity removal and suggested that the acceleration of acute toxicity removal was not solely due to ozonation, but rather the combination of ozonation and subsequent biodegradation (Martin et al., 2010; Wang et al., 2013).
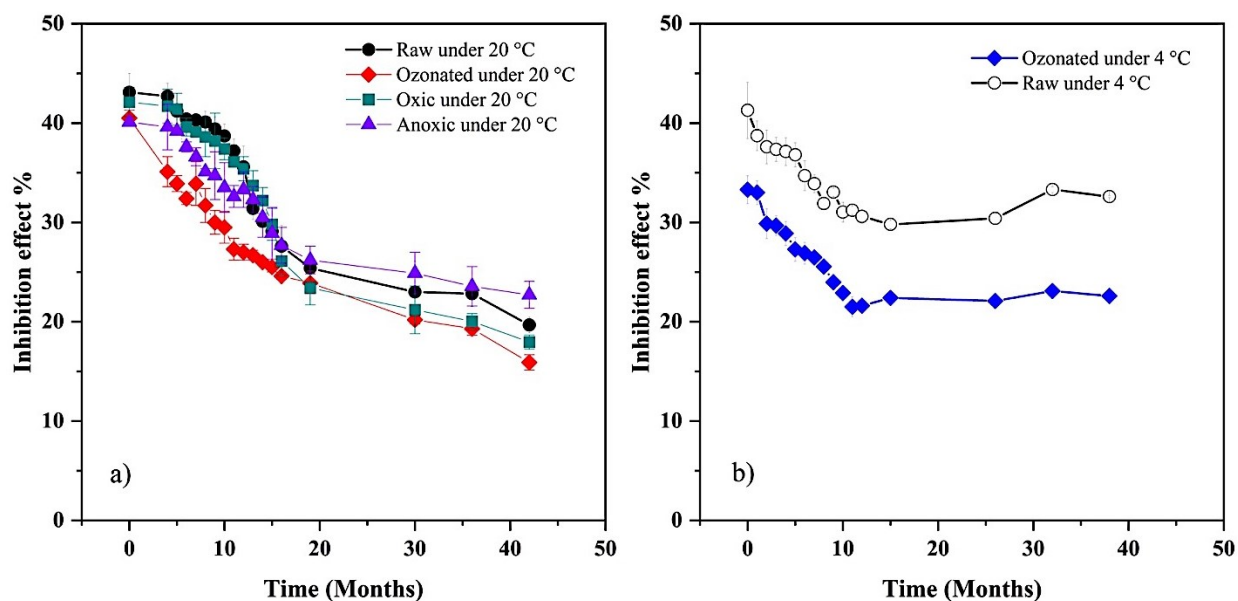
Figure 4.5 Reduction in acute toxicity to *A. fischeri* of OSPW stored at 20 °C (a) and 4 °C (b).

4.3.2 Correlation analysis

4.3.2.1 Correlation between NAs and other water quality parameters

The analysis of correlations between NAs and other quality parameters of OSPW can be important in predicting the degradation of NAs species during the aging of OSPW and in enhancing the understanding of the impact of NAs on the toxicity of OSPW. Fig. 4.6 presents the relationship between the concentration of total NAs and COD, DOC, Microtox®, and BE-SPME, as well as BE-SPME and Microtox®. As illustrated in Fig. 4.6a, 6b, total NAs exhibited a stronger

correlation with COD ($R^2 = 0.90$, *p-value* <0.001) compared to DOC ($R^2 = 0.72$, *p-value* <0.001), suggesting that COD is likely more appropriate than DOC as a surrogate variable to estimate NAs concentrations. These findings are in alignment with a previous study on NAs degradation in OSPW (Islam et al., 2014b). Additionally, ANOVA analysis for the regression model indicated that these linear relationships are statistically significant (*p-value* <0.001). Thus, it can be concluded that COD surrogate parameter presented a statistically significant linear relationship with the concentration of total NAs in OSPW. Considering the limited range of total NAs concentrations covered in this study, we incorporated three additional data points from the Mesocosm study (not yet published) in our research group. These data points included relationships between total NAs and inhibition effect, as well as between BE-SPME and inhibition effect. By integrating these supplementary data points, we were able to enhance the demonstration of the dose-response relationship. Based on Fig. 4.6c and Fig. 4.6d, similar fitting lines were observed between the total NAs concentration and inhibition effect, and BE-SPME concentration and inhibition effect. Our findings support the use of BE-SPME as a tool to predict acute toxicity during exposure to a complex mixture such as OSPW and are in agreement with prior research (Cancelli and Gobas, 2022; Redman et al., 2018). A significant linear relationship was observed between the concentration of total NAs and BE-SPME ($R^2 = 0.75$, *p-value* <0.001) in this work (Fig. 4.6e), as presented in an earlier OSPW study on the toxicity assessment of NAs (Swigert et al., 2015). The positive intercept in the correlation between total NAs and BE-SPME is expected because the organics measured by BE-SPME comprise both hydrocarbons and NAs (Cancelli and Gobas, 2022; Huang et al., 2021).
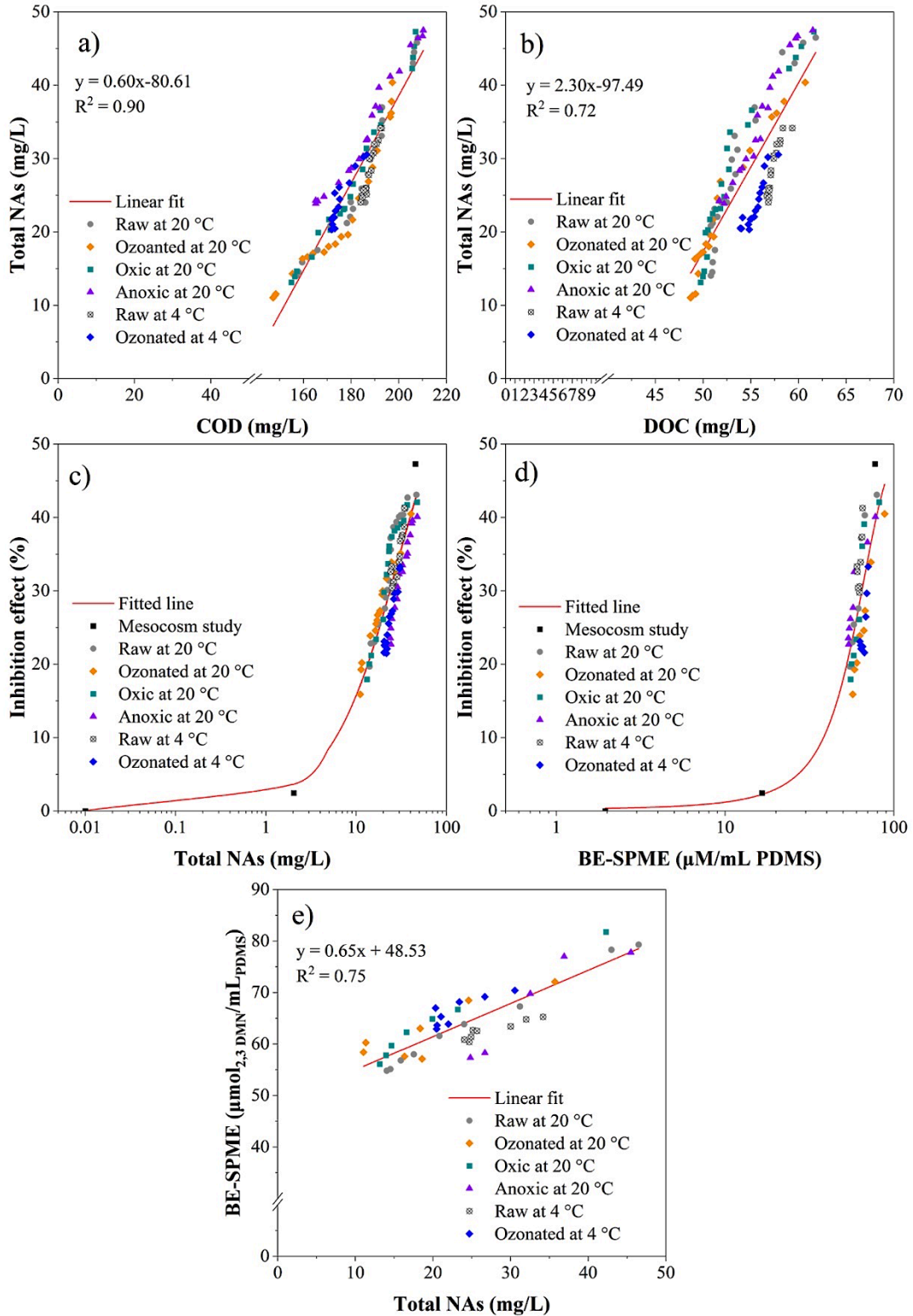
Figure 4.6 Relationships among OSPW chemistry: (a) COD-Total NAs, (b) DOC-Total NAs, (c) Total NAs-Inhibition effect (curve is logistic regressions of effects data), (d) BE-SPME-

Inhibition effect (curve is logistic regressions of effects data), and (e) Total NAs- BE-SPME (three dots were borrowed from the Mesocosm study in our research group: 1) control-river water; 2) 50% OSPW; 3) 100% OSPW).

4.3.2.2 Correlation between storage conditions and water quality

The quantitative correlation between the storage conditions (temperature, pH and DO) and the removal efficiency of water quality parameters (turbidity, COD, DOC, total NAs, classical NAs, Microtox®, and BE-SPME) was further investigated by using redundancy analysis (RDA) (Fig. 4.7a) and correlation matrix (Fig. 4.7b). As shown in Fig. 4.7a, the RDA analysis revealed that the RDA1 and RDA2 ordination axes explained 97.27% of the total variance data (*p-value* < 0.05). Temperature showed a significant positive correlation with the removal efficiency of all water quality parameters and correlation coefficients were above 0.90 (Fig. 4.7b), which aligns with prior studies where the positive effect of temperature was found on pollutant removal in various wastewater treatments (Arora and Kazmi, 2015; Luo et al., 2023). In contrast, there was a weak and negative correlation between DO and the removal efficiency of all water quality parameters with the correlation coefficients below -0.27, indicating a minimal inverse influence of DO on preserving water quality. Additionally, pH had the weakest positive correlation with the removal efficiency of COD and BE-SPME, with correlation coefficients being less than 0.1, and negative correlation with the removal efficiency of turbidity, DOC, total NAs, classical NAs, and Microtox®, with the correlation coefficients below -0.06. Overall, the statistical analysis results highlight that temperature had the most significant impact on OSPW quality, which also supports the common practice in OSPW studies of preserving OSPW samples in a cold room before laboratory experiments (Abdelrahman et al., 2023; Arslan et al., 2022; Huang et al., 2021).
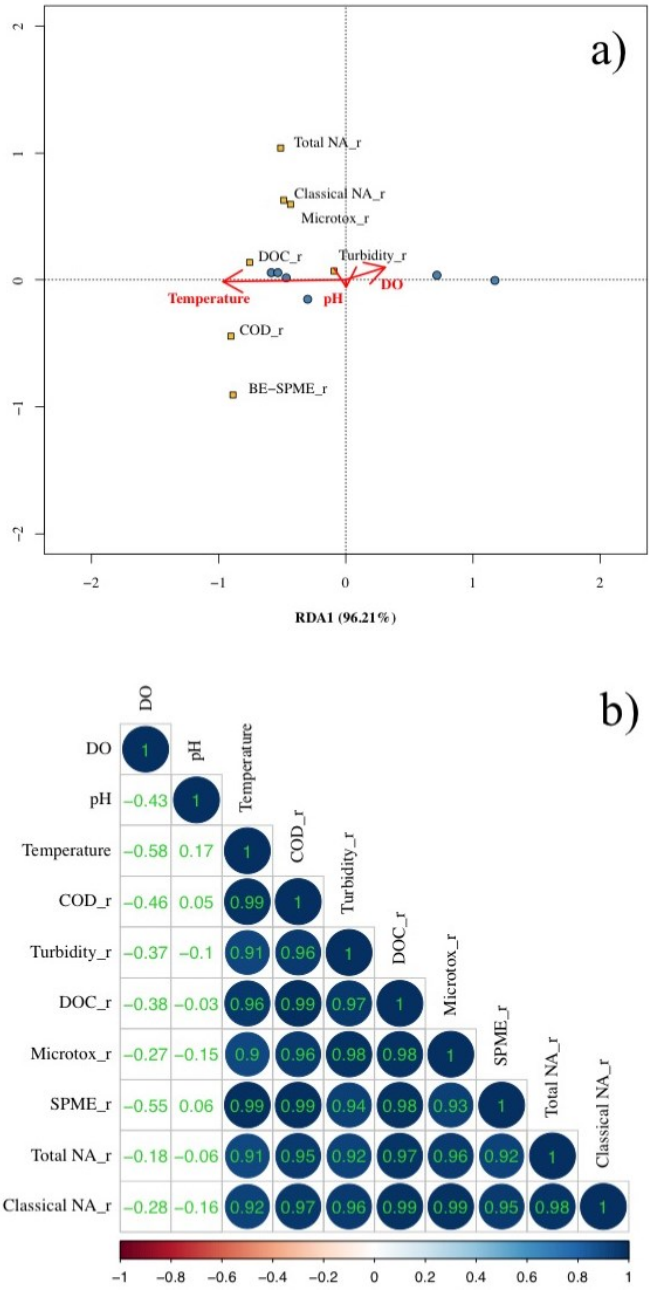
Figure 4.7 The statistical correlation of the storage conditions and the water quality: (a) redundancy analysis (RDA) and (b) correlation matrix.

4.3.3 Microbial community profiling in the reactors

The microbial community structures were studied to understand the role of microbial communities during OSPW storage in the laboratory under different conditions. A total of 3,730

phylotypes were observed at the 97% sequence similarity level, which comprised 29 phyla and 225 genera. Alpha diversity analysis was carried out to statistically interpret the changes in microbial community composition. The Shannon diversity index (H) was above 4.0 for the microbial communities in all OSPW samples, suggesting that microbial communities were abundant and diverse in OSPW (Fig. 4.8a). Furthermore, the results of H also illustrated that the microbial community in raw OSPW samples was higher than in ozonated OSPW stored at 20 °C, which could be due to the radicals generated from ozone pre-treatment, leading to unfavorable conditions for the bacterial growth and metabolism (Ganiyu et al., 2022), or the selection of ozonation in favor of certain species and against others (Huang et al., 2017; Hwang et al., 2013). In contrast, the Chao1 analysis showed no significant difference in microbial richness between raw OSPW and ozonated OSPW at 20 °C (Fig. 4.8a), suggesting that ozonation mainly affects the structure rather than the richness of the microbial community. Our findings are consistent with a previous study which found that low ozonation dosages (< 80 mg/L) did not severely affect the viability of microorganisms (Hwang et al., 2013). Interestingly, when the temperature decreased from 20 °C to 4 °C, the diversity and richness of the microbial community decreased in raw OSPW. This may be attributed to relatively higher toxicity and classical NAs present in raw OSPW at 4 °C. Conversely, the diversity and richness of the microbial community increased in ozonated OSPW when temperature decreased from 20 °C to 4 °C due to the lower toxicity and classical NAs found in ozonated OSPW at 4 °C. Moreover, compared to raw OSPW at 20 °C, oxic OSPW had a similar microbial diversity but lower microbial richness, indicating that higher DO might act as environmental stress on the microbial communities to affect the community composition (He et al., 2019). In contrast, anoxic OSPW had lower microbial diversity and richness, which can be explained by the anoxic OSPW having higher NAs concentration and least reduction in toxicity.

To study diversity patterns among microbial communities in the reactors under different conditions, beta diversity analysis was performed using principal coordinate analysis (PCoA) (Fig. 4.8b). For OSPW samples stored at 20 °C, the bacterial communities from the top and bottom layers of raw, ozonated, and oxic OSPW were grouped into two distinct clusters. This suggested that the microbial community dissimilarities existed between the top and bottom layers of anoxic and raw, ozonated, and oxic OSPW. Notably, the bacterial communities in the top and bottom layers of anoxic OSPW at 20 °C were distinctly separated from those in other OSPW samples stored at the same temperature, which is likely attributed to differences in oxygen availability. When the temperature was at 4 °C, bacterial communities in the top and bottom layers of raw and ozonated OSPW were found to be insignificantly different. However, ORP values at the top layer and bottom layer were similar in all OSPW samples stored at both 20 and 4 °C. These findings indicated that microbiological conditions, including temperature and oxygen, play a crucial role in shaping bacterial communities, with ORP may also contributing to some extent.

The primary aim of performing 16S rRNA amplicon sequencing was to elucidate underlying degradation mechanisms by identifying bacteria at lower ranks (e.g. genus-level taxonomy). Hence, the top twenty most abundant bacterial taxa were considered in this study to interpret abundant microbial processes in the reactor at top and bottom depths (Fig. 4.8c). In this work, Proteobacteria, Firmicutes, Bacteroidetes, Planctomycetes, and Patescibacteria were the dominant phyla in various OSPW samples. These phyla have been frequently observed in OSPW from oil sands tailings (Siddique et al., 2012; Zhang et al., 2020), Athabasca watershed and sediments (Yergeau et al., 2012), and in many other habitats (Herrmann et al., 2019). Several members of these phyla are known to be involved in NAs and hydrocarbons degradation or transformation via aerobic β-oxidation, combined α- and β-oxidation, aromatization and BPBA

degradation, and fermentation pathways (Foght et al., 2017; Johnson et al., 2011; Quagraine et al., 2005a).

In raw OSPW at 20 °C, the most abundant genera were *Fontimonas* (Bottom: 0.2%, Top: 10.7%), *AKYG587* (Bottom: 1.9%, Top: 0.8%), *SM1A02* (Bottom: 1.4%, Top: 1%), and *Hyphomicrobium* (Bottom: 0.2%, Top: 2.1%). The abundance of *Fontimonas* and *Hyphomicrobium* decreased at the bottom of raw OSPW because both of them are aerobic bacteria. In contrast, the abundance of *AKYG587* and *SM1A02* increased from top layer to bottom layer. The genus, *Hyphomicrobium,* was reported to metabolize organic matter at very low levels (Zhang et al., 2022), and *SM1A02* was proven to remove petroleum hydrocarbon (Bacosa et al., 2018). However, the ability of *Fontimonas* and *AKYG587* to degrade hydrocarbons and NAs has not been previously demonstrated.

In ozonated OSPW at 20 °C, the most enriched bacterial genera were *Bacillus* (Bottom: 0%, Top: 31.8 %), followed by *Fontimonas* (Bottom: 1.3%, Top: 22.3 %). *Bacillus* is aerobic and is known to degrade polyaromatic hydrocarbons and petroleum hydrocarbons, and likely plays a role in NAs removal (Das and Mukherjee, 2007; McKenzie et al., 2014). The relative abundance of this genus was substantially higher in ozonated OSPW (31.8%) than in other OSPW samples (0%), corroborating the observation that the highest NAs removal occurs in ozonated OSPW.

In oxic OSPW at 20 °C, the abundant genera were *Hyphomicrobium* (Bottom: 2.4%, Top: 10.8%), *Fontimonas* (Bottom: 0.2%, Top: 5.7%), *Legionella* (Bottom: 2.5%, Top: 0.8%), and *TX1A-55* (Bottom: 2.4%, Top: 0.1%). Given the high relative abundance of *Hyphomicrobium* in oxic OSPW (13.2%) when compared to other OSPW samples (<3%) and its strong ability to metabolize organic matter, the second highest removal of NAs was observed in oxic OSPW. The high abundance of *Legionella* warrants further investigation because some of the strains were

found to carry alkane hydroxylases (*alkB*) in their genome and were able to adhere to hydrocarbons (Halablab and Al-Dahlawi, 2008). *TX1A-55* has been founded in the soil but its impact on NAs and hydrocarbon degradation is required for future study.

In anoxic OSPW at 20 °C, methanogens were not highly abundant. The enriched bacterial genera were unclassified OTUs from the family of Saccharimonadales (Bottom: 1.3%, Top: 9.8%), *TX1A-55* (Bottom: 7%, Top: 0%), and *Legionella* (Bottom: 1%, Top: 3%). Saccharimonadales had small genomes with presumed symbiotic or parasitic lifestyles. Due to the difficulty in culture, their behavioral and adaptive traits are not understood deeply (Sánchez- Osuna et al., 2017). Recently, Saccharimonadales were found to be dominant bacteria in organic enriched sludge which could degrade plastics and show synergistic effects with the nitrogen cycling-related genes (Rüthi et al., 2020). Since the reduction in COD, DOC, and NAs fraction was limited in anoxic OSPW, it can be deduced that these bacterial genera had limited ability to degrade NAs.

In raw OSPW at 4 °C, abundant genera were *Nevskia* (Bottom: 2%, Top: 19.7%), an unclassified OTUs from the family of Chitinophagaceae (Bottom: 5.2%, Top: 8.1%), *Hyphomonas* (Bottom: 4.9%, Top: 4.9%), and *Legionelia* (Bottom: 4.3%, Top: 0.9%). *Nevskia* has been identified in oil-contaminated seawater or soil and has been demonstrated the ability to degrade petroleum hydrocarbon (Viggor et al., 2013; Wang et al., 2018). The bacteria of the Chitinophagaceae family have been extracted in heavy-oil-contaminated soil and were identified as polycyclic aromatic hydrocarbons (PAHs) degraders (Lladó et al., 2015). Besides, seven unclassified OTUs from the family of Xanthobacteraceae were found in abundance, occupying 32.3% and 18.8% in total at the bottom and top layer, respectively. It has been reported that several members of the Xanthobacteraceae are capable of degrading a variety of straight-chain and

aromatic hydrocarbons via aerobic β-oxidation, combined α- and β-oxidation and aromatization (Oren, 2014).

In ozonated OSPW at 4 °C, the enriched bacterial genera were *C1-B045* (Bottom: 4.2%, Top: 4.2%), *Legionella* (Bottom: 1.2%, Top: 5.9%), and an unclassified OTUs from the family of Xanthobacteraceae (Bottom: 0.2%, Top: 2.6%). All of these bacteria are previously reported as aerobes whose high abundance reflects microbiological conditions within ozonated OSPW at 4 °C were aerobic. Furthermore, both *C1-B045* and the Xanthobacteraceae family are well-known for their degradation of hydrocarbons (Bodor et al., 2021; Oren, 2014).

Overall, the results of microbial community structures indicated that the *Bacillus* and *Fontimonas* were the key microorganisms for degrading dissolved organics like NAs. Their enrichment in ozonated OSPW at 20 °C resulted the better performance on removal COD, DOC, and toxicity than other OSPW samples.
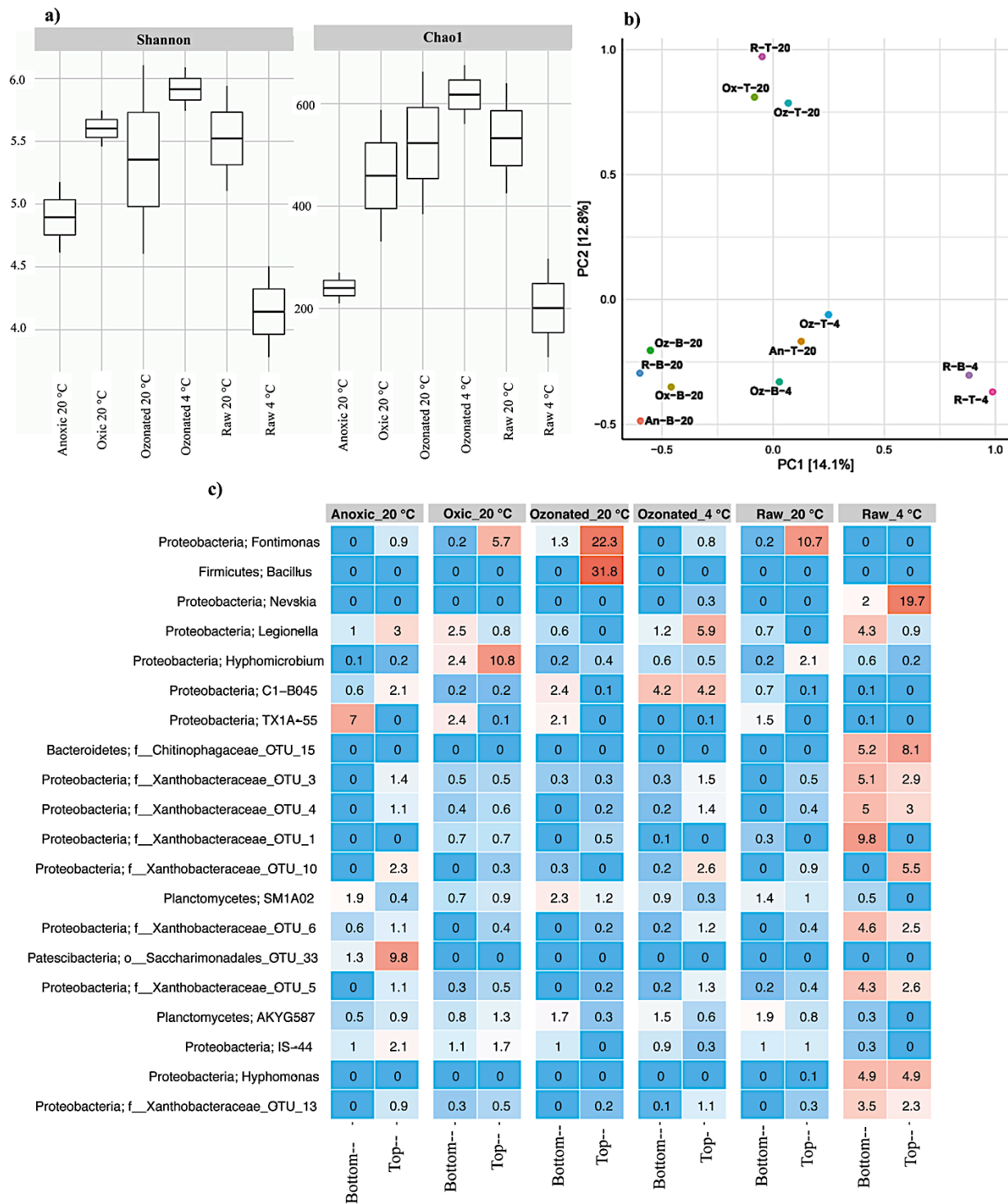
Figure 4.8 Alpha (a) and Beta (b) diversity analyses for microbial community and heat-map illustration of twenty most abundant bacterial genera at the top and bottom of each reactor (c).

4.4 Conclusions

The fate of dissolved organics in OSPW was studied under different storage conditions in the laboratory for 4 years. The highest removal of dissolved organics was observed in ozonated OSPW stored at 20 °C with the highest degradation of total NAs (72.6%), and the highest reduction of COD (25.3%) and DOC (19.8%). Biodegradation is likely to be the main reason for the decrease of NAs in OSPW and kinetics analysis revealed that the half-lives of total (474.8 days) and classical NAs (266.6 days) were shortest in ozonated OSPW at 20 °C, resulting the maximum reduction in toxicity as measured by Microtox® and BE-SPME. Our results suggested that ozonation pre-treatment could enhance the removal of dissolved organics and promote toxicity reduction in passive treatments, like constructed wetlands. COD concentration showed a positive correlation with total NAs in OSPW, indicating that COD can be used as a surrogate variable to estimate NAs concentrations. In addition, similar fitting lines were observed between the total NAs concentration and inhibition effect, and BE-SPME concentration and inhibition effect. Our findings support the use of BE-SPME as a tool to predict acute toxicity during exposure to OSPW, in agreement with prior research. The positive intercept was observed in the linear correlation between NAs concentration and BE-SPME, which can be explained by the organics measure by BE-SPME including both hydrocarbons and NAs. Another major finding of this study is that the temperature is the most important factor for the characteristics of OSPW, given the strong positive correlations between temperature and the removal of all of water parameters with their correlation coefficients above 0.90. The limited changes of various parameters including COD, DOC, NAs and toxicity in OSPW samples stored at 4 °C for 4 years supported the common practice of storing OSPW in the cold room as an effective way to preserve the water quality in the laboratory and

confirmed that the composition and properties of OSPW could be stable in the laboratory at least for several years.

The microbial communities in all OSPW at different conditions showed great richness and participated in the transformation of organics. The Shannon diversity index and the Chao1 value showed that the bacterial richness and microbial diversity in ozonated OSPW stored at 4 °C were significantly higher than the microbial diversity in other OSPW samples, which may be attributed to relatively lower toxicity and concentration of classical NAs. Principle coordinate analysis indicated that there were significant differences between microbes in OSPW stored at 20 °C and microbes in OSPW stored at 4 °C. Additionally, the microbes in anoxic OSPW at 20 °C were distinctly separated from those microbes in other OSPW samples at 20 °C given the negative ORP in anoxic OSPW while positive ORP in other OSPW samples. These findings suggested that bacterial communities were shaped mainly according to the temperature, although ORP was also playing a role in shaping the microbial communities. The microbial community analyses from 16S rRNA sequencing revealed that Proteobacteria, Firmicutes, Bacteroidetes, Planctomycetes, and Patescibacteria were the dominant phyla in various OSPW samples. The dominance of *Bacillus* and *Fontimonas* genera and the loss of microbial diversity in ozonated OSPW at 20 °C were observed. It is expected that bioaugmentation of endogenous OSPW microorganism may enhance the biodegradation of organics in ozonated OSPW. Overall, *Bacillus* and *Fontimonas* might be the key microorganisms for degrading dissolved organics like NAs in OSPW. Further research may focus on the interaction between microbes and dissolved organics, and biogeochemical mechanisms of organics removal from OSPW. Nevertheless, this study demonstrated the fate of dissolved organics in OSPW under various controlled conditions and highlights the impact of

temperature on OSPW characteristics, which can enhance the understanding of the long-term fate of organics in OSPW stored in reclamation ponds.

4.5 References

Abdalrhman, A.S., Ganiyu, S.O., Gamal El-Din, M., 2019. Degradation kinetics and structure-reactivity relation of naphthenic acids during anodic oxidation on graphite electrodes. Chemical Engineering Journal 370, 997-1007.

Abdelrahman, A., Ganiyu, S.O., Gamal El-Din, M., 2023. Degradation of surrogate and real naphthenic acids from simulated and real oil sands process water using electrochemically activated peroxymonosulfate (EO-PMS) process. Separation and Purification Technology 306, 122462.

Anderson, J., Wiseman, S.B., Moustafa, A., Gamal El-Din, M., Liber, K., Giesy, J.P., 2012. Effects of exposure to oil sands process-affected water from experimental reclamation ponds on Chironomus dilutus. water research 46(6), 1662-1672.

Arora, S., Kazmi, A.A., 2015. The effect of seasonal temperature on pathogen removal efficacy of vermifilter for wastewater treatment. Water research 74, 88-99.

Arslan, M., Gamal El-Din, M., 2021. Bacterial diversity in petroleum coke based biofilters treating oil sands process water. Science of The Total Environment 782, 146742.

Arslan, M., Müller, J.A., Gamal El-Din, M., 2022. Aerobic naphthenic acid-degrading bacteria in petroleum-coke improve oil sands process water remediation in biofilters: DNA-stable isotope probing reveals methylotrophy in Schmutzdecke. Science of The Total Environment 815, 151961.

Bacosa, H.P., Kamalanathan, M., Chiu, M.-H., Tsai, S.-M., Sun, L., Labonté, J.M., Schwehr, K.A., Hala, D., Santschi, P.H., Chin, W.-C., 2018. Extracellular polymeric substances (EPS)

producing and oil degrading bacteria isolated from the northern Gulf of Mexico. PLoS One 13(12), e0208406.

Bodor, A., Bounedjoum, N., Feigl, G., Duzs, Á., Laczi, K., Szilágyi, Á., Rákhely, G., Perei, K., 2021. Exploitation of extracellular organic matter from Micrococcus luteus to enhance ex situ bioremediation of soils polluted with used lubricants. Journal of Hazardous Materials 417, 125996.

Brown, L.D., Pérez-Estrada, L., Wang, N., Gamal El-Din, M., Martin, J.W., Fedorak, P.M., Ulrich, A.C., 2013. Indigenous microbes survive in situ ozonation improving biodegradation of dissolved organic matter in aged oil sands process-affected waters. Chemosphere 93(11), 2748-2755.

Butcher, J.B., Covington, S., 1995. Dissolved-oxygen analysis with temperature dependence. Journal of Environmental Engineering 121(10), 756-759.

Cancelli, A.M., Gobas, F.A., 2022. Treatment of naphthenic acids in oil sands process-affected waters with a surface flow treatment wetland: mass removal, half-life, and toxicity-reduction. Environmental Research 213, 113755.

Chheda, P., Grasso, D., 1994. Surface thermodynamics of ozone-induced particle destabilization. Langmuir 10(4), 1044-1053.

Clarke, T.P., 1980. Oil sands hot water extraction process. United States.

Das, K., Mukherjee, A.K., 2007. Crude petroleum-oil biodegradation efficiency of Bacillus subtilis and Pseudomonas aeruginosa strains isolated from a petroleum-oil contaminated soil from North-East India. Bioresource technology 98(7), 1339-1345.

Del Rio, L., Hadwin, A., Pinto, L., MacKinnon, M., Moore, M., 2006. Degradation of naphthenic acids by sediment micro- organisms. Journal of Applied Microbiology 101(5), 1049-1061.

Foght, J.M., Gieg, L.M., Siddique, T., 2017. The microbiology of oil sands tailings: past, present, future. FEMS Microbiology Ecology 93(5).

Ganiyu, S.O., Arslan, M., Gamal El-Din, M., 2022. Combined solar activated sulfate radical-based advanced oxidation processes (SR-AOPs) and biofiltration for the remediation of dissolved organics in oil sands produced water. Chemical Engineering Journal 433, 134579.

Garcia-Garcia, E., Ge, J.Q., Oladiran, A., Montgomery, B., Gamal El-Din, M., Perez-Estrada, L.C., Stafford, J.L., Martin, J.W., Belosevic, M., 2011. Ozone treatment ameliorates oil sands process water toxicity to the mammalian immune system. Water research 45(18), 5849-5857.

Goff, K.L., Headley, J.V., Lawrence, J.R., Wilson, K.E., 2013. Assessment of the effects of oil sands naphthenic acids on the growth and morphology of Chlamydomonas reinhardtii using microscopic and spectromicroscopic techniques. Science of the total environment 442, 116-122.

Halablab, M., Al-Dahlawi, A., 2008. Adherence of virulent and avirulent Legionella to hydrocarbons. J Medical Sciences 8, 234-238.

Han, X., MacKinnon, M.D., Martin, J.W., 2009. Estimating the in situ biodegradation of naphthenic acids in oil sands process waters by HPLC/HRMS. Chemosphere 76(1), 63-70.

He, Q., Chen, L., Zhang, S., Chen, R., Wang, H., 2019. Hydrodynamic shear force shaped the microbial community and function in the aerobic granular sequencing batch reactors for low carbon to nitrogen (C/N) municipal wastewater treatment. Bioresource technology 271, 48-58.

Herrmann, M., Wegner, C.-E., Taubert, M., Geesink, P., Lehmann, K., Yan, L., Lehmann, R., Totsche, K.U., Küsel, K., 2019. Predominance of Cand. Patescibacteria in groundwater is

caused by their preferential mobilization from soils and flourishing under oligotrophic conditions. Frontiers in microbiology 10, 1407.

Huang, C., Shi, Y., Sheng, Z., Gamal El-Din, M., Liu, Y., 2017. Characterization of microbial communities during start-up of integrated fixed-film activated sludge (IFAS) systems for the treatment of oil sands process-affected water (OSPW). Biochemical engineering journal 122, 123-132.

Huang, R., Chen, Y., Meshref, M.N., Chelme-Ayala, P., Dong, S., Ibrahim, M.D., Wang, C., Klamerth, N., Hughes, S.A., Headley, J.V., 2018. Characterization and determination of naphthenic acids species in oil sands process-affected water and groundwater from oil sands development area of Alberta, Canada. Water research 128, 129-137.

Huang, R., Yang, L., How, Z.T., Fang, Z., Bekele, A., Letinski, D.J., Redman, A.D., Gamal El-Din, M., 2021. Characterization of raw and ozonated oil sands process water utilizing atmospheric pressure gas chromatography time-of-flight mass spectrometry combined with solid phase microextractionun. Chemosphere 266, 129017.

Hwang, G., Dong, T., Islam, M.S., Sheng, Z., Pérez-Estrada, L.A., Liu, Y., Gamal El-Din, M., 2013. The impacts of ozonation on oil sands process-affected water biodegradability and biofilm formation characteristics in bioreactors. Bioresource technology 130, 269-277.

Islam, M.S., Dong, T., McPhedran, K.N., Sheng, Z., Zhang, Y., Liu, Y., Gamal El-Din, M., 2014a. Impact of ozonation pre-treatment of oil sands process-affected water on the operational performance of a GAC-fluidized bed biofilm reactor. Biodegradation 25(6), 811-823.

Islam, M.S., Moreira, J., Chelme-Ayala, P., Gamal El-Din, M., 2014b. Prediction of naphthenic acid species degradation by kinetic and surrogate models during the ozonation of oil sands process-affected water. Science of the total environment 493, 282-290.

Islam, M.S., Zhang, Y., McPhedran, K.N., Liu, Y., Gamal El-Din, M., 2015. Next-generation pyrosequencing analysis of microbial biofilm communities on granular activated carbon in treatment of oil sands process-affected water. Applied and environmental microbiology 81(12), 4037-4048.

Jasim, S., Ndiongue, S., Johnson, B., Schweitzer, L., Borikar, D., 2008. The effect of ozone on cold water coagulation. Ozone: Science and Engineering 30(1), 27-33.

Johnson, R.J., Smith, B.E., Sutton, P.A., McGenity, T.J., Rowland, S.J., Whitby, C., 2011. Microbial biodegradation of aromatic alkanoic naphthenic acids is affected by the degree of alkyl side chain branching. The ISME journal 5(3), 486-496.

Li, C., Fu, L., Stafford, J., Belosevic, M., Gamal El-Din, M., 2017. The toxicity of oil sands process-affected water (OSPW): A critical review. Science of the Total Environment 601, 1785-1802.

Li, T., Yan, X., Wang, D., Wang, F., 2009. Impact of preozonation on the performance of coagulated flocs. Chemosphere 75(2), 187-192.

Liang, J., Tumpa, F., Estrada, L.P., Gamal El-Din, M., Liu, Y., 2014. Impact of ozonation on particle aggregation in mature fine tailings. Journal of environmental management 146, 535-542.

Lillico, D.M., Hussain, N.A., Choo-Yin, Y.Y., Qin, R., How, Z.T., Gamal El-Din, M., Stafford, J.L., 2022. Using immune cell-based bioactivity assays to compare the inflammatory activities of oil sands process-affected waters from a pilot scale demonstration pit lake. Journal of Environmental Sciences.

Liu, H., Wang, D., Wang, M., Tang, H., Yang, M., 2007. Effect of pre-ozonation on coagulation with IPF–PACls: Role of coagulant speciation. Colloids and Surfaces A: Physicochemical and Engineering Aspects 294(1-3), 111-116.

Lladó, S., Covino, S., Solanas, A., Petruccioli, M., D'annibale, A., Viñas, M., 2015. Pyrosequencing reveals the effect of mobilizing agents and lignocellulosic substrate amendment on microbial community composition in a real industrial PAH-polluted soil. Journal of hazardous materials 283, 35-43.

Lo, C.C., Brownlee, B.G., Bunce, N.J., 2006. Mass spectrometric and toxicological assays of Athabasca oil sands naphthenic acids. Water Research 40(4), 655-664.

Luo, Y., Xie, H., Xu, H., Zhou, C., Wang, P., Liu, Z., Yang, Y., Huang, J., Wang, C., Zhao, X., 2023. Wastewater treatment plant serves as a potentially controllable source of microplastic: Association of microplastic removal and operational parameters and water quality data. Journal of Hazardous Materials 441, 129974.

Mahdavi, H., Prasad, V., Liu, Y., Ulrich, A.C., 2015. In situ biodegradation of naphthenic acids in oil sands tailings pond water using indigenous algae–bacteria consortium. Bioresource technology 187, 97-105.

Martin, J.W., Barri, T., Han, X., Fedorak, P.M., Gamal El-Din, M., Perez, L., Scott, A.C., Jiang, J.T., 2010. Ozonation of oil sands process-affected water accelerates microbial bioremediation. Environmental science & technology 44(21), 8350-8356.

Masliyah, J., Zhou, Z.J., Xu, Z., Czarnecki, J., Hamza, H., 2004. Understanding water- based bitumen extraction from Athabasca oil sands. The Canadian Journal of Chemical Engineering 82(4), 628-654.

McKenzie, N., Yue, S., Liu, X., Ramsay, B.A., Ramsay, J.A., 2014. Biodegradation of naphthenic acids in oils sands process waters in an immobilized soil/sediment bioreactor. Chemosphere 109, 164-172.

McQueen, A.D., Kinley, C.M., Hendrikse, M., Gaspari, D.P., Calomeni, A.J., Iwinski, K.J., Castle, J.W., Haakensen, M.C., Peru, K.M., Headley, J.V., 2017. A risk-based approach for identifying constituents of concern in oil sands process-affected water from the Athabasca Oil Sands region. Chemosphere 173, 340-350.

Meng, L., How, Z.T., Ganiyu, S.O., Gamal El-Din, M., 2021. Solar photocatalytic treatment of model and real oil sands process water naphthenic acids by bismuth tungstate: Effect of catalyst morphology and cations on the degradation kinetics and pathways. Journal of Hazardous Materials 413, 125396.

Meshref, M.N., Chelme-Ayala, P., Gamal El-Din, M., 2017. Fate and abundance of classical and heteroatomic naphthenic acid species after advanced oxidation processes: Insights and indicators of transformation and degradation. Water research 125, 62-71.

Morandi, G., Wiseman, S., Sun, C., Martin, J.W., Giesy, J.P., 2020. Effects of chemical fractions from an oil sands end-pit lake on reproduction of fathead minnows. Chemosphere 249, 126073.

Oren, A., 2014. The Family Xanthobacteraceae, in: Rosenberg, E., DeLong, E.F., Lory, S., Stackebrandt, E., Thompson, F. (Eds.), The Prokaryotes: Alphaproteobacteria and Betaproteobacteria. Springer Berlin Heidelberg, Berlin, Heidelberg, pp. 709-726. https://doi.org/10.1007/978-3-642-30197-1_258.

Petersen, M.A., Henderson, C.S., Ku, A.Y., Sun, A.Q., Pernitsky, D.J., 2015. Oil sands steam-assisted gravity drainage process water sample aging during long-term storage. Energy & Fuels 29(3), 2034-2041.

Quagraine, E., Headley, J., Peterson, H., 2005a. Is biodegradation of bitumen a source of recalcitrant naphthenic acid mixtures in oil sands tailing pond waters? Journal of Environmental Science and Health 40(3), 671-684.

Quagraine, E., Peterson, H., Headley, J., 2005b. In situ bioremediation of naphthenic acids contaminated tailing pond waters in the Athabasca oil sands region—demonstrated field studies and plausible options: a review. Journal of Environmental Science and Health 40(3), 685-722.

Reckhow, D.A., Legube, B., Singer, P.C., 1986. The ozonation of organic halide precursors: effect of bicarbonate. Water Research 20(8), 987-998.

Redman, A., Butler, J., Letinski, D., Di Toro, D., Paumen, M.L., Parkerton, T., 2018. Technical basis for using passive sampling as a biomimetic extraction procedure to assess bioavailability and predict toxicity of petroleum substances. Chemosphere 199, 585-594.

Rüthi, J., Bölsterli, D., Pardi-Comensoli, L., Brunner, I., Frey, B., 2020. The "plastisphere" of biodegradable plastics is characterized by specific microbial taxa of alpine and arctic soils. Frontiers in Environmental Science 8, 562263.

Sánchez- Osuna, M., Barbé, J., Erill, I., 2017. Comparative genomics of the DNA damage-inducible network in the Patescibacteria. Environmental Microbiology 19(9), 3465-3474.

Schindler, D., Donahue, W., Thompson, J., 2007. Running out of Steam? Oil Sands Development and Water Use in the Athabasca River Watershed: Science and Market based Solutions.

Scott, A.C., Mackinnon, M.D., Fedorak, P.M., 2005. Naphthenic acids in Athabasca oil sands tailings waters are less biodegradable than commercial naphthenic acids. Environmental science & technology 39(21), 8388-8394.

Shi, Y., Huang, C., Rocha, K.C., Gamal El-Din, M., Liu, Y., 2015. Treatment of oil sands process-affected water using moving bed biofilm reactors: with and without ozone pretreatment. Bioresource technology 192, 219-227.

Siddique, T., Penner, T., Klassen, J., Nesbø, C., Foght, J.M., 2012. Microbial communities involved in methane production from hydrocarbons in oil sands tailings. Environmental science & technology 46(17), 9802-9810.

Smith, D.F., Schaub, T.M., Kim, S., Rodgers, R.P., Rahimi, P., Teclemariam, A., Marshall, A.G., 2008. Characterization of acidic species in Athabasca bitumen and bitumen heavy vacuum gas oil by negative-ion ESI FT− ICR MS with and without acid− Ion exchange resin prefractionation. Energy & Fuels 22(4), 2372-2378.

Swigert, J.P., Lee, C., Wong, D.C., White, R., Scarlett, A.G., West, C.E., Rowland, S.J., 2015. Aquatic hazard assessment of a commercial sample of naphthenic acids. Chemosphere 124, 1-9.

Toor, N.S., Franz, E.D., Fedorak, P.M., MacKinnon, M.D., Liber, K., 2013. Degradation and aquatic toxicity of naphthenic acids in oil sands process-affected waters using simulated wetlands. Chemosphere 90(2), 449-458.

Van Loon, W.M., Verwoerd, M.E., Wijnker, F.G., vAN LEEUwEN, C.J., van Duyn, P., van deGuchte, C., Hermens, J.L., 1997. Estimating total body residues and baseline toxicity of complex organic mixtures in effluents and surface waters. Environmental Toxicology and Chemistry: An International Journal 16(7), 1358-1365.

Verbruggen, E.M., Vaes, W.H., Parkerton, T.F., Hermens, J.L., 2000. Polyacrylate-coated SPME fibers as a tool to simulate body residues and target concentrations of complex organic mixtures for estimation of baseline toxicity. Environmental science & technology 34(2), 324-331.

Viggor, S., Juhanson, J., Jõesaar, M., Mitt, M., Truu, J., Vedler, E., Heinaru, A., 2013. Dynamic changes in the structure of microbial communities in Baltic Sea coastal seawater microcosms modified by crude oil, shale oil or diesel fuel. Microbiological research 168(7), 415-427.

Wang, B., Teng, Y., Xu, Y., Chen, W., Ren, W., Li, Y., Christie, P., Luo, Y., 2018. Effect of mixed soil microbiomes on pyrene removal and the response of the soil microorganisms. Science of the Total Environment 640, 9-17.

Wang, N., Chelme-Ayala, P., Perez-Estrada, L., Garcia-Garcia, E., Pun, J., Martin, J.W., Belosevic, M., Gamal El-Din, M., 2013. Impact of ozonation on naphthenic acids speciation and toxicity of oil sands process-affected water to Vibrio fischeri and mammalian immune system. Environmental science & technology 47(12), 6518-6526.

Whale, G., Hjort, M., Di Paolo, C., Redman, A., Postma, J., Legradi, J., Leonards, P., 2022. Assessment of oil refinery wastewater and effluent integrating bioassays, mechanistic modelling and bioavailability evaluation. Chemosphere 287, 132146.

Xue, J., Huang, C., Zhang, Y., Liu, Y., Gamal El-Din, M., 2018. Bioreactors for oil sands process-affected water (OSPW) treatment: A critical review. Science of the Total Environment 627, 916-933.

Xue, J., Zhang, Y., Liu, Y., Gamal El-Din, M., 2016. Treatment of oil sands process-affected water (OSPW) using a membrane bioreactor with a submerged flat-sheet ceramic microfiltration membrane. Water research 88, 1-11.

Xue, J., Zhang, Y., Liu, Y., Gamal El-Din, M., 2017. Dynamics of naphthenic acids and microbial community structures in a membrane bioreactor treating oil sands process-affected water: impacts of supplemented inorganic nitrogen and hydraulic retention time. RSC advances 7(29), 17670-17681.

Yergeau, E., Lawrence, J.R., Sanschagrin, S., Waiser, M.J., Korber, D.R., Greer, C.W., 2012. Next-generation sequencing of microbial communities in the Athabasca River and its tributaries in relation to oil sands mining activities. Applied and environmental microbiology 78(21), 7626-7637.

Zhang, L., Graham, N., Kimura, K., Li, G., Yu, W., 2022. Targeting membrane fouling with low dose oxidant in drinking water treatment: Beneficial effect and biological mechanism. Water Research 209, 117953.

Zhang, L., Zhang, Y., Gamal El-Din, M., 2019. Integrated mild ozonation with biofiltration can effectively enhance the removal of naphthenic acids from hydrocarbon-contaminated water. Science of the Total Environment 678, 197-206.

Zhang, L., Zhang, Y., Patterson, J., Arslan, M., Zhang, Y., Gamal El-Din, M., 2020. Biofiltration of oil sands process water in fixed-bed biofilm reactors shapes microbial community structure for enhanced degradation of naphthenic acids. Science of the Total Environment 718, 137028.

Zhang, Y., Chelme-Ayala, P., Klamerth, N., Gamal El-Din, M., 2017. Application of UV-irradiated Fe (III)-nitrilotriacetic acid (UV-Fe (III) NTA) and UV-NTA-Fenton systems to degrade model and natural occurring naphthenic acids. Chemosphere 179, 359-366.

Zhang, Y., Xue, J., Liu, Y., Gamal El-Din, M., 2016. Treatment of oil sands process-affected water using membrane bioreactor coupled with ozonation: A comparative study. Chemical Engineering Journal 302, 485-497.

CHAPTER 5 AEROBIC DEGRADATION OF ANIONIC POLYACRYLAMIDE IN OIL SANDS TAILINGS: IMPACT FACTOR, DEGRADATION EFFECT, AND MECHANISM[3]

5.1 Introduction

Oil sands tailings, fluid wastes generated from mining to extract the bitumen (heavy crude oil) from the oil sands, consist of water, sands, fine clays and residue bitumen, as well as organic compounds such as naphthenic acids (NAs) (Brient et al., 2000). Until 2017, about 176 km^2 of tailings ponds in Northern Alberta have been generated due to the accumulated oil sands tailings on site (Allam et al., 2022). The storage of tailings could cause land disturbance and tailings could contain at most 83 % of water (by volume) which remains entrapped and unused (Vedoy and Soares, 2015). Therefore, it is essential to develop effective ways to recover and recycle the water and reclaim the land occupied by tailings ponds (Bazoubandi and Soares, 2020). Currently, synthetic polymeric flocculants are the basis of most dewatering technologies for oil sands tailings, among which polyacrylamide (PAM) is one of the most widely used flocculants (Zeng et al., 2022). Anionic polyacrylamides (A-PAM) with medium anionicity may be preferable than cationic and non-ionic in tailings flocculation due to lower toxicity and higher efficiency (Dwari et al., 2018).

However, there is a concern associated with the presence of residual acrylamide (AMD, monomer of PAM) due to incomplete polymerization process (Caulfield et al., 2002). In addition, AMD has been reported as a neurotoxin and carcinogen to humans (EPA, 2010). Concerns have been raised about the potential release of AMD from polyacrylamide degradation under certain

---

[3] This Chapter is based on the published paper: Li J, How ZT, Gamal El-Din M. Aerobic degradation of anionic polyacrylamide in oil sands tailings: Impact factor, degradation effect, and mechanism. Science of the Total Environment. 2023; 856:159079.

conditions, such as exposure of aqueous A-PAM/Fe^{3+} mixture to natural and simulated sunlight at acid/neutral pH (Zhao et al., 2018). However, most of the reported studies indicate that AMD is not a breakdown product of PAM degradation (Caulfield et al., 2003; Holliman et al., 2005). Although PAM applied in environmental systems usually has a high molecular weight, it can undergo degradation by different mechanisms, which results in chain scission, reduction of the molecular weight, and decrease in intrinsic viscosity (Guezennec et al., 2015; Xiong et al., 2018a). Most of the studies focus on the degradation of PAM solution as a result of thermal, mechanical, chemical, photolytic and biological processes. Details of each mechanism have been discussed previously by Guezennec et al. (2015 and Xiong et al. (2018a). Briefly, thermal degradation of PAM can cause substantial chain scission with the release of ammonia and carbon dioxide only when the temperature is above 300 °C. Mechanical degradation of PAM solutions involves irreversible changes, including viscosity reduction, main chain scission, and generation of free radicals. Chemical degradation mainly focuses on the reactivity of the amide group and numerous actions of free radicals causing chain scissions. Hydrolysis of amide groups yields poly(acrylamide-co-acrylic acid) and releases ammonium (NH_4^+) at low pH, while forming carboxylate anion and ammonia (NH_3) at high pH. Another free radical process is photolytic degradation, which generates free radicals from light exposure and leads to irreversible changes like backbone cleavage and cross-linking. Biodegradation of A-PAM can occur through two potential pathways with microorganisms: utilization of the amide group as a nitrogen source and/or the backbone as a carbon source under aerobic and anaerobic conditions (Bao et al., 2010; Wen et al., 2011). The amide nitrogen has been found to be susceptible to biodegradation of A-PAM, forming polyacrylate and releasing NH_3 (Nyyssölä and Ahlgren, 2019). In environmental applications of PAM, only thermal degradation is unlikely to occur due to the requirement of very

high temperature, while other degradation processes have been studied for a long period, mainly focusing on soil and hydro-systems. However, the release of AMD is inconsistent between studies. Woodrow et al. (2008) found that AMD could be rapidly released from aqueous A-PAM after exposure to natural and simulated sunlight under the presence of Fe^{3+} and acid conditions, while the majority of PAM degradation studies showed no evidence of AMD release (Caulfield et al., 2002; Xiong et al., 2018a). The biodegradation of PAM has been extensively investigated in recent years (Joshi and Abed, 2017). Although there is still an argument on how microorganisms degrade PAM, no release of AMD was observed in the biodegradation process (Wen et al., 2010). In terms of the residual AMD in commercial PAM products, various studies have demonstrated that they undergo rapid biodegradation under aerobic and anaerobic conditions, which limit their potential mobility in the environment (Guezennec et al., 2015).

Based on studies investigating PAM degradation in different environments, a number of factors including alkalinity, dissolved oxygen, high salinity, temperature, and microorganisms could affect the stability of PAM in oil sands tailings (Cossey et al., 2021; Dai et al., 2014; Xiong et al., 2018b). It is expected that aerobic biodegradation in the uppermost layer, anaerobic biodegradation in deeper layers, and alkaline hydrolysis of PAM would be the primary degradation processes in oil sands tailings after long storage time (Caulfield et al., 2002; Cossey et al., 2021; Xiong et al., 2018a). However, limited information is currently available regarding the fate of PAM and residual AMD, the characteristics of the PAM degraded products, and the effects of PAM degradation on water chemistry in oil sands tailings. This study would like to answer three questions: 1) whether PAM would degrade and release AMD in tailings water under different temperature and microbial conditions; 2) what are the effects of PAM degradation on the chemistry of tailings water; and 3) what is the possible mechanism of PAM degradation? Based on our best

knowledge, this is the first work revealing the possibility of PAM degradation and its effects on water chemistry in oil sands tailings. The findings obtained in this work will make a sound contribution to the enhanced understanding of the stability and fate of PAM and better management of oil sands tailings.

5.2 Materials and methods

5.2.1 Materials

Oil sands tailings samples were provided by an oil company from the oil sands in Northern Alberta and stored at 4 °C before use in the laboratory. The compositions of tailings and process water are listed in Table 5.1. A hydrolyzed polyacrylamide (SNF, Canada) with a medium anion charge density and a high molecular weight of around 2.12×10^6 Da, was employed as a polymer flocculant. Acrylamide (>99.9 % pure; powder) was purchased from Sigma Aldrich, while pure sand (silica, 40-100 mesh), sodium bicarbonate ($NaHCO_3$), potassium dihydrogen phosphate (KH_2PO_4), and methanol (HPLC grade) were purchased from Fisher Scientific. All chemicals were analytical grade and used as received without any further purification. All solutions were prepared with ultra-pure water (R≥18.2 MΩ) obtained from Millipore Millli-Q system. Five strains of bacteria were isolated from oil sands tailings as per their abilities to grow on A-PAM and were cultivated and used as microorganism augmentation in tailings water as well as added microorganisms in pure polymer solution. The detailed procedures of screening, isolation, and identification of the five A-PAM-degrading bacterial strains (Table B.1) can be found in the Supporting Information.

Table 5.1 Composition of oil sands tailings and process water.

Analysis (units); number of replicates	Value
DEAN-STARK (wt%); n = 2	

Water	45.3
Solids	53.4
Bitumen	1.2
Total	99.9
TEXTURE (wt%); n = 2	
Fine solids <44 μm	27.5
Coarse solids >44 μm	72.5
PROCESS WATER; n = 2	
Bulk pH; n = 2	8.6
Zeta potential	-35.2
TOC	104. 5
COD	434.9
Total NAs	51.8
SOLUBLE IONS (mg/L PROCESS WATER); n = 2	
NH_4^+	0.26
NO_2^-	0.05
NO_3^-	0.22

5.2.2 A-PAM degradation

The A-PAM degradation experiments were performed in both tailings and pure polymer solution. In oil sands tailings, 1000 ppm of A-PAM solution was added, as the same concentration was used in the majority of flocculation studies in oil sands tailings (Hripko et al., 2018; Zhang et al., 2021). Polymer dosage in ppm is expressed on the basis of total solids in tailings, meaning 1000 g polymer for 10^6 g solids (1000 ppm). The impact of different factors, including temperature, light, and microorganisms, on polymer degradation were evaluated. The conditions for each factor were summarized in Table 5.2. Duplicate reactors were used under each condition. Polymer stock solution with 0.1 wt% concentration in Milli-Q water was prepared 1 day earlier and would be kept for maximum 1 week. Mixing step was adapted from the method reported previously (Lu et al., 2016). In brief, 2 L of tailings samples were transferred into a 2 L standard baffled beaker and homogenized at 600 rpm for 2 min. Then the agitation speed was decreased and kept at 300 rpm when the desired amount of polymer stock solution was added to the slurries. Agitation was immediately stopped after polymer addition to avoid floc breakage. The resulted mixture was

transferred into a 2 L graduated cylinder, and the cylinder was then gently inverted 5 times for mixing before sedimentation. After settling for 30 min, supernatants (tailings water) were withdrawn from the cylinder for parameters measurement as samples $t = 0$. Sampling date was set at 2, 4, 6, and 11 weeks. All collected supernatant (tailings water) samples were stored at 4 °C until analysis.

Table 5.2 Conditions for different impact factors in A-PAM treated tailings water.

Factor	Condition	
	-	+
Temperature	4 °C	20 °C
Light	With light	Without light
Microorganism	Indigenous	Augmented (5-strain mixture, 58300-83300 CFU/100 mL)

In order to better understand the mechanism of polymer degradation in tailings, 1000 ppm of A-PAM was added into a simplified synthetic system, consisting of 300 mg/L $NaHCO_3$ solution with pure sands. $NaHCO_3$ was applied to adjust the pH of polymer solution at 8.5 ± 0.2 (Yousefzadeh et al., 2017). Based on the results from tailings, light was not a significant factor for the degradation of A-PAM in oil sands tailings (Fig. B.1 in appendix B). Therefore, a 2^2-factorial design (Table 5.3) was carried out to further investigate the interaction effect of temperature and microorganisms on the polymer degradation. Mixing step was the same as in tailings and each reactor had a duplicate. Supernatant samples were collected weekly for 11 weeks.

Table 5.3 Details of two-level factorial design for two factors of temperature and microorganism.

Reactor	Temperature	Microorganism
1	4 °C	No microorganism
2	4 °C	Added microorganism (5-strain mixture, 75066-76000 CFU/100 mL)
3	20 °C	No microorganism
4	20 °C	Added microorganism (5-strain mixture, 75066-76000 CFU/100 mL)

5.2.3 A-PAM concentration and molecular weight

Polymer concentration, molecular weight, and viscosity are important parameters for the characterization of polymer degradation. In oil sands tailings pond, the water body was expected to be static with no significant flow. Our study was centered on the *in vitro* degradation characteristics in a static context with aqueous buffers; therefore, the viscosity was not further considered. Both the concentration and molecular weights of A-PAM were analyzed by gel permeation chromatography (GPC). Polymer concentration was determined according to the method proposed by Lu et al. (2003). In brief, a high-performance liquid chromatography (HPLC, Agilent 1100) with an autosampler and an ultraviolet (UV) multiple wavelength detector, a TSK-Gel GMPW$_{XL}$ column (Tosoh Bioscience, 13 μm particle size, 7.8 mm ID × 30 cm) and a TSK-Gel guard PW$_{XL}$ column (Tosoh Bioscience, 12 μm particle size, 6.0 mm ID × 4.0 cm) were used. A solution of 0.05 M KH$_2$PO$_4$ (passed through a 0.2 μm filter) was used as mobile phase to elute the column at a flow rate of 0.7 mL/min under ambient temperature. The wavelength of the UV detector was set at 205 nm. The injection volume of prefiltered (0.45 μm) sample was 100 μL. The retention time for A-PAM was about 8.4 min. The concentration of polymer was calibrated and quantified based on its peak area. Calibration curve of polymer concentration is shown in the Fig.

B.2. The weight-average (M_w) and number-average (M_n) molecular weights and molecular weight distribution (MWD) of A-PAM were determined by HPLC (Agilent 1260 Infinity Multi-Detector Suite) with triple detectors (viscometer, differential refractive index and dual angle light scattering) and two columns (Agilent PL aquagel-OH MIXED-H) in series. Similar as the method proposed by Vajihinejad et al. (2021), the molecular weight was calibrated by using polyethylene oxide standards. A solution of 0.2 M sodium nitrate was used as a mobile phase for all analyses. All polymer samples were freeze dried before the molecular weight analysis.

5.2.4 AMD concentration

AMD concentration was determined using HPLC with UV multiple wavelength detector (Agilent 1100). The procedure was adapted from methods reported previously (Sang et al., 2015). In brief, 25 µL of prefiltered (0.45 µm) sample was delivered automatically onto a SB-C18 column (Agilent, ZORBAX, 3.5 µm particle size, 4.6 mm ID × 150 mm) with a guard column (Agilent, 1.8 µm particle size, 3.0 mm ID × 5.0 mm). The mobile phase consisted of 90 v/v% of phosphate buffer (0.006 M KH_2PO_4) and 10 v/v% of methanol. Separation was at room temperature with a flow rate of 0.5 mL/min and a wavelength of 208 nm. The retention time for acrylamide was approximately 4.6 min. The concentration of acrylamide was calibrated from 0.01 to 10 mg/L and quantified based on its peak area. Calibration curve of AMD concentration is presented in the Fig. B.3.

5.2.5 Fourier transformation infrared (FT-IR) spectrograms analysis

The spectrogram (4000-400 cm^{-1}) analysis was performed on an attenuated total reflection Fourier transform infrared (ATR-FTIR) spectrometer (Nicolet 8700, Thermo Fisher Scientific) at room temperature and used to assess the chemical structure of A-PAM before (polymer powder)

and after degradation (freeze-dried samples). The functional groups were identified by comparing the observed intensity bands to standard values.

5.2.6 Water chemistry

Water chemistry parameters including pH, total organic carbon (TOC), chemical oxygen demand (COD), ammonium, nitrite and nitrate, zeta potential, dissolved oxygen (DO), and naphthenic acids (NAs) were monitored during the experiments. Total organic carbon (TOC) was determined using a high temperature combustion TOC analyzer (TOC-L analyzers, Shimadzu), according to the Standard Method 5310-B (APHA, 2017). Chemical oxygen demand (COD) was assessed by a COD reactor (DRB 200, Hach), as per Standard Method 5220-D (APHA, 2017). Samples were diluted 10 times by Milli-Q water and filtered by 0.45 µm nylon filters before TOC and COD measurement. Ammonium cation, nitrite and nitrate anions in pre-treated samples (diluted 10 times by Milli-Q water and filtered by 0.2 µm nylon filters) were quantified by Dionex ICS Ion Chromatography. Zeta potential (ZP) was measured by using Phase analysis light scattering (PALS) in a Nanobrook Omni instrument (Brook Haven Instrument). Dissolved oxygen (DO) concentration and pH were determined by using an YSI model 50B DO meter (YSI Incorporated,) and Accumet Research AR20 pH/conductivity meter (Fisher-Scientific), respectively.

The chromatographic separation of NAs was achieved by following a method developed by Huang et al. (2015). Briefly, 500 µL of sample supernatant (passed through 0.2 µm nylon filter) mixed with 100 µL of 4.0 mg/L myristic acid-1-^{13}C (internal standard) and 400 µL methanol was injected into a Waters BEH Phenyl column (150 × 1 mm, 1.7 µm). A gradient mobile phase of 10 mM ammonia acetate buffer in both water (solvent A) and 50/50 methanol/acetonitrile (solvent B) was used for the chromatographic separation. TOF-MS was set at ESI negative mode using MS

scan over the mass range of 50-1200 Da in high resolution mode (mass resolution = 40,000 FWHM at 1431 m/z). The identification of classical NAs and oxidized NAs were based on the empirical formula $C_nH_{2n+z}O_x$ (x (number of oxygen) = 2, 3, 4, 5, 6) with n (number of carbon) ranging from 7 to 26 and z (a negative even integer) indicating hydrogen deficiency from the formation of ring or double bond equivalent (DBE). The data were obtained by MassLynx (Waters) and processed by TargetLynx (Waters).

5.2.7 Toxicity tests

After adjusting the pH of water samples to around 7.5, the acute toxicity of water samples was assessed by using the Microtox bioassay with the bacterial reagent *Aliivibrio fischeri* (*A. fischeri*). A Synergy Microplate reader coupled with 96-well plates was used to conduct the bioluminescence inhibition tests and measure the luminescence. Phenol was used as a positive control and 2 % of NaCl in deionized water was used as a blank control for the Microtox® assay. The inhibition of light emission was calculated and plotted according to the method developed by Johnson (2005). Dimethyl sulfoxide (DMSO) extractions were performed for sludge samples before pH adjusting in order to increase the bioavailability of organic contaminants to the test organisms *A. fischeri*. Ten grams of sludge samples were extracted with 20 mL of 100% DMSO for 2 h at room temperature at 200 rpm (Kapanen et al., 2013). The toxicity analyses were performed in duplicates for each sample. The potential carcinogenic effect of adjusted-pH water samples was determined via SOS-ChromoTest (Environmental Bio-detection Products Inc.), which is a colorimetric method used to assess the relative strength of a potential genotoxic compound. Different serial dilutions of each sample were prepared by adding DMSO in 96-well plates and then *E. coli* PQ37 was added. The induction factor (IF) was calculated based on the absorbances at 420 nm and 600 nm before and after incubation at 30 °C. Although the criteria of

IF value for genotoxicity varied in different studies, a more common interpretation of IF values indicates that a value lower than 1.5 is not genotoxic (Campos-Avelar et al., 2021). In terms of sludge samples, 2 g samples were extracted with 4 mL of 100% DMSO at room temperature for 1 h at 150 rpm before adjusting pH as according to Kapanen et al. (2013).

5.3 Results and discussion

5.3.1 A-PAM degradation in tailings water

5.3.1.1 Removal of A-PAM and residual AMD

The A-PAM and residual AMD removals were defined by the A-PAM and AMD concentration removal ratio, respectively. The removal ratio of A-PAM and residual AMD were calculated according to the following Eq. 5.1-5.2:

$$\text{A–PAM removal ratio} = \frac{C(\text{A–PAM}_{initial})\text{-}C(\text{A–PAM}_i)}{C(\text{A–PAM}_{initial})} \times 100\% \tag{5.1}$$

$$\text{AMD removal ratio} = \frac{C(\text{AMD}_{initial})\text{-}C(\text{AMD}_i)}{C(\text{AMD}_{initial})} \times 100\% \tag{5.2}$$

where $C(\text{A–PAM}_{initial})$ and $C(\text{AMD}_{initial})$ are the initial concentrations of A-PAM and residual AMD at week 0, respectively; $C(\text{A–PAM}_i)$ and $C(\text{AMD}_i)$ are the concentrations of A-PAM and AMD at week i (i = 1-11), respectively.

Former studies have shown that temperature is one of significant factors which can affect the PAM degradation in various media (Akbar et al., 2020; Xiong et al., 2018b). In order to mimic the common temperature conditions in tailings pond, temperature values of 20 °C and 4 °C were selected based on previous studies which monitored the properties of tailings (Dompierre et al., 2016). The changes of removal efficiency of the A-PAM concentration with time are illustrated in

Fig. 5.1a. The highest removal efficiency of A-PAM concentration in tailings water under 20 °C was 34.3 %, while 24.8 % was observed in tailings water at 4 °C. Similarly, higher removal efficiency of A-PAM could be found at higher temperature in pure polymer solution, which confirmed that temperature has a positive effect on the degradation of A-PAM in tailings. However, no decrease of A-PAM concentration occurred at 4 °C (<10 %) and only slight decrease (~10 %) at 20 °C was observed in pure polymer solution without microorganisms, demonstrating that temperature within the range of 4-20 °C has limited effects on A-PAM degradation without microbial activities. Similarly, Caulfield et al. (2003) also showed that their synthetic PAM solution without microorganisms was stable at room temperature after 2 weeks. Therefore, the higher removal efficiencies of A-PAM found in tailings water than in pure polymer solution are highly likely due to the microorganism effects, indicating that biodegradation could be a pathway for A-PAM removal in tailings.

PAM has been used as sole carbon and nitrogen source for microorganisms under aerobic conditions (Wen et al., 2011). Therefore, the effect of microorganisms and bioaugmentation on A-PAM degradation in pure polymer solution and tailings water was assessed by evaluating the polyacrylamide removal efficiency as shown in Fig. 5.1b. The removal efficiency of A-PAM in tailings water with augmented microorganisms could achieve as high as 41.0 %, while indigenous microorganisms in the tailings water could only achieve up to 32.1 %. In pure polymer solutions, improved removal efficiencies of A-PAM were also observed when microorganisms were added into the solutions. The above results indicated that the biodegradation processes of A-PAM occurred and could be promoted by microorganism augmentation in tailings water. Compared to previous studies, the degradation efficiencies of A-PAM in tailings water and pure polymer solution were lower (<50 %) due to lack of optimal conditions. For example, Wen et al. (2010)

indicated that 60 mg/L PAM could be degraded by pure bacterial strains with a high efficiency (>70 %) at 30 °C after 3 days in liquid media with PAM as the sole carbon source and mineral salts medium. In order to maximize the degradation efficiency of PAM in tailings, optimization experiments on various factors such as temperature, DO concentration, initial concentration of PAM and microorganism culture are needed in the future.

Low concentrations of AMD (1.15 mg/L) were detected in all samples at the beginning, and no increase of AMD concentration was observed during the whole sampling period, indicating the AMD was only from residual AMD in the PAM stock and A-PAM did not degrade into AMD in both tailings water and pure polymer solution within 11 weeks. As demonstrated in Fig. 5.1c, over 90 % of residual AMD could be removed within 2 weeks in tailings water at 20 °C, while it took 4 weeks to achieve 90 % of AMD removal in tailings water at 4 °C, suggesting that an increase of temperature could promote the degradation of residual AMD. This observation aligned with a previous study which found that AMD concentrations in solutions with PAM thickening agent were reduced at a faster rate at high temperatures (25 °C and 37 °C) than those at low temperature (4 °C) over a period of 6 weeks (Smith et al., 1996). Unlike in the tailings water, there were very limited degradations (<10 %) of AMD in pure polymer solution without microorganisms. The stability of acrylamide concentration in water and soil without microorganisms has been reported in several studies. Brown et al. (1980) showed that no AMD was removed from distilled water for more than 8 weeks and no chemical degradation occurred for AMD in >11 weeks in sterile environmental samples over the pH range 4-10. Besides, the removal efficiency of AMD significantly increased in pure polymer solutions after adding bacteria mixture (Fig. 5.1d), indicating that the degradation of AMD was mainly due to biological processes. In spite of the general toxicity of AMD, various microorganisms could degrade AMD by using it as nitrogen or

carbon source for growth. Previous studies have reported that AMD-degrading bacteria are mesophiles with optimum temperature for growth between 25 and 40 °C (Zamora et al., 2015). These studies have also demonstrated that biodegradation is the main mechanism of AMD removal in environmental systems. In tailings water, no improvement was observed in the removal efficiency of AMD via microorganism augmentation. This is probably due to low initial AMD concentration (1.15 mg/L) and fast biodegradation processes (>90 % within 2 weeks) in tailings water.
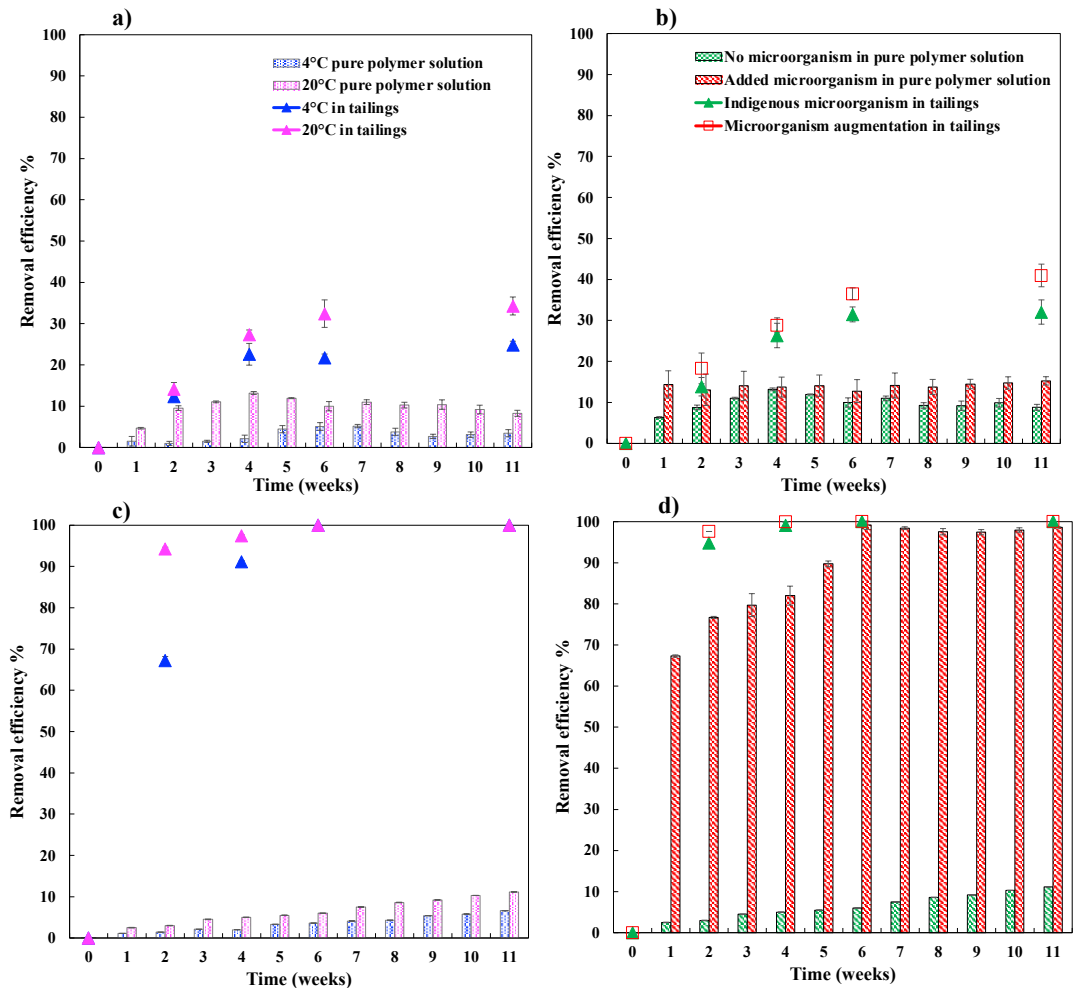
Figure 5.1 Removal efficiency of A-PAM (top) and residual AMD (bottom) in tailings water (dotted charts) and pure polymer solution (bar charts) under different temperature (a & c) and microorganism (b & d) conditions.

The interaction effects between temperature and microorganisms on the removal efficiency of A-PAM and AMD were investigated in pure polymer solutions. As shown in Table 5.4, for both A-PAM and AMD removal, microorganisms and temperature showed significant impacts due to low p-values (<0.05). However, the interaction effects of temperature and microorganisms only affected AMD removal significantly. The potential explanation for this phenomenon could be that AMD removal is mainly due to microorganism activity, while temperature could affect the metabolism activity of microorganism, resulting in a significant interaction effect. For A-PAM removal, both biodegradation and alkaline hydrolysis could result in its degradation, which might make the interaction of temperature and microorganism not significant.

Table 5.4 ANOVA results for the removal efficiency of A-PAM and AMD in pure polymer solutions after 11 weeks.

	Source of Variation	SS	df	MS	F	p-value
A-PAM removal %	Microorganism	61.54	1	61.54	53.18	0.002
	Temperature	78.44	1	78.44	67.78	0.001
	Interaction	1.69	1	1.69	1.46	0.29
	Within	4.63	4	1.16		
	Total	146.31	7			
AMD removal %	Microorganism	12502.51	1	12502.51	160215.88	<0.0001
	Temperature	335.80	1	335.80	4303.21	<0.0001
	Interaction	141.38	1	141.38	1811.72	<0.0001
	Within	0.31	4	0.08		

	Total	12980.00	7

5.3.1.2 Change in A-PAM molecular weight distribution

Table 5.5 illustrates the MW of polymer samples before and after degradation under different temperatures. In tailings water, the M_w of A-PAM declined from initial 2.12×10^6 g/mol to 2.00×10^6 g/mol at 4 °C, and further to 1.98×10^6 g/mol at 20 °C after 11 weeks. Similar to M_w, M_n also showed higher decreased at higher temperature. In addition, the polydispersity index (PDI) (M_w/M_n) of the polymer chains, was found to increase from 1.8 to 1.85 and to 2.39 at 4 °C and 20 °C, respectively, implying that the molecular weight distribution of A-PAM became less uniform. Unlike A-PAM in tailings water, M_n decreased while M_w and PDI increased in pure polymer solutions without microorganism under both 4 °C and 20 °C. A possible reason for the M_n decrease and an increased in M_w and PDI of A-PAM is that the inter and/or intra crosslinking of polymer chains could occur during the alkaline hydrolysis of A-PAM in pure solutions (Patel et al., 2021). Additionally, the decrease of M_n was promoted from 8.01×10^5 g/mol to 7.38×10^5 g/mol by increasing the temperature in pure polymer solution. Our finding was consistent with previous studies showing that temperature had a positive impact on crosslinking process of polymer chains (Ding et al., 2012; Molina et al., 2014).

In terms for A-PAM samples before and after degradation under different microorganism conditions. In tailings water with augmented microorganisms, the M_w and M_n of A-PAM were reduced to 1.81×10^5 g/mol and 8.02×10^5 g/mol, respectively, and PDI increased to 2.26 after 11 weeks. In contrast to the pure polymer solution without microorganism, A-PAM in pure polymer solution with added microorganisms showed lower value of M_w while higher value of M_n than the initial A-PAM, which resulted in the reduction in PDI from 1.80 to 1.42. Similar MW results in

both tailings water and pure polymer solution with added microorganisms suggested that the biodegradation could be the main pathway for the degradation of A-PAM in tailings. The average molecular weight results in both tailings water and pure polymer solutions indicated that the breakdown of C-C group occurred when A-PAM was consumed as carbon source for 11 weeks.

Table 5.5 GPC results of A-PAM samples before and after degradation under different temperature and microorganism conditions.

Sample	Mn (Da)	Mw (Da)	PDI
Raw A-PAM	1.18×10^6	2.12×10^6	1.80
4 °C pure polymer solution	8.01×10^5	2.68×10^6	3.34
20 °C pure polymer solution	7.38×10^5	2.48×10^6	3.36
4 °C in tailings	1.08×10^6	2.00×10^6	1.85
20 °C in tailings	8.29×10^5	1.98×10^6	2.39
No micro in pure polymer solution	7.38×10^5	2.48×10^6	3.36
Added micro in pure polymer solution	1.26×10^6	1.80×10^6	1.42
Indigenous micro in tailings	9.56×10^5	1.92×10^6	2.01
Micro augmentation in tailings	8.02×10^5	1.81×10^6	2.26

5.3.1.3 FT-IR analysis

In order to investigate the changes in A-PAM molecular structure, FT-IR was used to analyze A-PAM samples before and after degradation in tailings and in pure polymer solution

under different temperatures (Fig. 5.2a) and different microorganism (Fig. 5.2b) conditions. Table B.2 summarizes all the assignment of the FT-IR characterization of the bands and spectra of A-PAM. For the degraded A-PAM samples in tailings water under different temperature conditions (Fig. 5.2a), distinct decreases were observed at the 3340 cm^{-1} (-NH$_2$ asymmetric stretching), 3198 cm^{-1} (-NH$_2$ symmetric stretching) and 1657 cm^{-1} (C=O stretching of the primary amide), which could be due to the hydrolysis of the amide group. In addition, the wider band of carboxylate groups (1564 cm^{-1}) and increased intensities of 1401 cm^{-1} indicated the conversion of amide groups to ammonium and carboxylic acid. The peaks at 1126 cm^{-1} attributed to C-O-C stretching was confirmed after degradation. The result demonstrated that the adjoining amide group could be converted into ether group after hydrolysis. For the degraded A-PAM samples in pure polymer solutions, the FT-IR spectra were different from those in tailings water. The wide peaks at 3100-3340 cm^{-1} and strong peak at 1657 cm^{-1} in pure polymer solutions without microorganism confirmed that the intramolecular association could be carried out on the carbon chain during hydrolysis, which was consistent with GPC results of the inter and/or intra crosslinking of polymer chains. For degraded A-PAM samples in both tailings water and in pure polymer solution, the peaks of samples at 20 °C had higher intensities than the peaks in samples under 4 °C, confirming that hydrolysis, crosslinking, and degradation could be promoted with increasing temperature.

In terms of the microbial effect on the A-PAM degradation (Fig. 5.2b), compared with the degraded A-PAM in pure polymer solution without microorganisms, it is obvious that the absorption band near 2933 cm^{-1} assigned to -CH$_3$ or -CH$_2$- stretching partly disappeared; only a small shoulder of this peak remained in the spectrum of degraded A-PAM samples in pure polymer solution and tailings water with microorganisms. This was possibly due to the breakage of the carbon backbone of the polymer. In addition, the peak (1417 cm^{-1}) due to the C-N stretching

167

vibration of degraded A-PAM samples disappeared in pure polymer solution and tailings with microorganisms, suggesting that the amidase enzyme existed, and it could help microorganisms to cleave the C-N bond of polymer under aerobic condition. Based on the above results, it was verified that the microorganisms could degrade A-PAM and utilize the amide and carbon of the polymer as the source of carbon and nitrogen nutrition for their growth in aerobic environment. It is worthy to mention that a strong peak at 1657 cm^{-1} (due to the C=O bond) and some small peaks between 2900 and 2500 cm^{-1} appeared in the spectrum of A-PAM after degradation, which revealed that the -COOH existed in the intermediates of hydrolysis or/and metabolites of biodegradation.
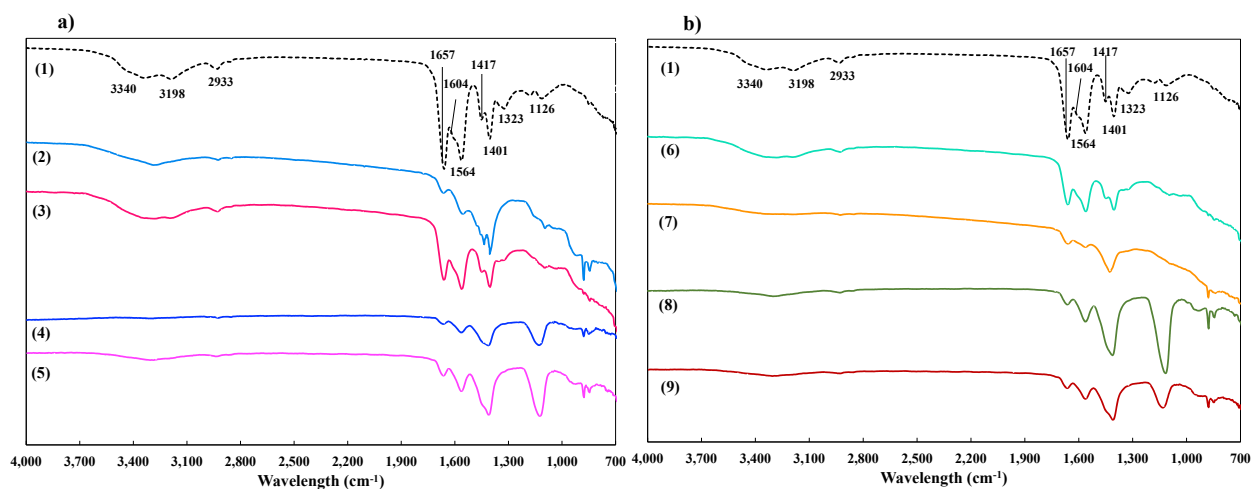
Figure 5.2 FT-IR spectrum of A-PAM before and after degradation under different temperature (a) and microorganism (b) conditions: (1) raw A-PAM before degradation; (2) degraded A-PAM in pure polymer solution at 4 °C; (3) degraded A-PAM in pure polymer solution at 20 °C; (4) degraded A-PAM in tailings water at 4 °C; (5) degraded A-PAM in tailings water at 20 °C; (6) degraded A-PAM in pure polymer solution without microorganisms; (7) A-PAM in pure polymer solution with added microorganisms after degradation; (8) degraded A-PAM in tailings

water with indigenous microorganisms; and (9) degraded A-PAM in tailings water with augmented microorganisms.

5.3.2 Effect of A-PAM degradation in tailings water

5.3.2.1 Water chemistry

5.3.2.1.1 Total inorganic nitrogen

Over the long-term timescales, nitrogen cycling could be one of the important biogeochemical processes in oil sands tailings (Risacher et al., 2018). However, apart from N_2 fixation, the nitrogen cycle and the effect of polymer degradation on nitrogen cycle in the tailings pond have been poorly studied. In this study, the total inorganic nitrogen concentrations ($\sum$(NH_4^+-N, NO_2^--N, NO_3^--N)) in tailings water and in pure polymer solution were monitored. As shown in Fig. 5.3, ammonium concentration was the major component (>80 %) of the total inorganic nitrogen concentration in both tailings water and pure polymer solution throughout the 11 weeks. Therefore, the changes in total inorganic nitrogen observed were due to the changes of ammonium concentration. Based on Table 5.1, the initial concentrations of ammonium (NH_4^+-N), nitrite (NO_2^--N) and nitrate (NO_3^--N) in oil sands tailings without PAM addition were quite low at 0.20, 0.02 and 0.05 mg/L, respectively, and remained relatively stable for 11 weeks (Fig. B.4). However, after adding PAM, the NH_4^+-N concentration in tailings water increased dramatically to around 5 mg/L due to the hydrolysis of the amide group in PAM and/or AMD. With the continuous degradation of PAM and AMD, the NH_4^+-N concentration continued increasing because ammonium is one of the possible breakdown products from PAM and AMD degradations. As the initial concentration of AMD was low (<2 mg/L), the main contribution of ammonium increase would be from the A-PAM degradation. The liberated ammonium in the water could be then oxidized to nitrate and nitrite under aerobic condition or/and used as a nitrogen source for growth

by the microbes, resulting in the reduction of ammonium concentration. Based on the low and relatively stable concentrations of nitrite and nitrate generated during the study, it is reasonable to assume that the liberated ammonium from A-PAM degradation in tailings water was utilized mainly for microbial growth rather than nitrification.

Since temperature and microorganisms showed significant impacts on the degradation of A-PAM and AMD in tailings water, it is expected that the NH_4^+-N concentration would change differently under various temperature and microorganism conditions. The NH_4^+-N concentration increased rapidly and then gradually decreased at 20 °C, while a gradual increase was observed at 4 °C (Fig. 5.3a), which was consistent with the results showing that faster degradation of A-PAM and AMD were observed at higher temperature. As biodegradation was the main process of removing A-PAM and AMD, the NH_4^+-N concentration in pure polymer solutions without microorganisms remained at low levels under both temperatures (Fig. 5.3c). Besides, the NH_4^+-N concentration in pure polymer solution with added microbes increased quickly where the concentration doubled in 2 weeks and then remained relatively stable (Fig. 5.3d). The lower NH_4^+-N concentrations and longer time required to reach the peak concentration were noticed in the tailings water with augmented microorganisms (Fig. 5.3b). This could be explained by the higher consumption of ammonium as nitrogen source due to the increase of total microorganisms, occurrence of the adaption for the introduced microorganism, and competition with indigenous microorganisms in tailings water. Therefore, the results showed that the biodegradation process had the biggest impact on NH_4^+-N concentration.
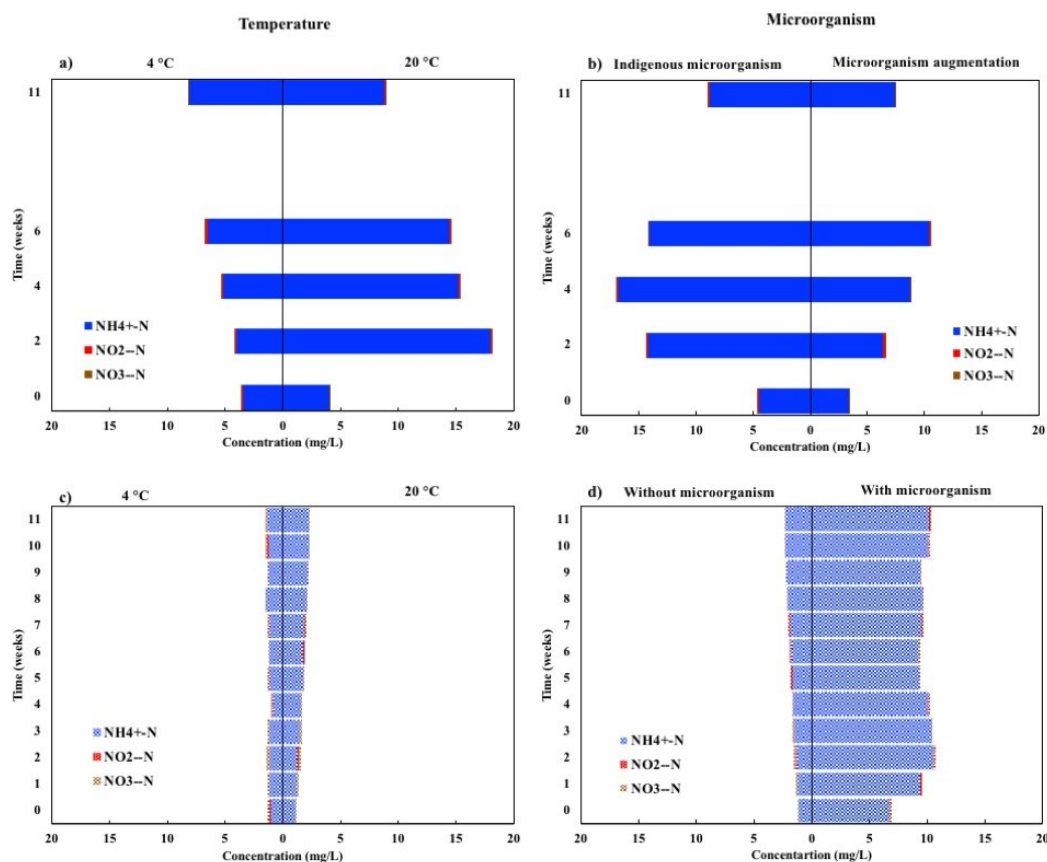
Figure 5.3 The concentration of total inorganic nitrogen ($\sum$(NH4+-N, NO2−-N, NO3−-N)) in tailings (a & b) and in pure polymer solution (c & d) with time under different temperature and microorganism conditions.

5.3.2.1.2 Naphthenic acids (NAs)

Among various organic compounds in tailings water, NAs are of particular environmental concerns due to their acute and chronic aquatic toxicity (Arslan et al., 2022). Flocculation by polymer-based flocculants has shown the capacity to remove NAs from oil sands process water (OSPW) (Pourrezaei et al., 2011). Additionally, the degradation of A-PAM could produce organic acids which might contribute to the NA measurement. Thus, it is worthy to study the effects of addition and degradation of A-PAM on the NA concentration in oil sands tailings. Here, we investigated the total concentration and relative abundance of different classes of NAs in water of

A-PAM treated tailings at beginning and after 11 weeks. The resutls were then compared to NAs in raw tailings without A-PAM addition at 20 °C.

As demonstrated in Fig. 5.4, the initial total concentration of NAs in raw tailings without A-PAM was 51.77 mg/L, with O_2 NAs being the most abundant classes (>60 %). After adding A-PAM, the initial total concentration of NAs was reduced, with the lowest value of 31.04 mg/L detected in the water of microorganism-augmented tailings. The reduction of NA concentration would likely be due to the removal of NAs by coagulation due to the A-PAM. Although the O_2 NAs were still the major components in A-PAM treated tailings water, they decreased to about 55 % among different conditions, suggesting that the addition of A-PAM was beneficial to the removal of O_2 NAs from tailings water. In addition, no remarkable changes were noticed in the total concentration of NAs in all systems after 11 weeks, indicating that the A-PAM degradation had no dramatic effect on the total concentration of NAs in tailings water. A decrease of O_2 NAs (which was below 50 %) and an increase in oxidized NAs with various extents were found in both the water of raw tailings and in A-PAM treated tailings with augmented microorganisms after 11 weeks. However, opposite changes, where the percentage of O_2 NAs increased to about 60 s% and O_3 NAs decreased below 20 %, were found in the A-PAM treated tailings water with indigenous microorganisms, suggesting that biodegradation of A-PAM might affect the distribution of NAs without affecting the total concentration. Furthermore, we highlight the DBE versus carbon number images for the dominant O_2 class in tailings water after 11 weeks. As illustrated in Fig. 5.5, compared to the abundant NAs with a wide range of DBE values (1-10) and carbon number (9-20) in raw tailings water without A-PAM, decreased concentrations of O_2 NAs with much narrower range of DBE values and carbon number were observed in A-PAM treated tailings water. Especially, for the A-PAM treated tailings water with augmented microorganisms, only two ranges

of NAs, including those with carbon numbers of 12-16 and DBE of 3-4, and carbon numbers of

15-17 and DBE of 6-9 remained, which could be explained by preferential removal due to the

addition and biodegradation of A-PAM.
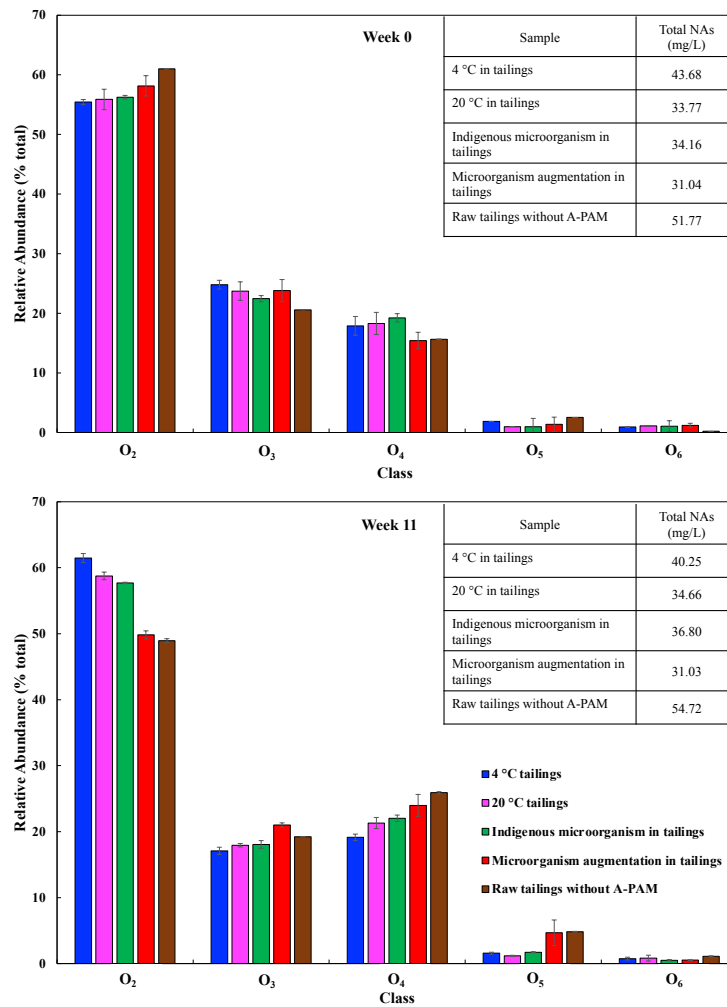
Figure 5.4 Diagram of total concentration and class distribution of NAs in tailings water with

and without A-PAM under different temperature and microorganism conditions at week 0 and

week 11.
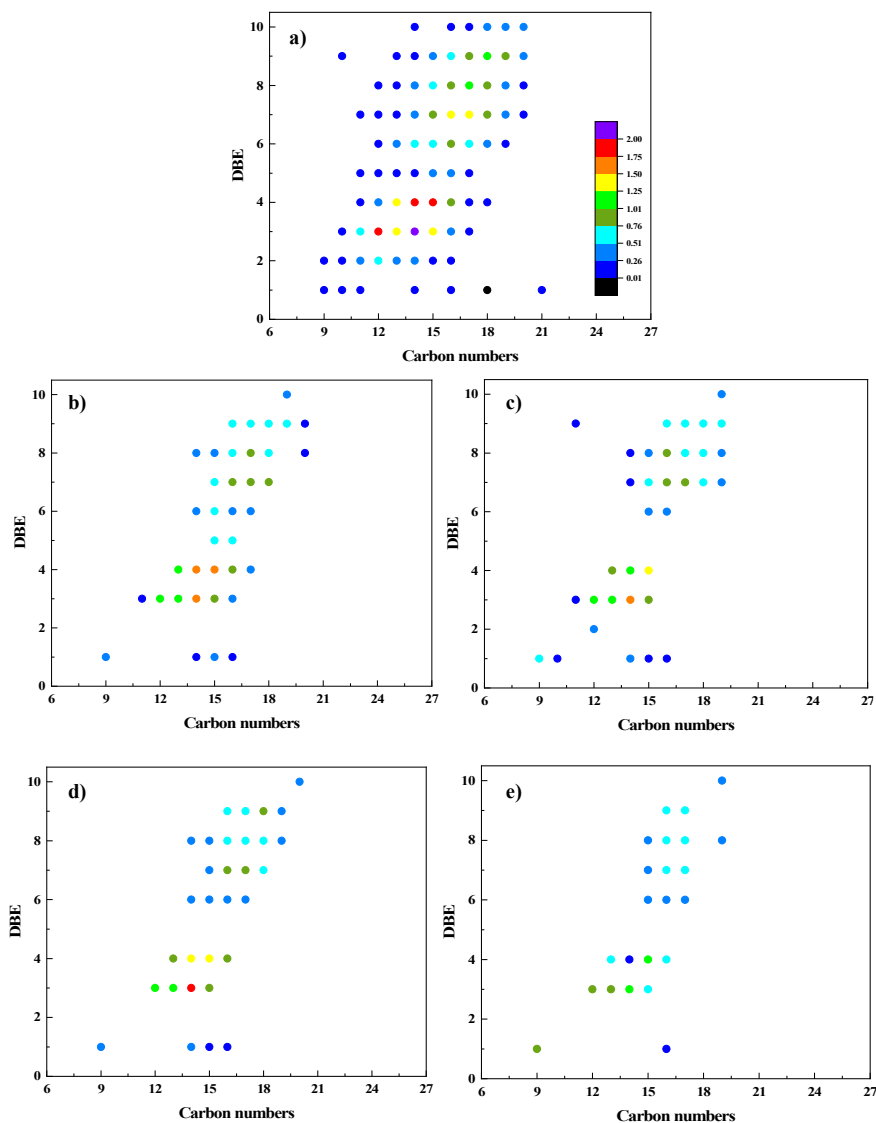
Figure 5.5 Isoabundance-contoured plots of DBE versus carbon number for the O2 class for tailing samples after 11 weeks: (a) control sample with no A-PAM under light and 20 °C ; (b) with A-PAM under no light and 4 °C; (c) with A-PAM under no light and 20 °C; (d) with A-PAM and indigenous microorganism under light and 20 °C; and (e) with A-PAM and microorganism augmentation under light and 20 °C.

In order to further understand the effect of A-PAM degradation on the dominant O_2 NAs, the DBE versus carbon number images for the classical NAs in pure polymer solutions were

studied (Fig. 5.6). The results showed that the generated O_2 NAs from A-PAM hydrolysis and degradation were in low concentrations (<2.5 mg/L) and were mainly NAs with DBE = 1 (z = 0). The carbon number range of NAs in pure polymer solution was 9-26, indicating that they are primarily saturated fatty acids and, therefore, very dissimilar from the NAs in tailings water. Therefore, we could assume that the increase in the relative abundance of O_2 NAs in A-PAM treated tailings water was mainly due to fatty acids. Besides, after adding microorganisms in the pure polymer solution, the concentration of saturated fatty acids decreased to < 0.9 mg/L which demonstrated that they were susceptible to biodegradation. Hence, these fatty acids would not persist as NAs in the water of A-PAM treated tailings though they could fit the NA formula. Similar results were obtained by previous studies (Brown and Ulrich, 2015; Scott et al., 2005). More detailed information of these fatty acids could to be investigated by GC-FID in the future.
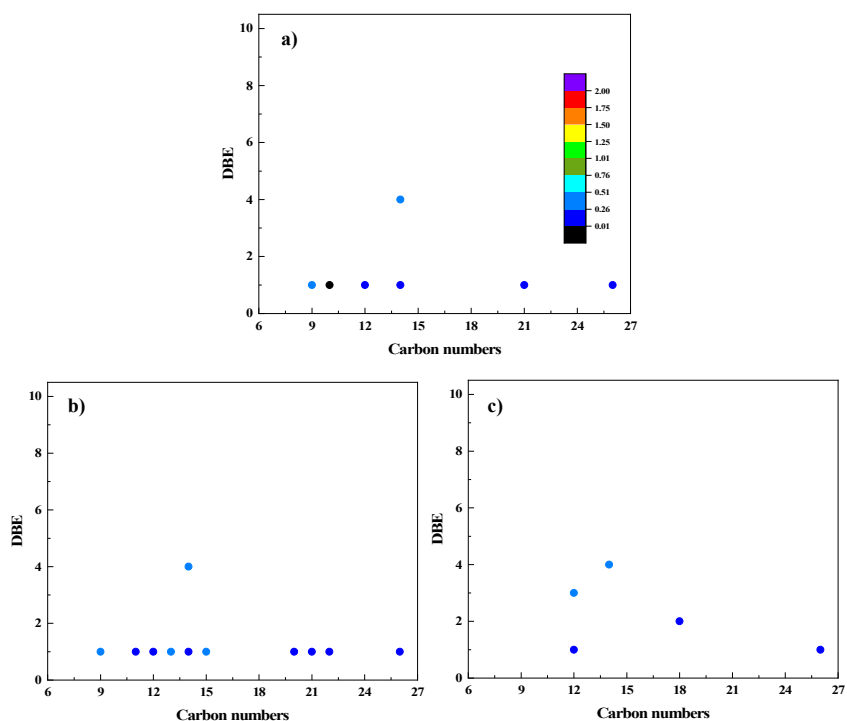
Figure 5.6 Isoabundance-contoured plots of DBE versus carbon number for the O2 class for pure polymer solution after 11 weeks: (a) samples with no microorganism at 4 °C; (b) with no microorganism at 20 °C; and (c) with microorganism at 20 °C.

5.3.2.1.3 TOC and COD

Both TOC and COD have been used to measure PAM degradation in various studies (Sang et al., 2015; Sun et al., 2021). The initial TOC and COD concentrations in the water of A-PAM treated tailings were measured as 480.9 mg/L-C and 1332.5 mg/L, respectively, which were 3-4 times higher than initial values in tailings water without A-PAM (Table 5.1). The removal efficiencies of TOC and COD of A-PAM treated tailings and pure polymer solution under different temperature and microorganism conditions were illustrated in Fig. 5.7. Interestingly, similar fluctuations were noticed in both TOC and COD removal efficiency in A-PAM treated tailings water where the values increased in the first 4 weeks, then decreased in the next 2 weeks, and started to increase again at week 11. The highest removal efficiencies of TOC and COD were found as 24.3 % and 32.8 %, respectively in A-PAM treated tailings water with augmented microorganisms. The low TOC and COD reduction indicated limited chain breakage of A-PAM which leads to partial mineralization in tailings water (Sun et al., 2017). The removal efficiencies of TOC and COD in pure polymer solution without microorganisms under different temperatures (Fig. 5.7a, 5.7c) were very low (<5 %) and relatively stable, while the removal values became similar to values in tailings water after adding microorganisms (Fig. 5.7b, 5.7d), suggesting that the chain scission was mainly due to the biodegradation of A-PAM. Besides, strong linear correlations with high R^2 values (>0.90) between the removal efficiency of A-PAM and the removal efficiency of TOC and COD were observed in A-PAM treated tailings water (Fig. B.5). This was expected because the initial concentration of A-PAM in tailings water was quite high

(1000 ppm), thus contributing to the high initial values of TOC and COD. In this case, TOC and COD could be used as indicators of A-PAM degradation in tailings water. Similar to A-PAM treated tailings water, TOC and COD were successfully used to assess A-PAM degradation in pure polymer solution under different conditions due to good linear correlations (all $R^2 > 0.89$) (Fig. B.6).
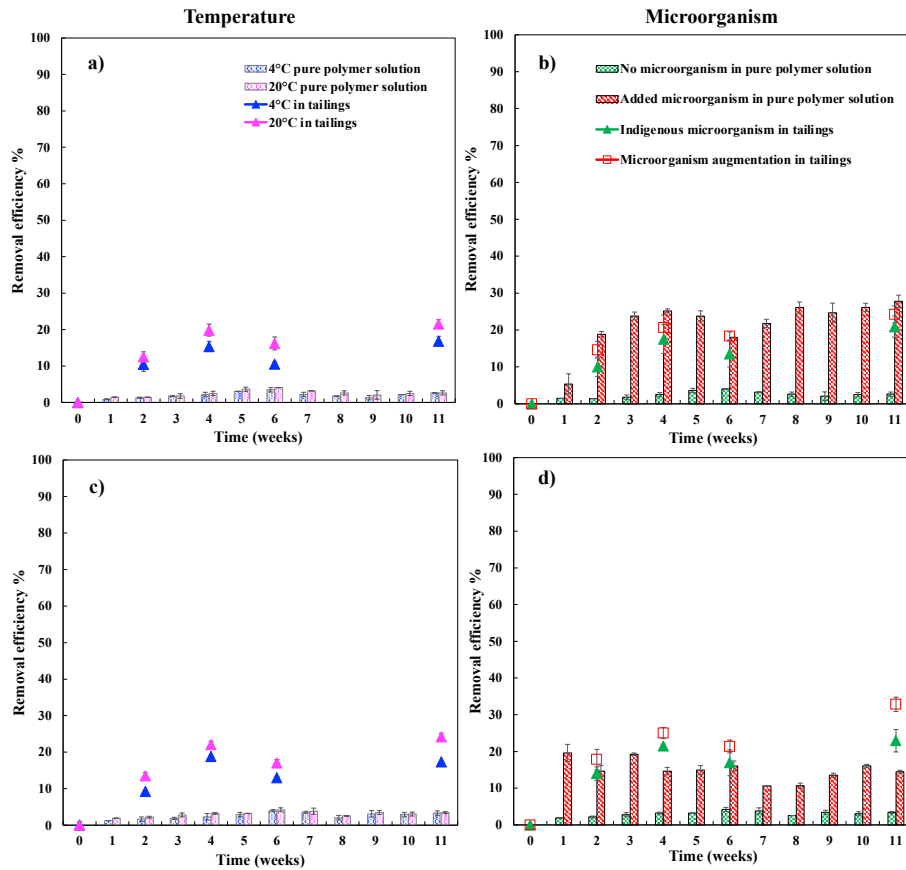
Figure 5.7 Removal efficiency of TOC (a & b) and COD (c & d) with time in tailings and pure polymer solution under different temperature (left) and microorganism (right) conditions.

5.3.2.1.4 Zeta potential and pH

Zeta potential is an important tool to indicate the stability of colloidal solution and it is driven by pH as well as ionic strength (Kumar and Dixit, 2017). Therefore, zeta potential and pH were monitored in tailings water and pure polymer solution. As shown in Fig. 5.8a, 8b, the initial

values of zeta potential in the water of A-PAM treated tailings under different conditions were about -60 mV, which were lower than the initial zeta potential value (-35 mV) in raw tailings water without A-PAM (Table 5.1) and hence indicated the higher stability by promoted settling from A-PAM addition. There was a slight increase of zeta potential value from -63 mV to -56 mV at 20 °C while no significant change of zeta potential was observed at 4 °C in A-PAM treated tailings water after 11 weeks. In addition, compared to the tailings water with indigenous microorganisms, zeta potential values were less negative in tailings water with augmented microorganisms. Similar changes of zeta potential were also observed in pure polymer solution. The zeta potential results were consistent with the degradation efficiency of A-PAM, suggesting that the degradation of A-PAM could result in the increase of zeta potential in tailings water. This implied that the stability of tailings water declined slightly and limited media interactions like decrease of hydrogen bonding and van der Waals could occur. The initial pH values of tailings water without A-PAM (Table 5.1) and with A-PAM (Fig. 5.8c, 8d) were both at 8.6, which indicated that A-PAM addition would not change the pH of tailings. The pH values rose slightly after 11 weeks in both A-PAM treated tailings water and in pure polymer solution, from 8.6 to 8.8 and from 8.4 to 8.6, respectively, which was probably due to the generation of ammonium from hydrolysis and degradation of A-PAM. Besides, the $NaHCO_3$ in both pure polymer solution and tailings water could act as buffer, which prevented the huge change in the pH values.
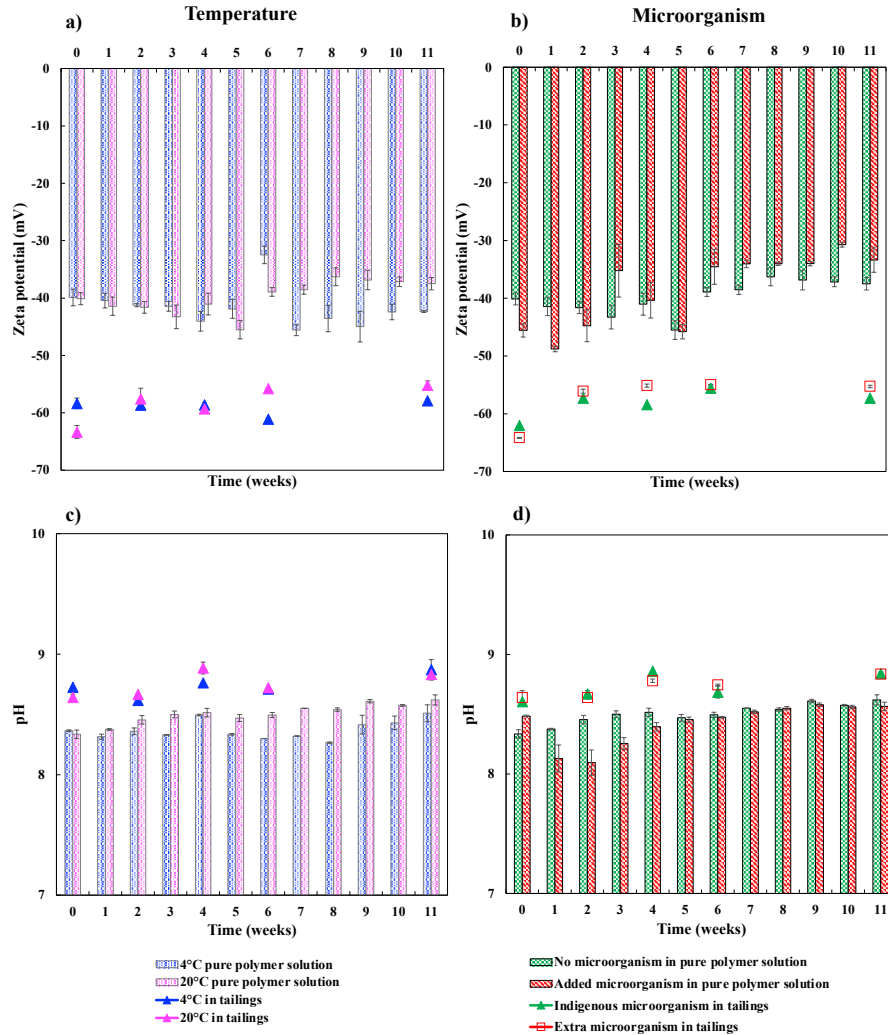
Figure 5.8 Zeta potential (a & b) and pH (c & d) of pure polymer solution and tailings at different time under different temperature and microorganism conditions.

5.3.2.2 Toxicity

5.3.2.2.1 Acute toxicity

The toxicity of tailings pond water has been the concern primarily with water release and long-term reclamation of oil sands tailings. As shown in Fig. 5.9, raw tailings water without A-PAM presented acute toxicity with highest inhibition effects of 52.0 % and 54.3 % at 5 min and 15 min, respectively, which was due to the presence of NAs and other organic compounds like phenol (Li et al., 2017). Although A-PAM is generally considered as relatively nontoxic (Buczek

179

et al., 2017), there is very limited publication assessing the toxicity of A-PAM with long exposure time and with potential degradation products such as AMD and other intermediates. Therefore, it is worthy to monitor the effect of A-PAM degradation on toxicity in tailings water under different conditions in order to ensure the safety of A-PAM application in tailings management for long period of time.

Acute toxicity tests performed with *A. fischeri* on tailings water and on pure polymer solution were compared under different temperature and microorganism conditions. As illustrated in Fig. 5.9, the highest inhibition effects were found in the A-PAM treated tailings water with augmented microorganisms at the beginning, 67 % (5 min) and 69.3 % (15 min), respectively, which revealed that even with high initial concentration of A-PAM (1000 ppm), the values were only 15 % higher than those in raw tailings water without A-PAM probably due to the AMD residual. In the pure polymer solutions, the maximum inhibition effects were also observed in the solution with added microorganisms at 33.6 % (5 min) and 34.2 % (15 min). That is, the reduction in luminescence intensity did not reach 50 %, confirming the non-toxic features of A-PAM at 1000 ppm in tailings. Similar decreases in inhibition effects from the beginning to week 11 (~20 % for 5 min and ~15 % for 15 min) were found in tailings water with and without A-PAM, indicating that the degradation of A-PAM did not dramatically affect the acute toxicity of tailings water. Previous studies have reported that the O_2 NAs, especially the tricyclic and bicyclic structures increased *A. fischeri* toxicity while fatty acids were not major contributors to toxicity (Yue et al., 2016). Hence, the reduction of acute toxicity in A-PAM treated tailings water confirmed that the increase in the O_2 NAs concentration was mainly due to fatty acids. Yet, small increases (<10 %) in the inhibition effects were found in pure polymer solution with added microorganisms and in A-PAM treated tailings water with augmented microorganisms. This implied that the toxicity of

metabolism intermediates from the biodegradation of A-PAM should not be neglected when assessing the long-term toxicity of A-PAM degradation in environmental systems. Furthermore, the acute toxicity of tailings sediments including pore water and sludge were also investigated at the beginning and the end of the sampling period (Fig. 5.9). Compared to the A-PAM treated tailings water, the acute toxicity of pore water in the sediments were relatively stable at about 60 % while the acute toxicity significantly increased for the sludge of tailings sediments under different conditions. The highest increases of acute toxicity of the sludge were observed at the sediments in A-PAM treated tailings with augmented microorganisms, from 55.4 % to 74.4 % (5 min) and from 57.8 % to 76.3 % (15 min), respectively. Although no noticeable differences of the acute toxicity of pore water and sludge at the beginning, after 11 weeks, the acute toxicity in sludge became at least 10 % higher than the toxicity in pore water, implying that toxic compounds gradually accumulated into the sludge by settling with A-PAM without being released into the pore water.
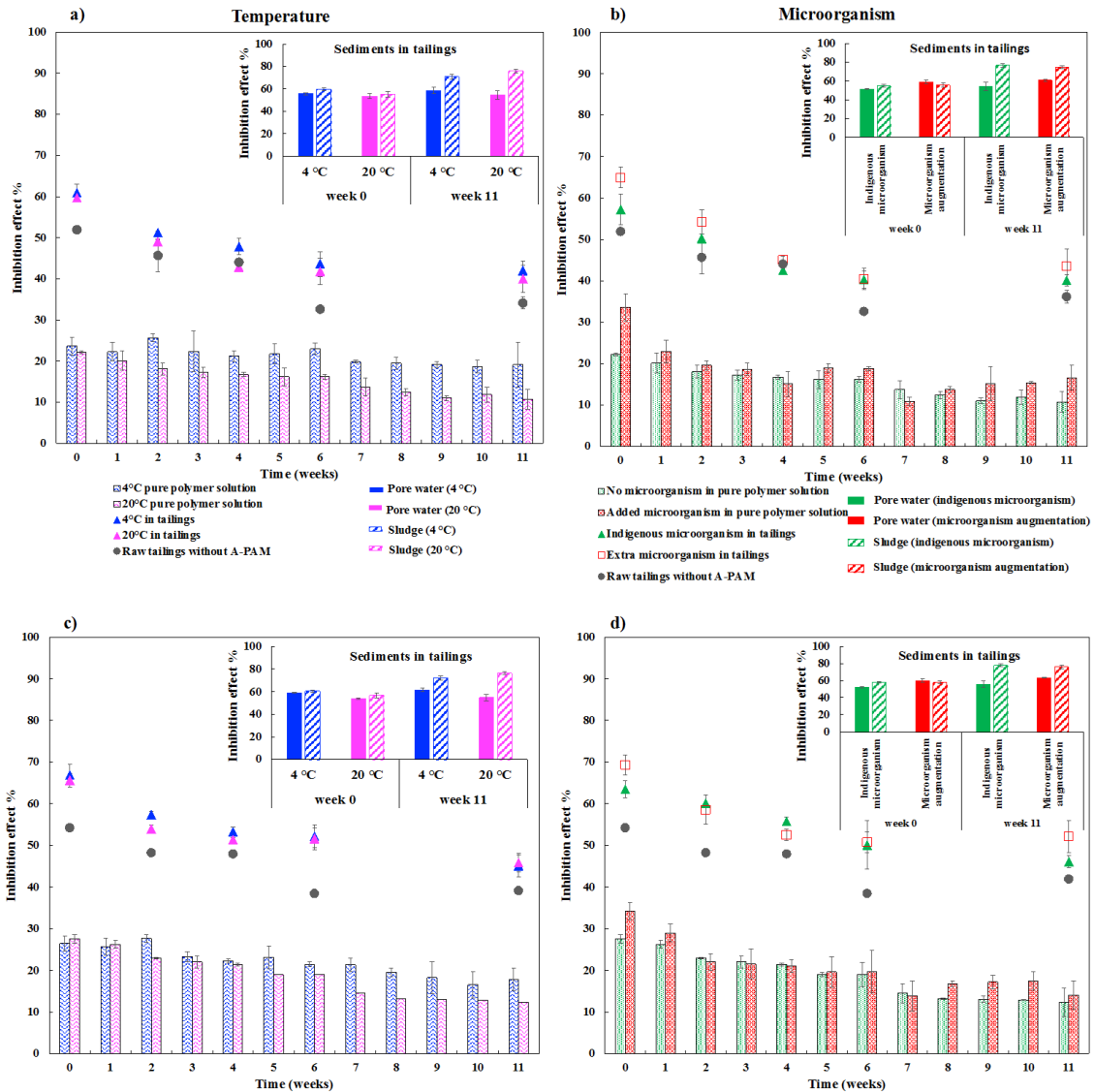
Figure 5.9 Acute toxicity (5 min (a & b) and 15 min (c & d)) to *A. fischeri* in tailings capping water, sediments and pure polymer solution under different temperature and microorganism conditions.

5.3.2.2.2 Genotoxicity

Despite AMD is readily biodegradable and former results show that complete degradation of AMD could be as fast as 4 weeks in oil sands tailings, careful monitoring of the genotoxicity could ensure that no hazardous chemicals were released from AMD or A-PAM under different conditions. Results of the genotoxicity test for the tailings capping water, tailings sediments, and

pure polymer solutions are summarized in Fig. 5.10. The survival rate in all samples exceeded 80 % which, based on the test's supplier, validated the test results, proving that the samples were not cytotoxic to the test bacteria. Besides, all the IF values of tailings water samples were lower than the threshold value of 1.5, which implied that the addition and degradation of A-PAM would not make tailings water become genotoxic, though they did slightly increase the IF values in tailings water. It was noticed that the genotoxicity in the sludge of A-PAM treated tailings increased after 11 weeks and the final IF values were close to the threshold under all conditions, demonstrating that the potentially genotoxic components may accumulate in the sludge of tailings sediments. However, no remarkable increase of genotoxicity was found in the pore water in A-PAM treated tailings sediments for 11 weeks. Longer tracking time for the genotoxicity of pore water and sludge in the tailings sediments is suggested for future studies to confirm whether the degradation of A-PAM in the sediments would result in the release of components with genotoxicity from sludge to pore water and then transferred to the capping water. It is interesting to observe that the genotoxicity of tailings water was lower than that of pure polymer solution under all conditions in most of sampling periods. Lower genotoxicity in A-PAM treated tailings water than that of pure polymer solution without microorganisms could result from the faster removal efficiency of AMD due to biodegradation while producing metabolites with lower toxicity by the more diverse microorganism community in tailings water as compared to the 5-strain microorganism mixtures in pure polymer solution. More details about the metabolites produced from biodegradation of AMD and A-PAM and the toxicity effect of these products are worthy to investigate in the future.
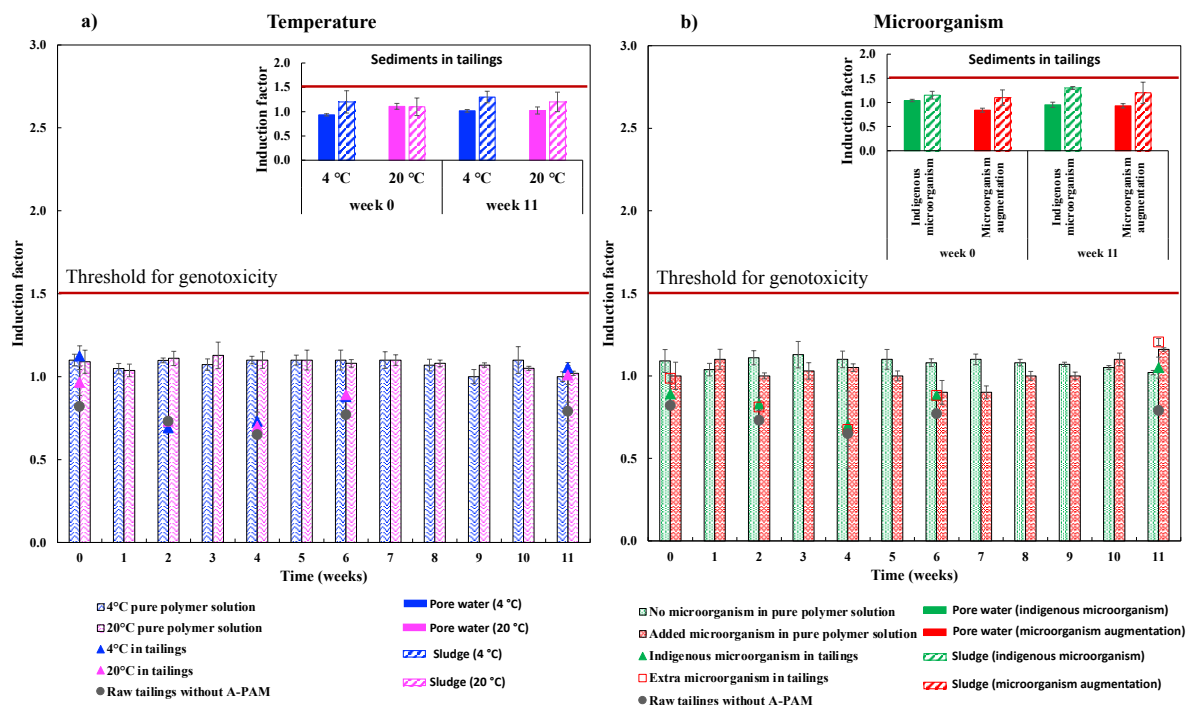
Figure 5.10 Genotoxicity of tailings capping water, sediments and pure polymer solution with time under different temperature (a) and microorganism (b) conditions.

5.3.3 Possible A-PAM degradation mechanisms

According to the degradation results of A-PAM under different temperature and microorganism conditions, biodegradation could be the primary mechanism of A-PAM degradation in oil sands tailings water. A-PAM biodegradation under aerobic condition occurred in tailings water because of the hydrolysis of amide nitrogen and the cleavage of the main carbon backbone. Based on the above results and proposed pathways in earlier studies (Bao et al., 2010; Joshi and Abed, 2017), the possible pathway for the aerobic biodegradation A-PAM and its derivatives in tailings water is outlined in Fig. 5.11. Biodegradation of A-PAM begins with amidase catalyzed deamination of A-PAM to ammonia and polyacrylic acid. The liberated ammonia is then utilized as a nitrogen source for growth by the microbes. As suggested by previous studies (Nyyssölä and Ahlgren, 2019; Yu et al., 2015), A-PAM would most likely be deaminated

by extracellular amidases rather than intracellular ones, because the large size of the polymers makes the transport into the cells difficult. After many cycles, subsequent catalysis by monooxygenases oxidation on the main PAM carbon chain results in the oxidation of α-[-CH$_2$-]-COH-, transferred to -CHO, and then oxidized to -COOH. During the biodegradation process, the main carbon backbone breaks down and large A-PAM molecules are transformed into smaller molecules, such as oligomers, acrylate, and organic acids like fatty acids. The smaller molecular fragment could be then used as the carbon source. No AMD is produced during the biodegradation process of A-PAM in oil sands tailings. The possible pathway of biodegradation of A-PAM was in line with the results of GPC, FT-IR, ammonium, and pH. Further study is needed to determine the detailed chemical structure of the A-PAM degradation products by using more advanced techniques like nuclear magnetic resonance spectroscopy and their subsequent fate. In addition, A-PAM was not fully biodegraded in oil sands tailings, which can be hypothesized that after biodegradation, the resulting carbon backbone structure, polyacrylate, is recalcitrant to further biodegradation.
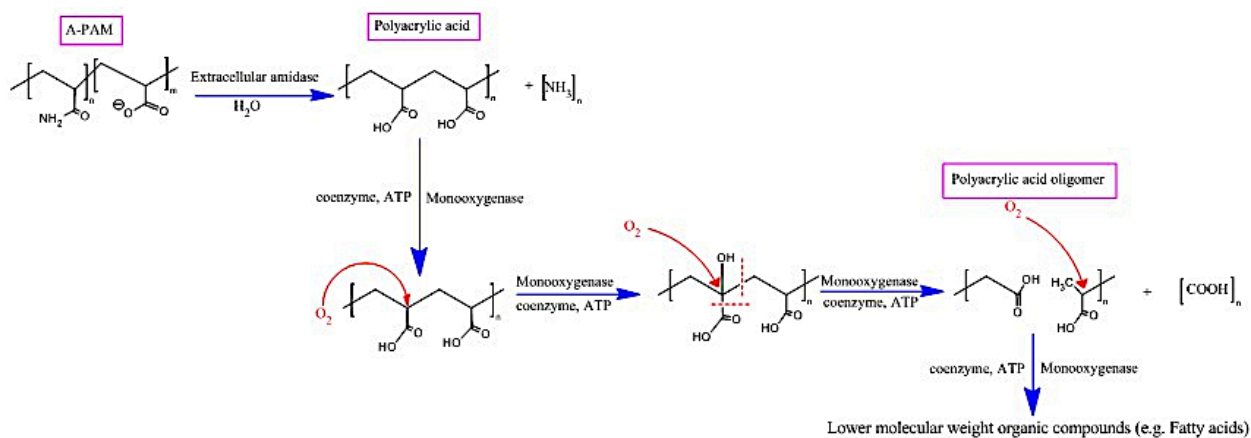
Figure 5.11 Possible aerobic biodegradation pathway for A-PAM and the potential intimidate compounds in tailings water.

5.4 Conclusion

The degradation of A-PAM in tailings water under different temperature and microorganism conditions was investigated and compared to its degradation in pure polymer solution. The highest removal efficiency of A-PAM could reach 41.0 % in tailings water at 20 °C with augmented microorganisms after 11 weeks. Under the experimental conditions examined in this work, no AMD was released from the A-PAM degradation and residual AMD, from the manufacturing process of A-PAM, was removed completely within 4 weeks in tailings water. Based on the results of GPC and FT-IR, it was proven that large A-PAM molecules were degraded into products with lower molecular weight. Besides, the hydrolysis of the amide groups in A-PAM with the conversion of amide groups to ammonium and carboxylic acid was confirmed. In tailings water, biodegradation was proposed as the main pathway for A-PAM degradation, and it was verified that the microorganisms could utilize the amide and carbon of A-PAM as the source of carbon and nitrogen nutrition for their growth in an aerobic environment. Both temperature and microorganisms increased the degradation of A-PAM and residual AMD in tailings water.

By monitoring the water characteristics of tailings, the impact of addition and degradation of A-PAM on the quality of tailings water was well explored. The concentration of total inorganic nitrogen, TOC, COD, and absolute value of zeta potential in tailings water dramatically increased, while the total concentration of NAs decreased, and pH remained relatively stable immediately after the A-PAM addition. No significant changes to the total concentration of NAs were observed in A-PAM treated tailings water, though low concentration of fatty acids (<2.5 mg/L), which fit NAs formula, were detected in pure polymer solution, indicating that A-PAM degradation would not affect the total concentration of NAs in tailings water though affect its distribution. Due to the strong linear correlation ($R^2 > 0.90$) between the A-PAM removal efficiency and the removal

efficiency of TOC and COD, our findings suggest that both parameters could be used as indicators of A-PAM degradation in tailings water. Slight increases in zeta potential and pH were found while A-PAM degraded in tailings water. To further evaluate the possible environmental risks of A-PAM and residual AMD degradation, both the acute toxicity and genotoxicity were assessed for tailings water and sediments, including pore water and sludge. Similar acute toxicity values between A-PAM treated tailings and raw tailings without A-PAM proved that the addition and degradation of A-PAM did not dramatically affect the acute toxicity of tailings water. No genotoxicity was identified in capping water and sediments in A-PAM treated tailings. Yet, increases of acute toxicity and genotoxicity were only noticed in the sludge of A-PAM treated tailings, demonstrating that the toxic components, which are not likely A-PAM component but rather what is being flocculated, could accumulate in the sludge without being released into the pore water.

Our results of A-PAM aerobic biodegradation in oil sands tailings suggest that A-PAM undergoes hydrolysis of amide groups by amidase enzymes, releasing ammonium and producing polyacrylic acid. Under aerobic condition, oxidation catalyzed by monooxygenase on the carbon chain might occur, resulting in the breakdown of carbon chain backbone and small molecular fragments like fatty acids. Further investigation could be completed to elucidate the degree and kinetics of A-PAM degradation in tailings. In addition, there is a need to examine biodegradation of PAM under anaerobic condition and the effect on microbial community in tailings to complete the knowledge gap of PAM degradation in tailings. Our results provide insights into the stability and impacts of A-PAM in oil sands tailings for long period of time, which are valuable for the management of oil sands tailings.

5.5 References

Akbar, M., Khan, M.F.S., Qian, L., Wang, H., 2020. Degradation of Polyacrylamide (PAM) and methane production by mesophilic and thermophilic anaerobic digestion: Effect of temperature and concentration. Frontiers of Environmental Science & Engineering 14(6), 1-11.

Akbari, S., Mahmood, S.M., Tan, I.M., Ghaedi, H., Ling, O.L., 2017. Assessment of polyacrylamide-based co-polymers enhanced by functional group modifications with regards to salinity and hardness. Polymers 9(12), 647.

Allam, N.E., Anwar, M.N., Kuznetsov, P.V., Ulrich, A.C., Dhar, B.R., 2022. Enzyme-assisted dewatering of oil sands tailings: Significance of water chemistry and biological activity. Chemical Engineering Journal 437, 135162.

Arslan, M., Müller, J.A., Gamal El-Din, M., 2022. Aerobic naphthenic acid-degrading bacteria in petroleum-coke improve oil sands process water remediation in biofilters: DNA-stable isotope probing reveals methylotrophy in Schmutzdecke. Science of The Total Environment 815, 151961.

Bao, M., Chen, Q., Li, Y., Jiang, G., 2010. Biodegradation of partially hydrolyzed polyacrylamide by bacteria isolated from production water after polymer flooding in an oil field. Journal of hazardous materials 184(1-3), 105-110.

Bazoubandi, B., Soares, J.B., 2020. Amylopectin-graft-polyacrylamide for the flocculation and dewatering of oil sands tailings. Minerals Engineering 148, 106196.

Brient, J.A., Wessner, P.J., Doyle, M.N., 2000. Naphthenic acids. Kirk‐ Othmer Encyclopedia of Chemical Technology.

Brown, L., Bancroft, K., Rhead, M., 1980. Laboratory studies on the adsorption of acrylamide monomer by sludge, sediments, clays, peat and synthetic resins. Water Research 14(7), 779-781.

Brown, L.D., Ulrich, A.C., 2015. Oil sands naphthenic acids: a review of properties, measurement, and treatment. Chemosphere 127, 276-290.

Buczek, S.B., Cope, W.G., McLaughlin, R.A., Kwak, T.J., 2017. Acute toxicity of polyacrylamide flocculants to early life stages of freshwater mussels. Environmental toxicology and chemistry 36(10), 2715-2721.

Campos-Avelar, I., Colas de la Noue, A., Durand, N., Cazals, G., Martinez, V., Strub, C., Fontana, A., Schorr-Galindo, S., 2021. Aspergillus flavus Growth Inhibition and Aflatoxin B1 Decontamination by Streptomyces Isolates and Their Metabolites. Toxins 13(5), 340.

Caulfield, M.J., Hao, X., Qiao, G.G., Solomon, D.H., 2003. Degradation on polyacrylamides. Part I. Linear polyacrylamide. Polymer 44(5), 1331-1337.

Caulfield, M.J., Qiao, G.G., Solomon, D.H., 2002. Some aspects of the properties and degradation of polyacrylamides. Chemical reviews 102(9), 3067-3084.

Cossey, H.L., Batycky, A.E., Kaminsky, H., Ulrich, A.C., 2021. Geochemical Stability of Oil Sands Tailings in Mine Closure Landforms. Minerals 11(8), 830.

Dai, X., Luo, F., Zhang, D., Dai, L., Chen, Y., & Dong, B. (2015). Waste-activated sludge fermentation for polyacrylamide biodegradation improved by anaerobic hydrolysis and key microorganisms involved in biological polyacrylamide removal. Scientific reports, 5(1), 1-13.

Dai, X., Luo, F., Yi, J., He, Q., Dong, B., 2014. Biodegradation of polyacrylamide by anaerobic digestion under mesophilic condition and its performance in actual dewatered sludge system. Bioresource technology 153, 55-61.

De Meyer, S.E., Willems, A., 2012. Multilocus sequence analysis of Bosea species and description of Bosea lupini sp. nov., Bosea lathyri sp. nov. and Bosea robiniae sp. nov., isolated from legumes. International Journal of Systematic and Evolutionary Microbiology 62(Pt_10), 2505-2510.

Ding, L., Yang, G., Xie, M., Gao, D., Yu, J., Zhang, Y., 2012. More insight into tandem ROMP and ADMET polymerization for yielding reactive long-chain highly branched polymers and their transformation to functional polymer nanoparticles. Polymer 53(2), 333-341.

Dompierre, K.A., Lindsay, M.B., Cruz-Hernández, P., Halferdahl, G.M., 2016. Initial geochemical characteristics of fluid fine tailings in an oil sands end pit lake. Science of the Total Environment 556, 196-206.

Dwari, R., Angadi, S., Tripathy, S., 2018. Studies on flocculation characteristics of chromite's ore process tailing: Effect of flocculants ionicity and molecular mass. Colloids and Surfaces A: physicochemical and engineering aspects 537, 467-477.

EPA, 2010. Toxicological review of acrylamide in support of summary information on the integrated risk information systems (IRIS). US Environmental Protection Agency.

Godwin Uranta, K., Rezaei-Gomari, S., Russell, P., Hamad, F., 2018. Studying the effectiveness of polyacrylamide (PAM) application in hydrocarbon reservoirs at different operational conditions. Energies 11(9), 2201.

Guezennec, A.-G., Michel, C., Bru, K., Touze, S., Desroche, N., Mnif, I., Motelica-Heino, M., 2015. Transfer and degradation of polyacrylamide-based flocculants in hydrosystems: a review. Environmental Science and Pollution Research 22(9), 6390-6406.

Holliman, P.J., Clark, J.A., Williamson, J.C., Jones, D.L., 2005. Model and field studies of the degradation of cross-linked polyacrylamide gels used during the revegetation of slate waste. Science of the Total Environment 336(1-3), 13-24.

Hripko, R., Vajihinejad, V., LopesMotta, F., Soares, J.B., 2018. Enhanced flocculation of oil sands mature fine tailings using hydrophobically modified polyacrylamide copolymers. Global Challenges 2(3), 1700135.

Huang, R., Sun, N., Chelme-Ayala, P., McPhedran, K.N., Changalov, M. and Gamal El-Din, M., 2015. Fractionation of oil sands-process affected water using pH-dependent extractions: a study of dissociation constants for naphthenic acids species. Chemosphere, 127, 291-296.

Huang, S., Guo, X., Duan, W., Cheng, X., Zhang, X., Li, Z., 2019. Degradation of high molecular weight polyacrylamide by alkali-activated persulfate: reactivity and potential application in filter cake removal before cementing. Journal of Petroleum Science and Engineering 174, 70-79

Johnson, B.T., 2005. Microtox® acute toxicity test, Small-scale freshwater toxicity investigations. Springer, pp. 69-105.

Joshi, S.J., Abed, R.M., 2017. Biodegradation of polyacrylamide and its derivatives. Environmental Processes 4(2), 463-476.

Kämpfer, P., Witzenberger, R., Denner, E.B., Busse, H.-J., Neef, A., 2002. Sphingopyxis witflariensis sp. nov., isolated from activated sludge. International Journal of Systematic and Evolutionary Microbiology 52(6), 2029-2034.

Kapanen, A., Vikman, M., Rajasärkkä, J., Virta, M., Itävaara, M., 2013. Biotests for environmental quality assessment of composted sewage sludge. Waste Management 33(6), 1451-1460.

Kumar, A., Dixit, C.K., 2017. Methods for characterization of nanoparticles, Advances in nanomedicine for the delivery of therapeutic nucleic acids. Elsevier, pp. 43-58.

Li, C., Fu, L., Stafford, J., Belosevic, M., Gamal El-Din, M., 2017. The toxicity of oil sands process-affected water (OSPW): A critical review. Science of the Total Environment 601, 1785-1802.

Lin, S.-Y., Wang, S.-L., Wei, Y.-S., Li, M.-J., 2007. Temperature effect on water desorption from methylcellulose films studied by thermal FT-IR microspectroscopy. Surface Science 601(3), 781-785.

Lu, J., Wu, L., Gan, J., 2003. Determination of polyacrylamide in soil waters by size exclusion chromatography. Journal of environmental quality 32(5), 1922-1926.

Lu, Q., Yan, B., Xie, L., Huang, J., Liu, Y., Zeng, H., 2016. A two-step flocculation process on oil sands tailings treatment using oppositely charged polymer flocculants. Science of the Total Environment 565, 369-375.

Mehboob, F., Junca, H., Schraa, G., Stams, A.J., 2009. Growth of Pseudomonas chloritidismutans AW-1T on n-alkanes with chlorate as electron acceptor. Applied Microbiology and Biotechnology 83(4), 739-747.

Mohn, W.W., Wilson, A.E., Bicho, P., Moore, E.R., 1999. Physiological and phylogenetic diversity of bacteria growing on resin acids. Systematic and Applied Microbiology 22(1), 68-78.

Molina, R., Jovancic, P., Vilchez, S., Tzanov, T., Solans, C., 2014. In situ chitosan gelation initiated by atmospheric plasma treatment. Carbohydrate polymers 103, 472-479.

Nyyssölä, A., Ahlgren, J., 2019. Microbial degradation of polyacrylamide and the deamination product polyacrylate. International Biodeterioration & Biodegradation 139, 24-33.

Patel, V., Dalsania, Y., Azad, M.S., Sharma, T., Trivedi, J., 2021. Characterization of co- and post- hydrolyzed polyacrylamide molecular weight and radius distribution under saline environment. Journal of Applied Polymer Science 138(26), 50616.

Pourrezaei, P., Drzewicz, P., Wang, Y., Gamal El-Din, M., Perez-Estrada, L.A., Martin, J.W., Anderson, J., Wiseman, S., Liber, K., Giesy, J.P., 2011. The impact of metallic coagulants on the removal of organic compounds from oil sands process-affected water. Environmental science & technology 45(19), 8452-8459.

Risacher, F.F., Morris, P.K., Arriaga, D., Goad, C., Nelson, T.C., Slater, G.F., Warren, L.A., 2018. The interplay of methane and ammonia as key oxygen consuming constituents in early stage development of Base Mine Lake, the first demonstration oil sands pit lake. Applied Geochemistry 93, 49-59.

Sang, G., Pi, Y., Bao, M., Li, Y., Lu, J., 2015. Biodegradation for hydrolyzed polyacrylamide in the anaerobic baffled reactor combined aeration tank. Ecological engineering 84, 121-127.

Scott, A.C., Mackinnon, M.D., Fedorak, P.M., 2005. Naphthenic acids in Athabasca oil sands tailings waters are less biodegradable than commercial naphthenic acids. Environmental science & technology 39(21), 8388-8394.

Smith, E.A., Prues, S.L., Oehme, F.W., 1996. Environmental degradation of polyacrylamides. 1. Effects of artificial environmental conditions: temperature, light, and pH. Ecotoxicology and Environmental Safety 35(2), 121-135.

Sun, M., Qiao, M.-X., Wang, J., Zhai, L.-F., 2017. Free-radical induced chain degradation of high-molecular-weight polyacrylamide in a heterogeneous electro-Fenton system. ACS Sustainable Chemistry & Engineering 5(9), 7832-7839.

Sun, Y., Zhang, S., Jin, B., Cheng, S., 2021. Efficient degradation of polyacrylamide using a 3-dimensional ultra-thin SnO2-Sb coated electrode. Journal of Hazardous Materials 416, 125907.

Vajihinejad, V., Gumfekar, S.P., Dixon, D.V., Silva, M.A., Soares, J.B., 2021. Enhanced dewatering of oil sands tailings by a novel water-soluble cationic polymer. Separation and Purification Technology 260, 118183.

Vedoy, D.R., Soares, J.B., 2015. Water- soluble polymers for oil sands tailing treatment: A Review. The Canadian Journal of Chemical Engineering 93(5), 888-904.

Wang, C., Guan, X., Yuan, Y., Wu, Y., Tan, S., 2019. Polyacrylamide crosslinked by bis-vinylimidazolium bromide for high elastic and stable hydrogels. RSC Advances 9(47), 27640-27645.

Wen, Q., Chen, Z., Zhao, Y., Zhang, H., Feng, Y., 2010. Biodegradation of polyacrylamide by bacteria isolated from activated sludge and oil-contaminated soil. Journal of Hazardous Materials 175(1-3), 955-959.

Wen, Q., Chen, Z., Zhao, Y., Zhang, H., Feng, Y., 2011. Performance and microbial characteristics of bioaugmentation systems for polyacrylamide degradation. Journal of Polymers and the Environment 19(1), 125-132.

Woodrow, J.E., Seiber, J.N., Miller, G.C., 2008. Acrylamide release resulting from sunlight irradiation of aqueous polyacrylamide/iron mixtures. Journal of agricultural and food chemistry 56(8), 2773-2779.

Xiong, B., Loss, R.D., Shields, D., Pawlik, T., Hochreiter, R., Zydney, A.L., Kumar, M., 2018a. Polyacrylamide degradation and its implications in environmental systems. NPJ Clean Water 1(1), 1-9.

Xiong, B., Miller, Z., Roman-White, S., Tasker, T., Farina, B., Piechowicz, B., Burgos, W.D., Joshi, P., Zhu, L., Gorski, C.A., 2018b. Chemical degradation of polyacrylamide during hydraulic fracturing. Environmental science & technology 52(1), 327-336.

Yousefzadeh, S., Ahmadi, E., Gholami, M., Ghaffari, H.R., Azari, A., Ansari, M., Miri, M., Sharafi, K., Rezaei, S., 2017. A comparative study of anaerobic fixed film baffled reactor and up-flow anaerobic fixed film fixed bed reactor for biological removal of diethyl phthalate from wastewater: a performance, kinetic, biogas, and metabolic pathway study. Biotechnology for biofuels 10(1), 1-15.

Yu, F., Fu, R., Xie, Y., Chen, W., 2015. Isolation and characterization of polyacrylamide-degrading bacteria from dewatered sludge. International journal of environmental research and public health 12(4), 4214-4230.

Yue, S., Ramsay, B.A., Wang, J., Ramsay, J.A., 2016. Biodegradation and detoxification of naphthenic acids in oil sands process affected waters. Science of the Total Environment 572, 273-279.

Zamora, R., Delgado, R.M., Hidalgo, F.J., 2015. Use of nucleophilic compounds, and their combination, for acrylamide removal. Acrylamide in food: analysis, content and potential health effects, 297-307.

Zeng, H., Tang, H., Sun, W., Wang, L., 2022. Strengthening Solid–liquid Separation of Bauxite Residue through the Synergy of Charge Neutralization and Flocculation. Separation and Purification Technology 285, 120296.

Zhang, D., Abraham, T., Dang-Vu, T., Xu, J., Gumfekar, S.P., Thundat, T., 2021. Optimal floc structure for effective dewatering of polymer treated oil sands tailings. Minerals Engineering 160, 106688.

Zhao, N., Al Bitar, H., Zhu, Y., Xu, Y., Shi, Z., 2018. Flocculation performance of anionic starch in oil sand tailings. Water Science and Technology 78(6), 1268-1275.

Zhou, C., Lee, S., Dooley, K., Wu, Q., 2013. A facile approach to fabricate porous nanocomposite gels based on partially hydrolyzed polyacrylamide and cellulose nanocrystals for adsorbing methylene blue at low concentrations. Journal of Hazardous Materials 263, 334-341.

CHAPTER 6 MOLECULAR AND MICROBIAL INSIGHTS TOWARDS UNDERSTANDING THE ANAEROBIC DEGRADATION OF ANIONIC POLYACRYLAMIDE IN OIL SANDS TAILINGS

6.1 Introduction

Polyacrylamide (PAM) is a high molecular weight, water-soluble polymer and one of the most commonly used flocculants for oil sands mining operations (Chen et al., 2021; Gumfekar et al., 2017). Among the different types of PAM, anionic polyacrylamide (A-PAM) has become a primary choice to enhance dewatering the oil sands tailings, which is an aqueous wastes suspension generated from bitumen mining and extraction processes (Dai et al., 2014; Qi et al., 2011). Although A-PAM is generally accepted as being non-toxic to humans (Seybold, 1994), it is reported that A-PAM could be broken down by physical-chemical factors, potentially releasing acrylamide (AMD) monomer, which is a neurotoxin and a carcinogen to humans (EPA, 2010; Woodrow et al., 2008; Xiong et al., 2018). Compared to the application of A-PAM in water and wastewater treatment, biodegradation of A-PAM in oil sands tailings is more likely to occur, given the higher dose applied (often 10 times higher) and the lack of other available nutrients in tailings (Cossey et al., 2021).

As oil sands tailings ponds are typically oxic at surface but are anoxic at about 1 m below the surface and deeper, aerobic biodegradation tends to occur in the upper layer whereas anaerobic biodegradation is more likely to occur in the deeper layer of tailings (Cossey et al., 2021; Li et al., 2023; Ramos-Padrón et al., 2011). Previous studies of A-PAM biodegradation in oilfield wastewater are mainly focused on aerobic environment (Bao et al., 2010; Dong et al., 2020; Liu et al., 2012; Li et al., 2023). For example, Dong et al. (2020) applied mixed strains isolated from

wastewater from a coking plant and a shale gas field to remove A-PAM. The maximum removal efficiency of A-PAM reached at 45.8% at 35 °C after 7 days. Recently, our previous study investigated the degradation of A-PAM at aerobic conditions in tailings (Li et al., 2023). Maximum degradation efficiency of A-PAM was found to be 41.0% at 20 °C with augmented indigenous microorganisms after 11 weeks. No acrylamide was reported during the biodegradation process in the above studies.

With respect to anaerobic environments, biodegradation of A-PAM has not been as widely investigated as aerobic degradation (Nyyssölä and Ahlgren, 2019). Few studies have reported the accumulation of AMD during the anaerobic degradation of A-PAM (Dai et al., 2014; Dai et al., 2015). However, recent research by Hu et al. (2018) has demonstrated that the anaerobic biodegradation of A-PAM could lead to the production of other less toxic metabolites, such as acrylate and propionate. While certain bacteria, such as Proteobacteria and Planctomycetes, have been found to have a strong correlation with anaerobic biodegradation of A-PAM (Dai et al., 2015; Haveroen et al., 2005; Hu et al., 2018), the responsible microbial communities for A-PAM degradation are still unclear (Cossey et al., 2021). In addition, the utilization of A-PAM by microorganisms in tailings is still a matter of debate. Haveroen et al. (2005) observed that A-PAM could be used as a nitrogen source and stimulated methanogenesis in different tailings mixed with domestic sewage sludge. However, Collins et al. (2016) found that the same A-PAM did not serve as a nitrogen source, and methanogenic activity was determined to be a result of nitrogen fixation in tailings. Various factors have been shown to affect the anaerobic biodegradation of A-PAM, including temperature, pH, polymer concentration, microbial communities, and the presence of other carbon sources (Berdugo-Clavijo et al., 2019; Akbar et al., 2020). For example, Akbar et al. (2020) found that increasing temperature from 35 °C to 55 °C could promote the A-PAM

degradation from 30% to 78% in anaerobic conditions. However, little is known about the effect of these factors on the biodegradation of A-PAM in tailings under anaerobic conditions.

Therefore, in order to better understand the A-PAM biodegradation pathways and its impacts on biogas production, water chemistry, and microbial community in tailings under anaerobic environment, this study focuses on (i) investigating the influence of A-PAM at different dosages on methane production during anaerobic degradation; (ii) exploring how A-PAM affects methane yield via organic transformation and the change of solid phase; (ii) determining the responsible microbial community for A-PAM degradation; and (iii) proposing the potential biodegradation mechanism of A-PAM.

6.2 Materials and methods

6.2.1 Materials

Tailings samples used in this study were from the oil sands extraction operation in Northern Alberta and stored at 4 °C before use in the laboratory. The inoculum was collected from mesophilic anaerobic digester from local wastewater treatment plant in Edmonton, Canada. The characteristics of tailings and inoculum listed in Table 6.1. The hydrolyzed anionic polyacrylamide (A-PAM) used in the present study was supplied by SNF, Canada. The weight averaged molecular weight (M_w) and number averaged molecular weight (M_n) of A-PAM were determined by gel permeation chromatography (GPC) to be around 2.12×10^6 Da and 1.2×10^6 Da, respectively, with the polydispersity index (PDI, M_w/M_n) of 1.80 and a medium anion charge density. Sodium hydroxide (NaOH) and acrylamide (>99.9 % pure; powder) were purchased from Sigma Aldrich. Methanol (HPLC grade) and potassium dihydrogen phosphate (KH_2PO_4) were obtained from Fisher Scientific. All solutions were prepared with ultra-pure water (R≥18.2 MΩ) obtained from a Millipore Millli-Q system.

Table 6.1 Properties of oil sands tailings and inoculum.

Properties	Value
Oil Sands tailings	
Water content %	47.6 ± 1.9
Solids content %	51.3 ± 2.2
Bitumen content%	1.1 ± 0.3
pH	8.5 ± 0.1
Zeta potential (mV)	-38.7 ± 2.4
TOC (mg/L)	173.7 ± 1.4
COD (mg/L)	560.5 ± 1.7
Inoculum	
Total solids (TS) (g/L)	35.7 ± 1.4
Volatile solids (VS) (g/L)	29.5 ± 1.6
pH	7.3 ± 0.05

6.2.2 A-PAM degradation experiment

The biodegradation of A-PAM was conducted in batch anaerobic reactors. At the start of batch experiments, 100 mL of tailings samples and 5 mL of inoculum were mixed in a 125 mL reactor. In order to investigate the effect of initial dosage on A-PAM degradation, different dosages of A-PAM (0, 50, 100, 250, 500, 1000, 2000 mg/kg TS) were added into reactors. N_2 was purged

in the headspace of reactors for 5 min to provide anaerobic conditions. The reactors were reversed several times to mix samples. The anaerobic reactors were operated at 37 ± 1 °C, and the batch experiment was conducted until constant methane yield achieved (about 36 days). The liquid samples were collected by using a syringe and then filtered (0.45 μm) and stored at 4 °C until analysis. The sludge samples were frozen at -20 °C for further microbial analysis and dried for 24 h at 105 °C for floc characterization.

6.2.3 Analytical methods

Methane that accumulated in the bottles was detected by a gas chromatography coupled with a thermal conductivity detector (GC-TCD) (7890B, Agilent Technologies Inc, USA), and helium was used as the carrier gas. Gas chromatography coupled with a flame ion detector (GC-FID) was used to characterize the composition of volatile fatty acids (VFAs). The concentration and molecular weights of A-PAM before and after degradation were determined by a GPC coupled with an ultraviolet multiple wavelength detector (Agilent Technologies Inc, USA). The columns used in this study were a TSK-Gel GMPW$_{XL}$ column (Tosoh Bioscience, 13 μm particle size, 7.8 mm ID × 30 cm) and a TSK-Gel guard PW$_{XL}$ column (Tosoh Bioscience, 12 μm particle size, 6.0 mm ID × 4.0 cm). The mobile phases for A-PAM concentration and molecular weight determination were 0.05 M KH$_2$PO$_4$ solution and 0.01 M NaH$_2$PO$_4$ with 0.1 M NaCl (pH 7) at the same rate (0.75 mL/min), respectively, under ambient temperature and 205 nm of UV wavelength. Both concentration and molecular weight were determined by a standard curve. Similarly, AMD concentration was measured by the using high-performance liquid chromatography (HPLC) with a UV multiple wavelength detector (Agilent 1100) that was coupled with a SB-C18 column (Agilent, ZORBAX, 3.5 μm particle size, 4.6 mm ID × 150 mm), a guard column (Agilent, 1.8 μm particle size, 3.0 mm ID × 5.0 mm) and the mobile phase consisting of 90 v/v% of phosphate

buffer (0.006 M KH_2PO_4) and 10 v/v% of methanol at a rate of 0.5 mL/min under ambient temperature and 208 nm of UV wavelength. Detailed procedure can be found in Sang et al. (2015). The supernatants after A-PAM degradation were freeze-dried and analyzed by an attenuated total reflection Fourier transform infrared spectrometer (ATR-FTIR, Nicolet 8700, Thermo Fisher Scientific).

The concentration of naphthenic acids (NAs) before and after A-PAM degradation was analyzed by ultra-performance liquid chromatography time-of-flight mass spectrometry (UPLC-TOF-MS) (Synapt G2, Waters) with negative electrospray ionization mode as explained previously (Huang et al., 2018). In brief, 0.5 mL of water samples (filtered by 0.2 μm nylon filter) was mixed with 0.4 mL of methanol and 0.1 mL of myristic acid-1-^{13}C (4.0 mg/L), which was used as an internal standard. Chromatographic separations were carried out using a Waters UPLC Phenyl BEH column (1.7 μm, 150 mm × 1 mm). Raw data was processed in TargetLynx® V 4.2 software. The total organic carbon (TOC) of the water sample was measured by a Shimadzu VCSH TOC analyzer (Shimadzu, Canada). Chemical oxygen demand (COD), ammonium nitrogen (NH_4^+-N) concentration, nitrite nitrogen (NO_2^--N), nitrate nitrogen (NO_3^--N), and total nitrogen (TN) concentration of water samples were determined by a Hach COD kit, a Hach ammonium kit, and a Hach TKN kit, respectively, coupled with a HACH DR-3900 spectrophotometer (Hach, USA).

6.2.4 Toxicity tests

The toxicity of water samples before and after A-PAM degradation were assessed by Microtox® for acute toxicity to *Allivibrio fischeri* (*A. fischeri*) and SOS-ChromoTest (Environmental Bio-detection Products Inc.) for potential carcinogenic effect to *E. coli* PQ37 as explained previously (Li et al., 2023). Briefly, after adjusting the pH of all samples to around 7

using 0.1 mM H_2SO_4, a Synergy Microplate reader coupled with 96-well plates was used for both Microtox® and SOS-ChromoTest. For acute toxicity, phenol was used as a positive control and 2 % of NaCl in deionized water was used as a blank control. The luminescence was measured, and the inhibition of light emission was calculated following the method of Johnson (2005). For the relative strength of potential genotoxicity, different serial dilutions of each sample were prepared by adding DMSO in 96-well plates and then *E. coli* PQ37 was added. The induction factor (IF) was calculated based on the absorbances at 420 nm and 600 nm before and after incubation at 30 °C. It is widely accepted that IF of 1.5 is a threshold value for genotoxicity (Alabi, 2022; Romano et al., 2020).

6.2.5 Floc characterization

Field emission scanning electron microscopy (FESEM, Zeiss Sigma 300 VP) was used to observe the surface structure of flocs before and after A-PAM degradation. The elemental composition of flocs was analyzed using energy-dispersive X-ray spectroscopy (EDS, Bruker) and X-ray powder diffraction (XRD, Rigaku Ultima IV powder X-ray diffractometer). The spectrogram (4000-400 cm^{-1}) analysis was used to assess the chemical structure of A-PAM before and after degradation via ATR-FTIR spectrometer at room temperature.

6.2.6 Microbial community analysis

DNA was first extracted from sludge samples at the beginning and the end of experiments by using a DNeasy blood and tissue kit (Qiagen Inc., USA). In order to investigate the microbial communities in the heavy and light DNA fractions, DNA samples were sent to the Applied Genomics Core facility (University of Alberta, Canada) for sequencing in an Illumina MiSeq instrument. For library preparation, the V3-V4 hypervariable region of the bacterial 16S rRNA gene was targeted and the 341F and 758R primers were used, following the procedure described

previously (Thijs et al., 2017). After sequencing, raw reads in R language were processed via the DADA2 computational pipeline (v1.8.0). True sequences were identified as amplicon sequence variants (ASVs). The alpha and beta diversity analyses were carried out to understand community diversity, richness, and pattern similarity (Arslan and Gamal El-Din, 2021). Then, taxonomic was assigned to each sequence using assignTaxonomy function in R and the non-redundant SILVA taxonomic training set ("silva_nr_v128_train_set.fa", https://www.arb-silva.de/). The microbial profiles were collapsed at different taxonomic levels (e.g. phylum to species). Taxonomy-assigned ASV table was imported in R language and subsequently heatmaps were produced for comparison of top 20 abundant ASVs using the "ampvis2" package.

6.3 Results and discussion

6.3.1 Effect of A-PAM concentration on methane production

The batch experiments of anaerobic degradation of A-PAM were conducted for 36 days until the maximum methane yields were achieved. Cumulative methane production from tailings sample with different concentrations of A-PAM (50 to 2000 mg/kg TS) are shown in Fig 6.1. The methane production in the absence of A-PAM increased with the time from the 1st to the 31st day and reached a maximum value of 8.5 mL CH_4. In the presence of A-PAM at concentration of 50 mg/kg TS and 100 mg/kg TS, slightly higher methane yield was observed at 8.9 and 8.7 mL, respectively, However, increasing A-PAM concentration from 250 to 2000 mg/kg TS caused the methane yield to decrease remarkably to 7.9, 7.5, 7.1, 6.4 mL, suggesting that higher A-PAM concentrations had a significantly negative effect on methane yield in the tailings at 37 °C. Similar results have been reported in prior studies where less methane was produced with increasing PAM concentrations under anaerobic degradation at 37 °C (Akbar et al., 2020; Dai et al., 2014; Wang et al., 2018). The lower methane yield in tailings with higher concentrations of A-PAM suggested

the slower and less degradation of A-PAM, which might be due to higher viscosities and large flocs that can inhibit the microbial activity (Chu et al., 2005; Dai et al., 2014). In the following sections, the details of how A-PAM concentration affects the methane production were explored.
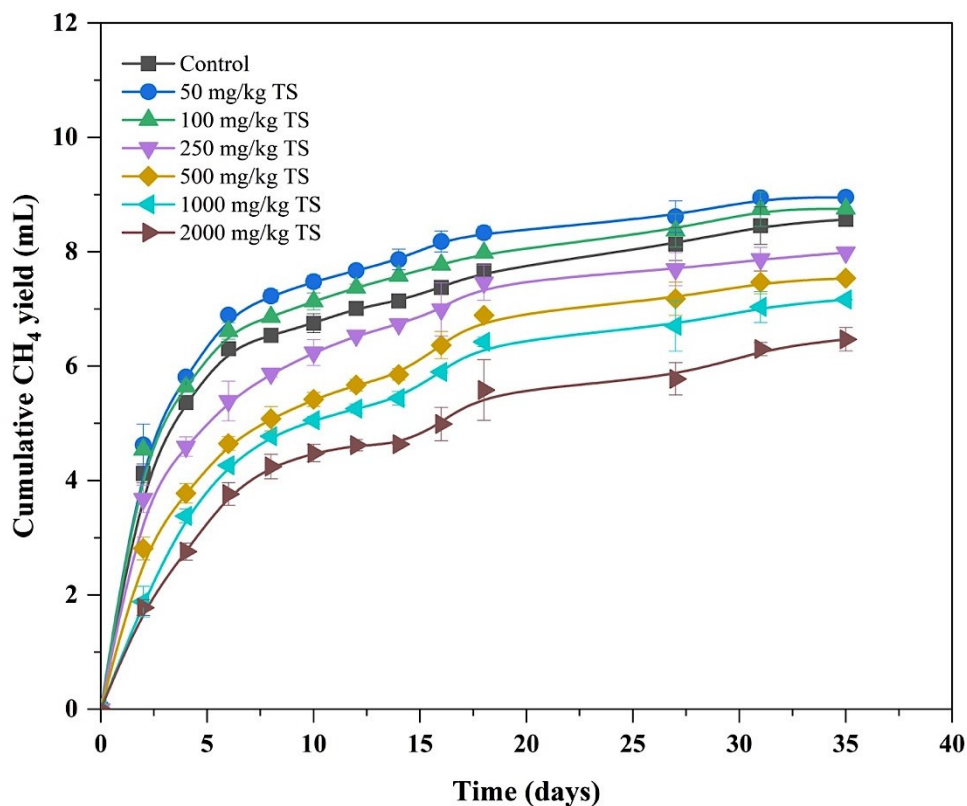
Figure 6.1 Cumulative methane production from A-PAM degradation.

6.3.2 Effect of A-PAM concentration on anaerobic degradation

Previous studies reported that PAM could be partly biodegraded and used as carbon and nitrogen sources under anaerobic conditions (Chu et al., 2002; Dai et al., 2015; Haveroen et al., 2005). The concentration of A-PAM in tailings before and after anaerobic condition is shown in Fig. 6.2. The concentration of A-PAM decreased significantly at low dosages as compared with high dosages in the tailings, following the order of 50 mg/kg TS (46.2%) > 100 mg/kg TS (40.0%) > 250 mg/kg TS (37.4%) > 500 mg/kg TS (33.2 %) > 1000 mg/kg TS (29.4%) > 2000 mg/kg TS

(24.8%). Similarly, the molecular weight of A-PAM in tailings decreased after anaerobic degradation (Table 6.2), with the highest reduction of M_w (76.2%) and M_n (80.2%) found in the A-PAM dose of 50 mg/kg TS. The decrease in M_w and M_n was due to the breakdown of C-C groups in the polymer (Xiong et al., 2020). In addition, the polydispersity index (PDI) of A-PAM with different concentrations also reduced after anaerobic degradation, suggesting that A-PAM in tailings under anaerobic condition was degraded to some extent and has undergone a downward shift in both M_w and M_n with narrowing of molecular weight distribution. Previously, Song et al. (2017) also observed the reduced molecular weight of PAM in anaerobic blanket reactors after operating 470 days and provided firm evidence that the cleavage of the main carbon chain backbone was attributed to biological degradation. When the concentration of A-PAM increased, especially for the highest dosage of 2000 mg/kg TS, the percentage of M_w and M_n decreased dramatically, dropping to 38.7% and 57.4%, respectively. The results indicated that the concentration of A-PAM plays a crucial role in anaerobic degradation of A-PAM in tailings and higher concentration of A-PAM results in less degradation, which is consistent with previous methane data. It is noted that the COD and TOC declined slowly with degradation of A-PAM (Table. B.3). With the highest A-PAM degradation occurring for dose of 50 mg/kg A-PAM, COD and TOC removal reached only 6.0 % and 21.5%, respectively, which were much lower than A-PAM removal. This result indicated that as A-PAM is exposed to anaerobic biodegradation in tailings, A-PAM molecules break down to intermediates, but achieving mineralization of these intermediates is challenging. In addition, the absolute value of the zeta potential of tailings water also decreased after A-PAM degradation. As explained in our previous study of aerobic degradation of A-PAM in tailings (Li et al., 2023), the zeta potential is an important tool to predict

the stability off the solution and reducing absolute value of zeta potential in this study implied that the interactions in tailings water, such as hydrogen bonding and van der Waals, reduced.
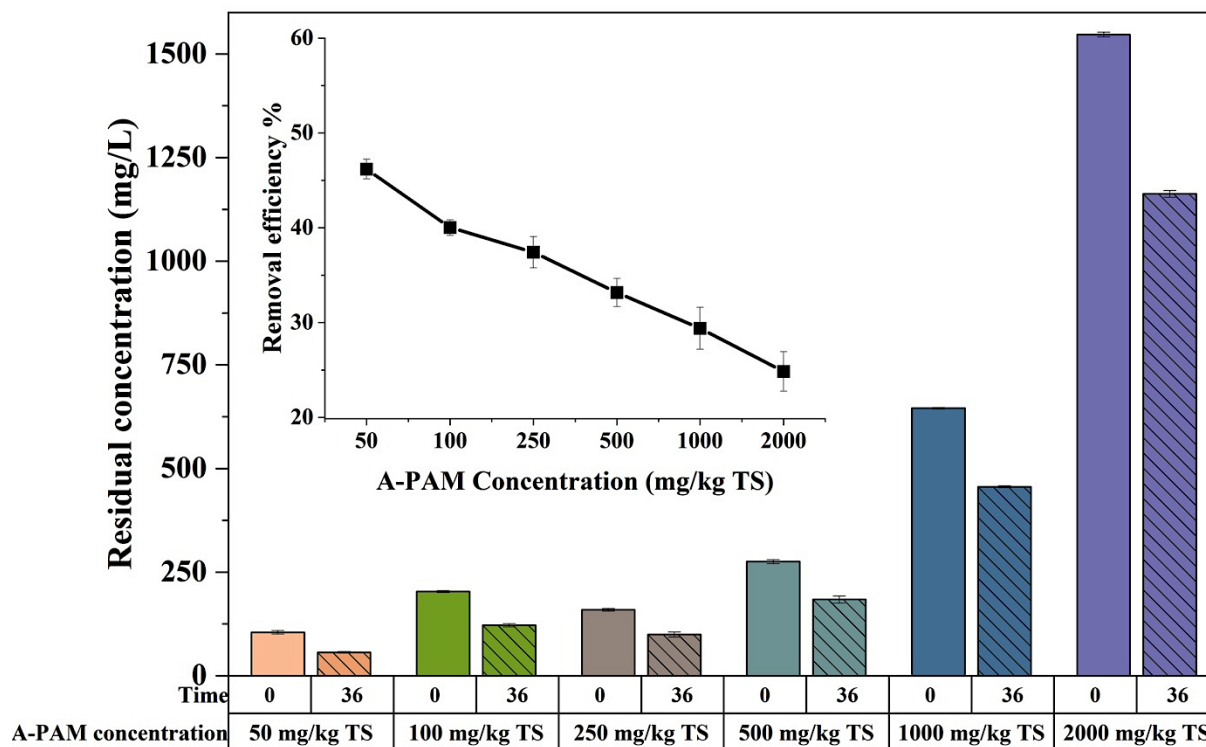
Figure 6.2 Concentration removal of A-PAM during anaerobic degradation.

Table 6.2 The molecular weight of A-PAM before and after anaerobic degradation.

Polymer sample	Mw (Da)	Mn (Da)	PDI
Before	2.1×10^6	1.2×10^6	1.80
50 mg/kg TS	5.0×10^5	4.2×10^5	1.20
100 mg/kg TS	5.1×10^5	4.2×10^5	1.21
250 mg/kg TS	6.0×10^5	4.8×10^5	1.24

500 mg/kg TS	7.2×10^5	5.7×10^5	1.27
1000 mg/kg TS	1.0×10^6	7.0×10^5	1.42
2000 mg/kg TS	1.3×10^6	9.0×10^5	1.44

To elucidate the change in the structure of A-PAM after degradation, the FT-IR spectrograms of the A-PAM before and after degradation were recorded and are shown in Fig. 6.3. As shown in Fig. 6.3, the regions at 1126 cm^{-1} (C-O-C) and 1401 cm^{-1} (-COO$^-$) increased while the regions at 3340 cm^{-1} (-NH$_2$), 3198 cm^{-1} (-NH$_2$), and 1657 cm^{-1} (C=O) decreased in A-PAM with low concentrations (50 and 100 mg/kg TS) after degradation, indicating that some amide groups (C-N) were hydrolyzed into ammonia and carboxylic acid and adjoining amide groups could be converted into ether group after hydrolysis at low A-PAM concentrations. With increasing A-PAM concentration, the peak intensities at 1126 cm^{-1} and 1401 cm^{-1} gradually reduced, whereas peak intensities at 3340 cm^{-1}, 3198 cm^{-1}, and 1657 cm^{-1} increased. These results demonstrated that higher concentration of A-PAM would inhibit the hydrolysis (Wang et al., 2018). Moreover, the band near 2933 cm^{-1} (-CH$_3$ or -CH$_2$) completely disappeared at lower concentrations of A-PAM (50-500 mg/kg TS), but only partly disappeared at higher concentrations of A-PAM (1000 and 2000 mg/kg TS), implying that more breakage of the carbon backbone occurred at lower concentrations of A-PAM. Similarly, the small peak at 1417 cm^{-1} (C-N) also disappeared for lower concentrations of A-PAM (50-500 mg/kg TS), while a small shoulder was left for higher concentrations of A-PAM (1000 and 2000 mg/kg TS), suggesting that more C-N bonds were cleaved to release -NH$_2$ and provide a nitrogen source to microbes under lower concentrations of A-PAM. The breakage of C-N could be further confirmed by the slight increase in pH after A-

PAM degradation (Table. B.3). Overall, the FT-IR results of A-PAM are consistent with previous results of methane production and degradation efficiency of the polymer.
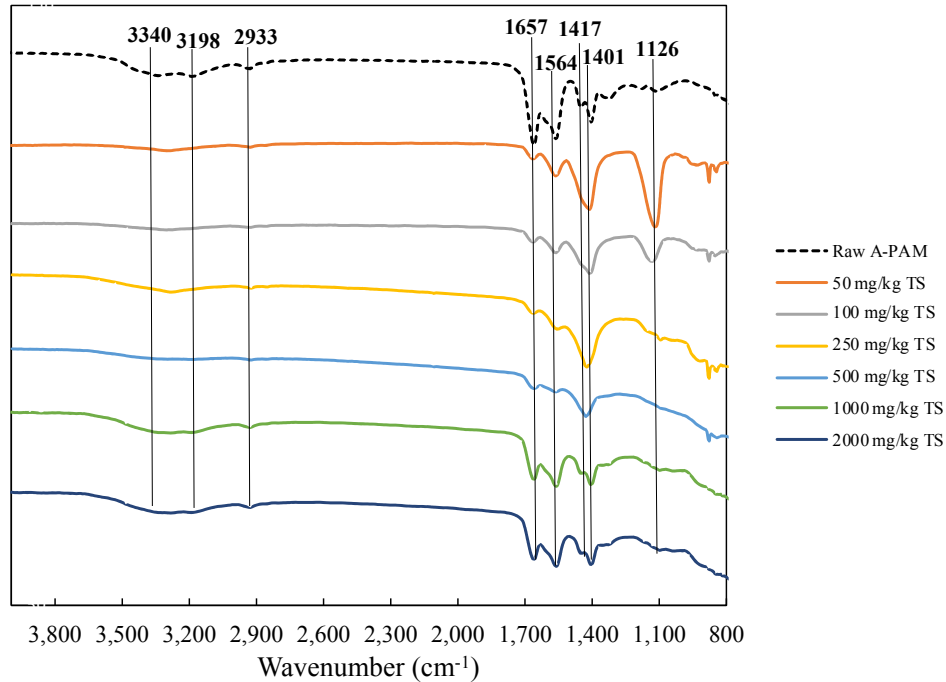
Figure 6.3 FT-IR analysis of A-PAM before and after degradation under anaerobic condition.

Besides being a carbon source, A-PAM has also been reported to be used as the nitrogen source by hydrolyzing the amide group into free ammonium (Dai et al., 2014) and to produce VFAs and methane under anaerobic conditions (Chu et al., 2002; Haveroen et al., 2005). Therefore, total nitrogen (TN), ammonium nitrogen (NH_4^+-N), nitrite nitrogen (NO_2^--N) and nitrate nitrogen (NO_3^--N) were measured to examine whether A-PAM can be used as the nitrogen source in tailings under anaerobic condition (Fig. 6.4). As shown in Fig. 6.4a, the concentration of TN decreased slightly in tailings with A-PAM addition, while it is relatively stable at 6.0 mg/L in control, which demonstrated that A-PAM could be utilized as an N source and converted to other forms of nitric salts (Yan et al., 2016). The higher NH_4^+-N concentrations were found in tailings with the addition of A-PAM compared to the control due to the hydrolysis of amide groups within A-PAM (Fig.

6.4b). Given that the NH_4^+-N could not be used immediately by microbes, the concentration of NH_4^+-N increased first and then decreased. It should be noticed that a longer time is needed for NH_4^+-N to climb to the maximum value in tailings with higher A-PAM concentrations. For example, for lower dosages of A-PAM (50 and 100 mg/kg TS) the highest NH_4^+-N concentrations were found at day 10, whereas for higher dosage of A-PAM (250 and 500 mg/kg TS) the maximum values were observed at day 15. This result indicated that increasing initial A-PAM amount would decrease the utilization rate of A-PAM as a nitrogen source, which is consistent with prior studies on anaerobic degradation of PAM (Dai et al., 2014; Haveroen et al., 2005). In addition, increasing A-PAM concentration resulted in higher NH_4^+-N concentration and previous publications have pointed out that both ammonium and free ammonia could suppress methane production under anaerobic degradation (Chen et al., 2008; Wang et al., 2018), which can provide additional explanation for lower methane production with higher A-PAM concentrations. Although there were fluctuations between 1 and 4 mg/L in the concentrations of NO_2^--N and NO_3^--N throughout the experiment (Fig. 6.4c), a slight increase was found in all tailings with A-PAM addition after A-PAM degradation. These observations suggest that the bacteria used A-PAM as their N source, which was obtained through the hydrolysis of the amide groups in the A-PAM, using an amidase enzyme produced by bacteria to cut the C-N bond in the amide group.
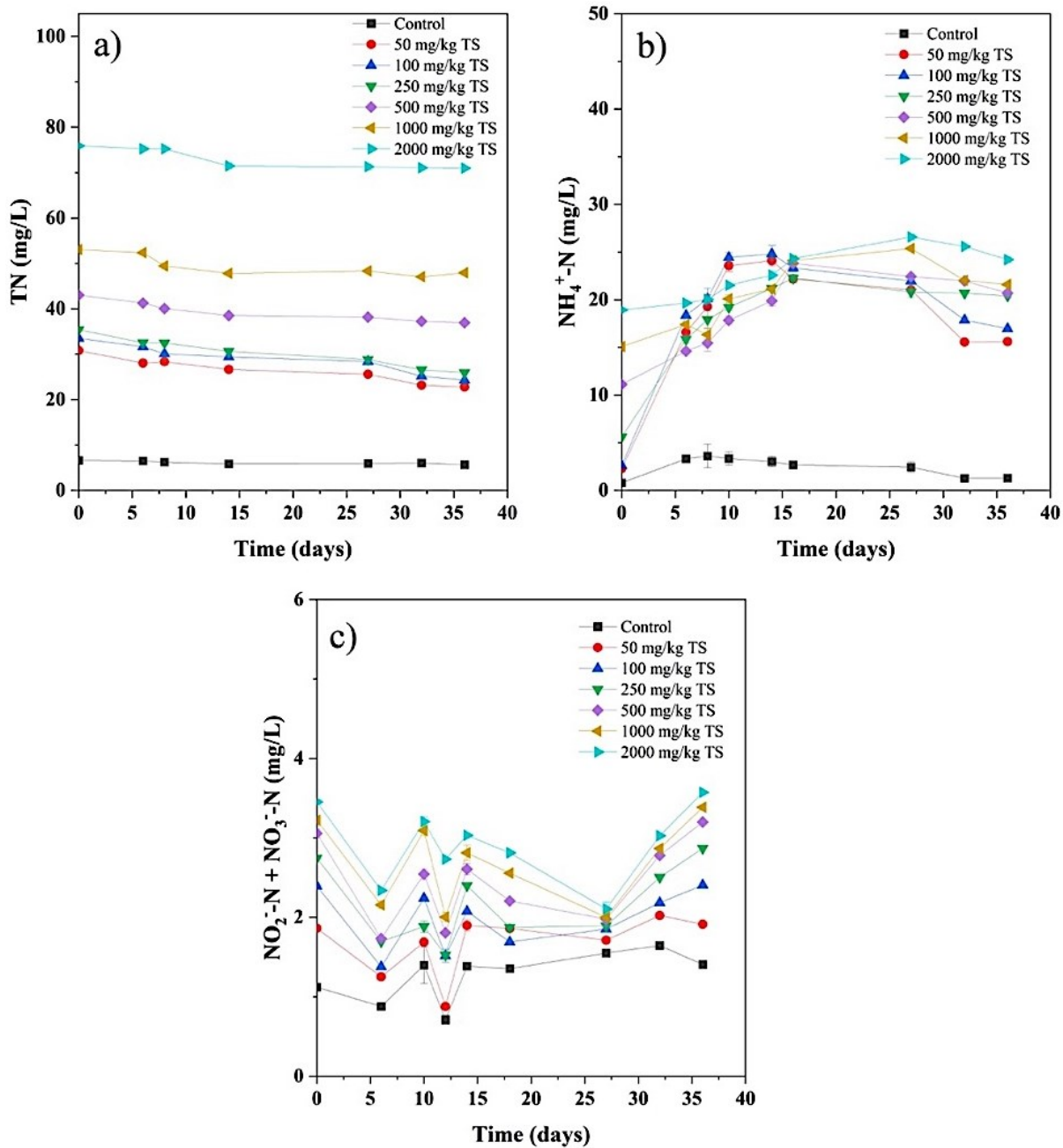
Figure 6.4 The concentration of TN, NH_4^+-N, NO_2^--N and NO_3^--N during degradation time.

6.3.3 Effect of A-PAM concentration on organic transformation during anaerobic degradation

To further study the intermediates produced during the anaerobic degradation of A-PAM in tailings, total VFAs production and AMD concentration were measured before and after A-PAM degradation (Fig. 6.5). Fig. 6.5a shows the contribution of A-PAM for VFAs production. Five distinct VFAs, including acetic acid, propionic acid, isobutyric acid, butyric acid, and caproic acid, were identified in tailings without A-PAM on both day 0 and day 36. On day 36, all tailings samples with A-PAM addition showed a dramatic increase in the total VFAs concentration compared to the control sample at day 0. Notably, valeric acid was also detected in the tailings samples with A-PAM addition on day 36, indicating its potential role as a product of A-PAM degradation. The maximum total VFAs production was 20.0 mg/L, with acetic (86.7%) and propionic (7.4%) acids as the main constituents in the tailings with 50 mg/kg TS of A-PAM at day 36. Although the total VFAs production decreased with increasing concentration of A-PAM, the main constituents remained acetic and propionic acids. This is consistent with a previous study that reported acetic acid and propionic acid as the major components produced during the anaerobic degradation of PAM under mesophilic conditions in a dewatered sludge system (Dai et al., 2014). Acetic acid is well-known to be the major component that is converted into methane (Wang et al., 2018). The low consumption of acetic acid in all tailings samples could explain the low production of methane (<10 mL) in this study. Moreover, the VFAs results suggest that the concentration of A-PAM plays a crucial role in the organic transformation during the anaerobic degradation of A-PAM. Lower concentrations (50 and 100 mg/kg TS) was found to lead to a higher accumulation of total VFAs (>16.0 mg/L) and a higher methane yield compared to higher concentrations of A-PAM (>100 mg/kg TS). In contrast, the lower production of total VFAs (< 14

mg/L) in tailings samples with higher A-PAM concentrations could be due to the inhibited microbial activity and major anaerobic degradation stages, including hydrolysis, acidogenesis, acetogenesis and methanogenesis (Liu et al., 2019). It is worth noting that the low consumption of total VFAs in low concentrations of A-PAM, which probably results from the partial inhibition of the acetogenesis and methanogenesis processes (Akbar et al., 2020), only led to a slight increase in methane yield compared to the control. Our results align with prior studies where the negative impact of excess VFAs production on methane yield was demonstrated (Akbar et al., 2020; Allam et al., 2023). Nevertheless, our findings highlight the potential benefit of using lower concentration of A-PAM for enhancing VFAs utilization and optimizing the anaerobic degradation process in future studies.

In addition to the VFAs, the changes of AMD concentration in tailings were also investigated (Fig. 6.5b). Traces of AMD (<0.8 mg/L) were found in the tailings with A-PAM addition at day 0, which was residual by-product due to the incomplete polymerization process of the commercial A-PAM (Caulfield et al., 2002). During anaerobic degradation, the breakdown of the carbon chain backbone in A-PAM led to a slight increase in AMD concentrations in tailings with A-PAM concentrations of 50, 100, 250 and 500 mg/kg, from 0.05, 0.07, 0.10, 0.13 mg/L to 0.12, 0.10, 0.12, 0.15 mg/L, respectively. However, the AMD concentration remained relatively stable at 0.53 mg/L when the A-PAM concentration was increased to 1000 mg/kg TS, and a slight reduction in AMD concentration (0.77 to 0.71 mg/L) was observed when the concentration of A-PAM was further increased to 2000 mg/kg TS. These results suggest that higher A-PAM concentrations could inhibit anaerobic degradation. Overall, the low concentrations of AMD found in all tailings samples with A-PAM addition suggested that the main intermediate products were low molecular weight polyacrylic acid rather than AMD from anaerobic degradation of A-PAM.

213

Similar findings were observed in earlier research on both aerobic and anaerobic degradation of PAM (Li et al., 2023; Liu et al., 2012; Wang et al., 2018; Yan et al., 2016). It has been reported that polyacrylic acid was the major inhibitor to the various processes of anaerobic degradation, such as solubilization, hydrolysis, acidogenesis, and methanogenesis, while AMD has been reported to significantly inhibit the methanogenesis stage (Wang et al., 2018). Given the low concentration of AMD in the tailings with A-PAM (<1 mg/L), our findings suggest that the negative impact of AMD on methane yield can be considered as minimal, and the low methane yield in tailings would be mainly due to the generation of polyacrylic acid from anaerobic degradation.
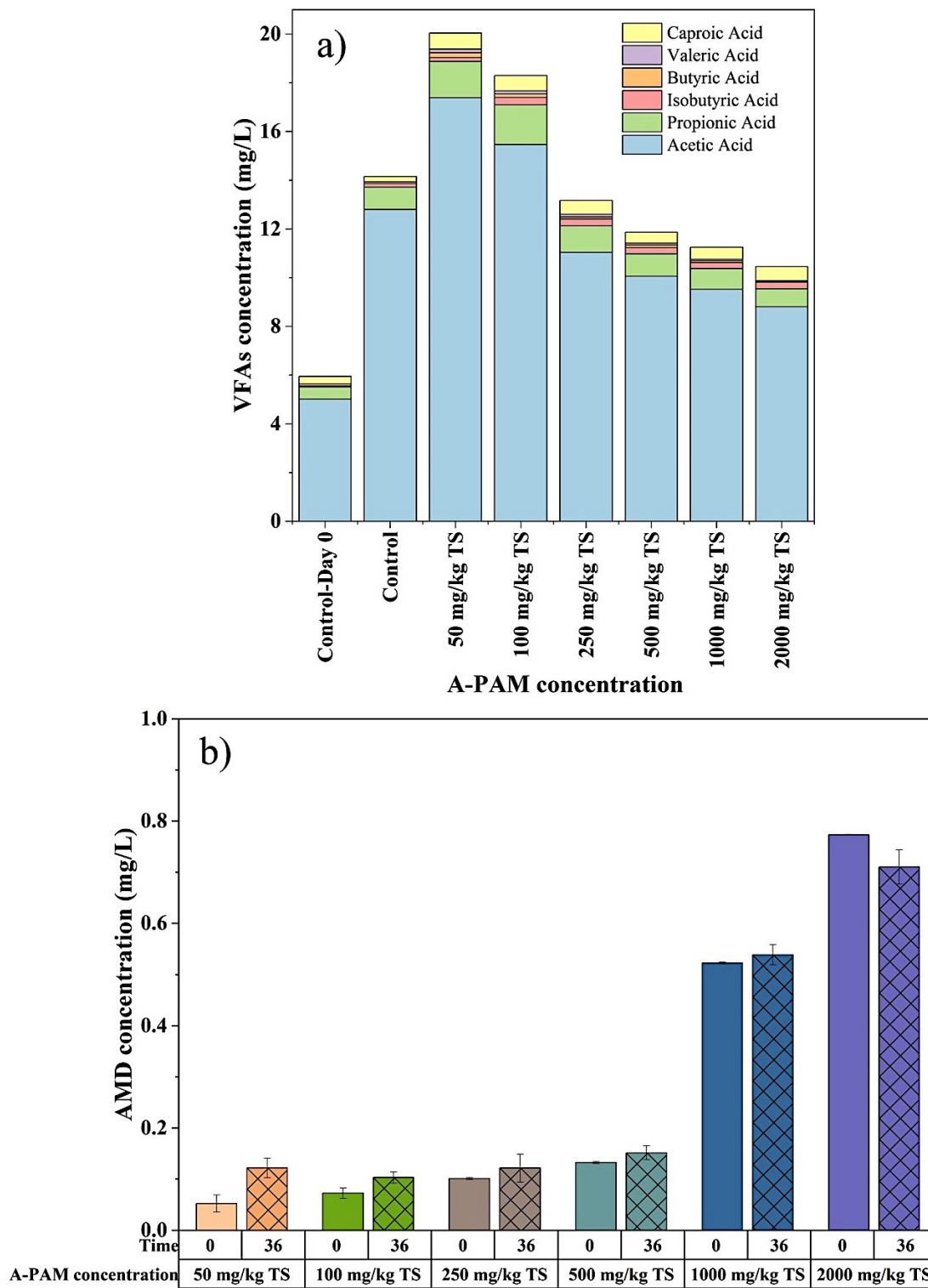
Figure 6.5 Concentration of VFAs (a) and AMD (b) in tailings with different A-PAM concentrations before and after anaerobic degradation of A-PAM.

It has been demonstrated that A-PAM can be degraded in tailings under anaerobic condition and its degradation intermediates may process potential biotoxicity, especially the AMD. Hence, the acute toxicity and genotoxicity of tailings water were evaluated before and after A-PAM degradation (Fig. 6.6). The initial tailings water without A-PAM addition showed 51.3% of inhibition effect to *A. fischeri* bacteria, which was mainly due to the presence of naphthenic acids (NAs) (Li et al., 2017) (Fig. 6.6a). When different dosages of A-PAM were added into tailings, the initial inhibition effect of tailings water reduced, of which the lowest inhibition effect (37.5%) was observed at 250 mg/kg TS of A-PAM. The reduction of acute toxicity in tailings with A-PAM addition was confirmed by the decrease in the concentration of total NAs (Fig. 6.6b), following the order of 250 mg/kg TS of A-PAM (14.6 mg/L) < 500 mg/kg TS of A-PAM (15.4 mg/L) < 1000 mg/kg TS of A-PAM (17.4 mg/L) < 2000 mg/kg TS of A-PAM (18.3 mg/L) < 100 mg/kg TS of A-PAM (50.6 mg/L) < 50 mg/kg TS of A-PAM (52.1 mg/L) < Control (55.0 mg/L). The lower total NAs concentrations at day 0 compared to control is likely due to the coagulation by A-PAM, as explained in our previous study on aerobic degradation of A-PAM in tailings (Li et al., 2023). After A-PAM degradation, more NAs were removed in tailings water with A-PAM addition (>22.0%) compared to the control (20.9%). Similarly, higher reduction of inhibition effect was observed in tailings water with A-PAM addition (>14.1%) than reduction in control (13.9%). Furthermore, there were no dramatic differences of reduction of inhibition effect and NAs concentration in tailings water with different A-PAM dosages. These results indicated that the anaerobic degradation of A-PAM in tailings would not produce NAs and contribute to the acute toxicity of tailings water. As shown in Fig. 6.6c, all IF values in tailings water with A-PAM addition were lower than the threshold value of 1.5 before and after A-PAM degradation, which

indicated that the addition of up to 2000 mg/kg TS of A-PAM and its anaerobic degradation would not cause genotoxicity in tailings water.
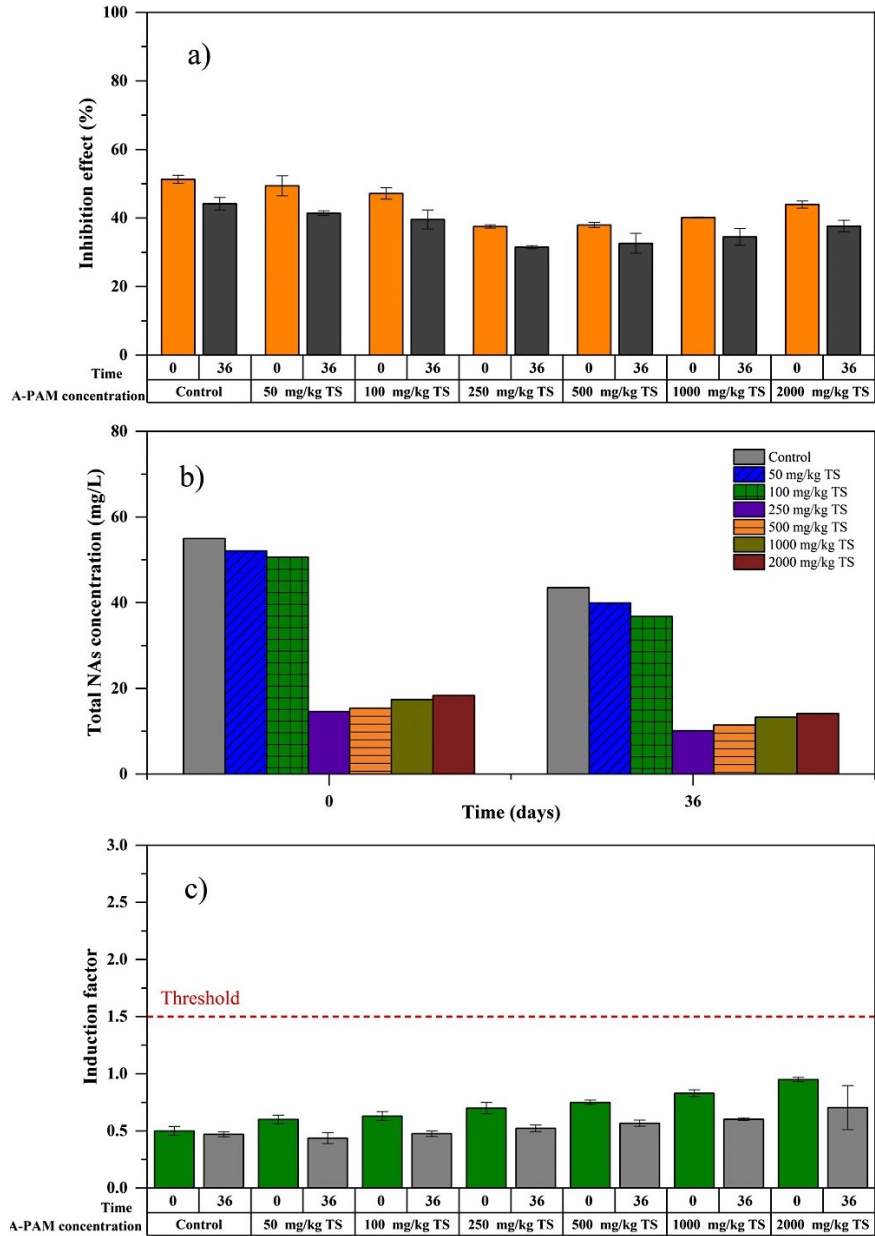
Figure 6.6 The acute toxicity to *A. fischeri* (a), concentration of total NAs (b), and genotoxicity in tailings water.

6.3.4 Effect of A-PAM concentration on solid phase during anaerobic degradation

In order to investigate the effect of anaerobic degradation of A-PAM with different initial concentrations on the flocs, SEM-EDS was use to compare the morphology and chemical composition on the surface of flocs. Images of solids in the control are compared to the sediments obtained before and after the degradation of A-PAM in Fig. 6.7. The solids in control samples exhibited a smooth surface without porous structures. When A-PAM was added into tailings at day 0, the formed flocs showed a coarse structure with an irregular porous surface, which is consistent with the fact that A-PAM could produce flocs through bridging bonding. With increasing A-PAM concentrations, an increased number of larger aggregates were found on the flocs. In addition, it is interesting to observe that after A-PAM degradation (day 36), the flocs produced by lower initial A-PAM concentrations (50 to 500 mg/kg TS) had more porous or honeycomb-like structures, which may provide more surface area and accessibility for microbial activity, leading to higher methane yield and degradation efficiency. Conversely, flocs formed by higher concentration of A-PAM remained relatively compact structures (1000 and 2000 mg/kg TS), which could limit microbial activity and result in lower methane yield and degradation efficiency. Therefore, the SEM findings indicated that the A-PAM concentration could affect the anaerobic degradation process via changing the floc structures. The porous or honeycomb-like structures observed in the flocs after A-PAM degradation in lower concentrations of A-PAM could result for various reasons: 1) methane produced from A-PAM degradation becomes trapped within the tailings flocs, resulting in the formation of gas pockets and pores (Chen et al., 2010); 2) the physical and chemical properties of the tailings flocs were altered due to A-PAM degradation, leading to changes in the stability and structure of flocs (Zhou et al., 2022); 3) the degradation metabolites of A-PAM, such as AMD and other organic compounds, can act as cationic surfactants

and interact with the negatively charged surfaces of flocs (Zheng et al., 2017); 4) the presence of microorganisms could break down A-PAM and form voids within the flocs (Wilén and Balmer, 1999).

Chemical composition of the solids and flocs is given in Table. B.4. Among various elements, C, O, and Si were found to be the dominant components in all solids and flocs (>90%) due to the presence of mineral matrices and organic compounds in tailings. In addition, compared to the control, the higher percentages of C, Na and Si in the flocs with A-PAM addition, along with the lower percentages of O and Al, could suggest that A-PAM co-precipitated with flocs resulting in changes in the mineral composition of the flocs. After A-PAM degradation, the increase in percentage of C, O, and Al, as well as the decrease in the percentage of Si, suggests that the A-PAM degradation may have contributed to changes in the composition and structure of the flocs, which could affect the microbial community and impact methane production. The increasing percentages of C and O could be due to the presence of organic compounds resulting from the A-PAM degradation or microbial activities. Given Al is known to affect the structural stability of minerals and clays due to the capability of forming strong chemical bonds with other elements (Sposito, 2008), the higher percentage of Al may play a role in the structural stability of flocs. In contrast, the decrease in the Si percentage could imply that there were changes in the mineral composition of the flocs, which could be due to the breakdown of silicate minerals by microbial activities (Konhauser and Ferris, 1996). Overall, EDS analysis could provide valuable insights into the composition and structure of flocs and support that the observed porous or honeycomb structures are due to the anaerobic degradation of A-PAM. However, further investigation of flocs would be necessary to better understand the impact of A-PAM concentration on floc structures and the anaerobic degradation process.

Control

Control

50 mg/kg TS

50 mg/kg TS

100 mg/kg TS

100 mg/kg TS

250 mg/kg TS

250 mg/kg TS

500 mg/kg TS

500 mg/kg TS

1000 mg/kg TS

1000 mg/kg TS

2000 mg/kg TS

2000 mg/kg TS
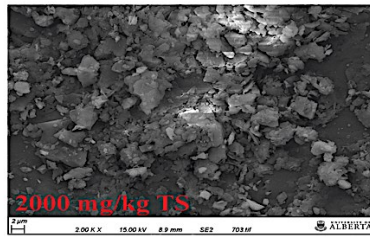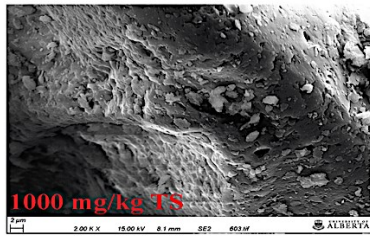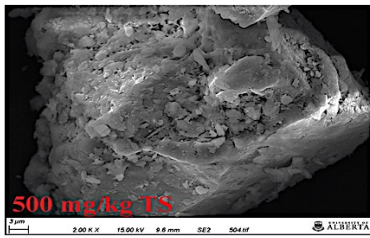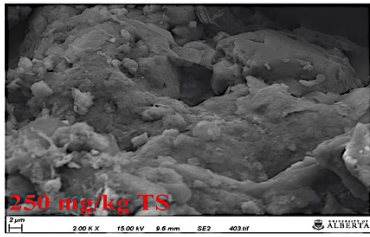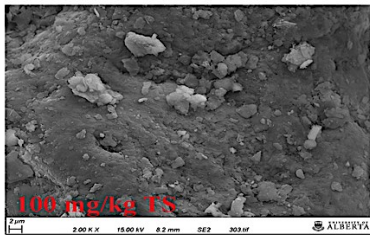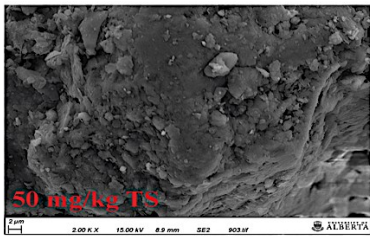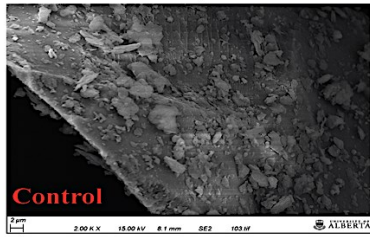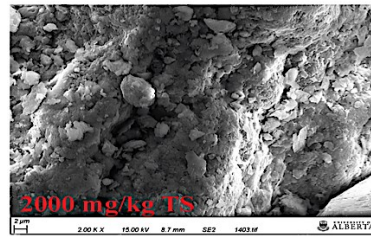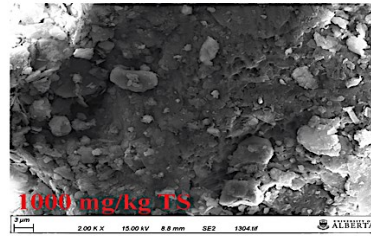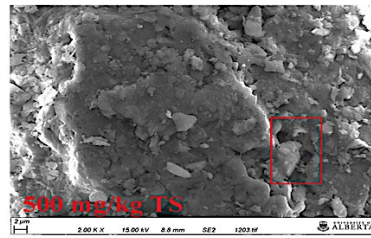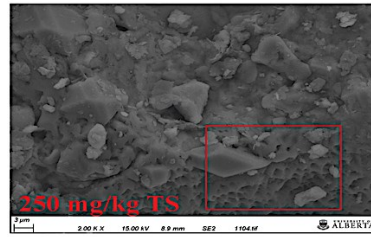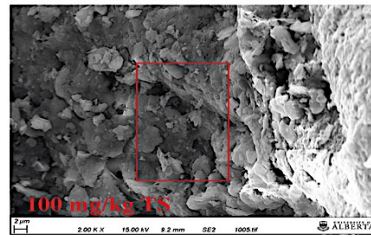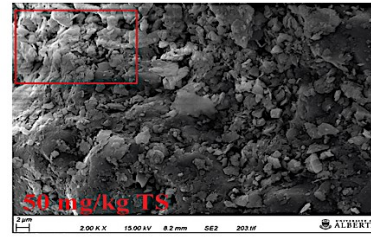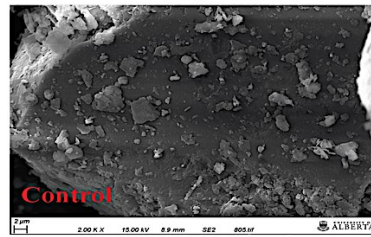
Figure 6.7 SEM images for flocs in control and tailings with A-PAM addition before (day 0) and after (day 36) anaerobic degradation of A-PAM.

In order to further investigate how the A-PAM concentration affects the flocs formed during anaerobic degradation in tailings, more analyses including FT-IR and XRD were conducted to study the structure and composition of the flocs (Fig. 6.8). As shown in Fig. 6.8a, similar peaks were found in solids from the control and from the flocs in tailings with A-PAM addition at day 0. These are the peaks found at 3693 cm^{-1} (O-H), 3619 cm^{-1} (O-H), 1602 cm^{-1} (C=C), 1480 cm^{-1} (C-H), 1033 cm^{-1} (Si-O-Si), 778 cm^{-1} (Si-O-Si), and 690 cm^{-1} (Si-O-Al). However, there were decreases in peak intensities at 1033 cm^{-1}, 778 cm^{-1}, and 690 cm^{-1} with increasing concentration of A-PAM. These intensities are characteristic of bonds occurring in silicate minerals and clays (Król et al., 2016; Naik et al., 2021). The reduction could be due to the elastic repulsions between the negatively charged A-PAM molecules and negatively charged silicate minerals and clays. As the concentration of A-PAM increased, the elastic repulsion also increased, which could alter the strength of the chemical bonds or vibrations responsible for the FT-IR peaks. Besides elastic repulsion, other interactions between A-PAM and minerals, like electrostatic interactions, could also play a role in changing peak intensities. After A-PAM degraded under anaerobic condition (Fig. 6.8b), the dramatic reductions in peak intensities at 1033 cm^{-1}, 778 cm^{-1}, and 690 cm^{-1} were found in lower concentrations of A-PAM (<500 mg/kg TS), which could be explained by the formation of organic products from A-PAM degradation. For example, polyacrylic acid, which is a polyelectrolyte and has a strong affinity for charged surfaces (Zaman et al., 2002). It could adsorb onto the surfaces of the silicate minerals and clays, potentially blocking or modifying the vibrations for the FT-IR. Another notable decrease at low concentrations of A-PAM (50 and 100 mg/kg TS) in the peak intensities were found at 1602 cm^{-1} and 1480 cm^{-1}, which are used to identify the

presence of organic compounds (Moosavinejad et al., 2019; Petibois et al., 2006). These decreases could also be due to A-PAM degradation and interactions between A-PAM and other organic compounds in tailings. In contrast, the increase in peak intensities at 1033 cm^{-1}, 778 cm^{-1}, and 690 cm^{-1} were observed in higher A-PAM concentrations (1000 and 2000 mg/kg TS). Given that A-PAM degradation decreased and occurred more slowly with high concentration in tailings, the longer residence times for A-PAM in the tailings could increase the likelihood of interactions with the solids. Therefore, the observed changes in the FT-IR peak intensities with varying concentration of A-PAM could be due to a complex interplay between the degradation products, the solid components in the tailings, and other factors that require further investigation to fully understand. Nevertheless, the FT-IR results are indicative of the changes in the interactions between the A-PAM and the flocs, which could contribute to changes in the physical structure of the flocs.

The XRD spectrum of flocs in the control and tailings samples with various concentrations of A-PAM at day 0 is presented in Fig. 6.8c. It can be observed that the two major peaks are at 24.3 and 31.0 angles (2θ) in all samples. These are characteristic peaks for quartz (Almutairi et al., 2021). The presence of these intensive peaks indicates the dominance of silica phase in the solids and flocs. Compared to the control, lower peak intensities were found in tailing samples with lower concentrations of A-PAM (50 to 500 mg/kg TS), suggesting that the presence of A-PAM could reduce the crystallinity of the minerals in the tailings. In contrast, higher peak intensities were found at higher concentrations of A-PAM (1000 and 2000 mg/kg TS), which may be due to the adsorption of A-PAM onto the surfaces of silica minerals, leading to the modification of the crystal structure of the mineral and subsequent increase in peak intensity. Previously, Deng et al. (2006) has observed that the adsorbed A-PAM could alter the charge properties of clays. After A-PAM

degradation (day 36) (Fig. 6.8d), the intensity of the peak at 24.3 and 31.0 angles (2θ) dropped for lower concentrations of A-PAM, which could be due to the breakdown of A-PAM molecules and their subsequent release from the flocs. On the other hand, the increase in peak intensities at higher concentrations of A-PAM could be attributed to the slower degradation of A-PAM, resulting in more interactions with minerals and increased adsorption onto their surfaces. Furthermore, the changes in the crystalline structure of the minerals, as demonstrated in XRD analysis, could have an impact on the microbial activity and methane production by affecting the properties of minerals surfaces and subsequently the microbial colonization and metabolic activity (Dong et al., 2022). Overall, the XRD results suggest that A-PAM could affect the crystalline structure of the solids components, such as silicate minerals in tailings, which is consistent with the SEM-EDS and FT-IR results. Together, the combined results provide valuable insights into the potential mechanisms underlying the observed effects of A-PAM on methane production and degradation in the tailings under anaerobic condition.
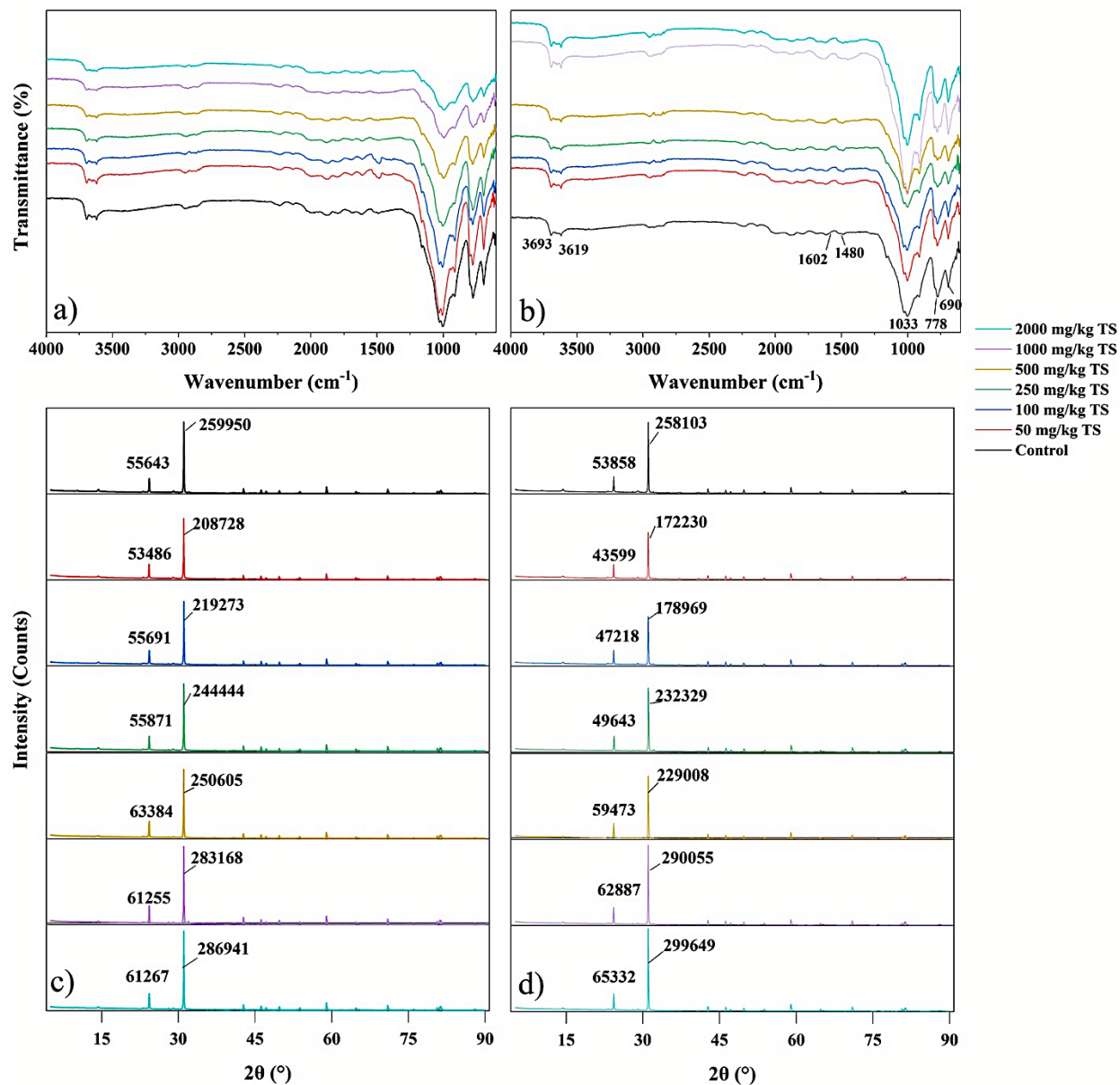
Figure 6.8 FT-IR (a and b) and XRD analysis (c and d) for solids and flocs before and after anaerobic degradation of A-PAM.

6.3.5 Effect of A-PAM concentration on microbial community during anaerobic degradation

The microbial community plays an important role in the anaerobic degradation process. To understand the impact of A-PAM addition and its degradation on the microbial community,

microorganism compositions were examined in the inoculum, pre-treatment control (control at day 0), and reactors with A-PAM addition as well as control at day 36. Overall, a total of 2251 phylotypes were observed at the 97% sequence similarity level, which comprised 41 phyla and 276 genera. In order to interpret the changes in microbial community composition, alpha diversity analyses, including the Shannon diversity index (H) and the Chao1 analysis, were carried out (Fig. 6.9a). The results showed that H values were above 5.0 and Chao1 values were above 250 in all samples, indicating a diverse microbial community that could participate in the degradation and transformation of organics like A-PAM under anaerobic condition. Similar H values varied between 5.0 to 5.4 and similar Chao1 values between 250 and 400 were found among pre-treatment control, control and tailing samples with various A-PAM concentrations, which suggested that the presence of A-PAM did not have a significant impact on overall microbial diversity. However, it is important to investigate the impact of A-PAM on the specific microbial community and their metabolic activity during the process of anaerobic degradation of A-PAM.

To assess the beta diversity of microbial communities in tailings with different concentrations of A-PAM, the principal coordinate analysis (PCoA) was performed (Fig. 6.9b). The PCoA plot clearly shows that the pre-treatment control was distinctly separated from the tailings samples with A-PAM addition at day 36, suggesting that the anaerobic degradation of A-PAM had an impact on microbial community composition. Interestingly, the tailings samples with different A-PAM concentrations at day 36 were grouped together, which indicated that the A-PAM concentration did not significantly affect the microorganism compositions during the degradation process and suggested that the microbial community is capable of adapting to and degrading A-PAM at a range of concentrations. At the same time, previous results such as higher methane yield

and higher degradation efficiency observed in lower concentration of A-PAM suggest that lower concentrations may be favorable for anaerobic degradation and biogas production.
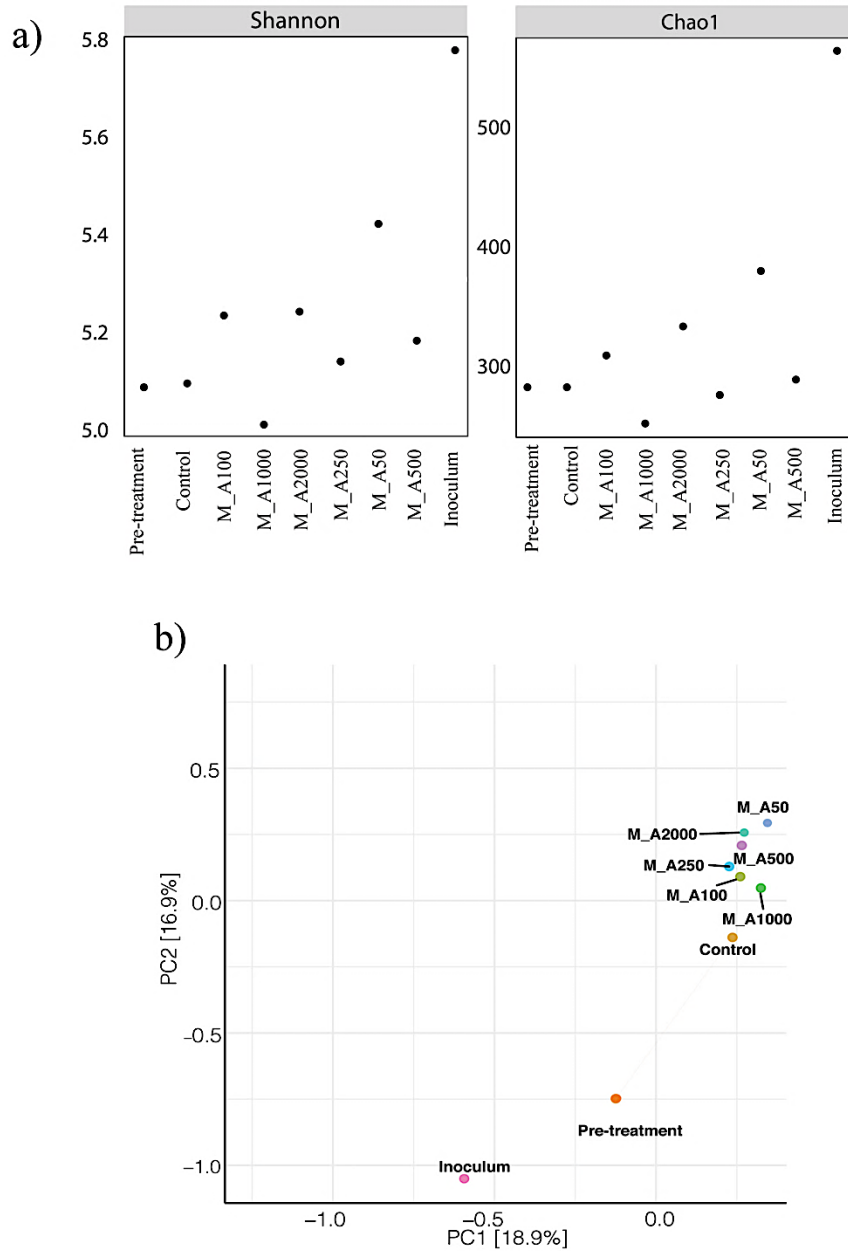
Figure 6.9 Alpha (a) and Beta (b) diversity of microbial communities in tailings before and after anaerobic degradation of A-PAM.

Considering different methane yields were obtained in tailings samples with different concentrations of A-PAM, which might be due to enrichment of different microbes (Akbar et al., 2020). By plotting the top 20 most abundant bacterial taxa (Fig 6.10a) and the composition of methanogens and methylotrophs (Fig 6.10b) in the heatmaps, it can be observed that Proteobacteria, Bacteroidetes, Chloroflexi, Firmicutes, Cloacimonetes, Synergistetes and Planctomycetes were dominant phyla in tailings samples (Fig 6.10a). The result is not surprising as these phyla are commonly found in anaerobic microbial communities and are known to play important roles in the degradation of organics. Proteobacteria and Bacteroidetes have been found to be involved in the hydrolysis and acidogenesis stages to produce acids like VFAs (Akbar et al., 2020; Dai et al., 2015). Besides, Proteobacteria has been previously reported to be capable of utilizing PAM as a carbon source (Hu et al., 2018). Chloroflexi and Firmicutes are commonly found in oilfields and have the ability to degrade high-molecular-weight n-alkanes (Cheng et al., 2014; Liang et al., 2015; Zhao et al., 2012). Both could play an important role in multiple stages in anaerobic degradation including hydrolysis, acidogenesis, and acetogenesis (Akbar et al., 2020; St-Pierre and Wright, 2014). Synergistetes and Planctomycetes, which are also commonly detected in oilfield produced water (Gieg et al., 2011; Zhao et al., 2015), have been reported to utilize PAM as a nitrogen source via producing amidase with growth under anaerobic conditions (Grula et al., 1994; Hu et al., 2018). Additionally, Synergistetes was also found to be capable of using small molecular organic substrate as a source of energy (Mnif et al., 2013), and some members of Planctomycetes are known as ammonium-oxidizing bacteria with the ability to oxidize NH_4^+-N under anaerobic conditions (Strous et al., 1999). Compared to other phyla, Cloacimonetes is a lesser well-studied phylum, but it has been reported as being comprised of acidification bacteria (Du et al., 2021) that

are believed to participate in degradation of refractory organic substances under anaerobic conditions (Westerholm et al., 2020).

Specifically, the dominant genera of Proteobacteria were *Comamonas*, *Pseudomonas*, *Smithella*, and *KCM-B-112*. Their relative abundance showed different trends among different samples after A-PAM degradation. Specifically, the relative abundance of *Comamonas* and *Pseudomonas* in the pre-treatment control were 10.9% and 4.7%, respectively. After A-PAM degradation, the relative abundance of *Comamonas* and *Pseudomonas* decreased in tailings samples, with a more significant reduction observed in tailing samples with lower concentrations of A-PAM (50 to 500 mg/kg TS). *Comamonas* and *Pseudomonas* genera are generally considered to be heterotrophic bacteria that have been found to be involved in the degradation of organic compounds such as aromatic hydrocarbons and PAHs (Liang et al., 2014; Ma et al., 2015). The decrease in the relative abundance of *Comamonas* and *Pseudomonas* after A-PAM degradation could be related to changes in the availability or composition of organic matter sources in the tailings. The result also indicated that the abundance of *Comamonas* and *Pseudomonas* could be influenced by the concentration of A-PAM in the tailings. In contrast, *Smithella* genus, with relative abundance of 1.2% in the pre-treatment control, was enriched in tailing samples with lower concentrations of A-PAM, with the maximum abundance value of 4.2% observed at 50 mg/kg TS of A-PAM, while it remained at 1-1.2% at higher concentrations of A-PAM (1000 and 2000 mg/kg TS). *Smithella* is commonly found in anaerobic environments, including anaerobic digestors and oil reservoirs (Liu et al., 2020), and is known to have the ability to degrade hydrocarbon and produce methane through syntrophic metabolism with other microorganisms such as hydrogenotrophic methanogens (Liang et al., 2015; Usman et al., 2019). Given the enrichment of *Smithella* and higher methane yield found in tailings samples with lower concentration of A-PAM,

228

Smithella could be involved in the anaerobic degradation of A-PAM and contribute to methane production in tailings. However, at higher concentrations of A-PAM, no significant increase was found for the relative abundance of *Smithella,* indicating that higher A-PAM concentration may have limited the growth or metabolic activity of *Smithella*. Interestingly, *KCM-B-112*, which is a recently discovered genus from the family Acidithiobacillaceae and has been detected in oil-contaminated soils (Hou et al., 2022), occupied a relative abundance of 1.5% in the pre-treatment control that dropped to 0-1% in tailings with lower concentrations of A-PAM (50 to 250 mg/kg TS) but slightly increased to 1.6-1.8% in tailings with higher concentrations of A-PAM (500 to 2000 mg/kg TS). Given that the metabolic capabilities and ecological role of *KCM-B-112* in tailings under anaerobic conditions are unknown, it is possible that the changes in relative abundance of *KCM-B-112* could be related to changes in the available organic matter sources or changes in environmental factors that could affect its growth or metabolic activity. Further research about *KCM-B-112* needs to be conducted. Unlike Proteobacteria, two dominant Cloacimonetes bacteria, uncultured *Candidatus_Cloacimonas* and *W5*, showed the similar trend in their relative abundance, which increased from 0.6% to 2.7-4.9%, and from 0.5% to 0.9-1.8% in tailings samples after A-PAM degradation. Both *Candidatus_Cloacimonas* and *W5* have been demonstrated to have a syntrophic lifestyle and are capable of propionate oxidation (Dyksma and Gallert, 2019). Therefore, these microorganisms may be functionally similar or may interact in similar ways within the tailings microbial community. Among Bacteroidetes bacteria, the abundance of *DMER64* and 9 other unclassified OTUs increased in most tailings samples after A-PAM degradation. Recently, *DMER64* has been proposed as a potential syntrophic bacterium that can transfer electron carrier H_2 to hydrogenotrophic methanogens during methanogenic degradation of VFAs (Lee et al., 2019). The enrichment of *DMER64* after A-PAM degradation

indicated that it plays a role in anaerobic degradation by affecting the methanogenesis stage. Similarly, the relative abundance of *XBB1006,* the dominant Firmicutes genus, also increased from 2 to 2-3.1% after A-PAM degradation. Due to the limited information about *XBB1006*, the increase in abundance could be related to the anaerobic degradation of A-PAM or to the utilization of other organic matter sources within tailings samples. It is interesting to notice that *Pirellula*, which is an obligate aerobic Planctomycetes bacteria, was detected in inoculum from anaerobic digestor, which could be associated with the influent substrate or indicate that a few aerobic areas existed in the digestor (Zhang et al., 2015). After A-PAM degradation, only slight changes were observed in the relative abundance of *Pirellula* in tailings samples, suggesting that these bacteria may not be playing a significant role in the anaerobic degradation of A-PAM. In regard to the composition of methylotrophs and methanogens in the archaea community (Fig. 6.10b**)**, the dominant methanogen in all samples was *Methanosaeta* (>50%), which is known to be an acetoclastic methanogen and can directly convert acetate into methane (Liang et al., 2015). Compared with that of the pre-treatment control, the relative abundance of hydrogenotrophic methanogens, including *Methanolinea* and *Methanospirillum,* increased in tailing samples with 250 mg/kg TS of A-PAM, while only *Methanolinea* increased in tailing samples with 1000 mg/kg TS of A-PAM, which is possibly due to the increase of H_2 and CO_2 production during the degradation of A-PAM. The *Candidatus_Dichloromethanomonas*, a methylotrophic methanogen, only appeared in the tailings sample with highest A-PAM concentration (2000 mg/kg TS), suggesting that some of the organic compounds in that tailings may be methylated and can be utilized by this methanogen for producing methane. It is interesting to find that one methylotroph, *Methylotenera*, that is capable of utilizing one-carbon compounds, such as methane, as a carbon source (Chistoserdova, 2015), was present in the control and in tailing samples with 100 and 1000 mg/kg TS of A-PAM after the

anaerobic degradation of A-PAM. Further studies are needed to confirm the role of *Methylotenera* in the anaerobic degradation of A-PAM in tailings.

Overall, based on the analysis of microbial community at different levels and the fact that tailings samples with 50 mg/kg TS of A-PAM had the highest methane yield and degradation efficiency of A-PAM, the key microorganisms for the anaerobic degradation of A-PAM in tailings might include *Smithella*, *Candidatus_Cloacimonas*, *W5*, *XBB1006* and *DMER64*. It is also worthy to note that besides *DMER64*, other unclassified Bacteroidetes could also play an important role in the anaerobic degradation of A-PAM due to their relatively high abundance in tailings with A-PAM.

a)

	Inoculum	Pre-treatment	Control	M_A50	M_A100	M_A250	M_A500	M_A1000	M_A2000
Proteobacteria; *Comamonas*	0.4	10.9	11.8	3.5	2.4	1.5	3	4.5	4.5
Proteobacteria; *Pseudomonas*	5.5	4.7	1.1	3.4	3.4	2.1	3.3	4.4	4.8
Cloacimonetes; *Candidatus_Cloacimonas*	4.3	0.6	5.4	2.7	2.5	3.5	4.9	4.3	3.7
Proteobacteria; *Immundisolibacter*	0	0.5	0	0.4	0.4	0.7	0.3	0.5	0.4
Bacteroidetes; *DMER64*	2.6	0.6	3.5	2.2	2.2	2.7	3.5	3.4	2.5
Epsilonbacteraeota; *Arcobacter*	18.3	0.7	0	0.8	0.5	0.2	0.6	0.6	0.4
Proteobacteria; *Smithella*	0.8	1.2	2.4	4.2	2.6	1.8	2.8	1.2	1
Bacteroidetes; f__ML635J−40_aquatic_group	0	2.4	0	2.8	2.3	2.7	2.2	2.4	2.9
Firmicutes; XBB1006	0.7	2	0.1	2	2.4	2.5	2.5	2.2	3.1
Bacteroidetes; f__ML635J−40_aquatic_group	0	2.1	0	2.5	2	2.5	2.2	2	2.2
Bacteroidetes; f__ML635J−40_aquatic_group	0	2.1	0	2.9	2	2	2.1	1.8	2.2
Proteobacteria; KCM−B−112	0	1.5	0	0	1	1	1.8	1.6	1.8
Planctomycetes; *Pirellula*	1.6	1.4	2.6	1.1	2.3	1.1	1.5	1.7	1.5
Bacteroidetes; f__ML635J−40_aquatic_group	0	2.7	0	0	2.7	3.3	0	2.6	3.1
Bacteroidetes; f__ML635J−40_aquatic_group	0	1.9	0	2.1	1.8	2	1.6	1.8	2.2
Bacteroidetes; f__ML635J−40_aquatic_group	0	2.1	0	2.2	1.9	2.1	1.9	1.5	2
Bacteroidetes; f__ML635J−40_aquatic_group	0	0	0	3.2	1.4	0	2.8	1.5	1.8
Bacteroidetes; f__ML635J−40_aquatic_group	0	1.6	0	2	1.4	1.8	1.5	1.4	1.6
Bacteroidetes; f__ML635J−40_aquatic_group	0	1.4	0	1.5	1.2	1.7	1.5	1.2	1.6
Cloacimonetes; W5	0.8	0.5	0.5	1	0.9	1.4	1.8	1.6	1.5

b)

	Inoculum	Pre-treatment	Control	M_A50	M_A100	M_A250	M_A500	M_A1000	M_A2000
Methanosaeta	68.1	100	46.3	100	59.2	76	100	73	77.4
Methylotenera	0	0	16.4	0	24.5	0	0	15.9	0
Methanospirillum	27.5	0	0	0	16.3	8	0	0	0
Methanolinea	0	0	23.9	0	0	16	0	11.1	0
Candidatus_Dichloromethanomonas	0	0	0	0	0	0	0	0	22.6
Methanomassiliicoccus	0	0	13.4	0	0	0	0	0	0
Methanocorpusculum	4.3	0	0	0	0	0	0	0	0

232

Figure 6.10 Heatmap illustrations of 20 top abundant bacterial genera (a) and composition of methylotrophs and methanogens (c) in different samples.

6.3.6 Degradation mechanism of A-PAM

Based on above results, the metabolic mechanism for the biodegradation of A-PAM in tailings under anaerobic condition was proposed (Fig. 6.11). A-PAM could be partially degraded to polyacrylate and polyacrylic acid after hydrolysis of the amide group, which was catalyzed by amidase (Zhao et al., 2019). Polyacrylate has been reported to be recalcitrant to further biodegradation (Cossey et al., 2021) whereas polyacrylic acid could be bio-converted to acetyl-CoA and pyruvic acid by dehydrogenase (Liu et al., 2019), which could be transformed to VFAs. Besides, AMD was also found to be one of the products from the anaerobic degradation of A-PAM, which could be later hydrolyzed into acrylic acid and converted to isobutyric acid detected in this study. Finally, VFAs could be transformed to CH_4 by methanogens. In addition, our results also suggested that A-PAM could be consumed as a carbon and nitrogen source in tailings during anaerobic degradation. Details of the metabolic pathway, including enzyme and the impact factors, could be determined in future studies.
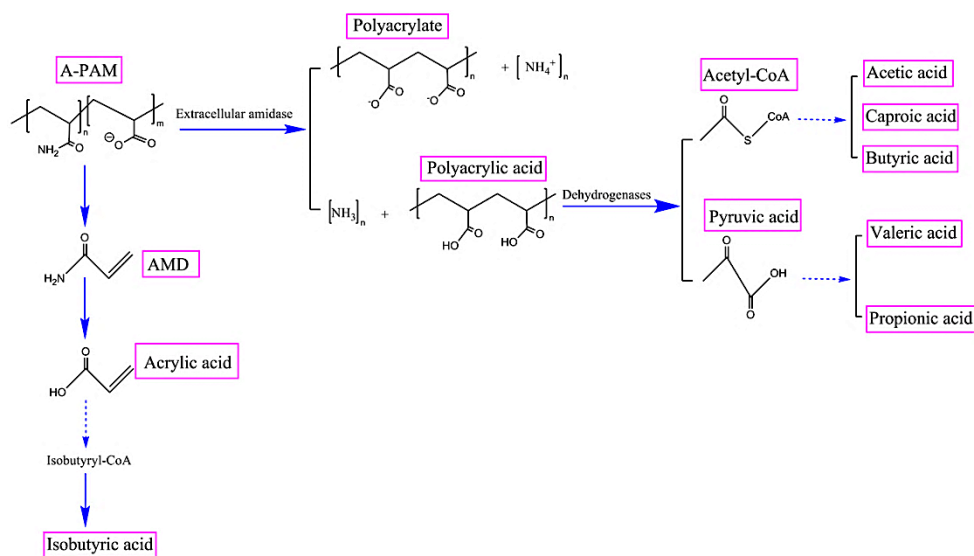
Figure 6.11 Proposed metabolic pathway of A-PAM biodegradation in tailings under anaerobic condition.

6.4 Conclusion

This work comprehensively investigated the anaerobic degradation of A-PAM in oil sands tailings, focusing on the impact of A-PAM concentration on methane production, A-PAM degradation, organic transformation, flocs structure and microbial community, which fills the knowledge gap. Our results showed that lower concentrations of A-PAM (10 and 100 mg/kg TS) resulted in higher methane yield compared to high concentrations of A-PAM (250 to 2000 mg/kg). The low methane yield (<10 mL) observed in all tailings samples could be due to the low consumption of acetic acid. Under anaerobic condition, A-PAM molecules could be degraded into smaller molecules, including AMD and polyacrylic acid, which were utilized as carbon and nitrogen sources for microbes. Different degradation efficiencies were observed with varying A-PAM concentrations, implying that polymer concentration could affect the degradation process. The results of Microtox® suggest that the degradation of A-PAM would not contribute the acute toxicity, and no genotoxicity was found before and after A-PAM degradation. The floc analyses suggest that A-PAM concentration could affect the degradation process by altering the flocs structure and composition, which subsequently affected the microbial colonization and metabolic activity. More importantly, *Smithella*, *Candidatus_Cloacimonas*, *W5*, *XBB1006* and *DMER64* were identified as the critical microorganisms involved in A-PAM degradation. These findings can contribute to the effective management of A-PAM treated oil sands tailings.

6.5 References

Akbar, M., Khan, M.F.S., Qian, L., Wang, H., 2020. Degradation of Polyacrylamide (PAM) and methane production by mesophilic and thermophilic anaerobic digestion: Effect of temperature and concentration. Frontiers of Environmental Science & Engineering 14(6), 1-11.

Alabi, O.A., 2022. Comparative chemical analysis, mutagenicity, and genotoxicity of Petroleum refinery wastewater and its contaminated river using prokaryotic and eukaryotic assays. Protoplasma, 1-13.

Allam, N.E., Zakaria, B.S., Kuznetsov, P.V., Dhar, B.R., Ulrich, A.C., 2023. Mitigating methane emission from oil sands tailings using enzymatic and lime treatments. Chemosphere 313, 137455.

Almutairi, A.L., Tayeh, B.A., Adesina, A., Isleem, H.F., Zeyad, A.M., 2021. Potential applications of geopolymer concrete in construction: A review. Case Studies in Construction Materials 15, e00733.

Arslan, M., Gamal El-Din, M., 2021. Bacterial diversity in petroleum coke based biofilters treating oil sands process water. Science of The Total Environment 782, 146742.

Bao, M., Chen, Q., Li, Y., Jiang, G., 2010. Biodegradation of partially hydrolyzed polyacrylamide by bacteria isolated from production water after polymer flooding in an oil field. Journal of hazardous materials 184(1-3), 105-110.

Berdugo-Clavijo, C., Sen, A., Seyyedi, M., Quintero, H., O'Neil, B., Gieg, L.M., 2019. High temperature utilization of PAM and HPAM by microbial communities enriched from oilfield produced water and activated sludge. Amb Express 9(1), 1-10.

Caulfield, M.J., Qiao, G.G., Solomon, D.H., 2002. Some aspects of the properties and degradation of polyacrylamides. Chemical reviews 102(9), 3067-3084.

Chen, H., Chen, Z., Nasikai, M., Luo, G., Zhang, S., 2021. Hydrothermal pretreatment of sewage sludge enhanced the anaerobic degradation of cationic polyacrylamide (cPAM). Water Research 190, 116704.

Chen, J., Ji, Q., Zheng, P., Chen, T., Wang, C., Mahmood, Q., 2010. Floatation and control of granular sludge in a high-rate anammox reactor. Water Research 44(11), 3321-3328.

Chen, Y., Cheng, J.J., Creamer, K.S., 2008. Inhibition of anaerobic digestion process: a review. Bioresource technology 99(10), 4044-4064.

Cheng, L., Shi, S., Li, Q., Chen, J., Zhang, H., Lu, Y., 2014. Progressive degradation of crude oil n-alkanes coupled to methane production under mesophilic and thermophilic conditions. PLoS One 9(11), e113253.

Chistoserdova, L., 2015. Methylotrophs in natural habitats: current insights through metagenomics. Applied microbiology and biotechnology 99, 5763-5779.

Chu, C., Lee, D., Chang, B.-V., You, C., Tay, J., 2002. "Weak" ultrasonic pre-treatment on anaerobic digestion of flocculated activated biosolids. Water research 36(11), 2681-2688.

Chu, C., Tsai, D., Lee, D., Tay, J., 2005. Size-dependent anaerobic digestion rates of flocculated activated sludge: role of intrafloc mass transfer resistance. Journal of environmental management 76(3), 239-244.

Collins, C.V., Foght, J.M., Siddique, T., 2016. Co-occurrence of methanogenesis and N2 fixation in oil sands tailings. Science of The Total Environment 565, 306-312.

Cossey, H.L., Batycky, A.E., Kaminsky, H., Ulrich, A.C., 2021. Geochemical Stability of Oil Sands Tailings in Mine Closure Landforms. Minerals 11(8), 830.

Dai, X., Luo, F., Yi, J., He, Q., Dong, B., 2014. Biodegradation of polyacrylamide by anaerobic digestion under mesophilic condition and its performance in actual dewatered sludge system. Bioresource technology 153, 55-61.

Dai, X., Luo, F., Zhang, D., Dai, L., Chen, Y., Dong, B., 2015. Waste-activated sludge fermentation for polyacrylamide biodegradation improved by anaerobic hydrolysis and key microorganisms involved in biological polyacrylamide removal. Scientific reports 5(1), 1-13.

Deng, Y., Dixon, J.B., White, G.N., 2006. Adsorption of polyacrylamide on smectite, illite, and kaolinite. Soil Science Society of America Journal 70(1), 297-304.

Dong, H., Huang, L., Zhao, L., Zeng, Q., Liu, X., Sheng, Y., Shi, L., Wu, G., Jiang, H., Li, F., 2022. A critical review of mineral–microbe interaction and co-evolution: mechanisms and applications. National science review 9(10), nwac128.

Dong, L., Su, F., Wang, Y.Z., 2020. Treatment of partially hydrolyzed polyacrylamide by mixed bacteria isolated from wastewater. Environmental Progress & Sustainable Energy 39(6), e13445.

Du, W., Huang, X., Zhang, J., Wang, D., Yang, Q., Li, X., 2021. Enhancing methane production from anaerobic digestion of waste activated sludge with addition of sodium lauroyl sarcosinate. Bioresource Technology 336, 125321.

Dyksma, S., Gallert, C., 2019. Candidatus Syntrophosphaera thermopropionivorans: a novel player in syntrophic propionate oxidation during anaerobic digestion. Environmental microbiology reports 11(4), 558-570.

EPA, 2010. Toxicological Review of Acrylamide in Support of Summary Information on the Integrated risk Information Systems (IRIS). US Environmental Protection Agency, Washington, DC.

Gieg, L.M., Jack, T.R., Foght, J.M., 2011. Biological souring and mitigation in oil reservoirs. Applied microbiology and biotechnology 92, 263-282.

Grula, M.M., Huang, M.-L., Sewell, G., 1994. Interactions of certain polyacrylamides with soil bacteria. Soil Science 158(4), 291-300.

Gumfekar, S.P., Rooney, T.R., Hutchinson, R.A., Soares, J.o.B., 2017. Dewatering oil sands tailings with degradable polymer flocculants. ACS applied materials & interfaces 9(41), 36290-36300.

Haveroen, M.E., MacKinnon, M.D., Fedorak, P.M., 2005. Polyacrylamide added as a nitrogen source stimulates methanogenesis in consortia from various wastewaters. Water Research 39(14), 3333-3341.

Hou, X., Ji, L., Li, T., Qi, Z., Sun, X., Li, Q., Zhang, Q., 2022. Effects of Salt Stress on the Structure and Function of Oil-Contaminated Soil Bacteria. Water, Air, & Soil Pollution 233(8), 349.

Hu, H., Liu, J.-F., Li, C.-Y., Yang, S.-Z., Gu, J.-D., Mu, B.-Z., 2018. Anaerobic biodegradation of partially hydrolyzed polyacrylamide in long-term methanogenic enrichment cultures from production water of oil reservoirs. Biodegradation 29(3), 233-243.

Huang, R., Chen, Y., Meshref, M.N., Chelme-Ayala, P., Dong, S., Ibrahim, M.D., Wang, C., Klamerth, N., Hughes, S.A., Headley, J.V., 2018. Characterization and determination of naphthenic acids species in oil sands process-affected water and groundwater from oil sands development area of Alberta, Canada. Water research 128, 129-137.

Johnson, B.T., 2005. Microtox® acute toxicity test, Small-scale freshwater toxicity investigations. Springer, pp. 69-105.

Konhauser, K., Ferris, F., 1996. Diversity of iron and silica precipitation by microbial mats in hydrothermal waters, Iceland: Implications for Precambrian iron formations. Geology 24(4), 323-326.

Król, M., Minkiewicz, J., Mozgawa, W., 2016. IR spectroscopy studies of zeolites in geopolymeric materials derived from kaolinite. Journal of Molecular Structure 1126, 200-206.

Lee, J., Koo, T., Yulisa, A., Hwang, S., 2019. Magnetite as an enhancer in methanogenic degradation of volatile fatty acids under ammonia-stressed condition. Journal of environmental management 241, 418-426.

Li, C., Fu, L., Stafford, J., Belosevic, M., Gamal El-Din, M., 2017. The toxicity of oil sands process-affected water (OSPW): A critical review. Science of the Total Environment 601, 1785-1802.

Li, J., How, Z.T., Gamal El-Din, M., 2023. Aerobic degradation of anionic polyacrylamide in oil sands tailings: Impact factor, degradation effect, and mechanism. Science of The Total Environment 856, 159079.

Liang, B., Wang, L.-Y., Mbadinga, S.M., Liu, J.-F., Yang, S.-Z., Gu, J.-D., Mu, B.-Z., 2015. Anaerolineaceae and Methanosaeta turned to be the dominant microorganisms in alkanes-dependent methanogenic culture after long-term of incubation. Amb Express 5, 1-13.

Liang, L., Song, X., Kong, J., Shen, C., Huang, T., Hu, Z., 2014. Anaerobic biodegradation of high-molecular-weight polycyclic aromatic hydrocarbons by a facultative anaerobe Pseudomonas sp. JP1. Biodegradation 25, 825-833.

Liu, J.-F., Lu, Y.-W., Liu, X.-B., Li, B.-G., Sun, Y.-F., Zhou, L., Liu, Y.-F., Yang, S.-Z., Gu, J.-D., Mu, B.-Z., 2020. Dominance of Pseudomonas in bacterial community and inhibition of fumarate addition pathway by injection of nutrients in oil reservoir revealed by functional gene and their transcript analyses. International Biodeterioration & Biodegradation 153, 105039.

Liu, L., Wang, Z., Lin, K., Cai, W., 2012. Microbial degradation of polyacrylamide by aerobic granules. Environmental technology 33(9), 1049-1054.

Liu, X., Xu, Q., Wang, D., Wu, Y., Yang, Q., Liu, Y., Wang, Q., Li, X., Li, H., Zeng, G., 2019. Unveiling the mechanisms of how cationic polyacrylamide affects short-chain fatty acids accumulation during long-term anaerobic fermentation of waste activated sludge. Water research 155, 142-151.

Ma, Q., Qu, Y., Shen, W., Zhang, Z., Wang, J., Liu, Z., Li, D., Li, H., Zhou, J., 2015. Bacterial community compositions of coking wastewater treatment plants in steel industry revealed by Illumina high-throughput sequencing. Bioresource Technology 179, 436-443.

Mnif, S., Bru- Adan, V., Godon, J.J., Sayadi, S., Chamkha, M., 2013. Characterization of the microbial diversity in production waters of mesothermic and geothermic Tunisian oilfields. Journal of Basic Microbiology 53(1), 45-61.

Moosavinejad, S.M., Madhoushi, M., Vakili, M., Rasouli, D., 2019. Evaluation of degradation in chemical compounds of wood in historical buildings using FT-IR and FT-Raman vibrational spectroscopy. Maderas. Ciencia y tecnología 21(3), 381-392.

Naik, A., Behera, B., Shukla, U., Sahu, H., Singh, P., Mohanty, D., Sahoo, K., Chatterjee, D., 2021. Mineralogical Studies of Mahanadi Basin coals based on FTIR, XRD and Microscopy: A Geological Perspective. Journal of the Geological Society of India 97, 1019-1027.

Nyyssölä, A., Ahlgren, J., 2019. Microbial degradation of polyacrylamide and the deamination product polyacrylate. International Biodeterioration & Biodegradation 139, 24-33.

Petibois, C., Gouspillou, G., Wehbe, K., Delage, J.-P., Déléris, G., 2006. Analysis of type I and IV collagens by FT-IR spectroscopy and imaging for a molecular investigation of skeletal muscle connective tissue. Analytical and bioanalytical chemistry 386, 1961-1966.

Qi, Y., Thapa, K.B., Hoadley, A.F., 2011. Application of filtration aids for improving sludge dewatering properties–a review. Chemical Engineering Journal 171(2), 373-384.

Ramos-Padrón, E., Bordenave, S., Lin, S., Bhaskar, I.M., Dong, X., Sensen, C.W., Fournier, J., Voordouw, G., Gieg, L.M., 2011. Carbon and sulfur cycling by microbial communities in a gypsum-treated oil sands tailings pond. Environmental science & technology 45(2), 439-446.

Romano, S., Perrone, M., Becagli, S., Pietrogrande, M., Russo, M., Caricato, R., Lionetto, M., 2020. Ecotoxicity, genotoxicity, and oxidative potential tests of atmospheric PM10 particles. Atmospheric Environment 221, 117085.

Sang, G., Pi, Y., Bao, M., Li, Y., Lu, J., 2015. Biodegradation for hydrolyzed polyacrylamide in the anaerobic baffled reactor combined aeration tank. Ecological engineering 84, 121-127.

Seybold, C., 1994. Polyacrylamide review: Soil conditioning and environmental fate. Communications in soil science and plant analysis 25(11-12), 2171-2185.

Song, W., Zhang, Y., Gao, Y., Chen, D., Yang, M., 2017. Cleavage of the main carbon chain backbone of high molecular weight polyacrylamide by aerobic and anaerobic biological treatment. Chemosphere 189, 277-283.

Sposito, G., 2008. The chemistry of soils. Oxford university press.

St-Pierre, B., Wright, A.-D.G., 2014. Comparative metagenomic analysis of bacterial populations in three full-scale mesophilic anaerobic manure digesters. Applied microbiology and biotechnology 98, 2709-2717.

Strous, M., Fuerst, J.A., Kramer, E.H., Logemann, S., Muyzer, G., van de Pas-Schoonen, K.T., Webb, R., Kuenen, J.G., Jetten, M.S., 1999. Missing lithotroph identified as new planctomycete. Nature 400(6743), 446-449.

Thijs, S., Op De Beeck, M., Beckers, B., Truyens, S., Stevens, V., Van Hamme, J.D., Weyens, N., Vangronsveld, J., 2017. Comparative evaluation of four bacteria-specific primer pairs for 16S rRNA gene surveys. Frontiers in microbiology 8, 494.

Usman, M., Hao, S., Chen, H., Ren, S., Tsang, D.C., Sompong, O., Luo, G., Zhang, S., 2019. Molecular and microbial insights towards understanding the anaerobic digestion of the wastewater from hydrothermal liquefaction of sewage sludge facilitated by granular activated carbon (GAC). Environment international 133, 105257.

Wang, D., Liu, X., Zeng, G., Zhao, J., Liu, Y., Wang, Q., Chen, F., Li, X., Yang, Q., 2018. Understanding the impact of cationic polyacrylamide on anaerobic digestion of waste activated sludge. Water Research 130, 281-290.

Westerholm, M., Liu, T., Schnürer, A., 2020. Comparative study of industrial-scale high-solid biogas production from food waste: Process operation and microbiology. Bioresource technology 304, 122981.

Wilén, B.-M., Balmer, P., 1999. The effect of dissolved oxygen concentration on the structure, size and size distribution of activated sludge flocs. Water research 33(2), 391-400.

Woodrow, J.E., Seiber, J.N., Miller, G.C., 2008. Acrylamide release resulting from sunlight irradiation of aqueous polyacrylamide/iron mixtures. Journal of Agricultural and Food Chemistry 56(8), 2773-2779.

Xiong, B., Loss, R.D., Shields, D., Pawlik, T., Hochreiter, R., Zydney, A.L., Kumar, M., 2018. Polyacrylamide degradation and its implications in environmental systems. NPJ Clean Water 1(1), 17.

Xiong, B., Purswani, P., Pawlik, T., Samineni, L., Karpyn, Z.T., Zydney, A.L., Kumar, M., 2020. Mechanical degradation of polyacrylamide at ultra high deformation rates during hydraulic fracturing. Environmental Science: Water Research & Technology 6(1), 166-172.

Yan, M., Zhao, L., Bao, M., Lu, J., 2016. Hydrolyzed polyacrylamide biodegradation and mechanism in sequencing batch biofilm reactor. Bioresource Technology 207, 315-321.

Zaman, A.A., Tsuchiya, R., Moudgil, B.M., 2002. Adsorption of a low-molecular-weight polyacrylic acid on silica, alumina, and kaolin. Journal of Colloid and Interface Science 256(1), 73-78.

Zhang, P., Shen, Y., Guo, J.-S., Li, C., Wang, H., Chen, Y.-P., Yan, P., Yang, J.-X., Fang, F., 2015. Extracellular protein analysis of activated sludge and their functions in wastewater treatment plant by shotgun proteomics. Scientific reports 5(1), 12041.

Zhao, F., Ma, F., Shi, R., Zhang, J., Han, S., Zhang, Y., 2015. Production of rhamnolipids by Pseudomonas aeruginosa is inhibited by H 2 S but resumes in a co-culture with P. stutzeri: applications for microbial enhanced oil recovery. Biotechnology letters 37, 1803-1808.

Zhao, L., Ma, T., Gao, M., Gao, P., Cao, M., Zhu, X., Li, G., 2012. Characterization of microbial diversity and community in water flooding oil reservoirs in China. World Journal of Microbiology and Biotechnology 28, 3039-3052.

Zhao, L., Song, T., Han, D., Bao, M., Lu, J., 2019. Hydrolyzed polyacrylamide biotransformation in an up-flow anaerobic sludge blanket reactor system: key enzymes, functional microorganisms, and biodegradation mechanisms. Bioprocess and biosystems engineering 42, 941-951.

Zheng, H., Feng, L., Gao, B., Zhou, Y., Zhang, S., Xu, B., 2017. Effect of the cationic block structure on the characteristics of sludge flocs formed by charge neutralization and patching. Materials 10(5), 487.

Zhou, S., Bu, X., Alheshibri, M., Zhan, H., Xie, G., 2022. Floc structure and dewatering performance of kaolin treated with cationic polyacrylamide degraded by hydrodynamic cavitation. Chemical Engineering Communications 209(6), 798-807.

CHAPTER 7 GENERAL CONCLUSIONS AND RECOMMENDATIONS

7.1 Thesis overview

Canada has the world's third largest proven oil reserves, where bitumen is extracted through either surface mining or in situ processes. During the extraction, upgrading and refining of oil sands, large amounts of wastewater such, as produced water from in situ Steam Assisted Gravity Drainage (SAGD) process and oil sands process water (OSPW) from surface mining, could be generated. SAGD produced water is characterized as having a slightly basic pH, high temperature, and high levels of colloidal impurities and total organic carbon (TOC). Due to the intensive use of water in the SAGD process, recycling the produced water to regenerate steam is essential for both the protection of the environment and minimizing operational costs. Different technologies have been developed to remove colloidal impurities from SAGD produced water, among which coagulation-flocculation (CF) with polymeric coagulants and flocculants is still considered as a promising and essential technology due to their stability under high temperatures. To better understand the impact of operational variables on the performance of softening-CF-sedimentation by using poly-DADMAC as coagulant and cationic polyacrylamide (PAM) as coagulant under high temperatures, numerical investigations based on response surface methodology (RSM) were performed. Additionally, the temperature effect on the removal mechanism and interactions between polymers and particles were also examined in Chapter 3.

In terms of OSPW, it is also a complex mixture containing toxic naphthenic acids (NAs) and is currently stored mainly in tailings ponds without release into the environment. With increasing water demands and more strict regulation, various treatment technologies, including active and passive applications, have been explored. Given that the comprehensive understanding

of systemic changes in physiochemical characteristics and the fate of dissolved organics during attenuation of OSPW is important to guarantee the applicability of technologies and to provide a reliable design in selecting and prioritizing treatment methods, Chapter 4 investigated the effect of temperature, oxygen and ozone pre-treatment on NAs degradation and toxicity reduction. In addition, quantitative statistical analyses were performed between NAs concentration and other water quality parameters, and between storage conditions and removal efficiency of water quality parameters. Finally, the key microorganisms for degrading dissolved organics in OSPW were identified.

As the main technology to recover water and reduce the volume of tailings stored in ponds, dewatering technologies rely heavily on the flocculation capacity of commercial polymer-based flocculants such as anionic polyacrylamide (A-PAM). However, limited information is currently available regarding the fate of A-PAM tailings. As oil sands tailings ponds are typically oxic closer to the surface and anoxic in the deeper layers, both aerobic and anaerobic degradation of A-PAM could occur. In Chapter 5, the degradation of A-PAM at oxic conditions in tailings was evaluated under different temperatures and microbial conditions. Moreover, the impacts of PAM degradation on the chemistry of tailings water and the possible degradation mechanism of PAM were also well studied. On the other hand, the anaerobic degradation of A-PAM in tailings was investigated in Chapter 6, focusing on the influence of A-PAM concentrations on methane production, organic transformation, and changes of solid phase during the anaerobic degradation process. More importantly, the responsible microbial community for A-PAM degradation and potential degradation mechanism were also examined.

7.2 Conclusions

The main conclusions of this research based on different projects are listed as follows:

Chapter 3: Thermal softening-coagulation-flocculation-sedimentation by using poly-DADMAC as coagulant and cationic polyacrylamide as flocculant in SAGD produced water

- Overall, poly-DADMAC dose and mixing time with softeners only were the most important factors for the treatment process.

- Increasing mixing time with softeners only could negate the negative effect of poly-DADMAC dose on both turbidity and TSS removal.

- The interaction effect of coagulation speed and mixing time with softeners was opposite on the removal of silica and particulate hardness, suggesting that their removal mechanisms were different even though they can be removed simultaneously in softening.

- TOC were affected mainly by softening and coagulation whereas coagulation and flocculation were important for TIC removal.

- The optimal conditions were 67 mg/L poly-DADMAC dose, 14 min mixing time with softeners only, coagulation speed of 200 rpm, and 16 min flocculation time, where the predicted maximum removal of turbidity, TSS, particulate hardness, silica, TOC and TIC were 99.2%, 99.1%, 99.4%, 27.0%, 69.0%, and 30.3%, respectively, and the value of SVI was 38.1 mL/g.

- Temperature increase could facilitate the removal of colloidal impurities via forming larger and denser flocs and changing their surface composition.

- Adsorption and subsequent bridging are the main removal mechanisms in the coagulation-flocculation process by using poly-DADMAC as the coagulant and cationic PAM as the flocculant.

Chapter 4: Fate of dissolved organics in OSPW during long-term storage

- The highest removal of dissolved organics was observed in ozonated OSPW stored at 20 °C with the highest degradation of total NAs (72.6%), and highest reduction of COD (25.3%) and DOC (19.8%).

- Biodegradation is likely to be the main reason for the decrease of NAs in OSPW and the shortest half-lives of total (474.8 days) and classical NAs (266.6 days) were observed in ozonated OSPW at 20 °C.

- Ozonation pre-treatment could enhance the removal of dissolved organics and promote the toxicity reduction in passive treatments like constructed wetlands.

- COD can be used as a surrogate variable to estimate NAs concentrations. BE-SPME could be used as a tool to predict acute toxicity during exposure to OSPW.

- Temperature is the most significant factor affecting OSPW quality. The limited changes of various parameters in OSPW stored at 4 °C for 4 years supported the common practice of storing OSPW in the cold room as an effective way to preserving the water quality in the laboratory and confirmed that the composition and properties of OSPW could be stable in the cold room for at least several years.

- Proteobacteria, Firmicutes, Bacteroidetes, Planctomycetes and Patescibacteria were the dominant phyla in various OSPW samples. *Bacillus* and *Fontimonas* might be the key microorganisms for degrading dissolved organics like NAs in OSPW.

Chapter 5: Aerobic degradation of A-PAM in oil sands tailings

- The maximum aerobic degradation removal efficiency of A-PAM was 41.0% in tailings water with augmented microorganisms at 20 °C.

- No acrylamide (AMD) monomer was released during the A-PAM degradation and residual AMD could be completely removed within 4 weeks.

- Both temperature and microorganisms showed significant effects ($p < 0.05$) on the degradation of A-PAM and residual AMD.

- Total organic carbon (TOC) and chemical oxygen demand (COD) could be used as indicators of A-PAM degradation in tailings.

- No substantial effects on acute toxicity and no genotoxicity were found in A-PAM treated tailings water.

- The potential mechanism of aerobic biodegradation of A-PAM in oil sands tailings is that with help of extracellular amidases, ammonia and smaller molecules, like organic acids, could be produced.

Chapter 6: Anaerobic degradation of A-PAM in oil sands tailings

- The addition of low concentrations of A-PAM (10 and 100 mg/kg TS) showed higher methane yield than high concentrations of A-PAM (250 to 2000 mg/kg).

- A-PAM molecules could be partially degraded into smaller molecules, such as AMD and polyacrylic acid, which could be utilized as both a carbon and nitrogen source for microbes.

- Addition of A-PAM could reduce the acute toxicity of tailings water by reducing NAs concentration and the degradation of A-PAM would not contribute to the acute toxicity and genotoxicity.

- A-PAM concentration could affect the degradation by altering the flocs structure and composition, which subsequently affected the microbial colonization and metabolic activity.

- Proteobacteria, Bacteroidetes, Chloroflexi, Firmicutes, Cloacimonetes, Synergistetes and Planctomycetes were dominant phyla in both the inoculum and tailings samples. *Smithella*, *Candidatus_Cloacimonas*, *W5*, *XBB1006* and *DMER64* were identified as the critical microorganisms involved in anaerobic degradation of A-PAM.

- The potential mechanism of anaerobic degradation of A-PAM was proposed: A-PAM could be partially degraded to polyacrylate and polyacrylic acid after hydrolysis of the amide group by amidase catalyzing. Polyacrylic acid could be bio-converted to acetyl-CoA and pyruvic acid by dehydrogenase, which could be transformed to VFAs. AMD could be hydrolyzed into acrylic acid and later converted to isobutyric acid.

7.3 Recommendations

Based on the results obtained from this research, recommendations for future works are proposed here:

- All SAGD experiments in this research were carried out in synthetic water, in which humic acid was used to represent the dissolved organics in SAGD produced water. Hence, real SAGD produced water is suggested in the future work to compare the interactions between particles with commercially available humic acid and organic fractions extracted from real wastewater. Additionally, the influence of residual bitumen and recycling sludge on the particles' interactions and removal mechanism in real SAGD produced water is recommended for further studies.

- The key microorganisms for degrading dissolved organics such as NAs in OSPW have been found. It is advisable to further investigate the metabolic pathway of these microorganisms in degrading dissolved organics under different conditions (temperature

and DO). Furthermore, there was some enrichment of relatively new microorganisms, such as *TX1A-55* and *AKYG587*, indicating they also played a role in degrading organics. Therefore, the impact of these microorganisms and their degradation pathways in OSPW are required for future study.

- In the study of aerobic degradation of A-PAM, microorganism augmentation showed significant impact on A-PAM degradation. To further explore the key microorganisms and the influence of A-PAM degradation on microorganism community, the analysis for microorganism profiling is recommended before and after A-PAM degradation under oxic conditions. In addition, besides temperature and microorganisms, other impact factors such as the concentration of A-PAM are also worth further examination in the future.

- The microbial community before and after A-PAM anaerobic degradation has been investigated. The relative abundance of many unclassified or newly discovered microorganisms, such as *KCM-B-112,* were found to be affected by A-PAM concentration and degradation. Their metabolic capabilities and ecological role in tailings under anaerobic conditions could be interesting to examine further. Moreover, degradation experiments were kept at 37 °C. A wider range of temperatures is recommended to enhance the knowledge about the temperature effect of anaerobic degradation of A-PAM in tailings.

- Both aerobic and anaerobic degradation experiments of A-PAM were conducted under controlled oxic or anoxic conditions in relatively small reactors. To fully understand the A-PAM degradation in oil sands tailings ponds, larger columns are suggested as reactors in future studies to mimic the environment of different depths in oil sands tailings.

- Considering the diverse toxicities associated with NAs and AMD, it is recommended to evaluate the toxicity of tailings water during A-PAM degradation using alternative toxicity assays, such as cell line-based methods.

Bibliography

Abdalrhman, A.S., Ganiyu, S.O., Gamal El-Din, M., 2019. Degradation kinetics and structure-reactivity relation of naphthenic acids during anodic oxidation on graphite electrodes. Chemical Engineering Journal 370, 997-1007.

Abdelrahman, A., Ganiyu, S.O., Gamal El-Din, M., 2023. Degradation of surrogate and real naphthenic acids from simulated and real oil sands process water using electrochemically activated peroxymonosulfate (EO-PMS) process. Separation and Purification Technology 306, 122462.

Ahmadi, M., Vahabzadeh, F., Bonakdarpour, B., Mofarrah, E., Mehranian, M., 2005. Application of the central composite design and response surface methodology to the advanced treatment of olive oil processing wastewater using Fenton's peroxidation. Journal of Hazardous Materials 123(1-3), 187-195.

Akbar, M., Khan, M.F.S., Qian, L., Wang, H., 2020. Degradation of Polyacrylamide (PAM) and methane production by mesophilic and thermophilic anaerobic digestion: Effect of temperature and concentration. Frontiers of Environmental Science & Engineering 14(6), 1-11.

Akbari, S., Mahmood, S.M., Tan, I.M., Ghaedi, H., Ling, O.L., 2017. Assessment of polyacrylamide based co-polymers enhanced by functional group modifications with regards to salinity and hardness. Polymers 9(12), 647.

Al-As'ad, A., Husein, M.M., 2014. Treatment of steam-assisted gravity drainage water using low coagulant dose and Fenton oxidation. Environ Technol 35(13-16), 1630-1638. https://doi.org/10.1080/09593330.2013.877086.

Alabi, O.A., 2022. Comparative chemical analysis, mutagenicity, and genotoxicity of Petroleum refinery wastewater and its contaminated river using prokaryotic and eukaryotic assays. Protoplasma, 1-13.

Alambets, A., 2014. Magnesium Oxide (MgO) Dosing Systems for Thermal Enhanced Oil Recovery, Alberta WaterSmart Water Management Solution. Calgary.

Alberta Energy Regulator, 2019. Directive 081: Water Disposal Limits and Reporting Requirements for Thermal In Situ Oil Sands Schemes, in: Regulator, A.E. (Ed.).

Alberta Energy Regulator, 2020. ST98: Alberta Energy Outlook 2020 executive summary. p. 11.

Allam, N.E., Anwar, M.N., Kuznetsov, P.V., Ulrich, A.C., Dhar, B.R., 2022. Enzyme-assisted dewatering of oil sands tailings: Significance of water chemistry and biological activity. Chemical Engineering Journal 437, 135162.

Allam, N.E., Zakaria, B.S., Kuznetsov, P.V., Dhar, B.R., Ulrich, A.C., 2023. Mitigating methane emission from oil sands tailings using enzymatic and lime treatments. Chemosphere 313, 137455.

Almutairi, A.L., Tayeh, B.A., Adesina, A., Isleem, H.F., Zeyad, A.M., 2021. Potential applications of geopolymer concrete in construction: A review. Case Studies in Construction Materials 15, e00733.

Anderson, J., Wiseman, S.B., Moustafa, A., Gamal El-Din, M., Liber, K., Giesy, J.P., 2012. Effects of exposure to oil sands process-affected water from experimental reclamation ponds on Chironomus dilutus. water research 46(6), 1662-1672.

Arora, S., Kazmi, A.A., 2015. The effect of seasonal temperature on pathogen removal efficacy of vermifilter for wastewater treatment. Water research 74, 88-99.

Arslan, M., Gamal El-Din, M., 2021. Bacterial diversity in petroleum coke based biofilters treating oil sands process water. Science of The Total Environment 782, 146742.

Arslan, M., Müller, J.A., Gamal El-Din, M., 2022. Aerobic naphthenic acid-degrading bacteria in petroleum-coke improve oil sands process water remediation in biofilters: DNA-stable isotope probing reveals methylotrophy in Schmutzdecke. Science of The Total Environment 815, 151961.

Atallah, C., Mortazavi, S., Tremblay, A.Y., Doiron, A., 2019. Surface-Modified Multi-lumen Tubular Membranes for SAGD-Produced Water Treatment. Energy & Fuels 33(6), 5766-5776. https://doi.org/10.1021/acs.energyfuels.9b00585.

Avadiar, L., Leong, Y., Fourie, A., Nugraha, T., 2013. Behaviours of kaolin suspensions with different polyacrylamide (PAM) flocculants under shear, Chemeca 2013: Challenging Tomorrow: Challenging Tomorrow. Engineers Australia Barton, ACT, pp. 249-254.

AWWA, 2017. Standard methods for the examination of water and wastewater. 23rd Edition. American Public Health Association, American Water Works Association, Water Envrionmental Federation, New York.

Bacosa, H.P., Kamalanathan, M., Chiu, M.-H., Tsai, S.-M., Sun, L., Labonté, J.M., Schwehr, K.A., Hala, D., Santschi, P.H., Chin, W.-C., 2018. Extracellular polymeric substances (EPS)

producing and oil degrading bacteria isolated from the northern Gulf of Mexico. PLoS One 13(12), e0208406.

Bao, M., Chen, Q., Li, Y., Jiang, G., 2010. Biodegradation of partially hydrolyzed polyacrylamide by bacteria isolated from production water after polymer flooding in an oil field. Journal of hazardous materials 184(1-3), 105-110.

Bartlett, A.J., Frank, R.A., Gillis, P.L., Parrott, J.L., Marentette, J.R., Brown, L.R., Hooey, T., Vanderveen, R., McInnis, R., Brunswick, P., 2017. Toxicity of naphthenic acids to invertebrates: Extracts from oil sands process-affected water versus commercial mixtures. Environmental pollution 227, 271-279.

Bazoubandi, B., Soares, J.B., 2020. Amylopectin-graft-polyacrylamide for the flocculation and dewatering of oil sands tailings. Minerals Engineering 148, 106196.

Berdugo-Clavijo, C., Sen, A., Seyyedi, M., Quintero, H., O'Neil, B., Gieg, L.M., 2019. High temperature utilization of PAM and HPAM by microbial communities enriched from oilfield produced water and activated sludge. Amb Express 9(1), 1-10.

Bergerson, J.A., Kofoworola, O., Charpentier, A.D., Sleep, S., MacLean, H.L., 2012. Life cycle greenhouse gas emissions of current oil sands technologies: surface mining and in situ applications. Environmental science & technology 46(14), 7865-7874.

Bhandari, V.M. and Ranade, V.V., 2014. Advanced physico-chemical methods of treatment for industrial wastewaters. Industrial wastewater treatment, recycling and reuse, 81-140.

Biryukova, O.V., Fedorak, P.M., Quideau, S.A., 2007. Biodegradation of naphthenic acids by rhizosphere microorganisms. Chemosphere 67(10), 2058-2064.

Black, A., Christman, R.F., 1961. Electrophoretic Studies of Sludge Particles Produced in Lime-Soda Softening. Journal- American Water Works Association 53(6), 737-747.

Blakley, E., 1974. The microbial degradation of cyclohexanecarboxylic acid: a pathway involving aromatization to form p-hydroxybenzoic acid. Canadian Journal of Microbiology 20(10), 1297-1306.

Blakley, E., Papish, B., 1982. The metabolism of cyclohexanecarboxylic acid and 3-cyclohexenecarboxylic acid by Pseudomonas putida. Canadian Journal of Microbiology 28(12), 1324-1329.

Bodor, A., Bounedjoum, N., Feigl, G., Duzs, Á., Laczi, K., Szilágyi, Á., Rákhely, G., Perei, K., 2021. Exploitation of extracellular organic matter from Micrococcus luteus to enhance ex

situ bioremediation of soils polluted with used lubricants. Journal of Hazardous Materials 417, 125996.

Bolto, B., Gregory, J., 2007. Organic polyelectrolytes in water treatment. Water research 41(11), 2301-2324.

Bouguerra, W., Ali, M.B.S., Hamrouni, B., Dhahbi, M., 2007. Equilibrium and kinetic studies of adsorption of silica onto activated alumina. Desalination 206(1-3), 141-146.

Brakstad, K., Rosenkilde, C., 2016. Modelling viscosity and mechanical degradation of polyacrylamide solutions in porous media, SPE Improved Oil Recovery Conference. OnePetro.

Bratby, J., 2006. Coagulation and flocculation in water and wastewater treatment, 430 IWA Publishing. London, UK 431.

Bratby, J., 2016. Coagulation and flocculation in water and wastewater treatment, IWA publishing.

Brient, J.A., Wessner, P.J., Doyle, M.N., 2000. Naphthenic acids. Kirk- Othmer Encyclopedia of Chemical Technology.

Brown, L., Bancroft, K., Rhead, M., 1980. Laboratory studies on the adsorption of acrylamide monomer by sludge, sediments, clays, peat and synthetic resins. Water Research 14(7), 779-781.

Brown, L.D., Pérez-Estrada, L., Wang, N., Gamal El-Din, M., Martin, J.W., Fedorak, P.M., Ulrich, A.C., 2013. Indigenous microbes survive in situ ozonation improving biodegradation of dissolved organic matter in aged oil sands process-affected waters. Chemosphere 93(11), 2748-2755.

Brown, L.D., Ulrich, A.C., 2015. Oil sands naphthenic acids: a review of properties, measurement, and treatment. Chemosphere 127, 276-290.

Buczek, S.B., Cope, W.G., McLaughlin, R.A., Kwak, T.J., 2017. Acute toxicity of polyacrylamide flocculants to early life stages of freshwater mussels. Environmental toxicology and chemistry 36(10), 2715-2721.

Butcher, J.B., Covington, S., 1995. Dissolved-oxygen analysis with temperature dependence. Journal of Environmental Engineering 121(10), 756-759.

Butler, R.M., 1994. Steam-assisted gravity drainage: concept, development, performance and future. Journal of Canadian Petroleum Technology 33(02), 44-50.

Campos-Avelar, I., Colas de la Noue, A., Durand, N., Cazals, G., Martinez, V., Strub, C., Fontana, A., Schorr-Galindo, S., 2021. Aspergillus flavus Growth Inhibition and Aflatoxin B1 Decontamination by Streptomyces Isolates and Their Metabolites. Toxins 13(5), 340.

Cancelli, A.M., Gobas, F.A., 2022. Treatment of naphthenic acids in oil sands process-affected waters with a surface flow treatment wetland: mass removal, half-life, and toxicity-reduction. Environmental Research 213, 113755.

Cao, B., Gao, B., Liu, X., Wang, M., Yang, Z., Yue, Q., 2011. The impact of pH on floc structure characteristic of polyferric chloride in a low DOC and high alkalinity surface water treatment. Water Res 45(18), 6181-6188. https://doi.org/10.1016/j.watres.2011.09.019.

Carman, P.S., Cawiezel, K., 2007. Successful breaker optimization for polyacrylamide friction reducers used in slickwater fracturing, SPE hydraulic fracturing technology conference. OnePetro.

Carreras, E.S., Passade-Boupat, N., Bourrel, M., Sedgwick, A., Yang, X., Junaid, A., 2013. Residual bitumen and flocculation: do we understand its effects?, Proceedings of the Seventeenth International Conference on Tailings and Mine Waste, November. pp. 3-6.

Caulfield, M.J., Hao, X., Qiao, G.G., Solomon, D.H., 2003. Degradation on polyacrylamides. Part I. Linear polyacrylamide. Polymer 44(5), 1331-1337.

Caulfield, M.J., Qiao, G.G., Solomon, D.H., 2002. Some aspects of the properties and degradation of polyacrylamides. Chemical reviews 102(9), 3067-3084.

Chan, S., 1989. A review on solubility and polymerization of silica. Geothermics 18(1-2), 49-56.

Chen, H., Chen, Z., Nasikai, M., Luo, G., Zhang, S., 2021. Hydrothermal pretreatment of sewage sludge enhanced the anaerobic degradation of cationic polyacrylamide (cPAM). Water Research 190, 116704.

Chen, H., Li, Q., Wang, M., Ji, D., Tan, W., 2020. XPS and two-dimensional FTIR correlation analysis on the binding characteristics of humic acid onto kaolinite surface. Science of the Total Environment 724, 138154.

Chen, J., Ji, Q., Zheng, P., Chen, T., Wang, C., Mahmood, Q., 2010. Floatation and control of granular sludge in a high-rate anammox reactor. Water Research 44(11), 3321-3328.

Chen, L., Xu, C., Zhang, X.-F., 2008. DFT calculations of vibrational spectra and nonlinear optical properties for MgO nanotube clusters. Journal of Molecular Structure: THEOCHEM 863(1-3), 55-59.

Chen, S., Chang, T., Lin, C., 2006. Silica pretreatment for a RO brackish water source with high magnesium. Water Science and Technology: Water Supply 6(4), 179-187.

Chen, Y., Cheng, J.J., Creamer, K.S., 2008. Inhibition of anaerobic digestion process: a review. Bioresource technology 99(10), 4044-4064.

Cheng, L., Shi, S., Li, Q., Chen, J., Zhang, H., Lu, Y., 2014. Progressive degradation of crude oil n-alkanes coupled to methane production under mesophilic and thermophilic conditions. PLoS One 9(11), e113253.

Cheng, W.P., Chi, F.H., 2002. A study of coagulation mechanisms of polyferric sulfate reacting with humic acid using a fluorescence-quenching method. Water research 36(18), 4583-4591.

Cheng, W.P., Chi, F.H., Li, C.C., Yu, R.F., 2008. A study on the removal of organic substances from low-turbidity and low-alkalinity water with metal-polysilicate coagulants. Colloids and Surfaces A: Physicochemical and Engineering Aspects 312(2-3), 238-244. https://doi.org/10.1016/j.colsurfa.2007.06.060.

Chheda, P., Grasso, D., 1994. Surface thermodynamics of ozone-induced particle destabilization. Langmuir 10(4), 1044-1053.

Chistoserdova, L., 2015. Methylotrophs in natural habitats: current insights through metagenomics. Applied microbiology and biotechnology 99, 5763-5779.

Chow, H., Pham, A.L.-T., 2019. Effective removal of silica and sulfide from oil sands thermal in-situ produced water by electrocoagulation. Journal of hazardous materials 380, 120880.

Chu, C., Lee, D., Chang, B.-V., You, C., Tay, J., 2002. "Weak" ultrasonic pre-treatment on anaerobic digestion of flocculated activated biosolids. Water research 36(11), 2681-2688.

Chu, C., Tsai, D., Lee, D., Tay, J., 2005. Size-dependent anaerobic digestion rates of flocculated activated sludge: role of intrafloc mass transfer resistance. Journal of environmental management 76(3), 239-244.

Clarke, T.P., 1980. Oil sands hot water extraction process. United States.

Collins, C.V., Foght, J.M., Siddique, T., 2016. Co-occurrence of methanogenesis and N2 fixation in oil sands tailings. Science of The Total Environment 565, 306-312.

COSIA, Water Performance Goals, https://cosia.ca/performance-goals/water.

Cossey, H.L., Batycky, A.E., Kaminsky, H., Ulrich, A.C., 2021. Geochemical Stability of Oil Sands Tailings in Mine Closure Landforms. Minerals 11(8), 830.

Dai, X., Luo, F., Yi, J., He, Q., Dong, B., 2014. Biodegradation of polyacrylamide by anaerobic digestion under mesophilic condition and its performance in actual dewatered sludge system. Bioresource technology 153, 55-61.

Dai, X., Luo, F., Zhang, D., Dai, L., Chen, Y., & Dong, B. (2015). Waste-activated sludge fermentation for polyacrylamide biodegradation improved by anaerobic hydrolysis and key microorganisms involved in biological polyacrylamide removal. Scientific reports, 5(1), 1-13.

Dai, X., Luo, F., Zhang, D., Dai, L., Chen, Y., Dong, B., 2015. Waste-activated sludge fermentation for polyacrylamide biodegradation improved by anaerobic hydrolysis and key microorganisms involved in biological polyacrylamide removal. Scientific reports 5(1), 1-13.

Das, K., Mukherjee, A.K., 2007. Crude petroleum-oil biodegradation efficiency of Bacillus subtilis and Pseudomonas aeruginosa strains isolated from a petroleum-oil contaminated soil from North-East India. Bioresource technology 98(7), 1339-1345.

Dayarathne, H., Angove, M.J., Jeong, S., Aryal, R., Paudel, S.R., Mainali, B., 2022. Effect of temperature on turbidity removal by coagulation: Sludge recirculation for rapid settling. Journal of Water Process Engineering 46, 102559.

De Meyer, S.E., Willems, A., 2012. Multilocus sequence analysis of Bosea species and description of Bosea lupini sp. nov., Bosea lathyri sp. nov. and Bosea robiniae sp. nov., isolated from legumes. International Journal of Systematic and Evolutionary Microbiology 62(Pt_10), 2505-2510.

Del Rio, L., Hadwin, A., Pinto, L., MacKinnon, M., Moore, M., 2006. Degradation of naphthenic acids by sediment micro- organisms. Journal of Applied Microbiology 101(5), 1049-1061.

Deng, Y., Dixon, J.B., White, G.N., 2006. Adsorption of polyacrylamide on smectite, illite, and kaolinite. Soil Science Society of America Journal 70(1), 297-304.

Deschner, F., Lothenbach, B., Winnefeld, F., Neubauer, J., 2013. Effect of temperature on the hydration of Portland cement blended with siliceous fly ash. Cement and concrete research 52, 169-181.

Ding, L., Yang, G., Xie, M., Gao, D., Yu, J., Zhang, Y., 2012. More insight into tandem ROMP and ADMET polymerization for yielding reactive long-chain highly branched polymers and their transformation to functional polymer nanoparticles. Polymer 53(2), 333-341.

Dompierre, K.A., Lindsay, M.B., Cruz-Hernández, P., Halferdahl, G.M., 2016. Initial geochemical characteristics of fluid fine tailings in an oil sands end pit lake. Science of the Total Environment 556, 196-206.

Dong, H., Huang, L., Zhao, L., Zeng, Q., Liu, X., Sheng, Y., Shi, L., Wu, G., Jiang, H., Li, F., 2022. A critical review of mineral–microbe interaction and co-evolution: mechanisms and applications. National science review 9(10), nwac128.

Dong, L., Su, F., Wang, Y.Z., 2020. Treatment of partially hydrolyzed polyacrylamide by mixed bacteria isolated from wastewater. Environmental Progress & Sustainable Energy 39(6), e13445.

Du, W., Huang, X., Zhang, J., Wang, D., Yang, Q., Li, X., 2021. Enhancing methane production from anaerobic digestion of waste activated sludge with addition of sodium lauroyl sarcosinate. Bioresource Technology 336, 125321.

Dwari, R., Angadi, S., Tripathy, S., 2018. Studies on flocculation characteristics of chromite's ore process tailing: Effect of flocculants ionicity and molecular mass. Colloids and Surfaces A: physicochemical and engineering aspects 537, 467-477.

Dyksma, S., Gallert, C., 2019. Candidatus Syntrophosphaera thermopropionivorans: a novel player in syntrophic propionate oxidation during anaerobic digestion. Environmental microbiology reports 11(4), 558-570.

Edzwald, J., Association, A.W.W., 2011. Water quality & treatment: a handbook on drinking water. McGraw-Hill Education.

EPA, 2010. Toxicological Review of Acrylamide in Support of Summary Information on the Integrated risk Information Systems (IRIS). US Environmental Protection Agency, Washington, DC.

EPA, 2010. Toxicological review of acrylamide in support of summary information on the integrated risk information systems (IRIS). US Environmental Protection Agency.

Fatema, J., Bhattacharjee, S., Pernitsky, D., Maiti, A., 2015. Study of the aggregation behavior of silica and dissolved organic matter in oil sands produced water using Taguchi experimental design. Energy & Fuels 29(11), 7465-7473.

Feng, B., Guo, W., Peng, J., Zhang, W., 2018. Separation of scheelite and calcite using calcium lignosulphonate as depressant. Separation and Purification Technology 199, 346-350.

Foght, J.M., Gieg, L.M., Siddique, T., 2017. The microbiology of oil sands tailings: past, present, future. FEMS Microbiology Ecology 93(5).

Forshomi, Z.D., Alva-Argaez, A., Bergerson, J.A., 2017. Optimal design of distributed effluent treatment systems in steam assisted gravity drainage oil sands operations. Journal of cleaner production 149, 1233-1248.

Frank, R.A., Fischer, K., Kavanagh, R., Burnison, B.K., Arsenault, G., Headley, J.V., Peru, K.M., Kraak, G.V.D., Solomon, K.R., 2009a. Effect of carboxylic acid content on the acute toxicity of oil sands naphthenic acids. Environmental science & technology 43(2), 266-271.

Frank, R.A., Kavanagh, R., Burnison, B.K., Arsenault, G., Headley, J.V., Peru, K.M., Van Der Kraak, G., Solomon, K.R., 2008. Toxicity assessment of collected fractions from an extracted naphthenic acid mixture. Chemosphere 72(9), 1309-1314.

Frank, R.A., Roy, J.W., Bickerton, G., Rowland, S.J., Headley, J.V., Scarlett, A.G., West, C.E., Peru, K.M., Parrott, J.L., Conly, F.M., 2014. Profiling oil sands mixtures from industrial developments and natural groundwaters for source identification. Environmental science & technology 48(5), 2660-2670.

Frank, R.A., Sanderson, H., Kavanagh, R., Burnison, B.K., Headley, J.V., Solomon, K.R., 2009b. Use of a (quantitative) structure–activity relationship [(Q) Sar] model to predict the toxicity of naphthenic acids. Journal of Toxicology and Environmental Health, Part A 73(4), 319-329.

Fu, L., Li, C., Lillico, D.M., Phillips, N.A., Gamal El-Din, M., Belosevic, M., Stafford, J.L., 2017. Comparison of the acute immunotoxicity of nonfractionated and fractionated oil sands process-affected water using mammalian macrophages. Environmental science & technology 51(15), 8624-8634.

Gamal El-Din, M., Fu, H., Wang, N., Chelme-Ayala, P., Pérez-Estrada, L., Drzewicz, P., Martin, J.W., Zubot, W., Smith, D.W., 2011. Naphthenic acids speciation and removal during petroleum-coke adsorption and ozonation of oil sands process-affected water. Science of the Total Environment 409(23), 5119-5125.

Ganiyu, S.O., Arslan, M., Gamal El-Din, M., 2022. Combined solar activated sulfate radical-based advanced oxidation processes (SR-AOPs) and biofiltration for the remediation of dissolved organics in oil sands produced water. Chemical Engineering Journal 433, 134579.

Gao, B., Yue, Q., Miao, J., 2003. Evaluation of polyaluminium ferric chloride (PAFC) as a composite coagulant for water and wastewater treatment. Water science and technology 47(1), 127-132.

Gao, B.Y., Wang, Y., Yue, Q.Y., Wei, J.C., Li, Q., 2008. The size and coagulation behavior of a novel composite inorganic–organic coagulant. Separation and Purification Technology 62(3), 544-550.

Garcia-Garcia, E., Ge, J.Q., Oladiran, A., Montgomery, B., Gamal El-Din, M., Perez-Estrada, L.C., Stafford, J.L., Martin, J.W., Belosevic, M., 2011. Ozone treatment ameliorates oil sands process water toxicity to the mammalian immune system. Water research 45(18), 5849-5857.

Geçer, A., 2022. Relation of the grain size, petrophysical parameters, and Fourier transform infrared analysis of Kusuri sandstones in the Zonguldak subbasin of the West Black Sea, Turkey. BULGARIAN CHEMICAL COMMUNICATIONS 4(3), 235-241.

Gieg, L.M., Jack, T.R., Foght, J.M., 2011. Biological souring and mitigation in oil reservoirs. Applied microbiology and biotechnology 92, 263-282.

Godwin Uranta, K., Rezaei-Gomari, S., Russell, P., Hamad, F., 2018. Studying the effectiveness of polyacrylamide (PAM) application in hydrocarbon reservoirs at different operational conditions. Energies 11(9), 2201.

Goff, K.L., Headley, J.V., Lawrence, J.R., Wilson, K.E., 2013. Assessment of the effects of oil sands naphthenic acids on the growth and morphology of Chlamydomonas reinhardtii using microscopic and spectromicroscopic techniques. Science of the total environment 442, 116-122.

Graham, S., Reitz, R., Hickman, C., 1989. Improving reverse osmosis performance through periodic cleaning. Desalination 74, 113-124.

Gröllmann, U., Schnabel, W., 1982. Free radical-induced oxidative degradation of polyacrylamide in aqueous solution. Polymer degradation and stability 4(3), 203-212.

Grula, M.M., Huang, M.-L., Sewell, G., 1994. Interactions of certain polyacrylamides with soil bacteria. Soil Science 158(4), 291-300.

Guezennec, A.-G., Michel, C., Bru, K., Touze, S., Desroche, N., Mnif, I., Motelica-Heino, M., 2015. Transfer and degradation of polyacrylamide-based flocculants in hydrosystems: a review. Environmental Science and Pollution Research 22(9), 6390-6406.

Guha Thakurta, S., Maiti, A., Pernitsky, D.J., Bhattacharjee, S., 2013. Dissolved organic matter in steam assisted gravity drainage boiler blow-down water. Energy & fuels 27(7), 3883-3890.

Gumfekar, S.P., Rooney, T.R., Hutchinson, R.A., Soares, J.o.B., 2017. Dewatering oil sands tailings with degradable polymer flocculants. ACS applied materials & interfaces 9(41), 36290-36300.

Halablab, M., Al-Dahlawi, A., 2008. Adherence of virulent and avirulent Legionella to hydrocarbons. J Medical Sciences 8, 234-238.

Han, X., MacKinnon, M.D., Martin, J.W., 2009. Estimating the in situ biodegradation of naphthenic acids in oil sands process waters by HPLC/HRMS. Chemosphere 76(1), 63-70.

Han, X., Scott, A.C., Fedorak, P.M., Bataineh, M., Martin, J.W., 2008. Influence of molecular structure on the biodegradability of naphthenic acids. Environmental science & technology 42(4), 1290-1295.

Haveroen, M.E., MacKinnon, M.D., Fedorak, P.M., 2005. Polyacrylamide added as a nitrogen source stimulates methanogenesis in consortia from various wastewaters. Water Research 39(14), 3333-3341.

Hay, M.B., Myneni, S.C., 2007. Structural environments of carboxyl groups in natural organic molecules from terrestrial systems. Part 1: Infrared spectroscopy. Geochimica et cosmochimica acta 71(14), 3518-3532.

Hayatbakhsh, M., Sadrzadeh, M., Pernitsky, D., Bhattacharjee, S., Hajinasiri, J., 2016. Treatment of an in situ oil sands produced water by polymeric membranes. Desalination and water treatment 57(32), 14869-14887.

He, Q., Chen, L., Zhang, S., Chen, R., Wang, H., 2019. Hydrodynamic shear force shaped the microbial community and function in the aerobic granular sequencing batch reactors for low carbon to nitrogen (C/N) municipal wastewater treatment. Bioresource technology 271, 48-58.

Heins, W., 2010. Is a paradigm shift in produced water treatment technology occurring at SAGD facilities? Journal of Canadian Petroleum Technology 49(01), 10-15.

Herrmann, M., Wegner, C.-E., Taubert, M., Geesink, P., Lehmann, K., Yan, L., Lehmann, R., Totsche, K.U., Küsel, K., 2019. Predominance of Cand. Patescibacteria in groundwater is caused by their preferential mobilization from soils and flourishing under oligotrophic conditions. Frontiers in microbiology 10, 1407.

Hogg, R., 2005. Flocculation and dewatering of fine-particle suspension. Coagulation and flocculation: Second Edition (FL). Boca Raton, CRC Press.

Holliman, P.J., Clark, J.A., Williamson, J.C., Jones, D.L., 2005. Model and field studies of the degradation of cross-linked polyacrylamide gels used during the revegetation of slate waste. Science of the Total Environment 336(1-3), 13-24.

Holowenko, F.M., MacKinnon, M.D., Fedorak, P.M., 2002. Characterization of naphthenic acids in oil sands wastewaters by gas chromatography-mass spectrometry. Water research 36(11), 2843-2855.

Hou, X., Ji, L., Li, T., Qi, Z., Sun, X., Li, Q., Zhang, Q., 2022. Effects of Salt Stress on the Structure and Function of Oil-Contaminated Soil Bacteria. Water, Air, & Soil Pollution 233(8), 349.

Hripko, R., Vajihinejad, V., LopesMotta, F., Soares, J.B., 2018. Enhanced flocculation of oil sands mature fine tailings using hydrophobically modified polyacrylamide copolymers. Global Challenges 2(3), 1700135.

Hu, H., Liu, J.-F., Li, C.-Y., Yang, S.-Z., Gu, J.-D., Mu, B.-Z., 2018. Anaerobic biodegradation of partially hydrolyzed polyacrylamide in long-term methanogenic enrichment cultures from production water of oil reservoirs. Biodegradation 29(3), 233-243.

Huang, C., Shi, Y., Gamal El-Din, M., Liu, Y., 2015. Treatment of oil sands process-affected water (OSPW) using ozonation combined with integrated fixed-film activated sludge (IFAS). Water research 85, 167-176.

Huang, C., Shi, Y., Sheng, Z., Gamal El-Din, M., Liu, Y., 2017. Characterization of microbial communities during start-up of integrated fixed-film activated sludge (IFAS) systems for the treatment of oil sands process-affected water (OSPW). Biochemical engineering journal 122, 123-132.

Huang, R., Chen, Y., Meshref, M.N., Chelme-Ayala, P., Dong, S., Ibrahim, M.D., Wang, C., Klamerth, N., Hughes, S.A., Headley, J.V., 2018. Characterization and determination of naphthenic acids species in oil sands process-affected water and groundwater from oil sands development area of Alberta, Canada. Water research 128, 129-137.

Huang, R., Sun, N., Chelme-Ayala, P., McPhedran, K.N., Changalov, M. and Gamal El-Din, M., 2015. Fractionation of oil sands-process affected water using pH-dependent extractions: a study of dissociation constants for naphthenic acids species. Chemosphere, 127, 291-296.

Huang, R., Yang, L., How, Z.T., Fang, Z., Bekele, A., Letinski, D.J., Redman, A.D., Gamal El-Din, M., 2021. Characterization of raw and ozonated oil sands process water utilizing atmospheric pressure gas chromatography time-of-flight mass spectrometry combined with solid phase microextractionun. Chemosphere 266, 129017.

Huang, S., Guo, X., Duan, W., Cheng, X., Zhang, X., Li, Z., 2019. Degradation of high molecular weight polyacrylamide by alkali-activated persulfate: reactivity and potential application in filter cake removal before cementing. Journal of Petroleum Science and Engineering 174, 70-79

Hughes, S.A., Mahaffey, A., Shore, B., Baker, J., Kilgour, B., Brown, C., Peru, K.M., Headley, J.V., Bailey, H.C., 2017. Using ultrahigh- resolution mass spectrometry and toxicity identification techniques to characterize the toxicity of oil sands process- affected water: The case for classical naphthenic acids. Environmental toxicology and chemistry 36(11), 3148-3157.

Hurwitz, G., Pernitsky, D.J., Bhattacharjee, S., Hoek, E.M., 2015. Targeted removal of dissolved organic matter in boiler-blowdown wastewater: integrated membrane filtration for produced water reuse. Industrial & Engineering Chemistry Research 54(38), 9431-9439.

Huzir, N.M., Aziz, M.M.A., Ismail, S., Mahmood, N.A.N., Umor, N., Muhammad, S.A.F.a.S., 2019. Optimization of coagulation-flocculation process for the palm oil mill effluent treatment by using rice husk ash. Industrial Crops and Products 139, 111482.

Hwang, G., Dong, T., Islam, M.S., Sheng, Z., Pérez-Estrada, L.A., Liu, Y., Gamal El-Din, M., 2013. The impacts of ozonation on oil sands process-affected water biodegradability and biofilm formation characteristics in bioreactors. Bioresource technology 130, 269-277.

Ilavsky, M., Hrouz, J., Stejskal, J., Bouchal, K., 1984. Phase transition in swollen gels. 6. Effect of aging on the extent of hydrolysis of aqueous polyacrylamide solutions and on the collapse of gels. Macromolecules 17(12), 2868-2874.

Islam, M.S., Dong, T., McPhedran, K.N., Sheng, Z., Zhang, Y., Liu, Y., Gamal El-Din, M., 2014a. Impact of ozonation pre-treatment of oil sands process-affected water on the operational performance of a GAC-fluidized bed biofilm reactor. Biodegradation 25(6), 811-823.

Islam, M.S., Moreira, J., Chelme-Ayala, P., Gamal El-Din, M., 2014b. Prediction of naphthenic acid species degradation by kinetic and surrogate models during the ozonation of oil sands process-affected water. Science of the total environment 493, 282-290.

Islam, M.S., Zhang, Y., McPhedran, K.N., Liu, Y., Gamal El-Din, M., 2015. Next-generation pyrosequencing analysis of microbial biofilm communities on granular activated carbon in treatment of oil sands process-affected water. Applied and environmental microbiology 81(12), 4037-4048.

Jasim, S., Ndiongue, S., Johnson, B., Schweitzer, L., Borikar, D., 2008. The effect of ozone on cold water coagulation. Ozone: Science and Engineering 30(1), 27-33.

Jennings, D.W., Shaikh, A., 2007. Heat-exchanger deposition in an inverted steam-assisted gravity drainage operation. Part 1. Inorganic and organic analyses of deposit samples. Energy & fuels 21(1), 176-184.

Ji, Y., Lu, Q., Liu, Q., Zeng, H., 2013. Effect of solution salinity on settling of mineral tailings by polymer flocculants. Colloids and Surfaces A: Physicochemical and Engineering Aspects 430, 29-38.

Johnson, B.T., 2005. Microtox® acute toxicity test, Small-scale freshwater toxicity investigations. Springer, pp. 69-105.

Johnson, R.J., Smith, B.E., Sutton, P.A., McGenity, T.J., Rowland, S.J., Whitby, C., 2011. Microbial biodegradation of aromatic alkanoic naphthenic acids is affected by the degree of alkyl side chain branching. The ISME journal 5(3), 486-496.

Joo, D.J., Shin, W.S., Choi, J.H., Choi, S.J., Kim, M.C., Han, M.H., Ha, T.W., Kim, Y.H., 2007. Decolorization of reactive dyes using inorganic coagulants and synthetic polymer. Dyes and Pigments 73(1), 59-64.

Joshi, S.J., Abed, R.M., 2017. Biodegradation of polyacrylamide and its derivatives. Environmental Processes 4(2), 463-476.

Jouenne, S., Klimenko, A., Levitt, D., 2017. Polymer flooding: Establishing specifications for dissolved oxygen and iron in injection water. SPE Journal 22(02), 438-446.

K. Labahn, S., C. Fisher, J., A. Robleto, E., H. Young, M., P. Moser, D., 2010. Microbially mediated aerobic and anaerobic degradation of acrylamide in a western United States irrigation canal. Journal of environmental quality 39(5), 1563-1569.

Kämpfer, P., Witzenberger, R., Denner, E.B., Busse, H.-J., Neef, A., 2002. Sphingopyxis witflariensis sp. nov., isolated from activated sludge. International Journal of Systematic and Evolutionary Microbiology 52(6), 2029-2034.

Kapanen, A., Vikman, M., Rajasärkkä, J., Virta, M., Itävaara, M., 2013. Biotests for environmental quality assessment of composted sewage sludge. Waste Management 33(6), 1451-1460.

Karami, H.R., Rahimi, M., Ovaysi, S., 2018. Degradation of drag reducing polymers in aqueous solutions. Korean Journal of Chemical Engineering 35(1), 34-43.

Karami, P., Khorshidi, B., McGregor, M., Peichel, J.T., Soares, J.B., Sadrzadeh, M., 2020. Thermally stable thin film composite polymeric membranes for water treatment: A review. Journal of Cleaner Production 250, 119447.

Kawaguchi, H., Li, Z., Masuda, Y., Sato, K., Nakagawa, H., 2012. Dissolved organic compounds in reused process water for steam-assisted gravity drainage oil sands extraction. Water Res 46(17), 5566-5574. https://doi.org/10.1016/j.watres.2012.07.036.

Keikhaei, M., Ichimura, M., 2019. Fabrication of Mg (OH) 2 thin films by electrochemical deposition with Cu catalyst. Thin Solid Films 681, 41-46.

Kimetu, J.M., Hill, J.M., Husein, M., Bergerson, J., Layzell, D.B., 2016. Using activated biochar for greenhouse gas mitigation and industrial water treatment. Mitigation and Adaptation Strategies for Global Change 21(5), 761-777.

Klein, C., Harbottle, D., Alagha, L., Xu, Z., 2013. Impact of fugitive bitumen on polymer- based flocculation of mature fine tailings. The Canadian Journal of Chemical Engineering 91(8), 1427-1432.

Konhauser, K., Ferris, F., 1996. Diversity of iron and silica precipitation by microbial mats in hydrothermal waters, Iceland: Implications for Precambrian iron formations. Geology 24(4), 323-326.

Król, M., Minkiewicz, J., Mozgawa, W., 2016. IR spectroscopy studies of zeolites in geopolymeric materials derived from kaolinite. Journal of Molecular Structure 1126, 200-206.

Ku, A.Y., Henderson, C.S., Petersen, M.A., Pernitsky, D.J., Sun, A.Q., 2012. Aging of water from steam-assisted gravity drainage (SAGD) operations due to air exposure and effects on ceramic membrane filtration. Industrial & engineering chemistry research 51(21), 7170-7176.

Kumar, A., Dixit, C.K., 2017. Methods for characterization of nanoparticles, Advances in nanomedicine for the delivery of therapeutic nucleic acids. Elsevier, pp. 43-58.

Kumar, K., Ravi, M., Pavani, Y., Bhavani, S., Sharma, A., VVR, N.R., 2012. Electrical conduction mechanism in NaCl complexed PEO/PVP polymer blend electrolytes. Journal of non-crystalline solids 358(23), 3205-3211.

Kusuma, H.S., Amenaghawon, A.N., Darmokoesoemo, H., Neolaka, Y.A., Widyaningrum, B.A., Anyalewechi, C.L., Orukpe, P.I., 2021. Evaluation of extract of Ipomoea batatas leaves as a green coagulant–flocculant for turbid water treatment: Parametric modelling and optimization using response surface methodology and artificial neural networks. Environmental Technology & Innovation 24, 102005.

Kusuma, H.S., Amenaghawon, A.N., Darmokoesoemo, H., Neolaka, Y.A., Widyaningrum, B.A., Onowise, S.U., Anyalewechi, C.L., 2022. A comparative evaluation of statistical empirical and neural intelligence modeling of Manihot esculenta-derived leaves extract for optimized bio-coagulation-flocculation of turbid water. Industrial Crops and Products 186, 115194.

Latour, I., Miranda, R., Blanco, A., 2014. Silica removal in industrial effluents with high silica content and low hardness. Environmental Science and Pollution Research 21(16), 9832-9842.

Latour, I., Miranda, R., Blanco, A., 2015. Silica removal with sparingly soluble magnesium compounds. Part II. Separation and Purification Technology 149, 331-338.

Lee, C.S., Robinson, J., Chong, M.F., 2014. A review on application of flocculants in wastewater treatment. Process Safety and Environmental Protection 92(6), 489-508.

Lee, J., Koo, T., Yulisa, A., Hwang, S., 2019. Magnetite as an enhancer in methanogenic degradation of volatile fatty acids under ammonia-stressed condition. Journal of environmental management 241, 418-426.

Leong, Y.-K., 2005. Yield stress and zeta potential of nanoparticulate silica dispersions under the influence of adsorbed hydrolysis products of metal ions—Cu (II), Al (III) and Th (IV). Journal of colloid and interface science 292(2), 557-566.

Li, C., Fu, L., Stafford, J., Belosevic, M., Gamal El-Din, M., 2017. The toxicity of oil sands process-affected water (OSPW): A critical review. Science of the Total Environment 601, 1785-1802.

Li, J., How, Z.T., Gamal El-Din, M., 2022a. Aerobic degradation of anionic polyacrylamide in oil sands tailings: Impact factor, degradation effect, and mechanism. Science of The Total Environment, 159079.

Li, J., How, Z.T., Gamal El-Din, M., 2023. Aerobic degradation of anionic polyacrylamide in oil sands tailings: Impact factor, degradation effect, and mechanism. Science of The Total Environment 856, 159079.

Li, J., How, Z.T., Zeng, H., Gamal El-Din, M., 2022. Treatment Technologies for Organics and Silica Removal in Steam-Assisted Gravity Drainage Produced Water: A Comprehensive Review. Energy & Fuels 36(3), 1205-1231.

Li, J., How, Z.T., Zeng, H., Gamal El-Din, M., 2022b. Treatment Technologies for Organics and Silica Removal in Steam-Assisted Gravity Drainage Produced Water: A Comprehensive Review. Energy & Fuels 36(3), 1205-1231.

Li, T., Yan, X., Wang, D., Wang, F., 2009. Impact of preozonation on the performance of coagulated flocs. Chemosphere 75(2), 187-192.

Liang, B., Wang, L.-Y., Mbadinga, S.M., Liu, J.-F., Yang, S.-Z., Gu, J.-D., Mu, B.-Z., 2015. Anaerolineaceae and Methanosaeta turned to be the dominant microorganisms in alkanes-dependent methanogenic culture after long-term of incubation. Amb Express 5, 1-13.

Liang, J., Tumpa, F., Estrada, L.P., Gamal El-Din, M., Liu, Y., 2014. Impact of ozonation on particle aggregation in mature fine tailings. Journal of environmental management 146, 535-542.

Liang, L., Song, X., Kong, J., Shen, C., Huang, T., Hu, Z., 2014. Anaerobic biodegradation of high-molecular-weight polycyclic aromatic hydrocarbons by a facultative anaerobe Pseudomonas sp. JP1. Biodegradation 25, 825-833.

Lightbown, V., 2015. New SAGD technologies show promise in reducing environmental impact of oil sand production. Journal of Environmental Solutions for Oil, Gas, and Mining 1(1), 47-58.

Lillico, D.M., Hussain, N.A., Choo-Yin, Y.Y., Qin, R., How, Z.T., Gamal El-Din, M., Stafford, J.L., 2022. Using immune cell-based bioactivity assays to compare the inflammatory activities of oil sands process-affected waters from a pilot scale demonstration pit lake. Journal of Environmental Sciences.

Lillico, D.M., Hussain, N.A., Choo-Yin, Y.Y., Qin, R., How, Z.T., Gamal El-Din, M., Stafford, J.L., 2023. Using immune cell-based bioactivity assays to compare the inflammatory activities of oil sands process-affected waters from a pilot scale demonstration pit lake. Journal of Environmental Sciences 128, 55-70.

Lin, S.-Y., Wang, S.-L., Wei, Y.-S., Li, M.-J., 2007. Temperature effect on water desorption from methylcellulose films studied by thermal FT-IR microspectroscopy. Surface Science 601(3), 781-785.

Lin, Z., Li, P., Hou, D., Kuang, Y., Wang, G., 2017. Aggregation mechanism of particles: Effect of Ca2+ and polyacrylamide on coagulation and flocculation of coal slime water containing illite. Minerals 7(2), 30.

Liu, H., Wang, D., Wang, M., Tang, H., Yang, M., 2007. Effect of pre-ozonation on coagulation with IPF–PACls: Role of coagulant speciation. Colloids and Surfaces A: Physicochemical and Engineering Aspects 294(1-3), 111-116.

Liu, J.-F., Lu, Y.-W., Liu, X.-B., Li, B.-G., Sun, Y.-F., Zhou, L., Liu, Y.-F., Yang, S.-Z., Gu, J.-D., Mu, B.-Z., 2020. Dominance of Pseudomonas in bacterial community and inhibition of fumarate addition pathway by injection of nutrients in oil reservoir revealed by functional gene and their transcript analyses. International Biodeterioration & Biodegradation 153, 105039.

Liu, L., Wang, Z., Lin, K., Cai, W., 2012. Microbial degradation of polyacrylamide by aerobic granules. Environmental technology 33(9), 1049-1054.

Liu, X., Xu, Q., Wang, D., Wu, Y., Yang, Q., Liu, Y., Wang, Q., Li, X., Li, H., Zeng, G., 2019. Unveiling the mechanisms of how cationic polyacrylamide affects short-chain fatty acids accumulation during long-term anaerobic fermentation of waste activated sludge. Water research 155, 142-151.

Lladó, S., Covino, S., Solanas, A., Petruccioli, M., D'annibale, A., Viñas, M., 2015. Pyrosequencing reveals the effect of mobilizing agents and lignocellulosic substrate amendment on microbial community composition in a real industrial PAH-polluted soil. Journal of hazardous materials 283, 35-43.

Lo, C.C., Brownlee, B.G., Bunce, N.J., 2006. Mass spectrometric and toxicological assays of Athabasca oil sands naphthenic acids. Water Research 40(4), 655-664.

Long, J., Li, H., Xu, Z., Masliyah, J., 2006. Role of colloidal interactions in oil sand tailings treatment. AIChE journal 52(1), 371-383.

Lu, J., Wu, L., Gan, J., 2003. Determination of polyacrylamide in soil waters by size exclusion chromatography. Journal of environmental quality 32(5), 1922-1926.

Lu, M., Wu, X., Wei, X., 2012. Chemical degradation of polyacrylamide by advanced oxidation processes. Environmental technology 33(9), 1021-1028.

Lu, Q., Yan, B., Xie, L., Huang, J., Liu, Y., Zeng, H., 2016. A two-step flocculation process on oil sands tailings treatment using oppositely charged polymer flocculants. Science of the Total Environment 565, 369-375.

Luo, Y., Xie, H., Xu, H., Zhou, C., Wang, P., Liu, Z., Yang, Y., Huang, J., Wang, C., Zhao, X., 2023. Wastewater treatment plant serves as a potentially controllable source of microplastic: Association of microplastic removal and operational parameters and water quality data. Journal of Hazardous Materials 441, 129974.

Ma, F., Wei, L., Wang, L., Chang, C.-C., 2008. Isolation and identification of the sulphate-reducing bacteria strain H1 and its function for hydrolysed polyacrylamide degradation. International journal of biotechnology 10(1), 55-63.

Ma, Q., Qu, Y., Shen, W., Zhang, Z., Wang, J., Liu, Z., Li, D., Li, H., Zhou, J., 2015. Bacterial community compositions of coking wastewater treatment plants in steel industry revealed by Illumina high-throughput sequencing. Bioresource Technology 179, 436-443.

Mahdavi, H., Prasad, V., Liu, Y., Ulrich, A.C., 2015. In situ biodegradation of naphthenic acids in oil sands tailings pond water using indigenous algae–bacteria consortium. Bioresource technology 187, 97-105.

Maiti, A., Sadrezadeh, M., Guha Thakurta, S., Pernitsky, D.J., Bhattacharjee, S., 2012. Characterization of boiler blowdown water from steam-assisted gravity drainage and silica–organic coprecipitation during acidification and ultrafiltration. Energy & fuels 26(9), 5604-5612.

Manfre Jaimes, D., Gates, I.D., Clarke, M., 2019. Reducing the Energy and Steam Consumption of SAGD Through Cyclic Solvent Co-Injection. Energies 12(20), 3860.

Mansour, A.M., Al-Maamari, R.S., Al-Hashmi, A.S., Zaitoun, A., Al-Sharji, H., 2014. In-situ rheology and mechanical degradation of EOR polyacrylamide solutions under moderate shear rates. Journal of Petroleum Science and Engineering 115, 57-65.

Marentette, J.R., Frank, R.A., Bartlett, A.J., Gillis, P.L., Hewitt, L.M., Peru, K.M., Headley, J.V., Brunswick, P., Shang, D., Parrott, J.L., 2015. Toxicity of naphthenic acid fraction components extracted from fresh and aged oil sands process-affected waters, and commercial naphthenic acid mixtures, to fathead minnow (Pimephales promelas) embryos. Aquatic Toxicology 164, 108-117.

Martin, J.W., Barri, T., Han, X., Fedorak, P.M., Gamal El-Din, M., Perez, L., Scott, A.C., Jiang, J.T., 2010. Ozonation of oil sands process-affected water accelerates microbial bioremediation. Environmental science & technology 44(21), 8350-8356.

Masliyah, J., Zhou, Z.J., Xu, Z., Czarnecki, J., Hamza, H., 2004. Understanding water- based bitumen extraction from Athabasca oil sands. The Canadian Journal of Chemical Engineering 82(4), 628-654.

McCollister, D., Oyen, F., Rowe, V., 1964. Toxicology of acrylamide. Toxicology and Applied Pharmacology 6(2), 172-181.

McKenzie, N., Yue, S., Liu, X., Ramsay, B.A., Ramsay, J.A., 2014. Biodegradation of naphthenic acids in oils sands process waters in an immobilized soil/sediment bioreactor. Chemosphere 109, 164-172.

McQueen, A.D., Kinley, C.M., Hendrikse, M., Gaspari, D.P., Calomeni, A.J., Iwinski, K.J., Castle, J.W., Haakensen, M.C., Peru, K.M., Headley, J.V., 2017. A risk-based approach for identifying constituents of concern in oil sands process-affected water from the Athabasca Oil Sands region. Chemosphere 173, 340-350.

Mehboob, F., Junca, H., Schraa, G., Stams, A.J., 2009. Growth of Pseudomonas chloritidismutans AW-1T on n-alkanes with chlorate as electron acceptor. Applied Microbiology and Biotechnology 83(4), 739-747.

Meng, L., How, Z.T., Ganiyu, S.O., Gamal El-Din, M., 2021. Solar photocatalytic treatment of model and real oil sands process water naphthenic acids by bismuth tungstate: Effect of catalyst morphology and cations on the degradation kinetics and pathways. Journal of Hazardous Materials 413, 125396.

Meshref, M.N., Chelme-Ayala, P., Gamal El-Din, M., 2017. Fate and abundance of classical and heteroatomic naphthenic acid species after advanced oxidation processes: Insights and indicators of transformation and degradation. Water research 125, 62-71.

Mesmer, R., Baes, C., 1990. Review of Hydrolysis Behavior of Ions in Aqueous Solutions. MRS Online Proceedings Library (OPL) 180.

Metcalf, W., 2003. Metcalf and Eddy wastewater engineering: treatment and reuse. In Wastewater engineering: treatment and reuse. New York, NY, McGraw Hill.

Miles, S.M., Hofstetter, S., Edwards, T., Dlusskaya, E., Cologgi, D.L., Gänzle, M., Ulrich, A.C., 2019. Tolerance and cytotoxicity of naphthenic acids on microorganisms isolated from oil sands process-affected water. Science of the Total Environment 695, 133749.

Mnif, S., Bru- Adan, V., Godon, J.J., Sayadi, S., Chamkha, M., 2013. Characterization of the microbial diversity in production waters of mesothermic and geothermic Tunisian oilfields. Journal of Basic Microbiology 53(1), 45-61.

Mohammadtabar, F., Pillai, R.G., Khorshidi, B., Hayatbakhsh, A., Sadrzadeh, M., 2019. Efficient treatment of oil sands produced water: Process integration using ion exchange regeneration wastewater as a chemical coagulant. Separation and Purification Technology 221, 166-174.

Mohd-Salleh, S.N.A., Mohd-Zin, N.S., Othman, N., 2019. A review of wastewater treatment using natural material and its potential as aid and composite coagulant. Sains Malaysiana 48(1), 155-164.

Mohn, W.W., Wilson, A.E., Bicho, P., Moore, E.R., 1999. Physiological and phylogenetic diversity of bacteria growing on resin acids. Systematic and Applied Microbiology 22(1), 68-78.

Molina, R., Jovancic, P., Vilchez, S., Tzanov, T., Solans, C., 2014. In situ chitosan gelation initiated by atmospheric plasma treatment. Carbohydrate polymers 103, 472-479.

Moosavinejad, S.M., Madhoushi, M., Vakili, M., Rasouli, D., 2019. Evaluation of degradation in chemical compounds of wood in historical buildings using FT-IR and FT-Raman vibrational spectroscopy. Maderas. Ciencia y tecnología 21(3), 381-392.

Morandi, G., Wiseman, S., Sun, C., Martin, J.W., Giesy, J.P., 2020. Effects of chemical fractions from an oil sands end-pit lake on reproduction of fathead minnows. Chemosphere 249, 126073.

Mpofu, P., Addai-Mensah, J., Ralston, J., 2004. Temperature influence of nonionic polyethylene oxide and anionic polyacrylamide on flocculation and dewatering behavior of kaolinite dispersions. Journal of Colloid and Interface Science 271(1), 145-156.

Naik, A., Behera, B., Shukla, U., Sahu, H., Singh, P., Mohanty, D., Sahoo, K., Chatterjee, D., 2021. Mineralogical Studies of Mahanadi Basin coals based on FTIR, XRD and Microscopy: A Geological Perspective. Journal of the Geological Society of India 97, 1019-1027.

Nair, A.T., Makwana, A.R., Ahammed, M.M., 2014. The use of response surface methodology for modelling and analysis of water and wastewater treatment processes: a review. Water science and technology 69(3), 464-478.

Nason, J.A., Lawler, D.F., 2009. Particle size distribution dynamics during precipitative softening: Declining solution composition. water research 43(2), 303-312.

Nguyen, Q., Boger, D., 1998. Application of rheology to solving tailings disposal problems. International Journal of Mineral Processing 54(3-4), 217-233.

Ni, M., Ratner, B.D., 2008. Differentiating calcium carbonate polymorphs by surface analysis techniques—an XPS and TOF- SIMS study. Surface and Interface Analysis: An International Journal devoted to the development and application of techniques for the analysis of surfaces, interfaces and thin films 40(10), 1356-1361.

Nimana, B., Canter, C., Kumar, A., 2015. Life cycle assessment of greenhouse gas emissions from Canada's oil sands-derived transportation fuels. Energy 88, 544-554.

Ning, R.Y., 2003. Discussion of silica speciation, fouling, control and maximum reduction. Desalination 151(1), 67-73.

NRC, 2022. Water Management in Oil Sands. Natural Resources Canada.

Nyyssölä, A., Ahlgren, J., 2019. Microbial degradation of polyacrylamide and the deamination product polyacrylate. International Biodeterioration & Biodegradation 139, 24-33.

Oladoja, N.A., 2016. Advances in the quest for substitute for synthetic organic polyelectrolytes as coagulant aid in water and wastewater treatment operations. Sustainable Chemistry and Pharmacy 3, 47-58. https://doi.org/10.1016/j.scp.2016.04.001.

Ooi, T.Y., Yong, E.L., Din, M.F.M., Rezania, S., Aminudin, E., Chelliapan, S., Rahman, A.A., Park, J., 2018. Optimization of aluminium recovery from water treatment sludge using Response Surface Methodology. Journal of environmental management 228, 13-19.

Oren, A., 2014. The Family Xanthobacteraceae, in: Rosenberg, E., DeLong, E.F., Lory, S., Stackebrandt, E., Thompson, F. (Eds.), The Prokaryotes: Alphaproteobacteria and

Betaproteobacteria. Springer Berlin Heidelberg, Berlin, Heidelberg, pp. 709-726. https://doi.org/10.1007/978-3-642-30197-1_258.

Osacky, M., Geramian, M., Ivey, D.G., Liu, Q., Etsell, T.H., 2013. Mineralogical and chemical composition of petrologic end members of Alberta oil sands. Fuel 113, 148-157.

Ovenden, C., Xiao, H., 2002. Flocculation behaviour and mechanisms of cationic inorganic microparticle/polymer systems. Colloids and Surfaces A: Physicochemical and Engineering Aspects 197(1-3), 225-234.

Özacar, M., Şengil, İ.A., 2003. Evaluation of tannin biopolymer as a coagulant aid for coagulation of colloidal particles. Colloids and Surfaces A: Physicochemical and Engineering Aspects 229(1-3), 85-96. https://doi.org/10.1016/j.colsurfa.2003.07.006.

Parks, J.L., Edwards, M., 2007. Boron removal via formation of magnesium silicate solids during precipitative softening. Journal of Environmental Engineering 133(2), 149-156.

Parsons, S.A., Jefferson, B., 2006. Introduction to potable water treatment processes. Blackwell publishing.

Parvathy, P.C., Jyothi, A.N., 2012. Synthesis, characterization and swelling behaviour of superabsorbent polymers from cassava starch- graft- poly (acrylamide). Starch- Stärke 64(3), 207-218.

Patel, V., Dalsania, Y., Azad, M.S., Sharma, T., Trivedi, J., 2021. Characterization of co- and post- hydrolyzed polyacrylamide molecular weight and radius distribution under saline environment. Journal of Applied Polymer Science 138(26), 50616.

Perdicakis, B., Petersen, M., Gerbino, A., McGregor, M., 2019. In High Temperature Reverse Osmosis Membrane SAGD Process Design Assessment, International Water Conference. Orlando, pp. 19-61.

Pereira, A.S., Bhattacharjee, S., Martin, J.W., 2013. Characterization of oil sands process-affected waters by liquid chromatography orbitrap mass spectrometry. Environmental science & technology 47(10), 5504-5513.

Pernitsky, D.J., Edzwald, J.K., 2006. Selection of alum and polyaluminum coagulants: principles and applications. Journal of Water Supply: Research and Technology—AQUA 55(2), 121-141.

Petersen, M.A., Henderson, C.S., Ku, A.Y., Sun, A.Q., Pernitsky, D.J., 2015. Oil sands steam-assisted gravity drainage process water sample aging during long-term storage. Energy & Fuels 29(3), 2034-2041.

Petibois, C., Gouspillou, G., Wehbe, K., Delage, J.-P., Déléris, G., 2006. Analysis of type I and IV collagens by FT-IR spectroscopy and imaging for a molecular investigation of skeletal muscle connective tissue. Analytical and bioanalytical chemistry 386, 1961-1966.

Pillai, R.G., Yang, N., Thi, S., Fatema, J., Sadrzadeh, M., Pernitsky, D., 2017. Characterization and Comparison of Dissolved Organic Matter Signatures in Steam-Assisted Gravity Drainage Process Water Samples from Athabasca Oil Sands. Energy & Fuels 31(8), 8363-8373. https://doi.org/10.1021/acs.energyfuels.7b00483.

Polizzotti, D.M., Khwaja, A.R., 2011. Use of cationic coagulant and acrylamide polymer flocculants for separating oil from oily water. Google Patents.

Polizzotti, D.M., Khwaja, A.R., 2014. Deoiling of SAGD produce water. Google Patents.

Pourrezaei, P., Alpatova, A., Chelme-Ayala, P., Perez-Estrada, L., Jensen-Fontaine, M., Le, X., Gamal El-Din, M., 2014. Impact of petroleum coke characteristics on the adsorption of the organic fractions from oil sands process-affected water. International Journal of Environmental Science and Technology 11(7), 2037-2050.

Pourrezaei, P., Drzewicz, P., Wang, Y., Gamal El-Din, M., Perez-Estrada, L.A., Martin, J.W., Anderson, J., Wiseman, S., Liber, K., Giesy, J.P., 2011. The impact of metallic coagulants on the removal of organic compounds from oil sands process-affected water. Environmental science & technology 45(19), 8452-8459.

Prakash, N., Sockan, V., Jayakaran, P., 2014. Waste water treatment by coagulation and flocculation. International Journal of Engineering Science and Innovative Technology (IJESIT) 3(2), 479-484.

Qi, Y., Thapa, K.B., Hoadley, A.F., 2011. Application of filtration aids for improving sludge dewatering properties–a review. Chemical Engineering Journal 171(2), 373-384.

Qin, C., Becerra, M., Shaw, J.M., 2017. Fate of Organic Liquid-Crystal Domains during Steam-Assisted Gravity Drainage/Cyclic Steam Stimulation Production of Heavy Oils and Bitumen. Energy & Fuels 31(5), 4966-4972.

Quagraine, E., Headley, J., Peterson, H., 2005a. Is biodegradation of bitumen a source of recalcitrant naphthenic acid mixtures in oil sands tailing pond waters? Journal of Environmental Science and Health 40(3), 671-684.

Quagraine, E., Peterson, H., Headley, J., 2005. In situ bioremediation of naphthenic acids contaminated tailing pond waters in the Athabasca oil sands region—demonstrated field studies and plausible options: a review. Journal of Environmental Science and Health 40(3), 685-722.

Quagraine, E., Peterson, H., Headley, J., 2005b. In situ bioremediation of naphthenic acids contaminated tailing pond waters in the Athabasca oil sands region—demonstrated field studies and plausible options: a review. Journal of Environmental Science and Health 40(3), 685-722.

Quinlan, P.J., Tam, K.C., 2015. Water treatment technologies for the remediation of naphthenic acids in oil sands process-affected water. Chemical Engineering Journal 279, 696-714.

Radpour, S., Gemechu, E., Ahiduzzaman, M., Kumar, A., 2021. Development of a framework for the assessment of the market penetration of novel in situ bitumen extraction technologies. Energy 220, 119666.

Ramos-Padrón, E., Bordenave, S., Lin, S., Bhaskar, I.M., Dong, X., Sensen, C.W., Fournier, J., Voordouw, G., Gieg, L.M., 2011. Carbon and sulfur cycling by microbial communities in a gypsum-treated oil sands tailings pond. Environmental science & technology 45(2), 439-446.

Ramsden, D., McKay, K., 1986a. Degradation of polyacrylamide in aqueous solution induced by chemically generated hydroxyl radicals: Part I—Fenton's reagent. Polymer degradation and stability 14(3), 217-229.

Ramsden, D., McKay, K., 1986b. The degradation of polyacrylamide in aqueous solution induced by chemically generated hydroxyl radicals: Part II—Autoxidation of Fe2+. Polymer degradation and stability 15(1), 15-31.

Rasouli, Y., Abbasi, M., Hashemifard, S.A., 2017. Investigation of in-line coagulation-MF hybrid process for oily wastewater treatment by using novel ceramic membranes. Journal of Cleaner Production 161, 545-559.

Reckhow, D.A., Legube, B., Singer, P.C., 1986. The ozonation of organic halide precursors: effect of bicarbonate. Water Research 20(8), 987-998.

Redman, A., Butler, J., Letinski, D., Di Toro, D., Paumen, M.L., Parkerton, T., 2018. Technical basis for using passive sampling as a biomimetic extraction procedure to assess bioavailability and predict toxicity of petroleum substances. Chemosphere 199, 585-594.

Rehman, K., Arslan, M., Müller, J.A., Saeed, M., Anwar, S., Islam, E., Imran, A., Amin, I., Mustafa, T., Iqbal, S., 2022. Operational parameters optimization for remediation of crude oil-polluted water in floating treatment wetlands using response surface methodology. Scientific Reports 12(1), 1-11.

Renault, F., Sancey, B., Charles, J., Morin-Crini, N., Badot, P.-M., Winterton, P., Crini, G., 2009. Chitosan flocculation of cardboard-mill secondary biological wastewater. Chemical Engineering Journal 155(3), 775-783.

Reynolds, T.D., Richards, P.A.C., 1995. Unit operations and processes in environmental engineering. PWS Publishing Company.

Rho, E., Evans, W., 1975. The aerobic metabolism of cyclohexanecarboxylic acid by Acinetobacter anitratum. Biochemical Journal 148(1), 11-15.

Risacher, F.F., Morris, P.K., Arriaga, D., Goad, C., Nelson, T.C., Slater, G.F., Warren, L.A., 2018. The interplay of methane and ammonia as key oxygen consuming constituents in early stage development of Base Mine Lake, the first demonstration oil sands pit lake. Applied Geochemistry 93, 49-59.

Romano, S., Perrone, M., Becagli, S., Pietrogrande, M., Russo, M., Caricato, R., Lionetto, M., 2020. Ecotoxicity, genotoxicity, and oxidative potential tests of atmospheric PM10 particles. Atmospheric Environment 221, 117085.

Rui, Z., Wang, X., Zhang, Z., Lu, J., Chen, G., Zhou, X., Patil, S., 2018. A realistic and integrated model for evaluating oil sands development with steam assisted gravity drainage technology in Canada. Applied Energy 213, 76-91.

Russell, C.G., Lawler, D.F., Speitel Jr, G.E., 2009a. NOM coprecipitation with solids formed during softening. Journal- American Water Works Association 101(4), 112-124.

Russell, C.G., Lawler, D.F., Speitel Jr, G.E., Katz, L.E., 2009b. Effect of softening precipitate composition and surface characteristics on natural organic matter adsorption. Environmental science & technology 43(20), 7837-7842.

Rüthi, J., Bölsterli, D., Pardi-Comensoli, L., Brunner, I., Frey, B., 2020. The "plastisphere" of biodegradable plastics is characterized by specific microbial taxa of alpine and arctic soils. Frontiers in Environmental Science 8, 562263.

Sadrzadeh, M., Hajinasiri, J., Bhattacharjee, S., Pernitsky, D., 2015. Nanofiltration of oil sands boiler feed water: Effect of pH on water flux and organic and dissolved solid rejection. Separation and Purification Technology 141, 339-353.

Sadrzadeh, M., Hajinasiri, J., Bhattacharjee, S., Pernitsky, D., 2015. Nanofiltration of oil sands boiler feed water: Effect of pH on water flux and organic and dissolved solid rejection. Separation and Purification Technology 141, 339-353. https://doi.org/10.1016/j.seppur.2014.12.011.

Sadrzadeh, M., Pernitsky, D., McGregor, M., 2018. Nanofiltration for the treatment of oil sands-produced water, Nanofiltration. InTech, pp. 25-45.

Sadrzadeh, M., Pernitsky, D., McGregor, M., 2018. Nanofiltration for the treatment of oil sands-produced water. InTech Rijeka.

Sahachaiyunta, P., Koo, T., Sheikholeslami, R., 2002. Effect of several inorganic species on silica fouling in RO membranes. Desalination 144(1-3), 373-378.

Sam-Tunsa Alarba, A., Epey, N., Nana, A., Tome, S., Mache, J.R., Nchare, M., 2022. Mineralogical and physicochemical characterization of clayey materials from Meiganga (Adamawa-Cameroon): potential application in traditional ceramic. Journal of Building Pathology and Rehabilitation 7(1), 1-12.

Samoshina, Y., Diaz, A., Becker, Y., Nylander, T., Lindman, B., 2003. Adsorption of cationic, anionic and hydrophobically modified polyacrylamides on silica surfaces. Colloids and Surfaces A: Physicochemical and Engineering Aspects 231(1-3), 195-205.

Sánchez- Osuna, M., Barbé, J., Erill, I., 2017. Comparative genomics of the DNA damage-inducible network in the Patescibacteria. Environmental Microbiology 19(9), 3465-3474.

Sang, G., Pi, Y., Bao, M., Li, Y., Lu, J., 2015. Biodegradation for hydrolyzed polyacrylamide in the anaerobic baffled reactor combined aeration tank. Ecological engineering 84, 121-127.

Sapkota, K., Oni, A.O., Kumar, A., Linwei, M., 2018. The development of a techno-economic model for the extraction, transportation, upgrading, and shipping of Canadian oil sands products to the Asia-Pacific region. Applied Energy 223, 273-292.

Schindler, D., Donahue, W., Thompson, J., 2007. Running out of Steam? Oil Sands Development and Water Use in the Athabasca River Watershed: Science and Market based Solutions.

Scott, A.C., Mackinnon, M.D., Fedorak, P.M., 2005. Naphthenic acids in Athabasca oil sands tailings waters are less biodegradable than commercial naphthenic acids. Environmental science & technology 39(21), 8388-8394.

Seright, R., Skjevrak, I., 2015. Effect of dissolved iron and oxygen on stability of hydrolyzed polyacrylamide polymers. SPE journal 20(03), 433-441.

Seybold, C., 1994. Polyacrylamide review: Soil conditioning and environmental fate. Communications in soil science and plant analysis 25(11-12), 2171-2185.

Shamaei, L., Khorshidi, B., Perdicakis, B., Sadrzadeh, M., 2018. Treatment of oil sands produced water using combined electrocoagulation and chemical coagulation techniques. Science of the Total Environment 645, 560-572.

Sharma, B., Dhuldhoya, N., Merchant, U., 2006. Flocculants—an ecofriendly approach. Journal of Polymers and the Environment 14(2), 195-202.

Sheikholeslami, R., Tan, S., 1999. Effects of water quality on silica fouling of desalination plants. Desalination 126(1-3), 267-280.

Shi, Y., Huang, C., Rocha, K.C., Gamal El-Din, M., Liu, Y., 2015. Treatment of oil sands process-affected water using moving bed biofilm reactors: with and without ozone pretreatment. Bioresource technology 192, 219-227.

Siddique, T., Penner, T., Klassen, J., Nesbø, C., Foght, J.M., 2012. Microbial communities involved in methane production from hydrocarbons in oil sands tailings. Environmental science & technology 46(17), 9802-9810.

Sillanpaa, M., Ncibi, M.C., Matilainen, A., Vepsalainen, M., 2018. Removal of natural organic matter in drinking water treatment by coagulation: A comprehensive review. Chemosphere 190, 54-71. https://doi.org/10.1016/j.chemosphere.2017.09.113.

Smith, D.F., Schaub, T.M., Kim, S., Rodgers, R.P., Rahimi, P., Teclemariam, A., Marshall, A.G., 2008. Characterization of acidic species in Athabasca bitumen and bitumen heavy vacuum gas oil by negative-ion ESI FT− ICR MS with and without acid− Ion exchange resin prefractionation. Energy & Fuels 22(4), 2372-2378.

Smith, E.A., Prues, S.L., Oehme, F.W., 1996. Environmental degradation of polyacrylamides. 1. Effects of artificial environmental conditions: temperature, light, and pH. Ecotoxicology and Environmental Safety 35(2), 121-135.

Song, W., Zhang, Y., Gao, Y., Chen, D., Yang, M., 2017. Cleavage of the main carbon chain backbone of high molecular weight polyacrylamide by aerobic and anaerobic biological treatment. Chemosphere 189, 277-283.

Sposito, G., 2008. The chemistry of soils. Oxford university press.

Srivastava, S., Saxena, K., Brighu, U., Gupta, A.B., 2022. Comparative evaluation of pilot-scale reactors based on pulsating floc blanket clarification and conventional clariflocculation technologies in simultaneous treatment of natural organic matter and turbidity. Water Supply 22(8), 6945-6958.

St-Pierre, B., Wright, A.-D.G., 2014. Comparative metagenomic analysis of bacterial populations in three full-scale mesophilic anaerobic manure digesters. Applied microbiology and biotechnology 98, 2709-2717.

Strous, M., Fuerst, J.A., Kramer, E.H., Logemann, S., Muyzer, G., van de Pas-Schoonen, K.T., Webb, R., Kuenen, J.G., Jetten, M.S., 1999. Missing lithotroph identified as new planctomycete. Nature 400(6743), 446-449.

Stumm, W., Morgan, J., 1992. Surface charge and the electric double layer. Chemistry of the Solid±Water Interface.

Sun, M., Qiao, M.-X., Wang, J., Zhai, L.-F., 2017. Free-radical induced chain degradation of high-molecular-weight polyacrylamide in a heterogeneous electro-Fenton system. ACS Sustainable Chemistry & Engineering 5(9), 7832-7839.

Sun, Y., Zhang, S., Jin, B., Cheng, S., 2021. Efficient degradation of polyacrylamide using a 3-dimensional ultra-thin SnO2-Sb coated electrode. Journal of Hazardous Materials 416, 125907.

Sun, Y., Zhu, C., Zheng, H., Sun, W., Xu, Y., Xiao, X., You, Z., Liu, C., 2017. Characterization and coagulation behavior of polymeric aluminum ferric silicate for high-concentration oily wastewater treatment. Chemical Engineering Research and Design 119, 23-32.

Suopajärvi, T., 2015. Functionalized nanocelluloses in wastewater treatment applications. Acta Universitatis Ouluensis C, 526.

Swigert, J.P., Lee, C., Wong, D.C., White, R., Scarlett, A.G., West, C.E., Rowland, S.J., 2015. Aquatic hazard assessment of a commercial sample of naphthenic acids. Chemosphere 124, 1-9.

Thijs, S., Op De Beeck, M., Beckers, B., Truyens, S., Stevens, V., Van Hamme, J.D., Weyens, N., Vangronsveld, J., 2017. Comparative evaluation of four bacteria-specific primer pairs for 16S rRNA gene surveys. Frontiers in microbiology 8, 494.

Toor, N.S., Franz, E.D., Fedorak, P.M., MacKinnon, M.D., Liber, K., 2013. Degradation and aquatic toxicity of naphthenic acids in oil sands process-affected waters using simulated wetlands. Chemosphere 90(2), 449-458.

Ulgut, B., Suzer, S., 2003. XPS studies of SiO2/Si system under external bias. The Journal of Physical Chemistry B 107(13), 2939-2943.

Usman, M., Hao, S., Chen, H., Ren, S., Tsang, D.C., Sompong, O., Luo, G., Zhang, S., 2019. Molecular and microbial insights towards understanding the anaerobic digestion of the wastewater from hydrothermal liquefaction of sewage sludge facilitated by granular activated carbon (GAC). Environment international 133, 105257.

Vajihinejad, V., Gumfekar, S.P., Dixon, D.V., Silva, M.A., Soares, J.B., 2021. Enhanced dewatering of oil sands tailings by a novel water-soluble cationic polymer. Separation and Purification Technology 260, 118183.

Van Aken, P., Van den Broeck, R., Degrève, J., Dewil, R., 2017. A pilot-scale coupling of ozonation and biodegradation of 2, 4-dichlorophenol-containing wastewater: The effect of biomass acclimation towards chlorophenol and intermediate ozonation products. Journal of Cleaner Production 161, 1432-1441.

Van Loon, W.M., Verwoerd, M.E., Wijnker, F.G., vAN LEEUwEN, C.J., van Duyn, P., van deGuchte, C., Hermens, J.L., 1997. Estimating total body residues and baseline toxicity of complex organic mixtures in effluents and surface waters. Environmental Toxicology and Chemistry: An International Journal 16(7), 1358-1365.

Vandamme, D., Foubert, I., Fraeye, I., Meesschaert, B., Muylaert, K., 2012. Flocculation of Chlorella vulgaris induced by high pH: role of magnesium and calcium and practical implications. Bioresource technology 105, 114-119.

Vedoy, D.R., Soares, J.B., 2015. Water- soluble polymers for oil sands tailing treatment: A Review. The Canadian Journal of Chemical Engineering 93(5), 888-904.

Veksha, A., Bhuiyan, T.I., Hill, J.M., 2016. Activation of aspen wood with carbon dioxide and phosphoric acid for removal of total organic carbon from oil sands produced water: Increasing the yield with bio-oil recycling. Materials 9(1), 20.

Verbruggen, E.M., Vaes, W.H., Parkerton, T.F., Hermens, J.L., 2000. Polyacrylate-coated SPME fibers as a tool to simulate body residues and target concentrations of complex organic mixtures for estimation of baseline toxicity. Environmental science & technology 34(2), 324-331.

Viggor, S., Juhanson, J., Jõesaar, M., Mitt, M., Truu, J., Vedler, E., Heinaru, A., 2013. Dynamic changes in the structure of microbial communities in Baltic Sea coastal seawater microcosms modified by crude oil, shale oil or diesel fuel. Microbiological research 168(7), 415-427.

Wang, B., Teng, Y., Xu, Y., Chen, W., Ren, W., Li, Y., Christie, P., Luo, Y., 2018. Effect of mixed soil microbiomes on pyrene removal and the response of the soil microorganisms. Science of the Total Environment 640, 9-17.

Wang, C., Guan, X., Yuan, Y., Wu, Y., Tan, S., 2019. Polyacrylamide crosslinked by bis-vinylimidazolium bromide for high elastic and stable hydrogels. RSC Advances 9(47), 27640-27645.

Wang, C., Han, C., Lin, Z., Masliyah, J., Liu, Q., Xu, Z., 2016. Role of preconditioning cationic zetag flocculant in enhancing mature fine tailings flocculation. Energy & Fuels 30(7), 5223-5231.

Wang, D., Liu, X., Zeng, G., Zhao, J., Liu, Y., Wang, Q., Chen, F., Li, X., Yang, Q., 2018. Understanding the impact of cationic polyacrylamide on anaerobic digestion of waste activated sludge. Water research 130, 281-290.

Wang, N., Chelme-Ayala, P., Perez-Estrada, L., Garcia-Garcia, E., Pun, J., Martin, J.W., Belosevic, M., Gamal El-Din, M., 2013. Impact of ozonation on naphthenic acids speciation and toxicity of oil sands process-affected water to Vibrio fischeri and mammalian immune system. Environmental science & technology 47(12), 6518-6526.

Wang, X., 2016. Review of characterization methods for water-soluble polymers used in oil sand and heavy oil industrial applications. Environmental Reviews 24(4), 460-470.

Wen, Q., Chen, Z., Zhao, Y., Zhang, H., Feng, Y., 2010. Biodegradation of polyacrylamide by bacteria isolated from activated sludge and oil-contaminated soil. Journal of Hazardous Materials 175(1-3), 955-959.

Wen, Q., Chen, Z., Zhao, Y., Zhang, H., Feng, Y., 2011. Performance and microbial characteristics of bioaugmentation systems for polyacrylamide degradation. Journal of Polymers and the Environment 19(1), 125-132.

Westerholm, M., Liu, T., Schnürer, A., 2020. Comparative study of industrial-scale high-solid biogas production from food waste: Process operation and microbiology. Bioresource technology 304, 122981.

Whale, G., Hjort, M., Di Paolo, C., Redman, A., Postma, J., Legradi, J., Leonards, P., 2022. Assessment of oil refinery wastewater and effluent integrating bioassays, mechanistic modelling and bioavailability evaluation. Chemosphere 287, 132146.

Wilén, B.-M., Balmer, P., 1999. The effect of dissolved oxygen concentration on the structure, size and size distribution of activated sludge flocs. Water research 33(2), 391-400.

Williams, P.A., 2008. Handbook of industrial water soluble polymers. John Wiley & Sons.

Wills, B.A., Finch, J., 2015. Wills' mineral processing technology: an introduction to the practical aspects of ore treatment and mineral recovery. Butterworth-Heinemann.

Wiseman, S., Anderson, J., Liber, K., Giesy, J., 2013. Endocrine disruption and oxidative stress in larvae of Chironomus dilutus following short-term exposure to fresh or aged oil sands process-affected water. Aquatic Toxicology 142, 414-421.

Wiśniewska, M., 2012. The temperature effect on the adsorption mechanism of polyacrylamide on the silica surface and its stability. Applied Surface Science 258(7), 3094-3101.

Woodrow, J.E., Seiber, J.N., Miller, G.C., 2008. Acrylamide release resulting from sunlight irradiation of aqueous polyacrylamide/iron mixtures. Journal of Agricultural and Food Chemistry 56(8), 2773-2779.

Wu, C., De Visscher, A., Gates, I.D., 2019. On naphthenic acids removal from crude oil and oil sands process-affected water. Fuel 253, 1229-1246. https://doi.org/10.1016/j.fuel.2019.05.091.

Wu, M., Yu, W., Qu, J., Gregory, J., 2019. The variation of flocs activity during floc breakage and aging, adsorbing phosphate, humic acid and clay particles. Water research 155, 131-141.

Xiao, D., Cheng, J., Liang, W., Sun, L., Zhao, J., 2021. Metal-phenolic coated and prochloraz-loaded calcium carbonate carriers with pH responsiveness for environmentally-safe fungicide delivery. Chemical Engineering Journal 418, 129274.

Xiong, B., Loss, R.D., Shields, D., Pawlik, T., Hochreiter, R., Zydney, A.L., Kumar, M., 2018a. Polyacrylamide degradation and its implications in environmental systems. NPJ Clean Water 1(1), 1-9.

Xiong, B., Miller, Z., Roman-White, S., Tasker, T., Farina, B., Piechowicz, B., Burgos, W.D., Joshi, P., Zhu, L., Gorski, C.A., 2018b. Chemical degradation of polyacrylamide during hydraulic fracturing. Environmental science & technology 52(1), 327-336.

Xiong, B., Purswani, P., Pawlik, T., Samineni, L., Karpyn, Z.T., Zydney, A.L., Kumar, M., 2020. Mechanical degradation of polyacrylamide at ultra high deformation rates during hydraulic fracturing. Environmental Science: Water Research & Technology 6(1), 166-172.

Xue, J., Huang, C., Zhang, Y., Liu, Y., Gamal El-Din, M., 2018. Bioreactors for oil sands process-affected water (OSPW) treatment: A critical review. Science of the Total Environment 627, 916-933.

Xue, J., Zhang, Y., Liu, Y., Gamal El-Din, M., 2016. Treatment of oil sands process-affected water (OSPW) using a membrane bioreactor with a submerged flat-sheet ceramic microfiltration membrane. Water research 88, 1-11.

Xue, J., Zhang, Y., Liu, Y., Gamal El-Din, M., 2017. Dynamics of naphthenic acids and microbial community structures in a membrane bioreactor treating oil sands process-affected water: impacts of supplemented inorganic nitrogen and hydraulic retention time. RSC advances 7(29), 17670-17681.

Yan, M., Zhao, L., Bao, M., Lu, J., 2016. Hydrolyzed polyacrylamide biodegradation and mechanism in sequencing batch biofilm reactor. Bioresource Technology 207, 315-321.

Yergeau, E., Lawrence, J.R., Sanschagrin, S., Waiser, M.J., Korber, D.R., Greer, C.W., 2012. Next-generation sequencing of microbial communities in the Athabasca River and its tributaries in relation to oil sands mining activities. Applied and environmental microbiology 78(21), 7626-7637.

Yousefzadeh, S., Ahmadi, E., Gholami, M., Ghaffari, H.R., Azari, A., Ansari, M., Miri, M., Sharafi, K., Rezaei, S., 2017. A comparative study of anaerobic fixed film baffled reactor and up-flow anaerobic fixed film fixed bed reactor for biological removal of diethyl phthalate from

wastewater: a performance, kinetic, biogas, and metabolic pathway study. Biotechnology for biofuels 10(1), 1-15.

Yu, F., Fu, R., Xie, Y., Chen, W., 2015. Isolation and characterization of polyacrylamide-degrading bacteria from dewatered sludge. International journal of environmental research and public health 12(4), 4214-4230.

Yu, W.-z., Gregory, J., Campos, L., Li, G., 2011. The role of mixing conditions on floc growth, breakage and re-growth. Chemical Engineering Journal 171(2), 425-430.

Yue, S., Ramsay, B.A., Wang, J., Ramsay, J.A., 2016. Biodegradation and detoxification of naphthenic acids in oil sands process affected waters. Science of the Total Environment 572, 273-279.

Zaman, A.A., Tsuchiya, R., Moudgil, B.M., 2002. Adsorption of a low-molecular-weight polyacrylic acid on silica, alumina, and kaolin. Journal of Colloid and Interface Science 256(1), 73-78.

Zamora, R., Delgado, R.M., Hidalgo, F.J., 2015. Use of nucleophilic compounds, and their combination, for acrylamide removal. Acrylamide in food: analysis, content and potential health effects, 297-307.

Zeng, H., Tang, H., Sun, W., Wang, L., 2022. Strengthening Solid–liquid Separation of Bauxite Residue through the Synergy of Charge Neutralization and Flocculation. Separation and Purification Technology 285, 120296.

Zeng, T., Li, R.J., Mitch, W.A., 2016. Structural modifications to quaternary ammonium polymer coagulants to inhibit N-nitrosamine formation. Environmental Science & Technology 50(9), 4778-4787.

Zeng, Y., Yang, C., Pu, W., Zhang, X., 2007a. Removal of silica from heavy oil wastewater to be reused in a boiler by combining magnesium and zinc compounds with coagulation. Desalination 216(1-3), 147-159.

Zeng, Y., Yang, C., Zhang, J., Pu, W., 2007. Feasibility investigation of oily wastewater treatment by combination of zinc and PAM in coagulation/flocculation. Journal of hazardous materials 147(3), 991-996.

Zeng, Y., Yang, C., Zhang, J., Pu, W., 2007b. Feasibility investigation of oily wastewater treatment by combination of zinc and PAM in coagulation/flocculation. J Hazard Mater 147(3), 991-996. https://doi.org/10.1016/j.jhazmat.2007.01.129.

Zhang, D., Abraham, T., Dang-Vu, T., Xu, J., Gumfekar, S.P., Thundat, T., 2021. Optimal floc structure for effective dewatering of polymer treated oil sands tailings. Minerals Engineering 160, 106688.

Zhang, K., Pernitsky, D., Jafari, M., Lu, Q., 2021. Effect of MgO slaking on silica removal during warm lime softening of SAGD produced water. Industrial & Engineering Chemistry Research 60(4), 1839-1849.

Zhang, K., Pernitsky, D., Jafari, M., Lu, Q., 2021. Effect of MgO Slaking on Silica Removal during Warm Lime Softening of SAGD Produced Water. Industrial & Engineering Chemistry Research.

Zhang, K., Pernitsky, D., Jafari, M., Lu, Q., 2021a. Effect of MgO slaking on silica removal during warm lime softening of SAGD produced water. Industrial & Engineering Chemistry Research 60(4), 1839-1849.

Zhang, L., Graham, N., Kimura, K., Li, G., Yu, W., 2022. Targeting membrane fouling with low dose oxidant in drinking water treatment: Beneficial effect and biological mechanism. Water Research 209, 117953.

Zhang, L., Mishra, D., Zhang, K., Perdicakis, B., Pernitsky, D., Lu, Q., 2020. Electrokinetic study of calcium carbonate and magnesium hydroxide particles in lime softening. Water Research 186, 116415.

Zhang, L., Mishra, D., Zhang, K., Perdicakis, B., Pernitsky, D., Lu, Q., 2021. Impact of influent deviations on polymer coagulant dose in warm lime softening of synthetic SAGD produced water. Water Research 200, 117202.

Zhang, L., Mishra, D., Zhang, K., Perdicakis, B., Pernitsky, D., Lu, Q., 2021b. Impact of influent deviations on polymer coagulant dose in warm lime softening of synthetic SAGD produced water. Water Research 200, 117202.

Zhang, L., Zhang, Y., Gamal El-Din, M., 2019. Integrated mild ozonation with biofiltration can effectively enhance the removal of naphthenic acids from hydrocarbon-contaminated water. Science of the Total Environment 678, 197-206.

Zhang, L., Zhang, Y., Patterson, J., Arslan, M., Zhang, Y., Gamal El-Din, M., 2020. Biofiltration of oil sands process water in fixed-bed biofilm reactors shapes microbial community structure for enhanced degradation of naphthenic acids. Science of the Total Environment 718, 137028.

Zhang, P., Shen, Y., Guo, J.-S., Li, C., Wang, H., Chen, Y.-P., Yan, P., Yang, J.-X., Fang, F., 2015. Extracellular protein analysis of activated sludge and their functions in wastewater treatment plant by shotgun proteomics. Scientific reports 5(1), 12041.

Zhang, Q., Yan, Z., Ouyang, J., Zhang, Y., Yang, H., Chen, D., 2018. Chemically modified kaolinite nanolayers for the removal of organic pollutants. Applied clay science 157, 283-290.

Zhang, Y., Chelme-Ayala, P., Klamerth, N., Gamal El-Din, M., 2017. Application of UV-irradiated Fe (III)-nitrilotriacetic acid (UV-Fe (III) NTA) and UV-NTA-Fenton systems to degrade model and natural occurring naphthenic acids. Chemosphere 179, 359-366.

Zhang, Y., Xue, J., Liu, Y., Gamal El-Din, M., 2016. Treatment of oil sands process-affected water using membrane bioreactor coupled with ozonation: A comparative study. Chemical Engineering Journal 302, 485-497.

Zhao, F., Ma, F., Shi, R., Zhang, J., Han, S., Zhang, Y., 2015. Production of rhamnolipids by Pseudomonas aeruginosa is inhibited by H 2 S but resumes in a co-culture with P. stutzeri: applications for microbial enhanced oil recovery. Biotechnology letters 37, 1803-1808.

Zhao, L., Bao, M., Yan, M., Lu, J., 2016. Kinetics and thermodynamics of biodegradation of hydrolyzed polyacrylamide under anaerobic and aerobic conditions. Bioresource Technology 216, 95-104.

Zhao, L., Ma, T., Gao, M., Gao, P., Cao, M., Zhu, X., Li, G., 2012. Characterization of microbial diversity and community in water flooding oil reservoirs in China. World Journal of Microbiology and Biotechnology 28, 3039-3052.

Zhao, L., Song, T., Han, D., Bao, M., Lu, J., 2019. Hydrolyzed polyacrylamide biotransformation in an up-flow anaerobic sludge blanket reactor system: key enzymes, functional microorganisms, and biodegradation mechanisms. Bioprocess and biosystems engineering 42, 941-951.

Zhao, N., Al Bitar, H., Zhu, Y., Xu, Y., Shi, Z., 2018. Flocculation performance of anionic starch in oil sand tailings. Water Science and Technology 78(6), 1268-1275.

Zhao, P., Geng, T., Zhao, Y., Tian, Y., Li, J., Zhang, H., Zhao, W., 2021. Removal of Cu (Ⅱ) ions from aqueous solution by a magnetic multi-wall carbon nanotube adsorbent. Chemical Engineering Journal Advances 8, 100184.

288

Zheng, H., Feng, L., Gao, B., Zhou, Y., Zhang, S., Xu, B., 2017. Effect of the cationic block structure on the characteristics of sludge flocs formed by charge neutralization and patching. Materials 10(5), 487.

Zhou, C., Lee, S., Dooley, K., Wu, Q., 2013. A facile approach to fabricate porous nanocomposite gels based on partially hydrolyzed polyacrylamide and cellulose nanocrystals for adsorbing methylene blue at low concentrations. Journal of Hazardous Materials 263, 334-341.

Zhou, S., Bu, X., Alheshibri, M., Zhan, H., Xie, G., 2022. Floc structure and dewatering performance of kaolin treated with cationic polyacrylamide degraded by hydrodynamic cavitation. Chemical Engineering Communications 209(6), 798-807.

Zhou, Z., Yang, Y., Li, X., Gao, W., Liang, H., Li, G., 2012. Coagulation efficiency and flocs characteristics of recycling sludge during treatment of low temperature and micro-polluted water. Journal of Environmental Sciences 24(6), 1014-1020.

Zhu, G., Zheng, H., Chen, W., Fan, W., Zhang, P., Tshukudu, T., 2012. Preparation of a composite coagulant: Polymeric aluminum ferric sulfate (PAFS) for wastewater treatment. Desalination 285, 315-323.

Appendix A

A-1. Permission of copyright

Chapter 2

Treatment Technologies for Organics and Silica Removal in Steam-Assisted Gravity Drainage Produced Water: A Comprehensive Review

ACS Publications
Most Trusted. Most Cited. Most Read.

Author: Jia Li, Zuo Tong How, Hongbo Zeng, et al

Publication: Energy & Fuels

Publisher: American Chemical Society

Date: Feb 1, 2022

Copyright © 2022, American Chemical Society

Fig. 2.1

Fig.2.5

License Number	5494590394155
License date	Feb 23, 2023
Licensed Content Publisher	Elsevier
Licensed Content Publication	Elsevier Books
Licensed Content Title	Wills' Mineral Processing Technology
Licensed Content Author	Barry A. Wills,James A. Finch
Licensed Content Date	Jan 1, 2016
Licensed Content Pages	22
Start Page	417
End Page	438
Type of Use	reuse in a thesis/dissertation
Portion	figures/tables/illustrations
Number of figures/tables/illustrations	1
Format	both print and electronic
Are you the author of this Elsevier chapter?	No
Will you be translating?	No
Title	Fate of Polymer-Based Coagulants/Flocculants in Oil and Gas Wastewater Treatment
Institution name	University of Alberta
Expected presentation date	Apr 2023
Order reference number	3
Portions	Figure 6

SPRINGER NATURE LICENSE
TERMS AND CONDITIONS

Feb 23, 2023

This Agreement between Miss. JIA LI ("You") and Springer Nature ("Springer Nature") consists of your license details and the terms and conditions provided by Springer Nature and Copyright Clearance Center.

License Number	5494590651895
License date	Feb 23, 2023
Licensed Content Publisher	Springer Nature
Licensed Content Publication	Journal of Polymers and the Environment
Licensed Content Title	Flocculants—an Ecofriendly Approach
Licensed Content Author	B. R. Sharma et al
Licensed Content Date	May 4, 2006
Type of Use	Thesis/Dissertation
Requestor type	academic/university or research institute
Format	print and electronic
Portion	figures/tables/illustrations
Number of figures/tables/illustrations	1
Will you be translating?	no
Circulation/distribution	1 - 29
Author of this Springer Nature content	no
Title	Fate of Polymer-Based Coagulants/Flocculants in Oil and Gas Wastewater Treatment
Institution name	University of Alberta
Expected presentation date	Apr 2023
Order reference number	4
Portions	Figure.2

4. STM Permission Guidelines

4. 1. An alternative scope of license may apply to signatories of the STM Permissions Guidelines ("STM PG") as amended from time to time and made available at https://www.stm-assoc.org/intellectual-property/permissions/permissions-guidelines/.

4. 2. For content reuse requests that qualify for permission under the STM PG, and which may be updated from time to time, the STM PG supersede the terms and conditions contained in this License.

4. 3. If a License has been granted under the STM PG, but the STM PG no longer apply at the time of publication, further permission must be sought from the Rightsholder. Contact journalpermissions@springernature.com or bookpermissions@springernature.com for these rights.

5. Duration of License

5. 1. Unless otherwise indicated on your License, a License is valid from the date of purchase ("License Date") until the end of the relevant period in the below table:

Reuse in a medical communications project	Reuse up to distribution or time period indicated in License
Reuse in a dissertation/thesis	Lifetime of thesis
Reuse in a journal/magazine	Lifetime of journal/magazine
Reuse in a book/textbook	Lifetime of edition
Reuse on a website	1 year unless otherwise specified in the License
Reuse in a presentation/slide kit/poster	Lifetime of presentation/slide kit/poster. Note: publication whether electronic or in print of presentation/slide kit/poster may require further permission.
Reuse in conference proceedings	Lifetime of conference proceedings
Reuse in an annual report	Lifetime of annual report
Reuse in training/CME materials	Reuse up to distribution or time period indicated in License
Reuse in newsmedia	Lifetime of newsmedia
Reuse in coursepack/classroom materials	Reuse up to distribution and/or time period indicated in license

6. Acknowledgement

6. 1. The Licensor's permission must be acknowledged next to the Licensed Material in print. In electronic form, this acknowledgement must be visible at the same time as the figures/tables/illustrations or abstract and must be hyperlinked to the journal/book's homepage.

6. 2. Acknowledgement may be provided according to any standard referencing system and at a minimum should include "Author, Article/Book Title, Journal name/Book imprint, volume, page number, year, Springer Nature".

7. Reuse in a dissertation or thesis

7. 1. Where 'reuse in a dissertation/thesis' has been selected, the following terms apply: Print rights of the Version of Record are provided for; electronic rights for use only on institutional repository as defined by the Sherpa guideline (www.sherpa.ac.uk/romeo/) and only up to what is required by the awarding institution.

7. 2. For theses published under an ISBN or ISSN, separate permission is required. Please contact journalpermissions@springernature.com or bookpermissions@springernature.com for these rights.

7. 3. Authors must properly cite the published manuscript in their thesis according to current citation standards and include the following acknowledgement: '*Reproduced with permission from Springer Nature*'.

8. License Fee

You must pay the fee set forth in the License Agreement (the "License Fees"). All amounts payable by you under this License are exclusive of any sales, use, withholding, value added or similar taxes, government fees or levies or other assessments. Collection and/or remittance of such taxes to the relevant tax authority shall be the responsibility of the party who has the legal obligation to do so.

9. Warranty

9. 1. The Licensor warrants that it has, to the best of its knowledge, the rights to license reuse of the Licensed Material. **You are solely responsible for ensuring that the material you wish to license is original to the Licensor and does not carry the copyright of another entity or third party (as credited in the published version).** If the credit line on any part of the Licensed Material indicates that it was reprinted or adapted with permission from another source, then you should seek additional permission from that source to reuse the material.

9. 2. EXCEPT FOR THE EXPRESS WARRANTY STATED HEREIN AND TO THE EXTENT PERMITTED BY APPLICABLE LAW, LICENSOR PROVIDES THE LICENSED MATERIAL "AS IS" AND MAKES NO OTHER REPRESENTATION OR WARRANTY. LICENSOR EXPRESSLY DISCLAIMS ANY LIABILITY FOR ANY CLAIM ARISING FROM OR OUT OF THE CONTENT, INCLUDING BUT NOT LIMITED TO ANY ERRORS, INACCURACIES, OMISSIONS, OR DEFECTS CONTAINED THEREIN, AND ANY IMPLIED OR EXPRESS WARRANTY AS TO MERCHANTABILITY OR FITNESS FOR A PARTICULAR PURPOSE. IN NO EVENT SHALL LICENSOR BE LIABLE TO YOU OR ANY OTHER PARTY OR ANY OTHER PERSON OR FOR ANY SPECIAL, CONSEQUENTIAL, INCIDENTAL, INDIRECT, PUNITIVE, OR EXEMPLARY DAMAGES, HOWEVER CAUSED, ARISING OUT OF OR IN CONNECTION WITH THE DOWNLOADING, VIEWING OR USE OF THE LICENSED MATERIAL REGARDLESS OF THE FORM OF ACTION, WHETHER FOR BREACH OF CONTRACT, BREACH OF WARRANTY, TORT, NEGLIGENCE, INFRINGEMENT OR OTHERWISE (INCLUDING, WITHOUT LIMITATION, DAMAGES BASED ON LOSS OF PROFITS, DATA, FILES, USE, BUSINESS OPPORTUNITY OR CLAIMS OF THIRD PARTIES), AND WHETHER OR NOT THE PARTY HAS BEEN ADVISED OF THE POSSIBILITY OF SUCH DAMAGES. THIS LIMITATION APPLIES NOTWITHSTANDING ANY FAILURE OF ESSENTIAL PURPOSE OF ANY LIMITED REMEDY PROVIDED HEREIN.

10. Termination and Cancellation

10. 1. The License and all rights granted hereunder will continue until the end of the applicable period shown in Clause 5.1 above. Thereafter, this license will be terminated and all rights granted hereunder will cease.

10. 2. Licensor reserves the right to terminate the License in the event that payment is not received in full or if you breach the terms of this License.

11. General

11. 1. The License and the rights and obligations of the parties hereto shall be construed, interpreted and determined in accordance with the laws of the Federal Republic of Germany without reference to the stipulations of the CISG (United Nations Convention on Contracts for the International Sale of Goods) or to Germany's choice-of-law principle.

11. 2. The parties acknowledge and agree that any controversies and disputes arising out of this License shall be decided exclusively by the courts of or having jurisdiction for Heidelberg, Germany, as far as legally permissible.

11. 3. This License is solely for Licensor's and Licensee's benefit. It is not for the benefit of any other person or entity.

Questions? For questions on Copyright Clearance Center accounts or website issues please contact springernaturesupport@copyright.com or +1-855-239-3415 (toll free in the US) or +1-978-646-2777. For questions on Springer Nature licensing please visit https://www.springernature.com/gp/partners/rights-permissions-third-party-distribution

Other Conditions:

Version 1.4 - Dec 2022

Questions? customercare@copyright.com.

Chapter 3

Removal of colloidal impurities by thermal softening-coagulation-flocculation-sedimentation in steam assisted gravity drainage (SAGD) produced water: Performance, interaction effects and mechanism study

Author:
Jia Li,Zuo Tong How,Chelsea Benally,Yongxiang Sun,Hongbo Zeng,Mohamed Gamal El-Din

Publication: Separation and Purification Technology

Publisher: Elsevier

Date: 15 May 2023

Journal Author Rights

BACK   CLOSE WINDOW

Chapter 5

Aerobic degradation of anionic polyacrylamide in oil sands tailings: Impact factor, degradation effect, and mechanism

Author: Jia Li,Zuo Tong How,Mohamed Gamal El-Din

Publication: Science of The Total Environment

Publisher: Elsevier

Date: 15 January 2023

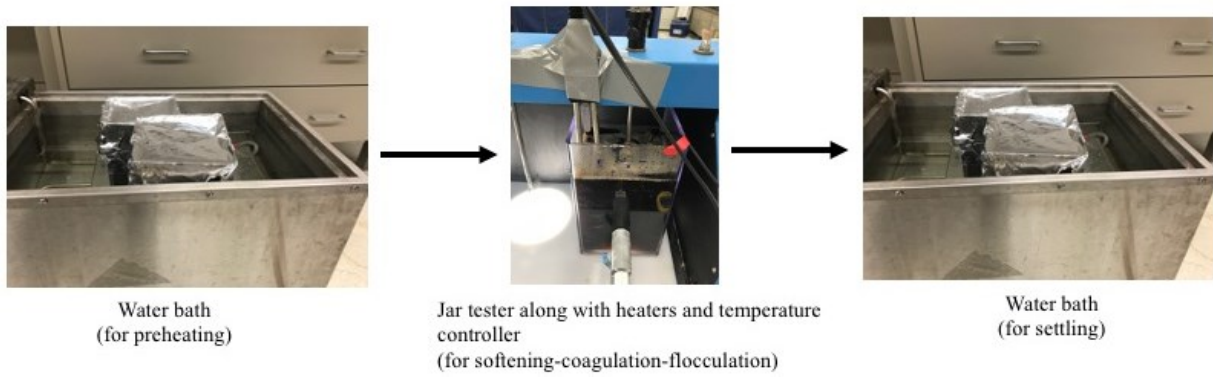**Journal Author Rights**

BACK   CLOSE WINDOW

Figure A.1 Setup for jar tests under high temperature.

Table A.1 RSM experimental design along with observed and predicated responses values.

Run	Poly-DADMAC dose (x₁)	Mixing time with softeners only (x₂)	Coagulation speed (x₃)	Flocculation time (x₄)	Turbidity removal %		TSS removal %		Particulate hardness removal %		Silica removal %		TOC removal %		TIC removal %		SVI mL/g	
	x_1	x_2	x_3	x_4	Experimental	Predicted	Experimental	Predicted	Experimental	Predicted	Experimental	Predicted	Experimental	Predicted	Experimental	Predicted	Experimental	Predicted
1	0	0	0	2	97.45	98.18	97.42	98.17	98.65	98.99	22.05	21.24	70.91	70.34	28.11	29.05	37.49	37.43
2	0	0	0	2	98.39	98.18	98.15	98.17	99.28	98.99	21.39	21.24	70.01	70.34	28.09	29.05	36.76	37.43
3	1	1	1	1	98.87	98.70	98.52	98.77	99.45	99.29	28.13	29.41	70.38	72.83	30.61	30.85	39.33	36.30
4	-1	1	1	1	99.55	99.17	99.15	99.29	99.16	99.40	25.77	25.55	65.66	65.03	30.18	30.54	39.55	39.12
5	1	-1	1	1	96.6	96.81	96.15	95.40	98.84	98.50	14.8	15.93	77.93	77.46	32.83	31.18	35.26	33.76
6	-1	-1	1	1	99.02	99.32	98.52	98.26	98.42	98.61	19.68	18.95	70.73	69.66	31.44	30.87	30.36	32.26
7	1	1	-1	1	98.33	97.95	98.15	97.23	99.29	99.53	26.1	25.62	75.87	75.96	31.74	32.81	37.61	40.61
8	-1	1	-1	1	98.78	98.41	98.15	97.75	99.53	99.64	17.07	16.60	69.12	68.16	25.61	24.03	43.54	43.43
9	1	-1	-1	1	94.38	94.63	93.26	93.87	97.45	97.21	17.67	17.46	75.03	73.75	32.96	33.14	39.1	38.07
10	-1	-1	-1	1	97.52	97.14	97.05	96.72	97.81	97.32	15.03	15.32	65.82	65.95	24.89	24.36	38.21	36.57
11	0	0	2	0	99.42	99.84	99.63	99.49	99.83	99.57	23.12	22.73	72.89	73.08	29.17	29.07	32.94	34.61
12	0	0	2	0	99.44	99.84	99.52	99.49	99.32	99.57	22.87	22.73	72.92	73.08	28.94	29.07	33.77	34.61
13	0	2	0	0	98.7	98.76	98.42	98.11	98.87	98.78	25.7	25.93	71.11	71.58	29.22	28.47	40.83	38.65
14	0	2	0	0	98.54	98.76	98.15	98.11	99.19	98.78	25.38	25.93	71.83	71.58	27.54	28.47	37.45	38.65
15	2	0	0	0	95.43	96.06	93.73	94.22	99.79	99.47	19.29	19.89	75.68	75.87	34.6	33.53	34.93	35.05
16	2	0	0	0	96.51	96.06	94.04	94.22	99.77	99.47	19.74	19.89	75.75	75.87	32.98	33.53	33.54	35.05
17	0	0	0	0	99.17	98.37	96.68	95.91	98.96	99.58	16.03	16.89	71	72.79	30.86	30.38	39.24	38.83
18	0	0	0	0	98.99	98.37	96.31	95.91	99.87	99.58	15.44	16.89	71.74	72.79	29.51	30.38	39.58	38.83
19	0	0	0	0	98.51	98.37	96.1	95.91	99.47	99.58	17.49	16.89	70.48	72.79	30.55	30.38	38.75	38.83
20	0	0	0	0	97.89	98.37	95	95.91	99.26	99.58	17.97	16.89	75.56	72.79	31.28	30.38	36.88	38.83
21	-2	0	0	0	98.89	99.02	98.68	97.60	99.57	99.69	15.55	13.89	59.15	60.27	29.76	30.44	42.65	42.61
22	-2	0	0	0	99.22	99.02	97.15	97.60	99.66	99.69	12.4	13.89	59.5	60.27	29.5	30.44	43.27	42.61
23	0	-2	0	0	96.2	95.60	92.83	93.71	96.07	96.53	16.43	18.33	74.52	74.00	28.4	29.13	26.8	29.25
24	0	-2	0	0	95.16	95.60	93.73	93.71	96.18	96.53	19.82	18.33	72.59	74.00	28.94	29.13	28.96	29.25
25	0	0	-2	0	97.27	96.90	95.88	96.42	96.34	96.58	21.1	21.62	72.37	72.50	31.76	31.69	36.05	36.15
26	0	0	-2	0	96.35	96.90	96.73	96.42	96.52	96.58	20.29	21.62	71.93	72.50	32.33	31.69	36.98	36.15
27	1	1	1	-1	98.73	98.90	97.41	98.07	98.7	99.37	25.38	22.68	74.8	72.42	25.05	25.59	32.87	32.24
28	-1	1	1	-1	99.59	99.36	98.31	98.59	99.75	99.48	17.42	18.82	65.77	64.62	32.38	31.29	40.85	41.30
29	1	-1	1	-1	97.67	97.00	95.31	94.70	99.78	99.44	16.65	16.36	76.92	77.05	25.47	25.92	31.12	29.70
30	-1	-1	1	-1	99.54	99.51	97.05	97.56	99.88	99.55	19.38	19.38	70.24	69.25	32.86	31.62	36.56	34.44
31	1	1	-1	-1	98.19	98.14	96.68	96.53	97.7	97.68	25.22	25.21	75.81	75.55	35.47	34.72	29.86	29.47
32	-1	1	-1	-1	97.81	98.60	95.94	97.05	97.94	97.79	17.82	16.19	68.72	67.75	32.19	31.93	37.2	38.53
33	1	-1	-1	-1	94.61	94.83	93.73	93.16	95.91	96.21	26.42	24.21	74.45	73.34	35.21	35.05	27.69	26.93

34	-1	-1	-1	-1	96.98	97.33	95.94	96.02	97.03	96.32	22.2	22.07	66.04	65.54	31.68	32.26	32.3	31.67
35	0	0	0	-2	98.14	98.56	97.2	96.77	98.08	98.07	20.06	21.26	68.51	69.52	30.92	31.71	27.38	28.47
36	0	0	0	-2	99.19	98.56	97.05	96.77	97.81	98.07	20.34	21.26	68.04	69.52	30.86	31.71	28.35	28.47

Table A.2 ANOVA results for the RSM models' terms.

Effect	Term	Turbidity removal (%)		TSS removal (%)		Particulate hardness removal (%)		Silica removal (%)		TOC removal (%)		TIC removal (%)		SVI (mL/g)	
		Mean square	p-value	Mean square	p-value	Mean square	p-value	Mean square	p-value	Mean square	p-value	Mean square	p-value	Mean square	p-value
linear	x_1-Poly-DADMAC dose	17.63	< 0.0001	22.82	< 0.0001	0.09	0.43	72.48	< 0.0001	485.55	< 0.0001	19.14	< 0.0001	114.87	< 0.0001
	x_2-mixing time with softeners only	19.99	< 0.0001	38.98	< 0.0001	10.15	< 0.0001	115.29	< 0.0001	11.72	0.01	0.87	0.32	176.96	< 0.0001
	x_3-coagulation speed	17.18	< 0.0001	18.91	< 0.0001	17.85	< 0.0001	2.46	0.26	0.66	0.53	13.64	0.0004	4.69	0.19
	x_4-flocculation time	0.29	0.28	3.93	0.003	1.68	0.003	0.0008	0.98	1.33	0.38	14.06	0.0004	159.98	< 0.0001
Interaction	x_1x_2	4.19	0.0003	5.43	0.0006	-	-	47.27	< 0.0001	-	-	-	-	18.51	0.01
	x_1x_3	-	-	-	-	-	-	26.47	0.0009	-	-	71.87	< 0.0001	-	-
	x_1x_4	-	-	-	-	-	-	-	-	-	-	35.79	< 0.0001	39.09	0.0006
	x_2x_3	2.04	0.008	-	-	2.34	0.0005	28.36	0.0007	46.89	< 0.0001	-	-	-	-
	x_2x_4	-	-	-	-	0.73	0.04	51.48	< 0.0001	-	-	-	-	-	-
	x_3x_4	-	-	-	-	3.74	<0.0001	40.13	0.0001	-	-	51.30	< 0.0001	50.09	0.0002

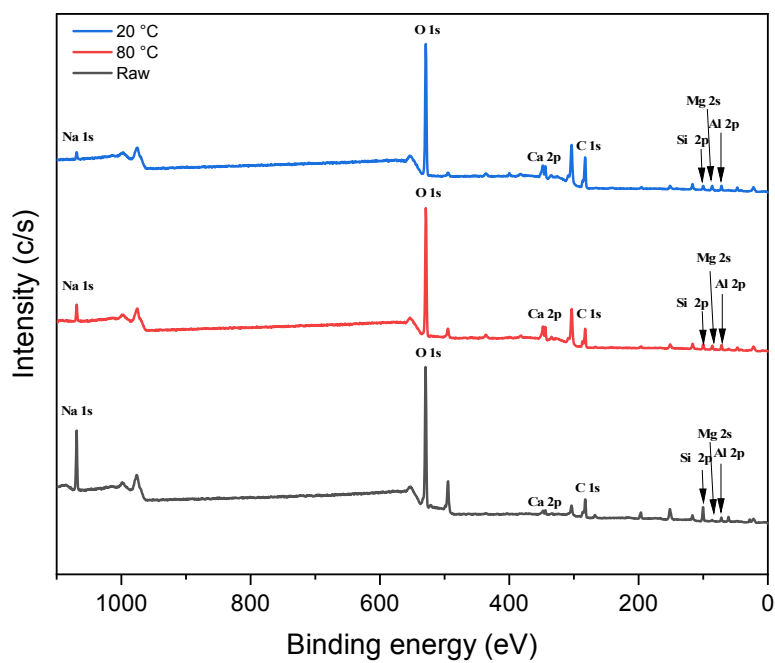|														
	x_1^2	2.09	0.007	-	-	-	-	-	-	67.17	< 0.0001	7.80	0.005	-	-
Quadratic	x_2^2	4.32	0.0003	-	-	10.13	< 0.0001	75.10	< 0.0001	-	-	7.59	0.006	64.80	< 0.0001
	x_3^2	-	-	12.68	<0.0001	6.16	0.0001	75.46	< 0.0001	-	-	-	-	32.45	0.001
	x_4^2	-	-	7.38	0.0001	3.01	0.0001	52.21	< 0.0001	24.77	0.0006	-	-	94.60	< 0.0001

Figure A.2 XPS spectra of survey scan for raw particles and flocs after optimal treatment under 20 °C and 80 °C.
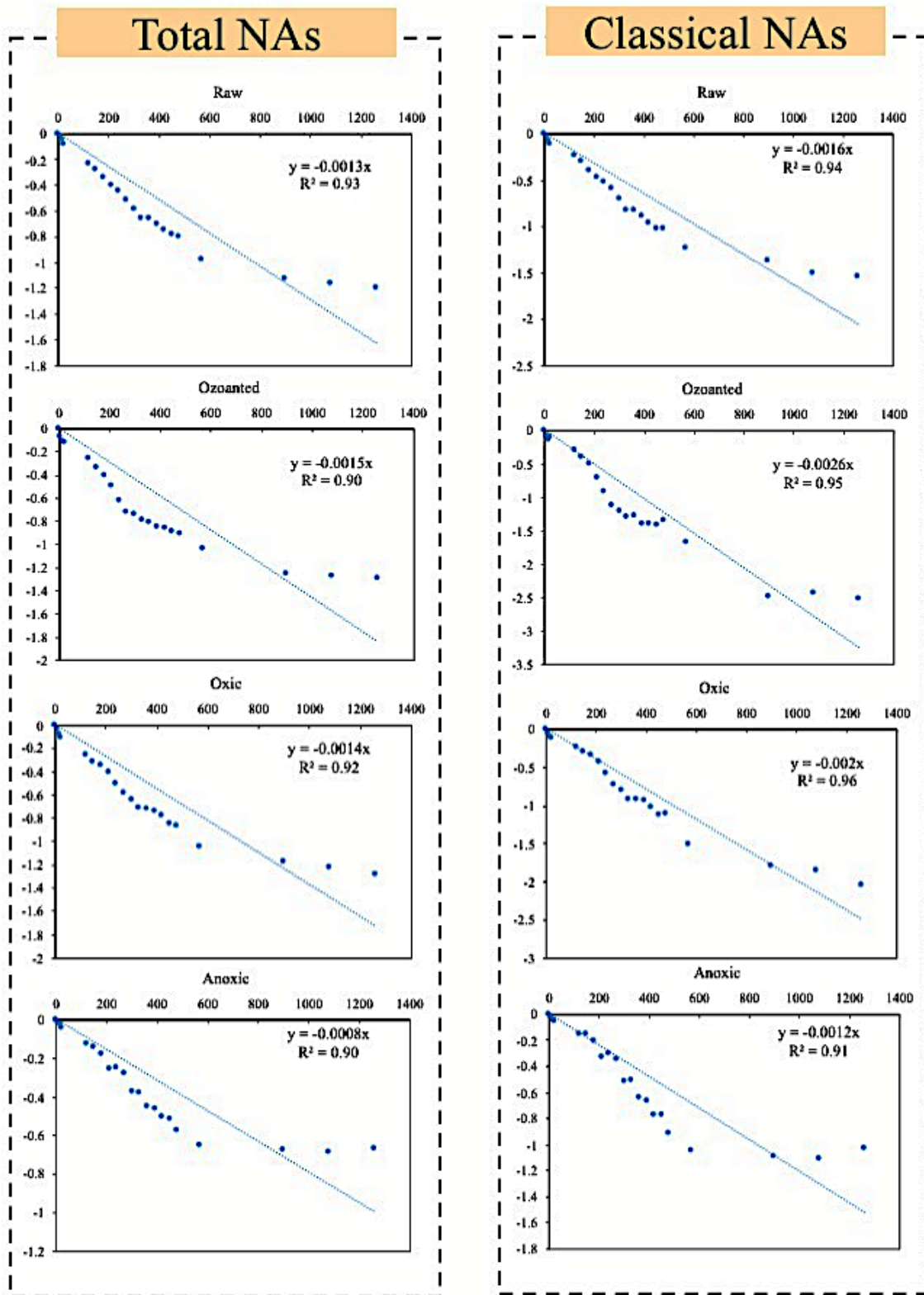
Figure A.3 Biodegradation kinetics evaluation for total and classical NAs in aged OSPW.

Appendix B

Table B .1 Percent similarity of cultivable bacterial strains from oil sands tailings and their characterization.

| Strain name	Percent identity	Characteristics	Reference
Pseudomonas chloritidismutans strain AW-1	99.76%	Facultative anaerobic, gram-negative, chlorate-reducing bacterium	(Mehboob et al., 2009)
Bosea lathyri strain R-46060	99.26%	Aerobe, mesophilic, gram-negative bacterium	(De Meyer and Willems, 2012)
Sphingopyxis witflariensis strain W-50	99.36%	Aerobe, mesophilic, gram-negative bacterium	(Kämpfer et al., 2002)
Pseudomonas vancouverensis strain DhA-51	94.23%	Aerobe, mesophilic, gram-negative bacterium	(Mohn et al., 1999)
Pseudomonas knackmussii strain B13	96.98%	Aerobe, mesophilic, gram-negative bacterium	(Stolz et al., 2007)
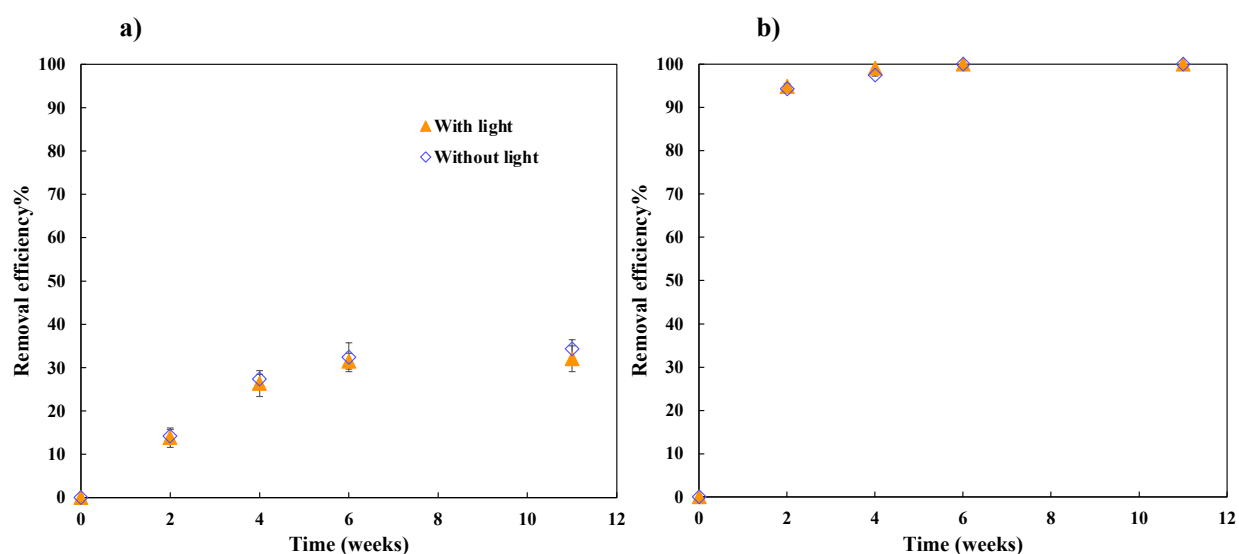
Figure B.1 Removal efficiency of A-PAM (a) and residual AMD (b) in tailings water under different light conditions.
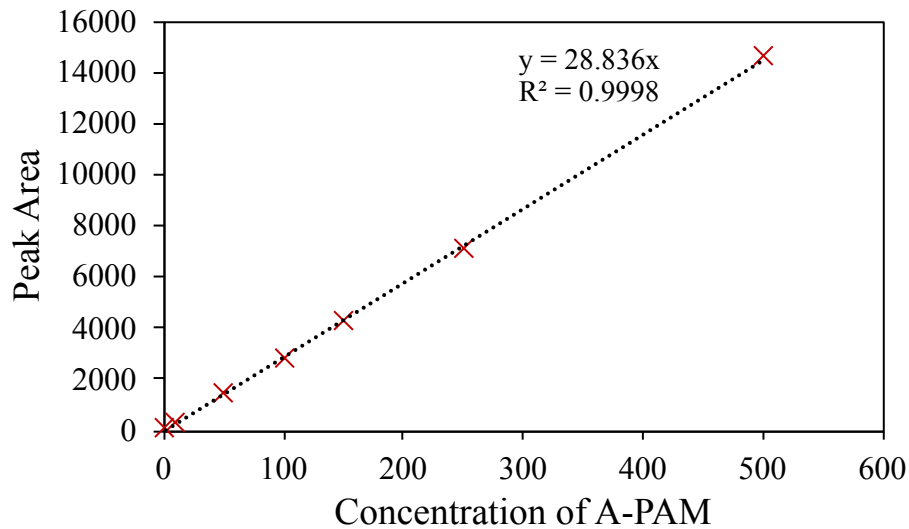

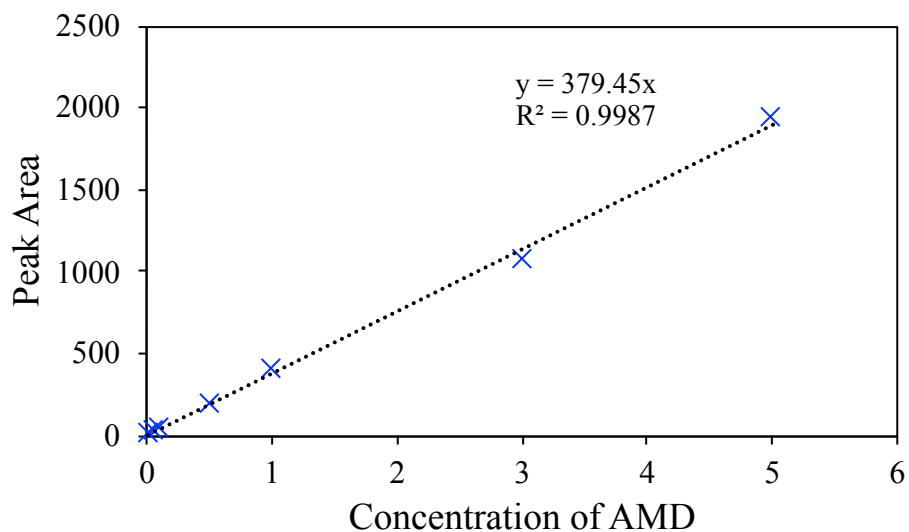**Figure B.2** Calibration curve for the concentration of A-PAM.

Figure B.3 Calibration curve for the concentration of AMD.

Table B.2 Assignment of the Fourier transform infrared (FTIR) characterization of bands of the A-PAM.

Peak position (cm^{-1})	Assignment	Reference
3340	Primary amide NH$_2$ asymmetric stretching	(Godwin Uranta et al., 2018; Xiong et al., 2018)
3198	Primary amide NH$_2$ symmetric stretching	(Godwin Uranta et al., 2018; Xiong et al., 2018)
2933	-CH$_3$ or -CH$_2$- stretching	(Akbari et al., 2017; Huang et al., 2019)
1657	Primary amide C=O stretching	(Akbari et al., 2017; Xiong et al., 2018)
1604	Secondary amide N-H bending	(Zhou et al., 2013)
1564	C=O asym stretching of -COO$^-$	(Godwin Uranta et al., 2018; Xiong et al., 2018)
1417	C-N stretching of amide	(Wang et al., 2019)
1401	-COO$^-$ sysmetric stretching	(Godwin Uranta et al., 2018)
1323	C-O stretching	(Godwin Uranta et al., 2018)
1126	C-O-C stretching	(Lin et al., 2007)
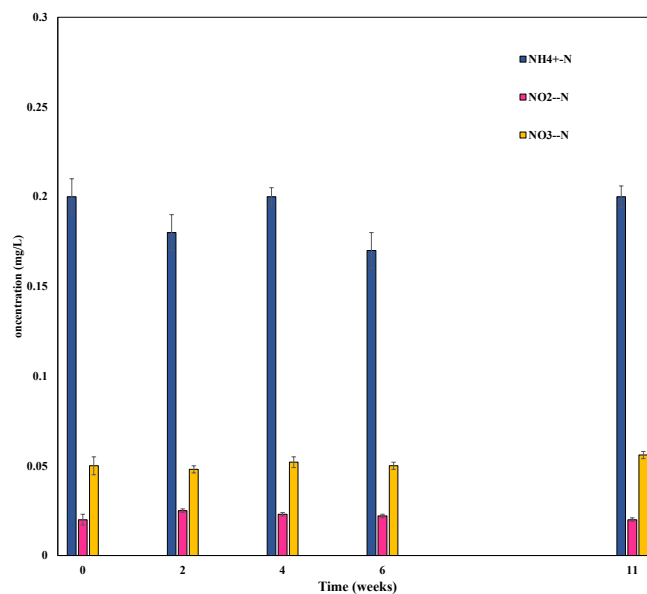
Figure B.4 The concentration of NH_4^+-N, NO_2^--N, NO_3^--N in raw tailings water without A-PAM.
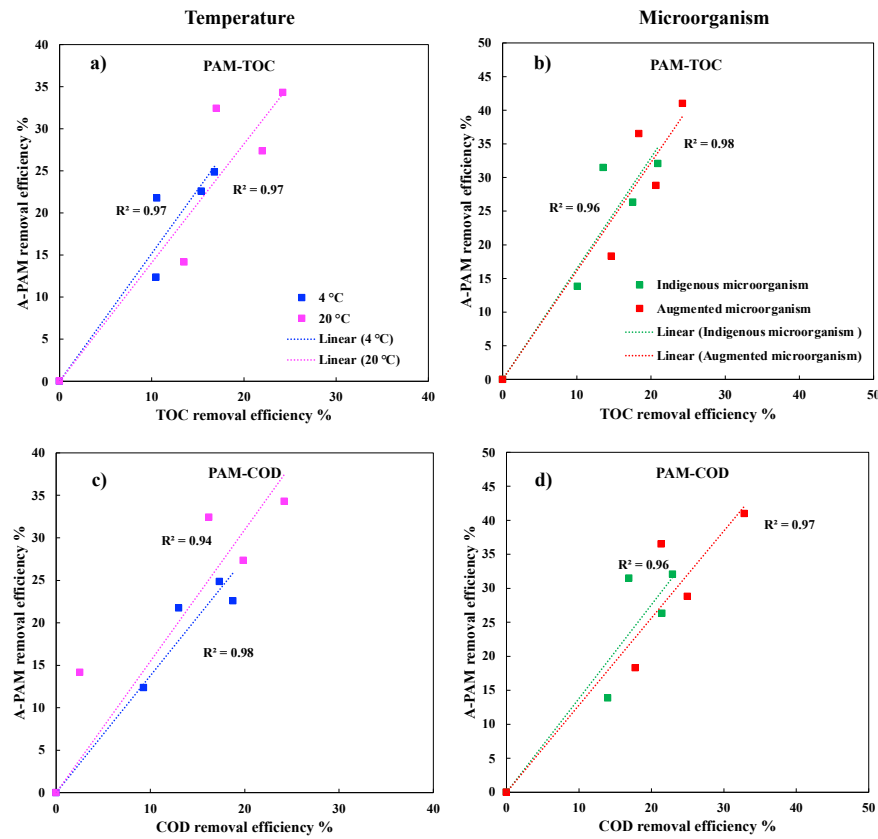

Figure B.5 Linear relationship between the removal efficiency of A-PAM with the removal efficiency of TOC (a & b) and COD (c & d) in tailings water under different temperature and microorganism conditions.
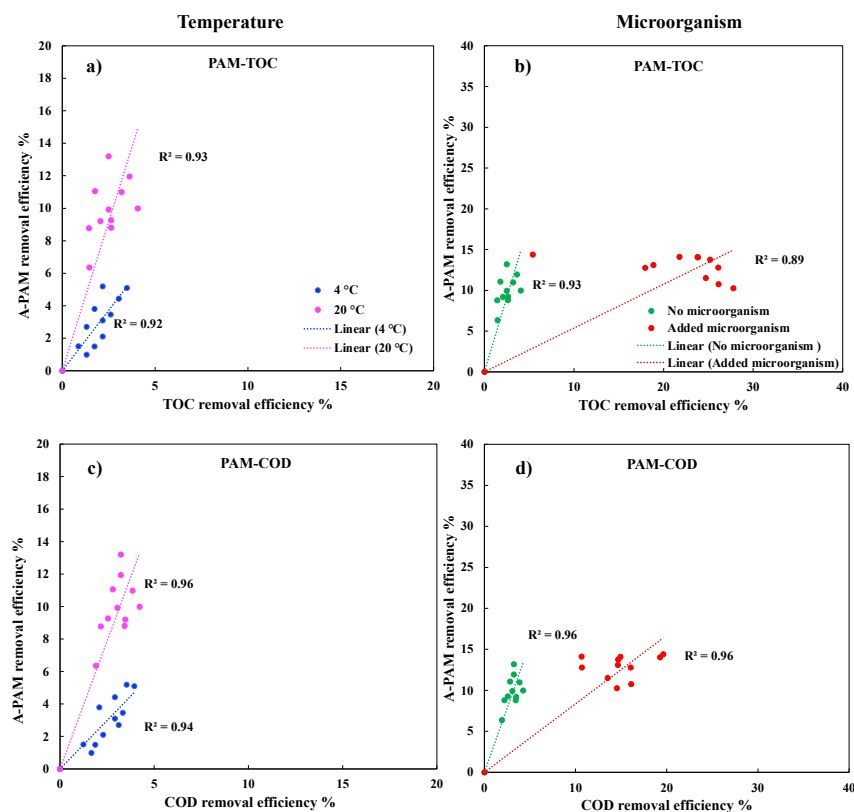
Figure B.6 Linear relationship between the removal efficiency of A-PAM with the removal efficiency of TOC (a & b) and COD (c & d) in pure polymer solution under different temperature and microorganism conditions.

Table B.3 The mean value of COD, TOC, zeta potential and pH of tailings water with different A-PAM concentrations before and after anaerobic degradation of A-PAM.

Sample	COD (mg/L)		TOC (mg/L)		Zeta potential (mV)		pH	
	Day 0	Day 36	Day 0	Day 36	Day 0	Day 36	Day 0	Day 36
Control	560.5	479.8	173.7	141.4	-38.7	-41.3	8.5	8.8
50 mg/kg TS	618.3	580.90	191.0	150.0	-40.9	-38.5	8.6	8.8
100 mg/kg TS	677.5	645.8	208.2	166.9	-43.3	-40.9	8.6	8.7
250 mg/kg TS	776.7	745.8	211.8	173.2	-62.2	-45.6	8.7	8.9
500 mg/kg TS	853.5	836.7	246.4	202.4	-63.1	-52.0	8.7	8.8
1000 mg/kg TS	1100.0	1083.0	266.5	227.1	-65.1	-59.9	8.8	9.0

| 2000 mg/kg TS | 1880.8 | 1874.0 | 268.0 | 235.8 | -75.3 | -71.5 | 8.8 | 9.0 |

Table B.4 Chemical composition of flocs in control and tailings with A-PAM addition before and after anaerobic degradation of A-PAM by EDS analysis.

Sample	Elements (wt%)															
	C		O		Na		Mg		Al		Si		K		Fe	
	Day 0	Day 36	Day 0	Day 36	Day 0	Day 36	Day 0	Day 36	Day 0	Day 36	Day 0	Day 36	Day 0	Day 36	Day 0	Day 36
Control	11.7	14.4	50.7	49.8	0.1	0.3	0.2	0.2	4.3	3.9	30.9	30.0	1.2	0.7	1.1	0.7
50 mg/kg TS	11.9	16.5	46.1	48.9	0.3	0.4	0.2	0.3	3.7	7.8	36.4	22.7	0.6	1.8	0.8	1.7
100 mg/kg TS	12.1	13.5	46.1	48.5	0.3	0.3	0.1	0.2	4.2	4.5	35.4	30.6	0.8	0.9	1.0	1.0
250 mg/kg TS	12.6	15.1	46.3	48.1	0.2	0.1	0.1	0.1	2.4	1.8	37.8	34.1	0.2	0.3	0.4	0.4
500 mg/kg TS	12.9	16.2	47.2	45.9	0.2	1.9	0.1	0.4	1.6	8.5	37.2	23.3	0.3	1.7	0.6	2.0
1000 mg/kg TS	13.0	15.1	47.9	47.8	0.2	0.4	0.1	0.3	2.0	8.1	36.1	25.1	0.3	1.7	0.4	1.5
2000 mg/kg TS	13.2	17.8	48.2	48.5	0.5	0.2	0.2	0.2	2.4	6.1	32.5	26.1	1.1	0.7	1.6	0.9